Final Report

Project #20-004

Galveston Offshore Ozone Observations (GO_3)

Submitted by

James Flynn, University of Houston
Yuxuan Wang, University of Houston
Paul Walter, St. Edward's University
Gary Morris, St. Edward's University

Prepared by
Travis Griggs, University of Houston
Xueying Liu, University of Houston

November 15th, 2021

Executive Summary

The following report presents the observational data, initial analysis, and modeling results from the GO3 field campaign, operating from July – October 2021 due to a COVID-19 delay. The GO3 campaign addressed the observational gap in collection of meteorological, ozone (surface measurements and ozonesonde vertical profiles) and boundary layer height data over Galveston Bay and the offshore waters of the Gulf of Mexico to validate and improve the photochemical modeling used for air quality forecasting.

Three active boats were selected to outfit with instrumentation in order to obtain the ozone, meteorological and boundary layer data. These boats, a 100' commercial ocean-going boat operated out of Galveston, TX that primarily services large marine vessel traffic offshore in the Gulf of Mexico, a commercial shrimper operated on the east side of Galveston Bay out of Smith Point, TX and a pontoon boat operated by the science team out of Kemah, TX were equipped to measure meteorological parameters and surface ozone. The pontoon boat and shrimp boat (July-August) were equipped with ceilometers to measure the boundary layer data. The pontoon boat also measured Ox (O_3 + NO_2) for six weeks and provided a platform to launch ozonesondes over Galveston Bay.

Instruments were calibrated prior to deployment by comparison with ozone (O_3) standards directly traceable to the EPA Region 6 standard reference photometer for O_3 as well as routine baseline assessments while deployed. Regression and spatial analysis have been used to investigate patterns and trends in the data collected. These analyses were complemented by three-dimensional air quality modeling using the Weather Research and Forecasting-GEOS Chem platform.

The small sampling systems were found to be a highly effective and economical way to collect routine measurements over the water. The selection of boats and operational areas can be tailored to study different areas of interest. High ozone was found over the water numerous times, once exceeding 130 ppbv over Galveston Bay and 110 ppbv over the Gulf. Several recirculation events of land-bay breeze and land-sea breeze which resulted in elevated ozone levels reaching one or more monitors were also observed. Measurements of Ox allowed for the calculation of NO_2 which was found to be elevated over Galveston Bay at times, even when excluding discrete ship exhaust plumes.

Boundary layer height measurements from the eastern and western shores of Galveston Bay showed distinctly different average diurnal profiles, with the western shore presenting a more traditional land-based low morning and high afternoon boundary layer while the eastern shore appeared to be more marine influenced with possible impacts from the sea breeze off the Gulf in the late afternoon and evening. Upper layers detected at both locations were quite similar, indicating a larger regional feature decoupled from the surface.

Modeling data tended to overpredict ozone, particularly on low ozone days. Possible reasons for this include an underprediction of boundary layer height over the water. Additional chemical, meteorological, and boundary layer measurements over the water are recommended for future work in addition to further modeling and analysis of this rich data set.

1 Table of Contents

2 Introduction

Studies have observed high ozone periods in the Houston-Galveston-Brazoria (HGB) area driven by large circulation patterns and mesoscale land-sea breeze circulations (Berlin et al., 2013; Caicedo et al., 2019; Langford et al., 2009; Wang et al., 2016). Regional background (non-locally produced) O_3 transported into the area by large-scale winds were significantly correlated with peak O_3 levels in the HGB region (Berlin et al., 2013; Langford et al., 2009; Nielsen-

Gammon et al., 2005). High O_3 events in the HGB were most associated with continental outflow, while the lowest O_3 levels were from onshore winds (Berlin et al., 2013). However, the onshore bay breeze, which passes over the industrial regions (e.g. Houston Ship Channel), had significantly elevated regional background O_3 levels than the stronger onshore sea breeze, which passes through the Caribbean before entering the Gulf of Mexico (Berlin et al., 2013; Langford et al., 2009). Though episodic, the bay and sea breeze circulation patterns are also found to be important causes for high O_3 events in urban/industrial coastal sites in the U.S. (Banta et al., 2005; Caicedo et al., 2019; Loughner et al., 2011; Mazzuca et al., 2017; Stauffer and Thompson, 2015).

The land/bay/sea breeze phenomenon occurs under weak synoptic forcing when offshore winds sweep urban/industrial pollutants onto open waters before reversing as an onshore breeze and bringing the photochemically aged air, which can be high in O_3, back on shore. There is great interest in understanding the O_3 levels in these open waters (i.e. Galveston Bay), which is exposed to a combination of land-based urban and industrial emissions (Wallace et al., 2018), ship emissions (Schulze et al., 2018; Williams et al., 2009), and complex marine O_3 chemistry (i.e. halogen) (Tuite, et al., 2018; Osthoff et al., 2008; Tanaka et al., 2003). Previous studies have observed elevated O_3 levels in these open waters relative to land-based sites (Sullivan et al., 2018; Goldberg et al., 2014). However, unlike land-based measurements, historical records and/or routine measurement of O_3 levels over these waters (i.e. areas where measurement can be difficult) are limited. Available measurements in these regions are generally from ship or airborne measurements during short-intensive sampling campaigns, which were not designed with a focus on O_3 over the water (Mazzuca et al., 2017; Parrish et al., 2009).

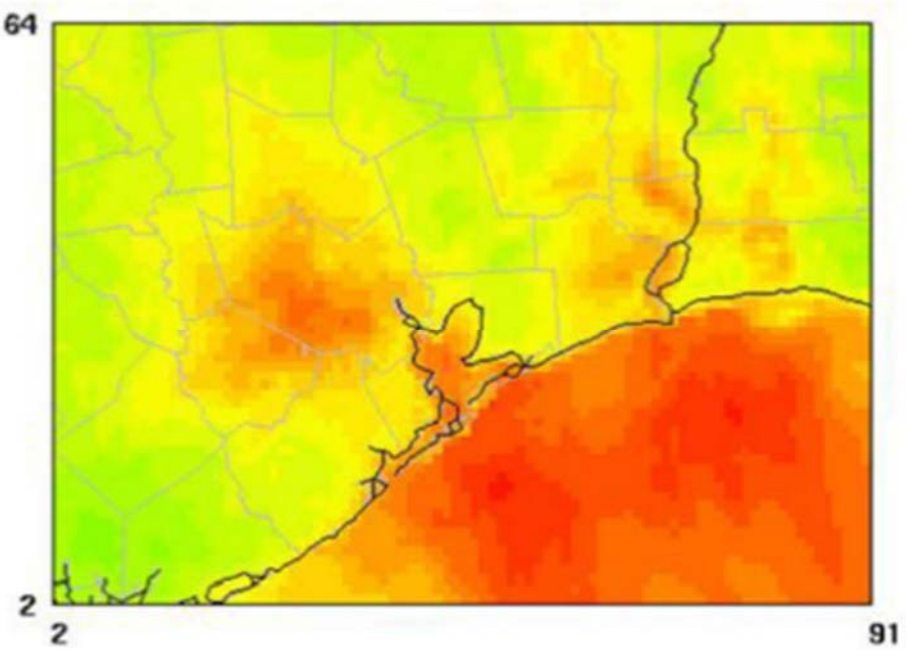

Figure 1. Future case simulation showing high O_3 over water, from Dunker, et al. (2019).

While photochemical models can be powerful tools in detecting and forecasting O_3 levels in these maritime environments (Figure 1), the models are typically built upon parameterizations or simple assumptions to represent small-scale meteorological and chemical processes over the

waters. These assumptions/parameterizations need suitable measurements for validation and/or tuning. In addition, current models may not include all important processes, and to identify which processes are missing and their impacts will also require extensive measurements. Routine observations over the waters have been lacking. Due to this, model performance over the marine environments has been largely unconstrained and thus highly uncertain. Previous studies have observed both positive and negative biases of modeled O_3 concentration in these coastal, transitional regions (Caicedo et al., 2019; Dunker et al. 2019; Sullivan et al., 2018; Goldberg et al., 2014; Li et al., 2012; Yerramilli et al., 2012). A recent study of the HGB region and the Galveston Bay compared observation and modeled planetary boundary layer (PBL), wind direction and speed, and O_3 concentrations during a high O_3 event in Houston (Caicedo et al., 2019). They observed a lower correlation between observations and models over bodies of water and coastal regions compared to measurements closer inland (Caicedo et al., 2019). For that study, the discrepancy observed in the coastal and land-water regions was due to a delay in the simulation of onset bay and sea breezes, which are important factors for modeling O_3 (Caicedo et al., 2019). A recent O_3 model study accounted for the changes in local and regional background O_3 levels and found that similar to previous studies, the model performed well for inland sites but overestimated O_3 at the coastal sites, specifically for days with lower O_3 levels (less than 60 ppbv) (Dunker et al. 2019). These model studies incorporated the halogen chemistry proposed by Tuite et al. (2018). However, the chemistry alone was insufficient to match observations, leading the authors to suspect inaccurate emissions in the Gulf of Mexico or incorrect meteorology with respect to the marine boundary layer height and residual layer mixing. Further measurement of O_3 and meteorological conditions directly on Galveston Bay are necessary to understand the high O_3 events in the HGB region and to improve and refine models.

3 Objectives

The goals for this project are described by the science questions below:

1. How frequently does high O_3 reside over the water during the O_3 season, and how does the observed frequency compare to that simulated by photochemical models? Under what conditions do the modeled and measured O_3 agree or disagree? Is O_3 consistently elevated over water relative to over land, or is there a spatial variability in O_3 over water?

2. How does O_3 and O_X over water compare with O_3 and O_X over adjacent land? Are there indications that O_3 is higher over water due to a lack of titration from point and mobile sources? Are the offshore O_3 values consistent with the findings from previous studies, including the coastal measurements at San Luis Pass in 2016 (Tuite et al., 2018)?

3. How is O_3 formation over the water impacted by local circulation patterns? How does the diurnal pattern over water differ from over land and from coastal measurement locations, such as Smith Point? How frequently does the bay breeze result in a local circulation that brings urban plumes into Galveston Bay? What effect does this circulation have on O_3 in the Houston area in an era of reduced VOC emissions from the Houston Ship Channel area?

4. What are the characteristics of the boundary layer over the water during high O_3 events, and how to the observed boundary layer heights compare to model predicted values? Boundary

layer heights over water are often parameterized and may not accurately represent reality, especially in areas with complex land-water interaction and circulation patterns, such as in Galveston Bay and the offshore waters (Dunker et al., 2019). How do the measured boundary layer heights compare to other land-based coastal measurements, such as those from Smith Point during DISCOVER-AQ Houston or from the Galveston 99th St. site (C1034)?

5. How do small O_3, O_X, and meteorology sampling systems installed on commercial vessels help us better understand O_3 and O_X in Galveston Bay and the Gulf of Mexico? Measurements of O_3 and meteorological parameters have been installed on commercial aircraft, such as in the MOZAIC project (Marenco et al., 1998). Do the vessels operating in Galveston Bay and the offshore coastal areas provide appropriate spatial coverage to investigate O_3 over water under a variety of weather conditions? Can a small sampling system be designed such that it operates with little to no impact on the routine vessel operations?

4 Methodology - Field Measurements

For this project, we developed and installed two automated sampling systems on commercial boats and one traditional measurement system on a UH research boat operating in Galveston Bay. One of the commercial boats and the UH boat operated in Galveston Bay while the second commercial boat primarily operated in the waters offshore of Galveston Island in the Gulf of Mexico. Ozonesondes were also launched from the UH boat within Galveston Bay under this project and from the boat in the Gulf of Mexico under support of another TCEQ program (PGA 582-21-22179-015). One of the conceptual models for high O_3 in the Houston area involves weak synoptic forcing which allows offshore flow due to a combination of the Galveston Bay breeze (GBB) and Gulf of Mexico breeze (GMB) to circulate pollutants over the water before recirculating the aged pollution back over land in the afternoon.

4.1 Instrument Packages

The automated instrument packages consist of a 2B Technology Model 205 dual-beam O_3 analyzer provided by St. Edward's University (Gary Morris, Co-PI), Global Positioning System (GPS), and a ruggedized industrial computer (PC). The PC was configured to boot and shut down with an external switch or with the application or loss of power which automatically started or stopped the instrumentation and data logging. A compact, all-in-one weather station was installed to measure temperature, relative humidity, pressure, and wind speed and direction. An internal digital compass was used with GPS data to correct winds for the motion of the boat. This equipment was installed into a light-colored (yellow) weatherproof enclosure to protect the instrumentation and reduce heat. Additional insulation and a radiant barrier further reduced solar heating. A thermoelectric heat exchanger attached to the enclosure further reduced heat and maintained a stable environment for the instrumentation. Desiccant bags were also used to help control internal relative humidity. This enclosure was secured to the boat exterior on top of the cabin. A Teflon sample line was run from the sample pump in the O_3 monitor to an elevated location on each boat for the sample inlet. A Teflon rain shroud prevented water from entering

the 90 mm Teflon particle filter before being sampled. The relatively large area of the filter required less frequent access to the boat and equipment for filter changes.

A valve was used to periodically route the sample through an ozone-destroying charcoal volume to assess the instrument baseline. Instruments were calibrated prior to and after deployment by comparison with O_3 standards directly traceable to the EPA Region 6 standard reference photometer for O_3. Data was also compared to other O_3 monitors when in proximity to sites such as Galveston 99th Street (C1034), Sylvan Beach (C556), and UH Smith Point (C1606).
Data was logged internally and then transferred to servers at UH via integrated cellular modems when the boat was within the cellular coverage area. There was excellent cellular coverage over most of the areas where the boats operated in Galveston Bay, with the exception of spotty signal at Smith Point itself. Coverage in the Gulf was also present typically as far out as the main anchoring locations but not at the lightering area. The data, which included performance information such as instrument temperatures, pressures, and flows, was displayed on the same system used to visualize and edit data from the network of UH monitoring sites. The network connection also allowed investigators to log into the computers on the boat via LogMeIn to evaluate instrument performance and aid in troubleshooting.

Vaisala CL-51 ceilometers were installed on the UH pontoon boat and the Shrimp Boat. The ceilometers operated and collected data continuously, however the ceilometer on the UH pontoon boat suffered a failure on August 30th. Since the Shrimp Boat was not going out as frequently as hoped due to poor shrimping conditions, the team removed the ceilometer from the Shrimp Boat and installed it on the UH pontoon boat. The data, both mobile and stationary, is used to better understand O_3 processes in and around the Galveston and Trinity Bay area.

The main shortcoming of the project was that the manufacturer failed to deliver working NO_2 photocells. Ultimately an alternate NO_2 photocell was installed during the downtime caused by Hurricane Nicholas and deployed on the UH pontoon boat system. The Ox measurement was captured from September 17th – October 25th, 2021, the end of field measurements.

4.2 Platforms

Several different types of marine vessels and operators were considered for this project. The two chosen were based on their typical operating profiles and openness to working with the science team. In Galveston Bay, a shrimper from Smith Point was chosen (Figure 2). As described to the science team, their operating pattern would follow the shrimp in the Bay as they slowly migrated through various portions of the eastern portion of the Bay, unlike oyster boats which visit fixed locations. Since the boat docked at Smith Point it would provide excellent opportunities for comparison with C1606. For the Gulf of Mexico, a charter boat (Figure 3) service was selected as their operations would take them to the various anchoring and lightering areas off of Galveston Island frequently, sometimes multiple times per day.

Figure 2. Shrimp boat operated in Galveston Bay by Larry Willis.

Figure 2 shows the shrimp boat with the mobile sampling package installed onto the roof of the pilothouse. A dedicated high output marine alternator and battery was installed for additional power to operate the science equipment while underway. State regulations dictate different seasons and legal catch amounts; however, except for bad weather, he was expected to be on the bay typically four days a week. Based on precampaign discussions, on a typical day he would leave the Smith Point area around dawn and return around 2:00 PM, depending on the season and catch. Mr. Willis based his boat at the basin in the RV park where the UH Smith Point (C1606) monitoring site is located, allowing for routine comparisons with the O_3 monitor just 260 m east of the dock. The early season influence of fresh water in the Bay from local rains decreased the quality of catch this season and resulted in significantly lower number of outings and spatial coverage by the Shrimp Boat. COVID related issues also limited his ability to operate for a couple of weeks in August and September.

Figure 3. The M/V Red Eagle operated by Ryan Marine out of Galveston, TX in the Gulf of Mexico

The Red Eagle (Figure 3) is a 100’ long crew/utility vessel with two 40 kW 110/208V three-phase power generators. The typical operating profile for the Red Eagle was to depart the Galveston docks for the Galveston Anchorages and Lightering areas roughly every other day, depending on their clients’ needs. The Red Eagle also conducted some operations as far west as Matagorda Bay (one occasion) and north through the ship channel to the port of Houston. On occasion, the boat would go up to 50 miles offshore. These activities would occur at any time of day and in all weather conditions.

Figure 4. The UH pontoon boat is owned by the University of Houston and operated in Galveston Bay

Additionally, the R/V Mishipeshu (Figure 4), a pontoon boat owned and operated by the UH Earth & Atmospheric Science Department (named after a Native American mythical water cougar) received the third sampling system and was deployed on selected days in July, August, September and October (outings listed in Table 1) to sample in situ O_3, Ox (O_3 + NO_2 - added September 17th), boundary layer heights & meteorological variables around Galveston Bay. Twenty-seven ozonesondes were launched from the UH pontoon boat throughout the sampling period to determine the vertical distribution of O_3 and the marine boundary layer height. Together, the three boats characterized much of Galveston Bay and the offshore waters. This operational area and pattern provided a robust data set for analysis and evaluating model outputs.

Table 1. Days the UH pontoon boat (Pontoon) operated on Galveston Bay. The color of the cells represents the TCEQ Air Quality Forecast, with an asterisk representing an Ozone Action Day.

Date	Time	Sonde Launch
07-13-2021	06:30 – 16:00	Morning & Afternoon
07-14-2021	07:20 – 12:00	-
07-18-2021	06:45 – 13:45	Morning & Afternoon
07-21-2021*	07:00 – 13:45	Morning & Afternoon
07-22-2021*	06:45 – 10:00	Morning
07-26-2021*	06:25 – 16:40	Morning & Afternoon
07-27-2021*	06:15 – 14:25	Morning
07-28-2021*	07:30 – 11:40	Afternoon
08-04-2021*	07:15 – 13:00	-
08-12-2021	06:45 – 10:45	Morning
08-16-2021	06:45 – 14:05	Morning & Afternoon
08-24-2021	13:30 – 16:40	-
08-25-2021*	09:20 – 14:55	-
09-01-2021	07:30 – 13:30	Morning
09-03-2021	07:10 – 11:50	Morning & Afternoon
09-07-2021*	08:55 – 14:35	Afternoon
09-08-2021*	07:05 – 16:45	Morning & Afternoon
09-09-2021*	08:20 – 15:30	Morning & Afternoon
09-17-2021	13:20 –16:40	-
09-20-2021	08:25 – 13:40	-
09-21-2021	07:20 – 15:15	-
09-25-2021*	07:40 – 17:10	Morning & Afternoon
09-26-2021*	07:25 – 14:40	Morning & Afternoon
10-06-2021*	08:30 – 14:40	Afternoon
10-07-2021*	08:30 – 14:40	Afternoon

5 Methodology: Modeling

5.1 WRF-GC Model

WRF-GC v2.0 is a regional air quality model (Feng et al., 2021) that couples the Weather Research and Forecasting (WRF) meteorological model (v3.9.1.1) and the GEOS-Chem atmospheric chemistry model (v12.7.2). Nested-domain capabilities are included in WRF-GC v2.0 to better simulate regional meteorology, air quality and their interactions at high resolution.

The WRF-GC simulation was driven by the National Centers for Environmental Prediction (NCEP) Global Forecast System (GFS) analysis data at 0.25° × 0.25° resolution (https://rda.ucar.edu/datasets/ds083.3/). Table 2 listed the physics schemes used in this study. We adopted the Mellor-Yamada-Nakanishi-Niino (MYNN) planetary boundary layer scheme (Mellor and Yamada, 1982; Nakanishi and Niino, 2006; Nakanishi and Niino, 2009), the Morrison double-moment microphysics scheme (Morrison et al., 2009), the Monin-Obukhov Similarity surface layer, the Noah land surface scheme (Chen and Dudhia, 2001), the Rapid Radiative Transfer Model (RRTMG) longwave and shortwave radiation schemes (Iacono et al., 2008), and the New Tiedtke cumulus parameterization.

WRF-GC used the most updated full O_x-NO_x-VOC-halogen-aerosol chemistry from GEOS-Chem v12.7.2. The emissions used are year-2011 National Emission Inventory scaled to year 2013 for the US and year-2014 CEDS for the rest of the world. Biogenic emissions are from the Model of Emissions of Gases and Aerosols from Nature (MEGAN) (Guenther et al., 2012). Soil NO_x (Hudman et al., 2012) and lightning NO_x (Murray et al., 2012) emissions are included.

We set up three domains with different horizontal resolutions that cover Texas, Southeast Texas, and the Houston-Galveston region, referred to as domain 1, 2, and 3, respectively, as shown in Figure 5. Domain 2 is nested within domain 1, while domain 3 is nested within domain 2. The corresponding horizontal resolutions and grid numbers for domains 1–3 are 25 km x 25 km (73 × 64 grids), 5 km x 5 km (131 × 91 grids), and 1 km x 1 km (161 × 131 grids), respectively. All domains have identical vertical resolutions with 50 hybrid sigma-eta vertical levels spanning from surface up to 10 hPa. The boundary conditions of chemical species for domain 1 were taken from a GEOS-Chem global simulation at 2° × 2.5° resolution and 6-hourly output frequency. In nested-domain simulations, the parent domain provided lateral boundary conditions to the inner domain; specifically, the 25 km-resolution outputs (domain 1) were used as boundary conditions in the 5-km resolution simulation (domain 2), and the 5-km resolution outputs (domain 2) were used as boundary conditions in the 1-km simulations (domains 3). Simulations were performed from 1 June to 1 October 2021, with initial conditions for three domains provided by the GEOS-Chem global simulation. For every monthly simulation, the first 5 days (e.g. 27–31 May) were used for spin-up to remove the influences of initial conditions and the subsequent monthly simulations (e.g. 1 June – 30 June) were used for analysis.

Table 2. WRF-GC physics configurations.

Configuration	Setting	Scheme
PBL scheme	bl_pbl_physics = 5	MYNN 2.5
Surface layer	sf_sfclay_physics = 1	Monin-Obukhov Similarity
Land surface	sf_surface_physics = 2	Noah Land Surface Model
Microphysics	mp_physics = 10	Morrison 2-moment
Shortwave radiation	ra_sw_physics = 4	RRTMG
Longwave radiation	ra_lw_physics = 4	RRTMG
Cumulus parametrization	cu_physics = 16	New Tiedtke

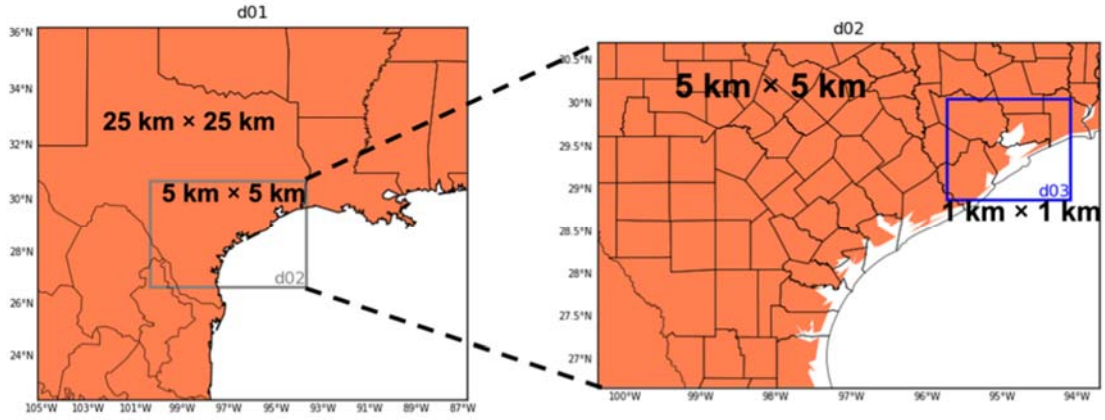

Figure 5. WRF-GC domains. D01, d02, and d03 stand for domain 1, 2, and 3 respectively.

Table 3 Description of WRF-GC domain setting.

Domain	Region	Horizontal Resolution	Domain Size	Output frequency
1	Texas	25 km × 25 km	73 × 64	6-hourly
2	Southeast Texas	5 km × 5 km	131 × 91	3-hourly
3	Houston-Galveston	1 km × 1 km	161 × 131	hourly

5.2 Performance Metrics

WRF-GC uses chemistry schemes from the GEOS-Chem global chemical transport model, which has a standard benchmarking procedure for each major code release, using observations compiled from surface monitoring network, aircraft campaigns, and satellite retrievals around the globe. In addition to these efforts, an in-depth evaluation of the model's performance in simulating field observations was performed and described in the next Section. Table 4 shows the performance metrics employed throughout the reporting periods for this study. In addition to the performance metrics, descriptive statistics such as mean, median, standard deviation, minimum, and maximum are used.

Table 4. Performance metrics used in observation and model comparison.

Performance metric	**Formula**
Correlation Coefficient (R)	$R = \frac{\sum_{i=1}^{N}(M_i - \overline{M})(O_i - \overline{O})}{\sqrt{\sum_{i=1}^{N}(M_i - \overline{M})^2}\sqrt{\sum_{i=1}^{N}(O_i - \overline{O})^2}}$

Normalized Mean Bias (NMB)	$NMB = \frac{\sum_{i=1}^{N}(M_i - O_i)}{\sum_{i=1}^{N} O_i} \times 100\%$
Root Mean Square Error (RMSE)	$RMSE = \sqrt{\frac{1}{N}\sum_{i=1}^{N}(M_i - O_i)^2}$

Note: M is the model output, O is the observation, N is the number of samples, and the means of M and O are given by $\overline{M} = \frac{1}{N}\sum_{i=1}^{N} M_i$ and $\overline{O} = \frac{1}{N}\sum_{i=1}^{N} O_i$.

6 Discussion

6.1 Question 1: Ozone Over the Water

6.1.1 How frequently does high O_3 reside over the water during the O_3 season, and how does the observed frequency compare to that simulated by photochemical models?

Figure 6 (b) shows the frequency of modeled high ozone days over July 1st – September 11th, 2021. On average, 45% of the days (33 among 73 days) during July 1–September 11, 2021, are characterized as high ozone days by the model. High ozone days are defined as days with maximum hourly ozone exceeding 70 ppbv, as shown in Table 5. Urban Houston experienced high ozone more frequently than Galveston Bay and the Gulf of Mexico. 40-80% of days in urban Houston experienced hourly ozone exceeding 70 ppbv, while only 30-50% and 20% of days in Galveston Bay and the Gulf of Mexico experienced such high ozone, respectively. Table 5 shows that 10 high ozone days, 6 moderate ozone days, and 2 low ozone days are identified by TCEQ forecast out of the 18-days outing period before September 11th, 2021. The TCEQ high ozone days are 100% captured by the WRF-GC model. The TCEQ moderate ozone days are 67% captured, with August 16th and 24th being overestimated by the model. The two TCEQ low ozone days are overestimated by the model. Meanwhile, in comparison to the ozone level measured by boats, the model captured the same high ozone days as observations in 17% of the days (3 among 18 days) before September 11th, 2021, but overestimates ozone in 83% of the days (15 among 18 days). In addition, both the WRF-GC model and TCEQ predictions are relatively higher than the measured ozone levels, as shown in Table 5.

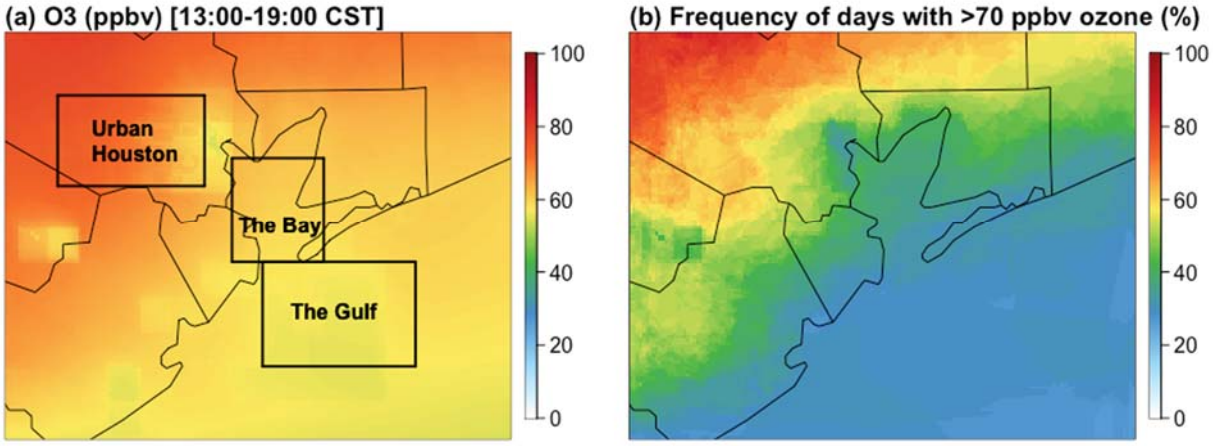

Figure 6. (a) afternoon mean ozone, and (b) frequency of high ozone days over July 1–September 11, 2021. The high ozone days are defined as days with any hourly ozone exceeding 70 ppbv.

6.1.2 Under what conditions do the modeled and measured O3 agree or disagree?

The model is biased high in most cases, as shown in Figure 7. The relative differences are higher over the Gulf of Mexico than over Galveston Bay in general, as shown in Figure 7d. The large ozone overestimation over the Gulf could have possibly resulted from overestimation of planetary boundary layer (PBL) height over the Gulf waters in Figure 11. Model estimates high PBL where high ozone aloft could potentially mix into the PBL and produce a less steep vertical profile than over the land and the Bay, as shown in Figure 11. The downmixing could bring ozone aloft to the surface, causing high surface ozone concentration. The modeled vertical profile shows less ozone at 2-4 km aloft but more ozone below 1.5 km in comparison to ozonesonde measurements at the Gulf, which suggests the high ozone bias over the Gulf could be partly caused by high PBL with strong downmixing ozone estimated by the model.

Figure 12 shows ozone biases as a function of observed temperature and relative humidity. One cluster of high biases is found with high observed temperature (> 30 °C) and low relative humidity (< 50%), suggesting hot and dry days tend to yield higher ozone bias from the model. This, for example, could be the case in the northwest part of Galveston Bay with high ozone, high temperature, and low humidity in Figure 7–9. Meanwhile, there are also high biases when the temperature is low (< 25 °C), and the relative humidity is high (> 60%).

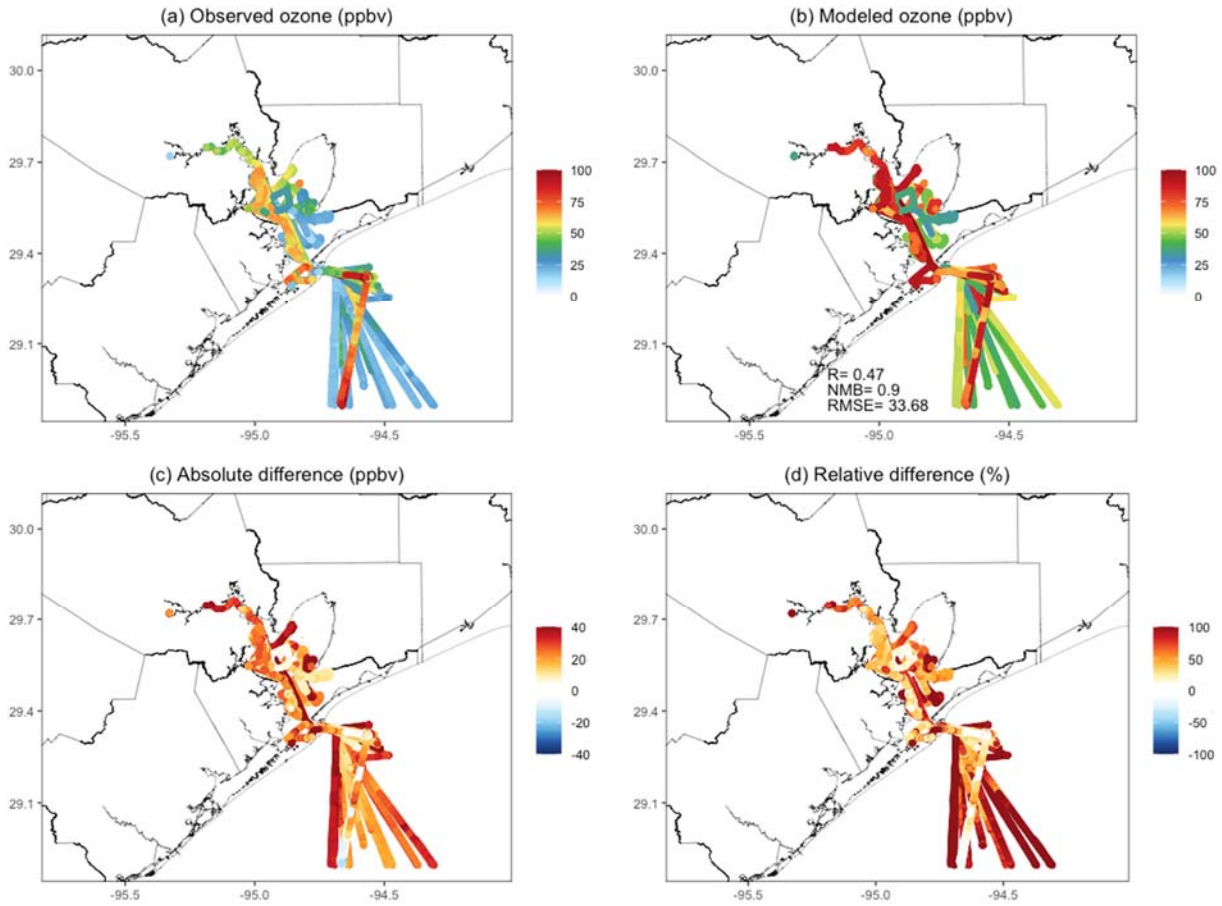

Figure 7. Observed and modeled surface ozone from July 7 to September 11, 2021. Absolute differences are model minus observation (i.e. model–observation), and relative differences are absolute differences divided by observation (i.e. (model–observation)/observation).

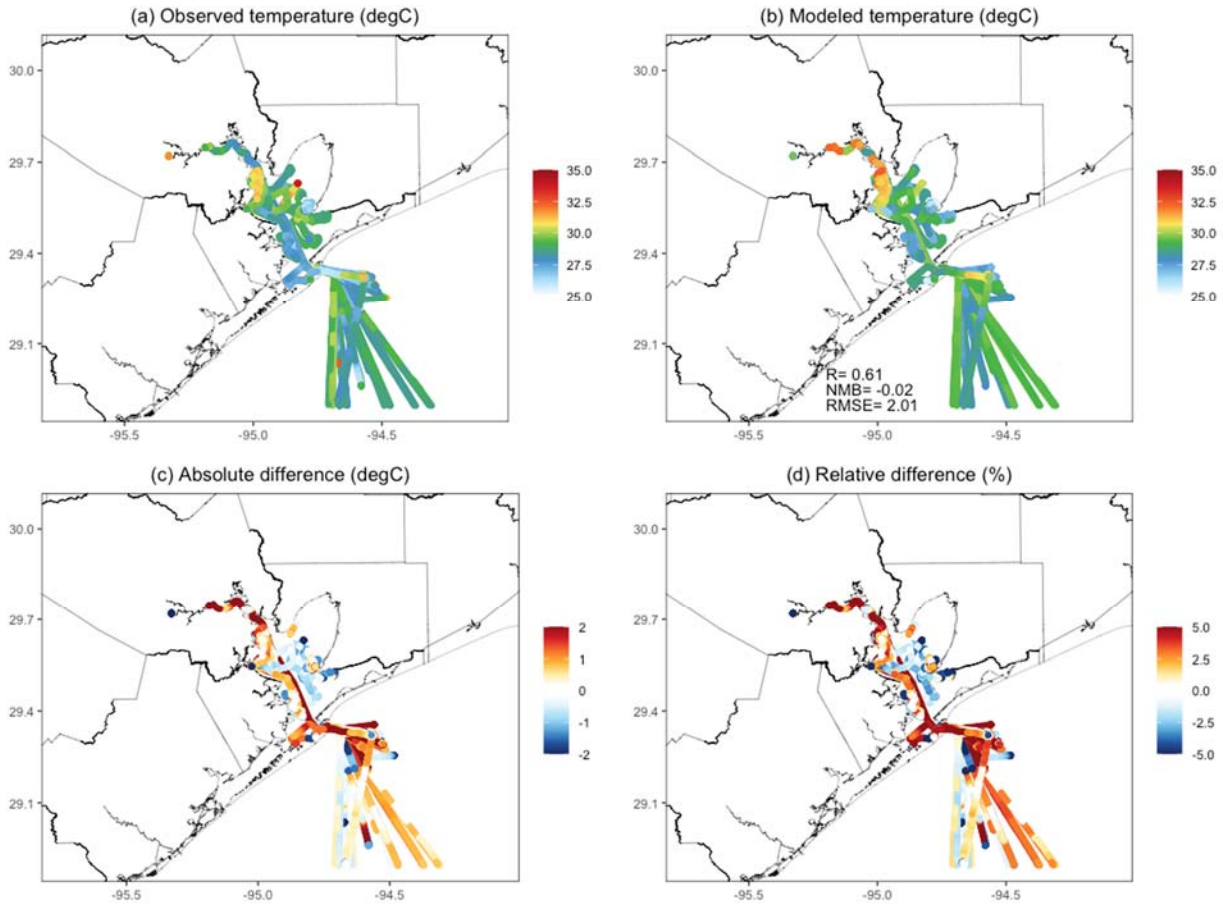

Figure 8. Observed and modeled air temperature from July 7 to September 11, 2021. Absolute differences are model minus observation (i.e. model–observation), and relative differences are absolute differences divided by observation (i.e. (model–observation)/observation).

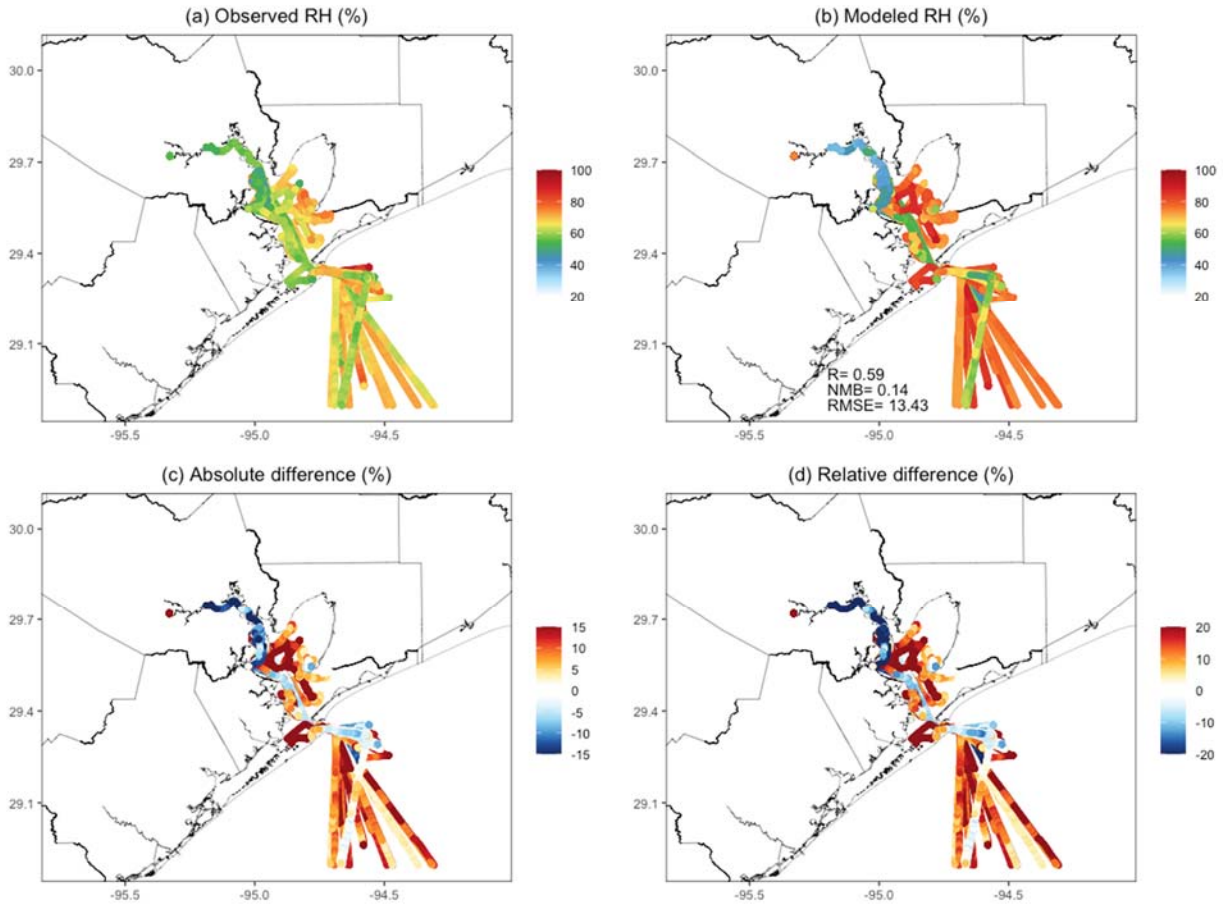

Figure 9. Observed and modeled relative humidity from July 7 to September 11, 2021. Absolute differences are model minus observation (i.e. model–observation), and relative differences are absolute differences divided by observation (i.e. (model–observation)/observation).

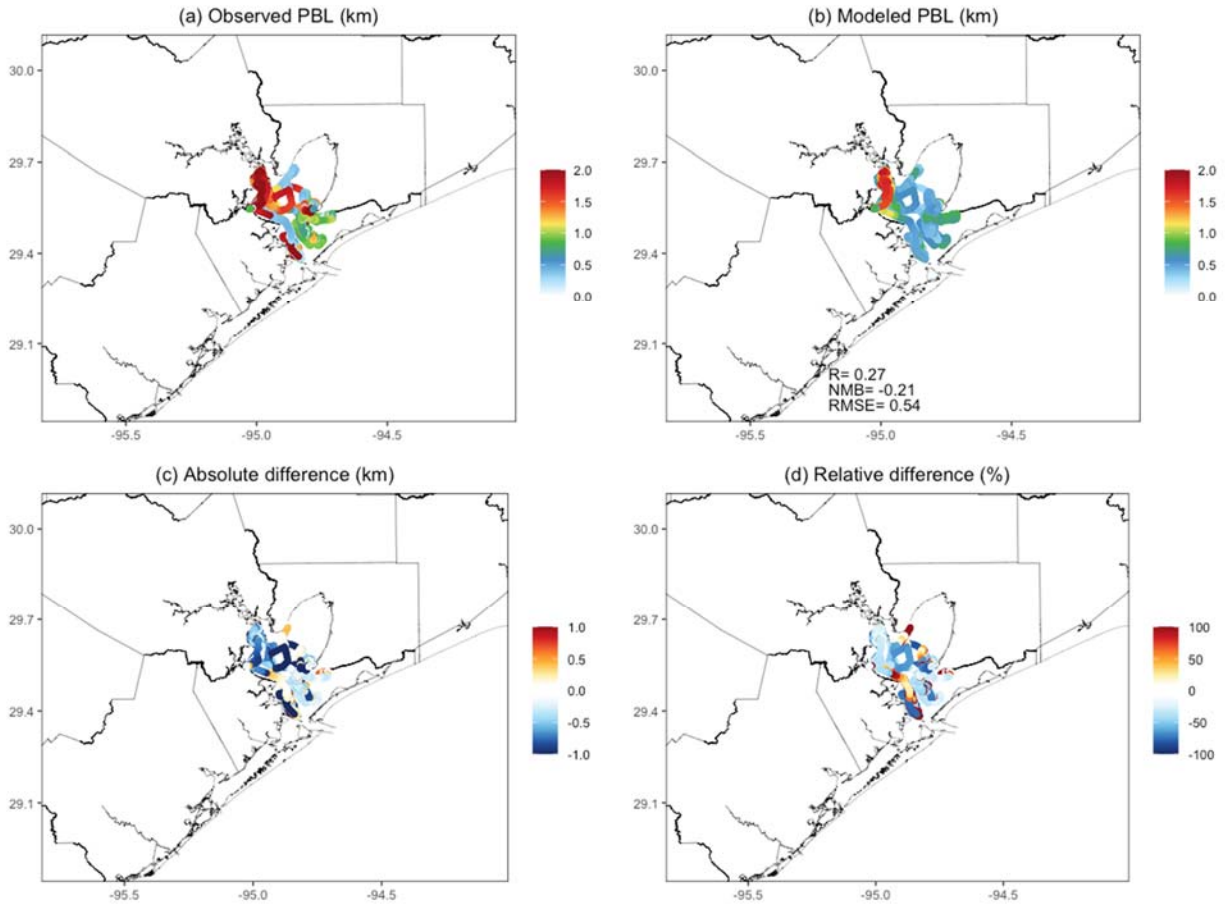

Figure 10. Observed and modeled planetary boundary layer height from July 7 to September 11, 2021. Absolute differences are model minus observation (i.e. model–observation), and relative differences are absolute differences divided by observation (i.e. (model–observation)/observation).

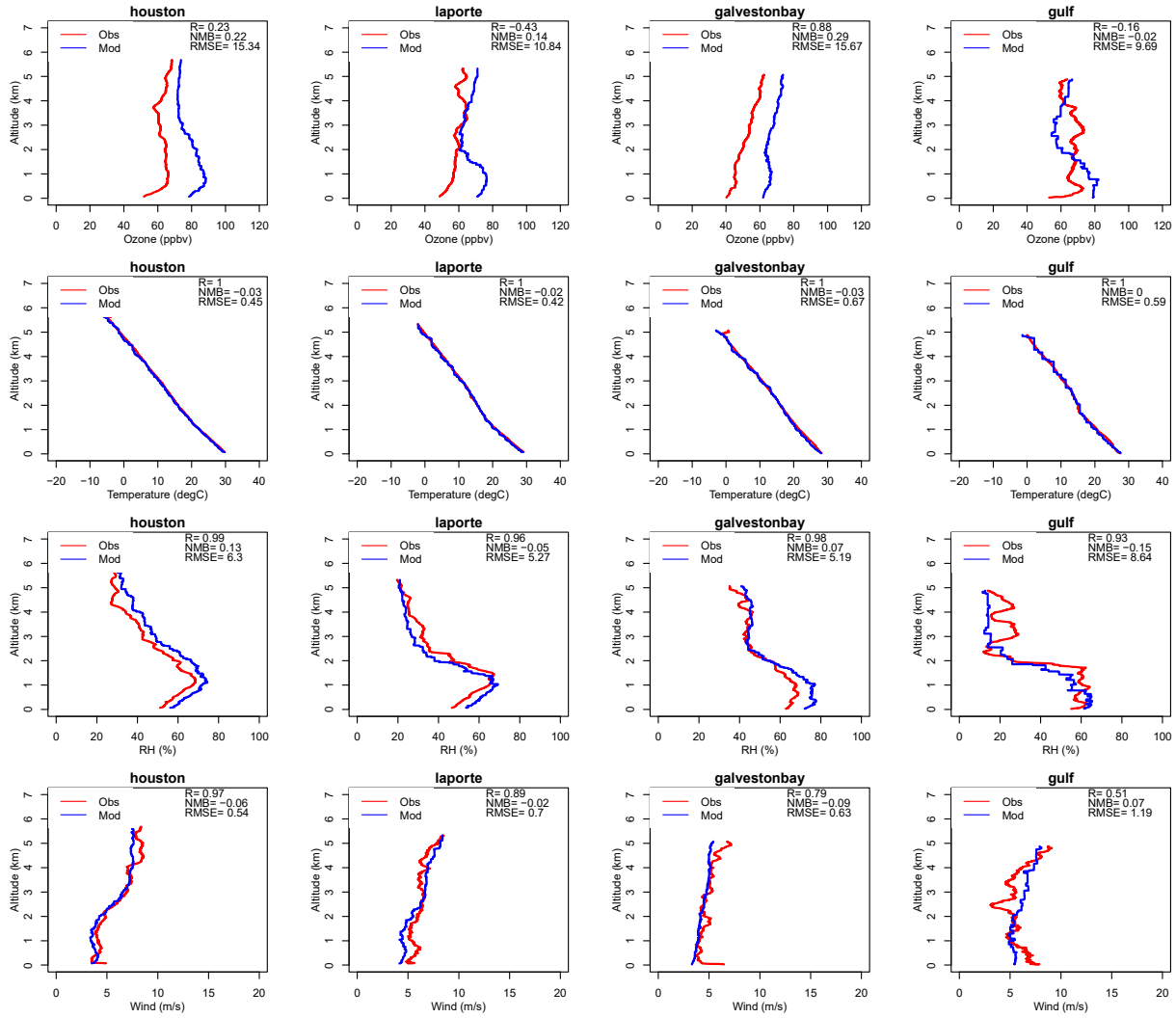

Figure 11. Comparisons of vertical profiles between observed and modeled ozone (first row), temperature (second row), relative humidity (third row), and wind speed (fourth row) over urban Houston, La Porte, Galveston Bay, and the Gulf of Mexico for June, July, and August 2021. Thick solid lines show the mean, and shadings show the range between minimum and maximum. Correlation coefficient (R) normalized mean bias (NMB), and root mean square error (RMSE) are inserted.

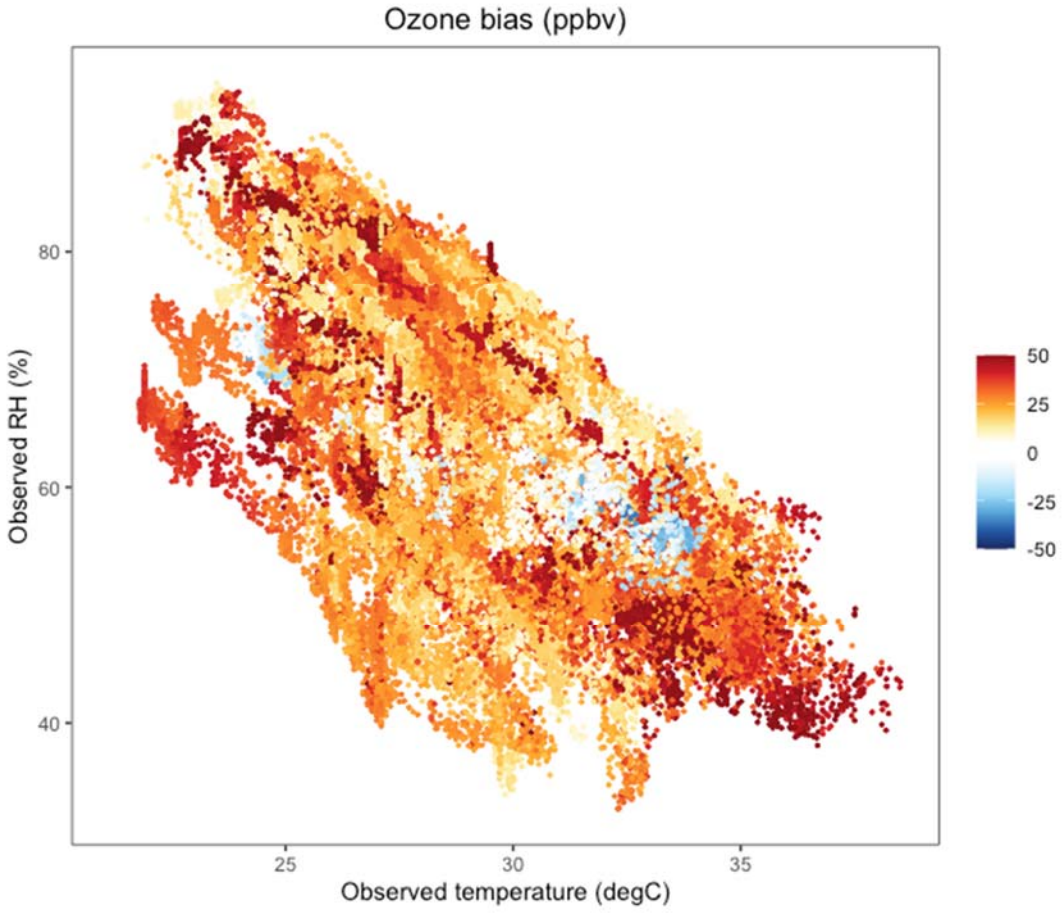

Figure 12.Ozone biases (model minus observation) as a function of observed temperature and relative humidity.

An overview of all meteorological, O_3, and NO_2 collected by the three research vessels over the entire sample period is shown in Figures 13-15. From the time series, periods of high ozone occur over the water throughout the ozone season. The highest ozone periods over the water do generally coincide with a wind flow reversal shifting the winds from generally onshore (southerly flow) to generally offshore (northerly flow). This scenario would typically occur after the passing of a frontal boundary. The highest ozone of the sample period of 133 ppb was observed on October 7th, 2021, approximately 4 days after the passing of a frontal boundary. This measurement was recorded by the UH pontoon boat during a mobile sampling period on Galveston Bay in the W/NW regions.

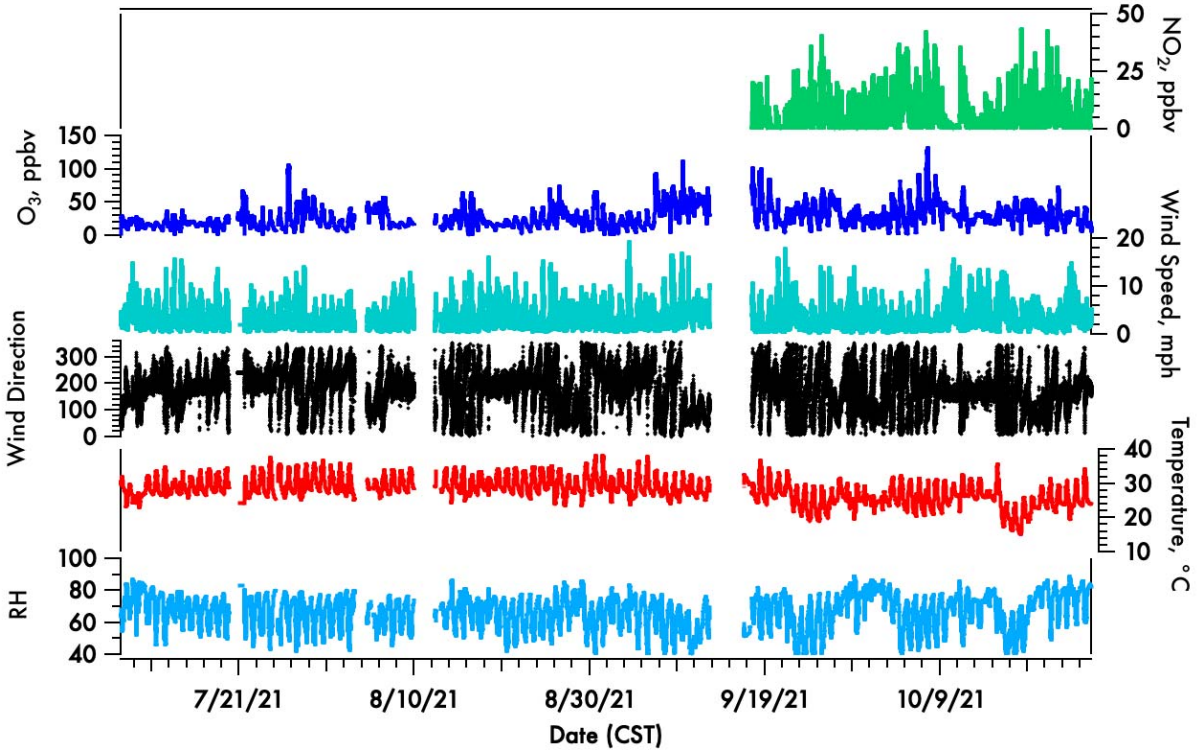

Figure 13. Ozone and Meteorological data collected on the UH pontoon boat operated by the University of Houston from July 13th - October 11th, 2021.

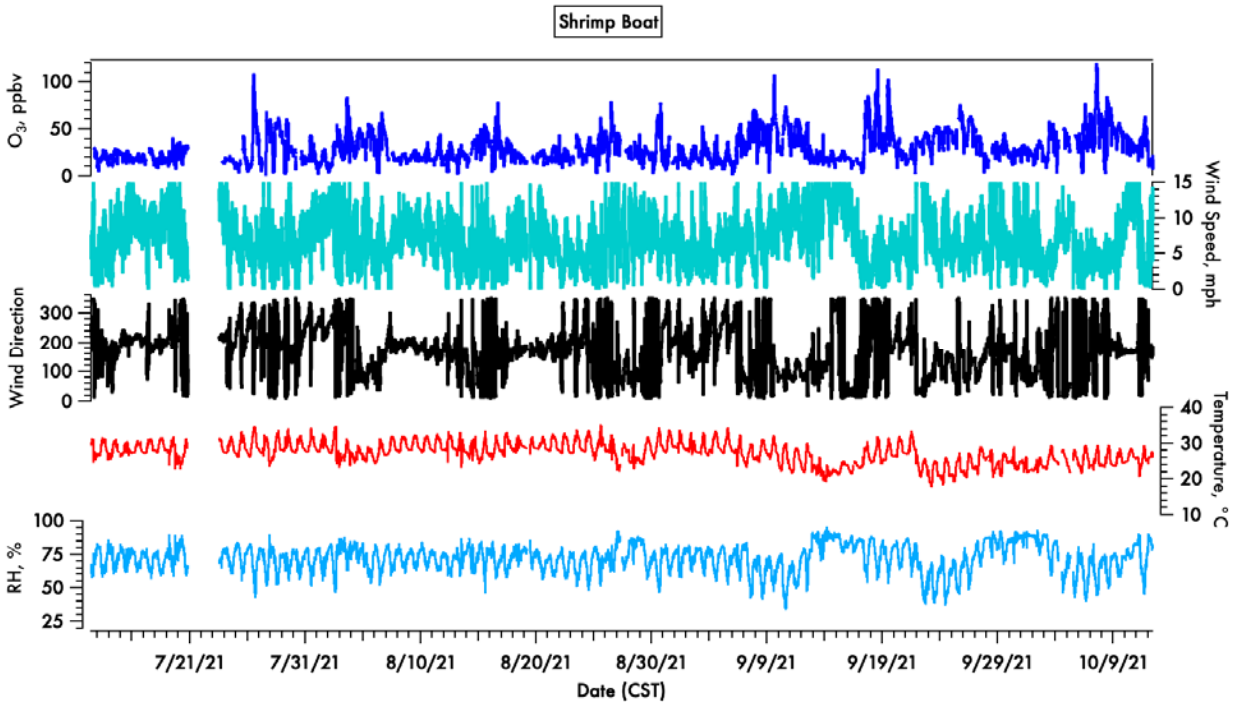

Figure 14. Ozone and Meteorological data collected on the Shrimp Boat operated by Larry Willis from July 12th - October 11th, 2021.

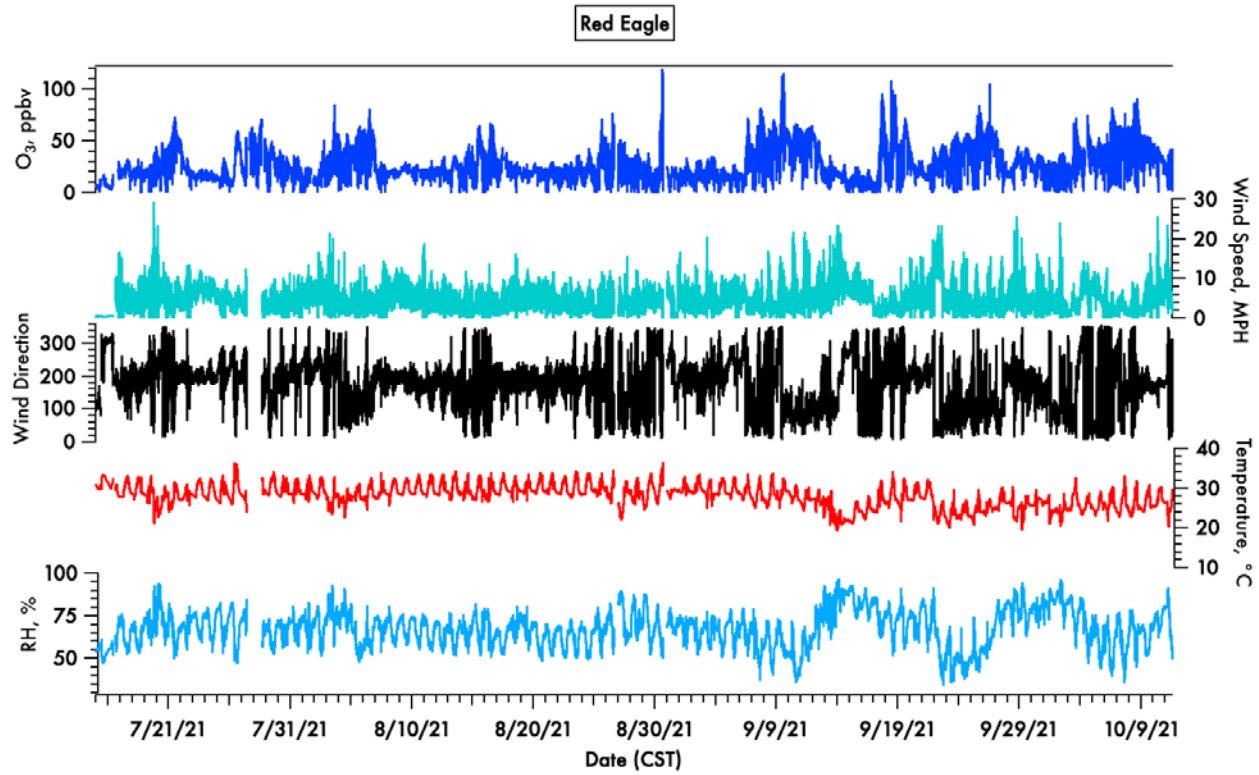

Figure 15. Ozone and Meteorological data collected on the Red Eagle operated by Ryan Marine from July 17th - October 11th, 2021.

The spatial plots of O_3 and NO_2 (UH pontoon boat only) for the UH pontoon boat, Shrimp Boat, and the M/V Red Eagle are shown in Figures 16-19. The UH pontoon boat was docked in Kemah, TX, labeled in Figure 16, on the West side of Galveston Bay. The primary operating areas were on the west side of the Houston ship channel. The Shrimp Boat was docked at Smith Point when not being operated in Galveston Bay. The M/V Red Eagle, which primarily operated in the Gulf of Mexico, was docked on the bayside of Galveston Island when not being operated. The Red Eagle regularly serviced both anchorage locations, approximately 10 miles offshore, as well as the lightering area approximately 30 miles offshore. During the sample period, the Red Eagle also traversed the Houston ship channel to service clients near the port of Houston on two occasions.

The spatial plot of ozone collected during the sample period from the UH pontoon boat is shown in Figure 16. The spatial plot shows an overlapping picture of spatial and temporal ranges. However, some trends were apparent, specifically that high ozone was more frequently observed over Galveston Bay west of the ship channel and north of Kemah, TX, although sampling bias is likely influencing this observation. These areas are nearest to emissions sources and most likely subject to recirculation processes associated with the bay/sea breeze and potentially less affected by penetration of the Gulf breeze.

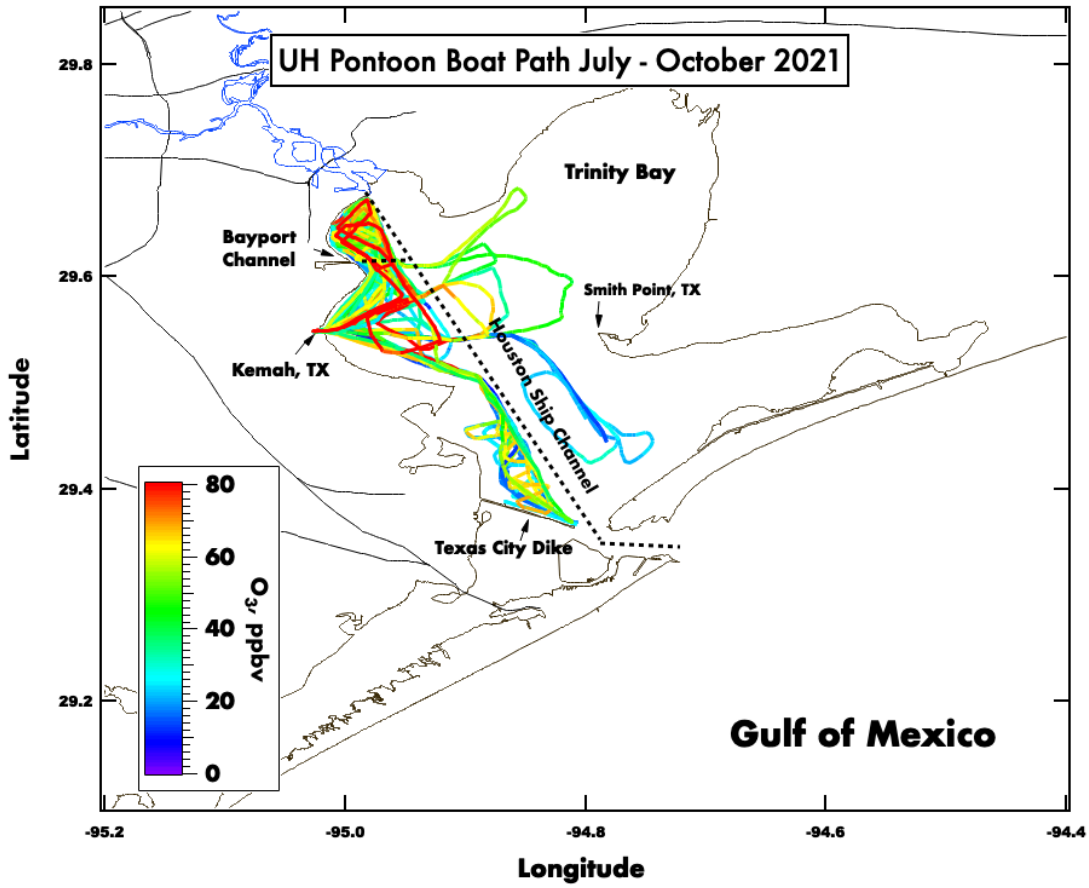

Figure 16. Spatial Map of ozone collected from July – October 2021 on the UH pontoon boat.

Regions of Galveston Bay near the Houston ship channel and nearest the urban and industrial emissions sources showed frequent spikes in NO_2, as shown in Figure 17. The sample period for NO_2 was considerably shorter (09/17/2021 - 10/24/2021) compared with the time period for the ozone data collection on the UH pontoon boat displayed in Figure 16.

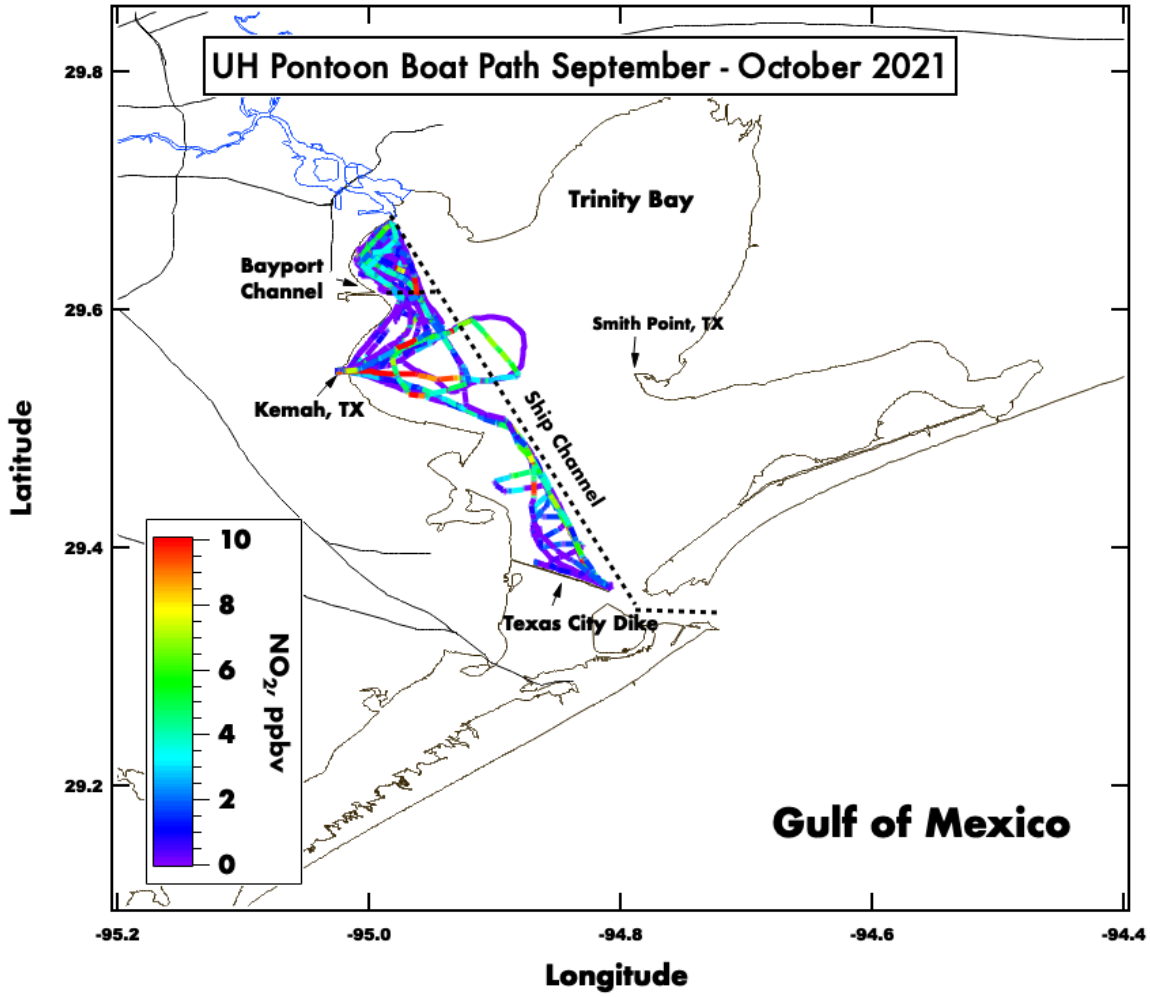

Figure 17. Spatial Map of NO_2 collected from September 17th – October 11th, 2021, on the UH pontoon boat.

The spatial overview for the shrimp boat, operated by Larry Willis out of Smith Point, is shown in Figure 18. The spatial plot shows less ozone variability in the coverage region, primarily around the Smith Point area on the East side of Galveston Bay. The shrimp boat operated less frequently than the Red Eagle or UH pontoon boat. Unfortunately, the shrimp boat did not operate out on the Bay during the majority of the high ozone episodes, staying at the dock at Smith Point.

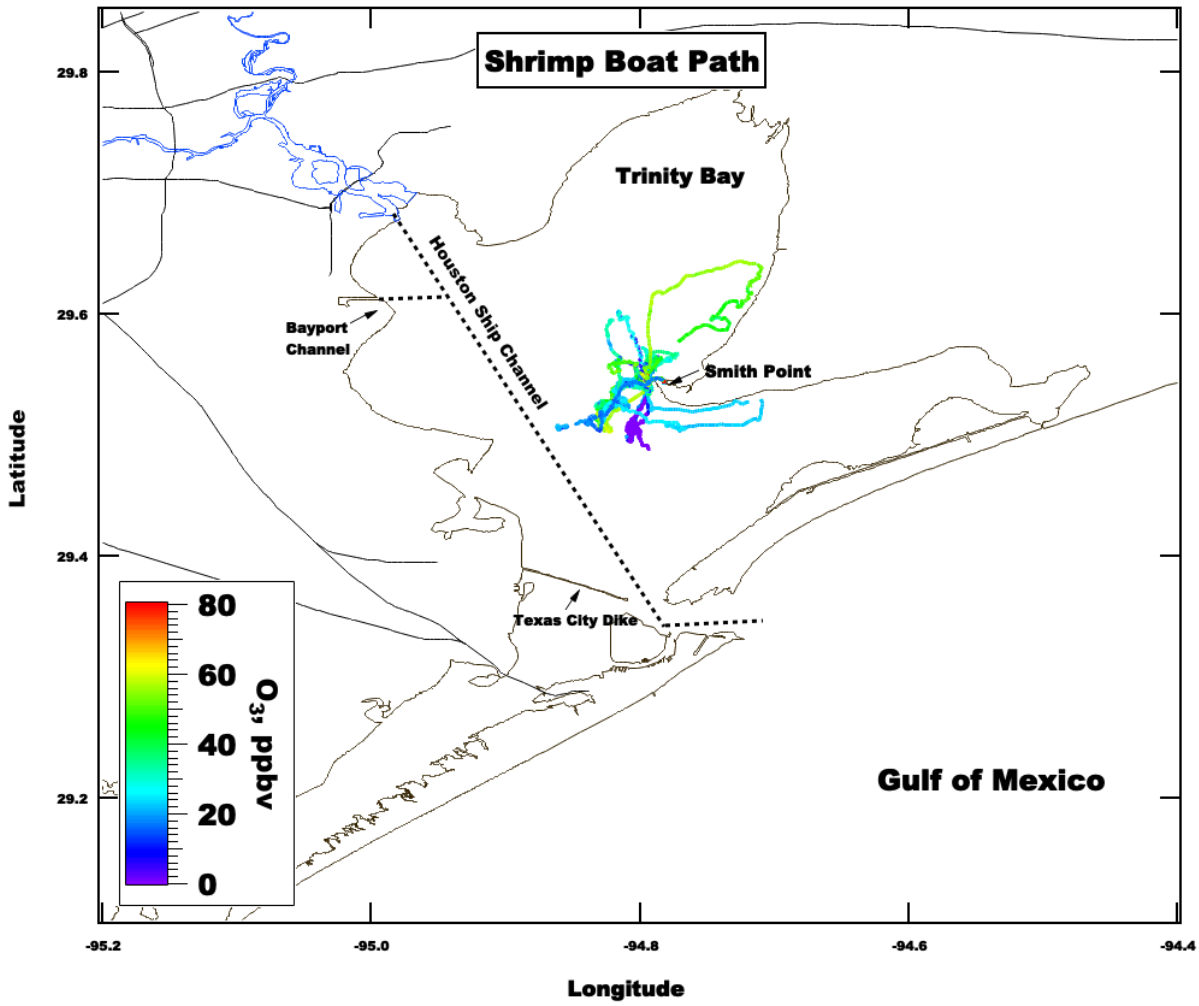

Figure 18. Spatial Map of ozone collected from July 12th – October 11th, 2021, on the Shrimp Boat operated by Larry Willis.

The M/V Red Eagle operated primarily in the offshore waters of the Gulf of Mexico, servicing large commercial vessels in the anchorage and lightering areas. The Red Eagle operated at any time of day or night and in most weather conditions. The wide spatial and temporal variability of ozone observed offshore, as seen in Figure 19, is an interesting feature. The highest ozone observed offshore was on September 9th, 2021, with concentrations exceeding 110 ppbv. The high ozone observations typically occurred in the post-frontal environment with a flow reversal from onshore (southerly) to offshore (northerly).

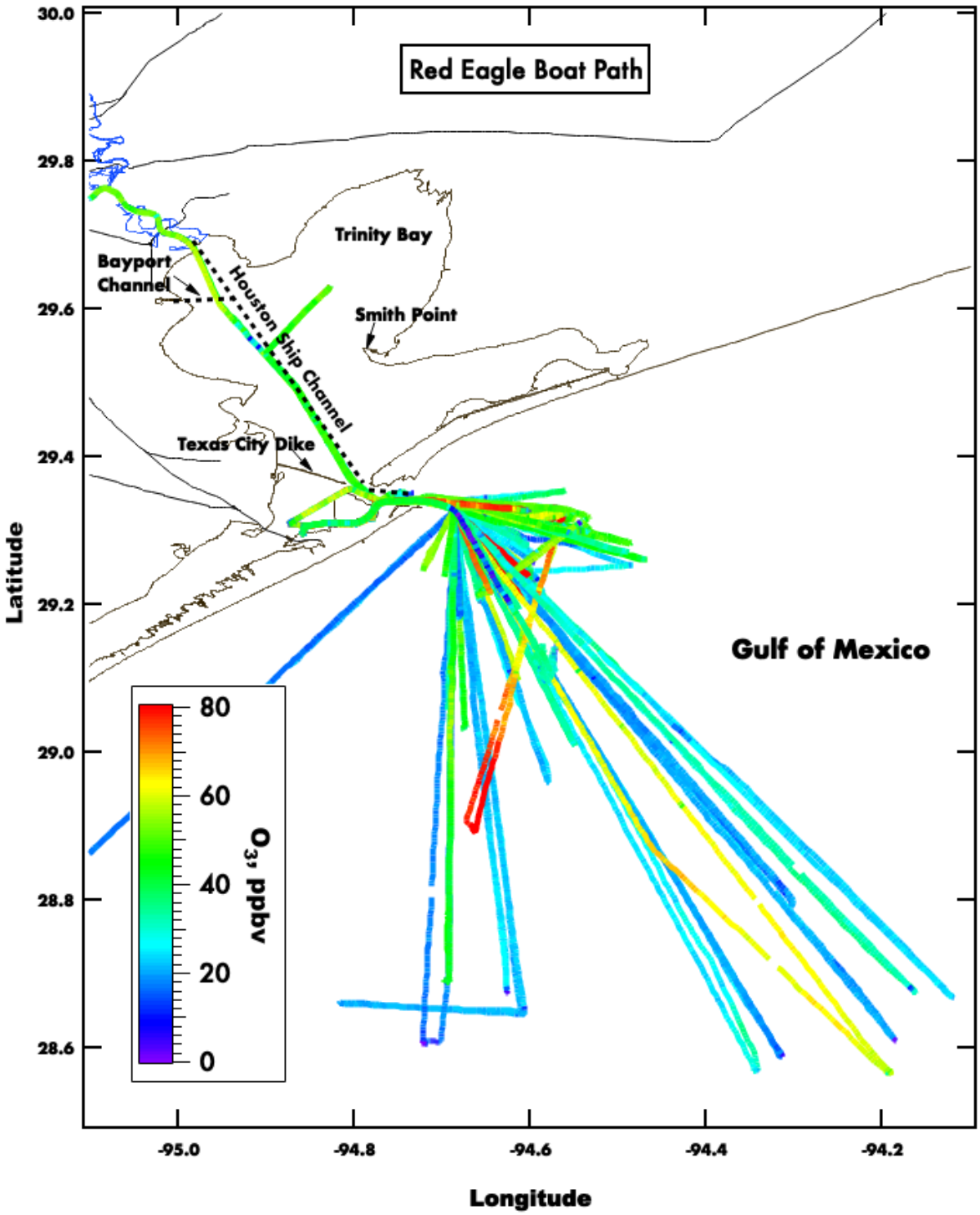

Figure 19. Spatial Map of ozone collected from July 17th – October 11th, 2021, on the Red Eagle operated by Ryan Marine.

6.1.3 Is O3 consistently elevated over water relative to over land, or is there a spatial variability in O3 over water?

Figure 20 shows that modeled daily ozone concentrations over land are slightly lower than those over waters. The land-to-water gradient is different depending on the time of day. Daytime mean ozone follows the descending land-to-water gradient with ozone concentrations of 60 ppbv, 55 ppbv, and 53 ppbv at urban Houston, Galveston Bay, and the Gulf of Mexico, respectively. This is reasonable considering descending land-to-water gradient of temperature and PBL, but ascending land-to-water gradient of humidity, as shown in Figure 20. Higher temperature enhances ozone mainly through increased biogenic emissions and higher abundance of NOx, while lower humidity reduces the chemical loss rate of ozone (Jacob and Winner, 2009), both of which could lead to a cascade of meteorological feedbacks onto ozone concentration itself (Liu et al., 2021; Wang et al., 2020; Sadiq et al., 2017). On the other hand, the model's trend of nighttime ozone is estimated to the reverse of the daytime model estimates, with an ascending land-to-water nighttime gradient with ozone concentrations of 35 ppbv, 48 ppbv, and 49 ppbv at urban Houston, Galveston Bay, and the Gulf of Mexico, respectively.

Vertically, ozone profiles over land are steeper than those over offshore waters, as shown in Figure 11. Ozone profiles over urban Houston (R = 0.23) and Galveston Bay (R = 0.88) are better captured than those over La Porte (R = –0.43) and the Gulf (R = –0.16). At La Porte, ozone overestimation between 0–2 km may be caused by an overestimation of surface NOx emissions near the Shipping Channel. At the Gulf, ozone is overestimated between 0–2 km but underestimated between 2–4 km, which may suggest too strong downmixing of ozone aloft in the model. Wind speed underestimations at the Gulf, causing less ventilation and dispersion of air pollutants, may be part of the reason for the ozone overestimation between 0–2 km in the Gulf. Meteorological variables including temperature (R = 1), relative humidity (R = 0.93–0.99), and wind speed (R = 0.51–0.97) are generally well captured by the model. Yet, the Gulf shows the poorest performance among the four regions, indicating the current model physics schemes that have good performances over land may not work well over offshore waters.

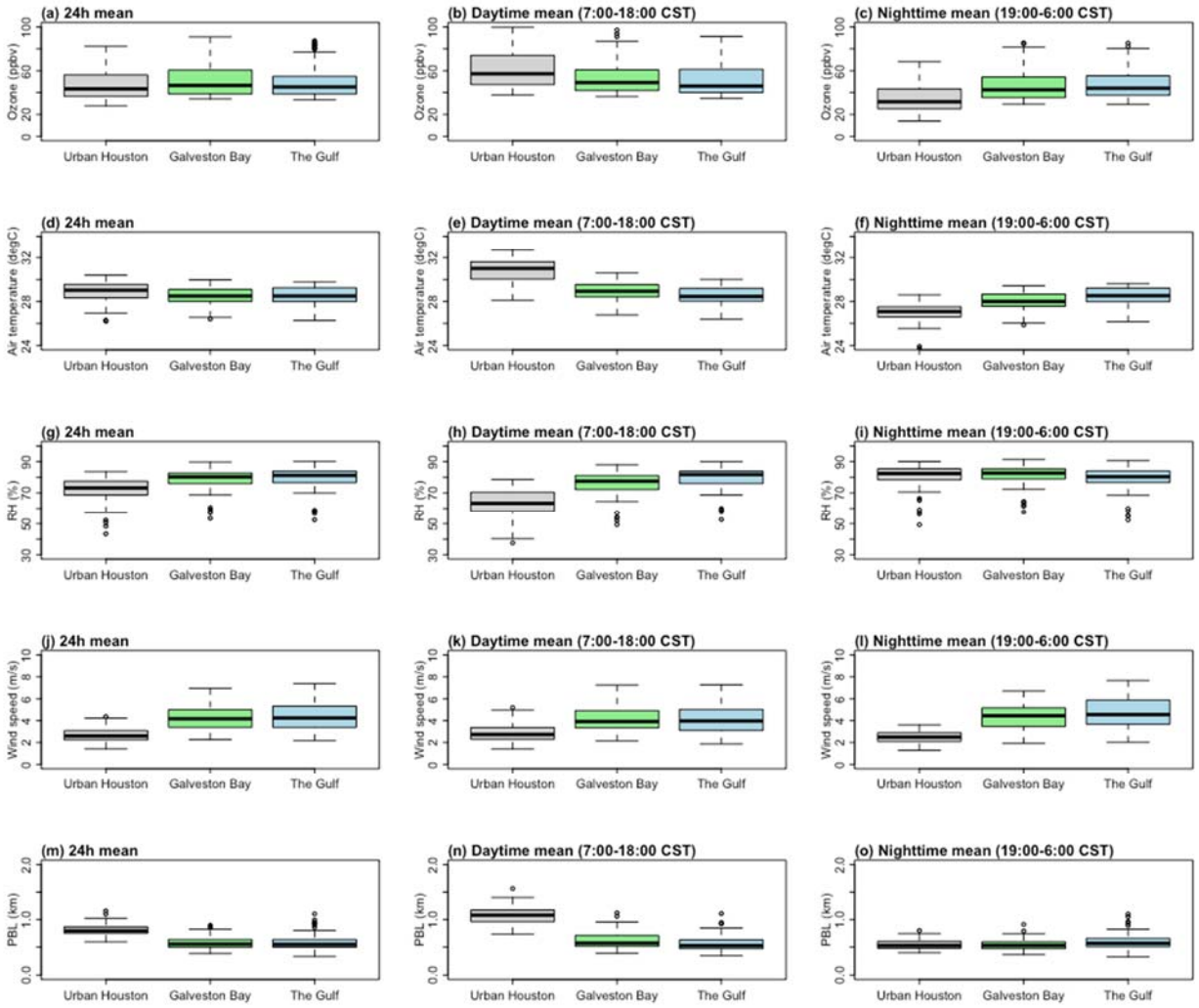

Figure 20. Land-water gradient of ozone, temperature, relative humidity, wind speed and planetary boundary layer height. Left, middle, and right columns show daily mean, daytime mean, and nighttime mean, respectively. Urban Houston, Galveston Bay, and the Gulf of Mexico are defined by black boxes in Figure 6a.

Table 5. Contains the UH Pontoon outing dates, Bay sector, 1-minute O_3 average, standard deviation, maximum, minimum, in parts per billion (ppb), and modeled ozone level. The color coding represents the ozone levels from 1) boat-measured observations, 2) WRF-GC model estimates, and 3) TCEQ air quality forecast for the Houston area with green, yellow and orange representing 'low', 'moderate', and 'high' ozone levels respectively. For measured and modeled ozone levels, high ozone days are defined as days with maximum hourly ozone exceeding 70 ppbv. Moderate ozone days are defined as days with maximum hourly ozone exceeding 40 but not 70 ppbv. Low ozone days are defined as days with all hourly ozone below 40 ppbv. For TCEQ forecast, air quality index (AQI) color coding is adopted where high, moderate, and low levels are defined as 8-hour ozone exceeding 70 ppbv, exceeding 55 but not 70 ppbv, and below 55 ppbv, respectively.

Outing Date	Section of Bay	Mean	SD.	Max.	Min.	Measured ozone level	Modeled ozone level	TCEQ Forecast ozone level
07-13-2021	SE	21.5	3.8	32.8	6.4	Low	Moderate	Moderate
07-14-2021	W/NW	22.4	6.6	39.8	4.1	Low	Moderate	Low
07-18-2021	SW	20.5	3.5	27.5	8.3	Low	Moderate	Low
07-21-2021	NW	51.1	12.9	68.9	18.0	Moderate	High	High
07-22-2021	NW	24.4	3.6	30.6	10.0	Low	High	High
07-26-2021	SW -> NW	49.4	33.6	107.5	4.5	High	High	High
07-27-2021	E/SE	24.8	12.7	52.8	7.2	Moderate	High	High
07-28-2021	N/NW	49.2	9.2	69.8	25.1	Moderate	High	High
08-04-2021	NW	31.6	3.5	39.8	22.4	Low	High	High
08-12-2021	SE	21.4	5.0	32.3	7.0	Low	Moderate	Moderate
08-16-2021	N/NW	44.2	13.5	65.5	11.0	Moderate	High	Moderate
08-24-2021	NW	39.6	2.5	43.6	28.0	Moderate	High	Moderate
08-25-2021	NW	42.5	8.5	71.9	19.0	Moderate	High	High
09-01-2021	NW	22.9	6.8	34.6	5.1	Low	Moderate	Moderate
09-03-2021	NW/W	29.6	3.7	36.1	21.8	Low	Moderate	Moderate
09-07-2021	NW	57.6	5.3	69.1	36.4	Moderate	High	High
09-08-2021	SW -> NW	61.7	9.7	75.5	24.8	High	High	High
09-09-2021	SW -> NW	61.3	5.6	67.9	31.0	High	High	High
09-17-2021	NW/W	79.6	13.0	104.3	44.5	High		Moderate
09-20-2021	NW	33.6	6.8	55.4	20.3	Moderate		Low
09-21-2021	SW -> NW	23.5	7.2	43.0	10.8	Low		Moderate
09-25-2021	NW -> SW	57.0	9.3	71.6	18.0	Moderate		High
09-26-2021	NW	55.7	9.4	68.8	26.4	Moderate		High
10-06-2021	SW -> NW	57.7	17.6	93.7	24.9	High		High
10-07-2021	NW/W	93.1	21.4	134.8	33.3	High		High

A summary of the UH pontoon ozone observations while operating in a mobile capacity on Galveston Bay is shown in Table 5. Because of the large temporal variation associated with this dataset, it is challenging to compare spatial variability from outing to outing. However, looking at the standard deviation values of the outings does show there can be considerable spatial variability during an outing. The minimum ozone values can sometimes be impacted by titration effects when intercepting large ship emissions plumes, but the standard deviation value should be low if the ozone is relatively constant. 'High' ozone days, as classified in Table 5, generally showed higher standard deviations throughout the study period. The highest standard deviation of 33.6 ppb was observed during an outing on July 26th, 2021. This day is discussed in further detail in Section 6.3 and was characterized by a bay breeze recirculation resulting in considerable heterogeneity of ozone across Galveston Bay as seen in Figure 36.

6.2 Results Question 2: O_3 Vs. Ox

6.2.1 How does O_3 and O_X over water compare with O_3 and O_X over adjacent land?

The addition of a UV photocell into the mobile platforms was delayed due to manufacturing issues and ultimately unable to be installed into the instrument packages on the commercial boats in the project's timeline. After traditional photocell replacement lamps arrived (delayed due to supply chain issues), a blue light converter was installed into the UH pontoon boat while the boat was removed from the water for Hurricane Nicholas. The UH pontoon boat measured Ox upon redeployment on September 17th until the end of the observation period, October 25th, 2021.

A comparison of the three mobile boat platforms with the nearest TCEQ continuous air monitoring stations (CAMS) is shown in the following figures. Comparison between stationary ozone and mobile platforms generally shows good agreement. The comparison of the calculated NO_2 derived from the Ox measurement shows considerably more variability.

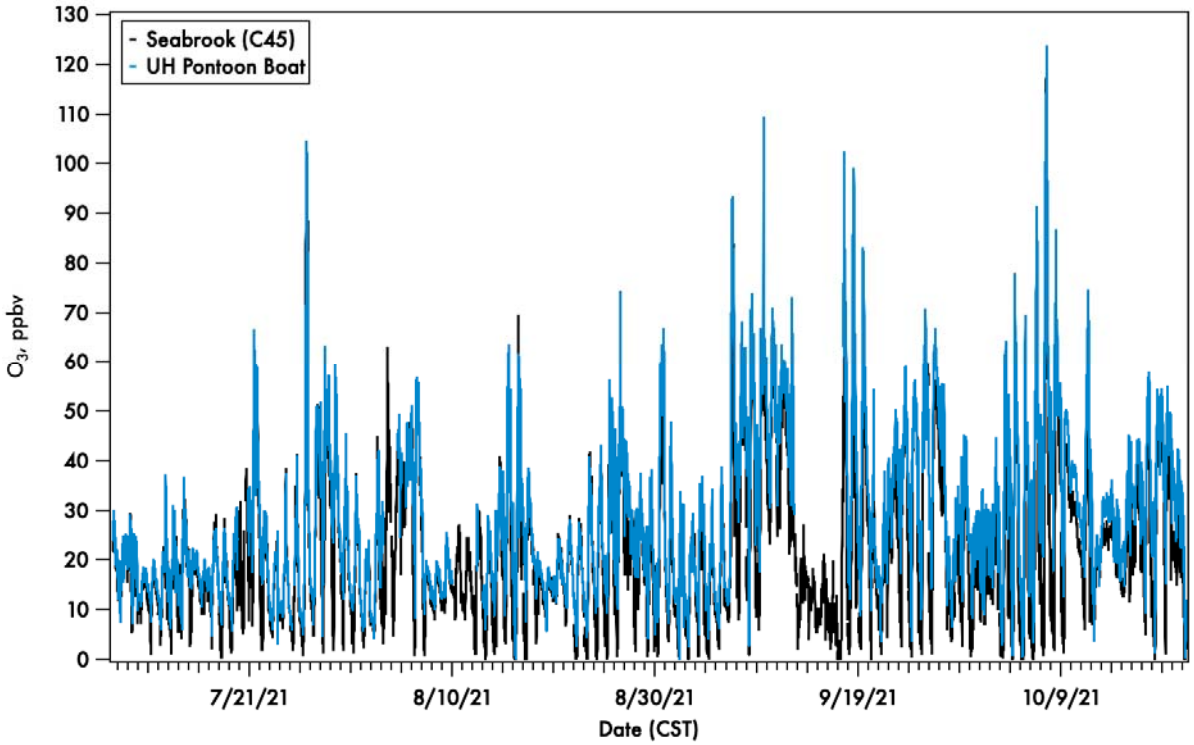

Figure 21. Time-series of 5-minute averaged ozone (O_3) concentration from the UH pontoon boat mobile monitor and the nearest TCEQ monitor, Seabrook (C45). Measurements are from July 7th, – October 21st, 2021.

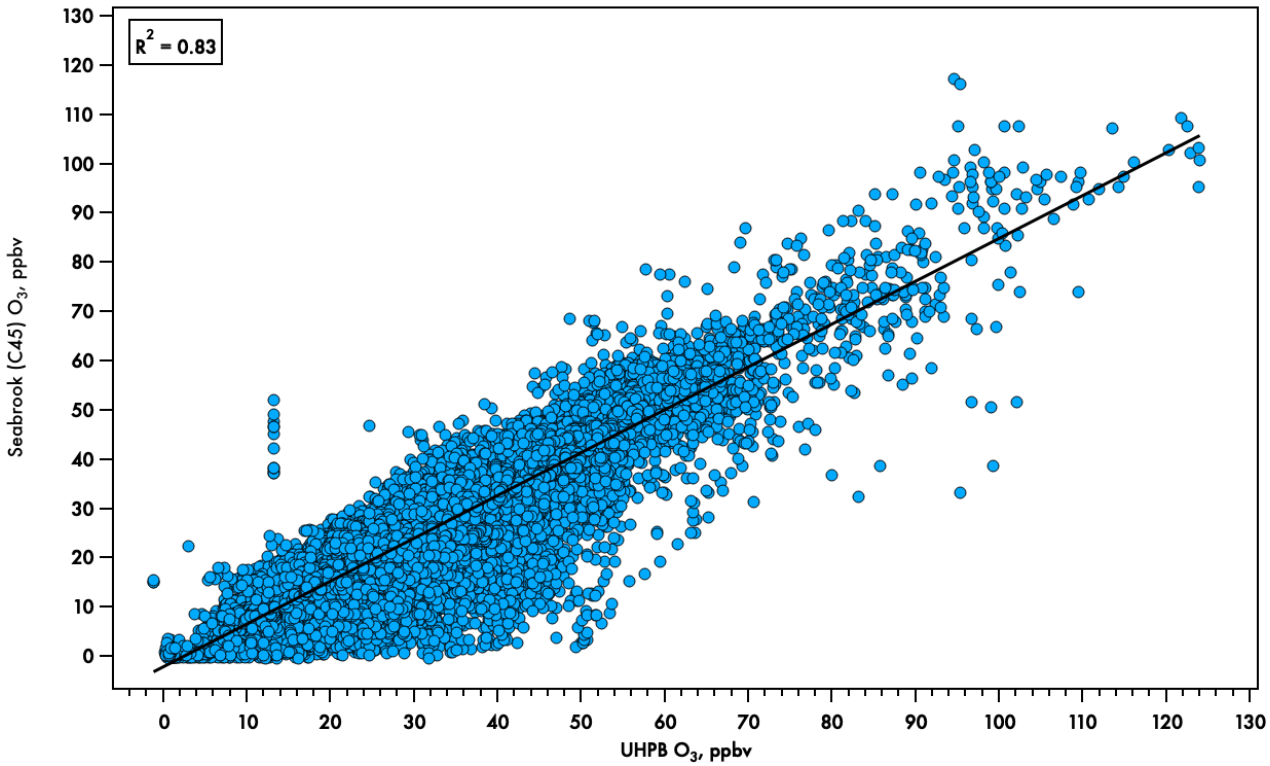

Figure 22. Scatter plot of 5-minute averaged ozone (O_3) concentration from the UH pontoon boat mobile monitor and the nearest TCEQ monitor, Seabrook (C45). Measurements are from July 7th, – October 21st, 2021.

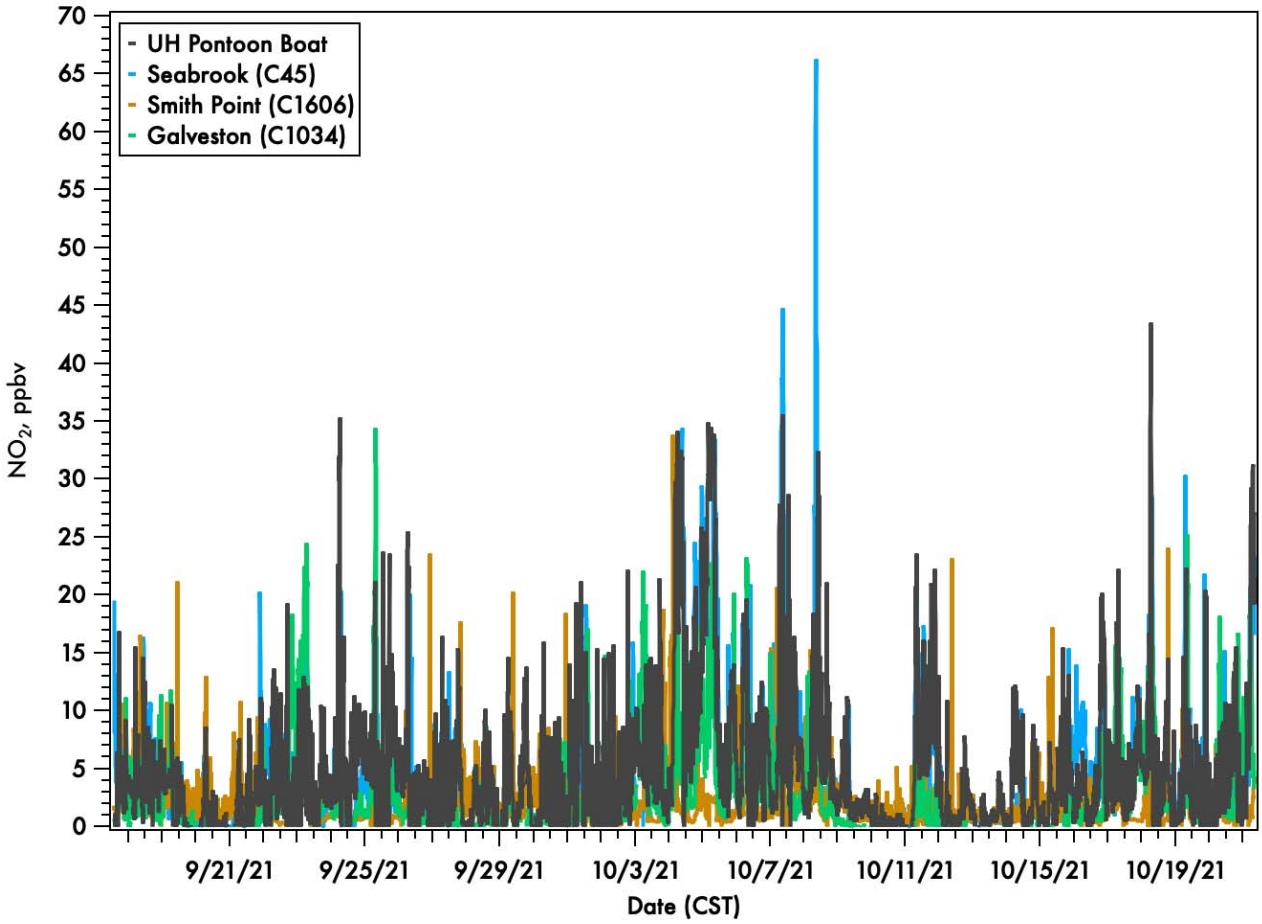

Figure 23. Time series of 5-minute averaged nitrogen dioxide (NO_2) concentration from the UH Pontoon boat mobile monitor and other stationary monitors around Galveston Bay.

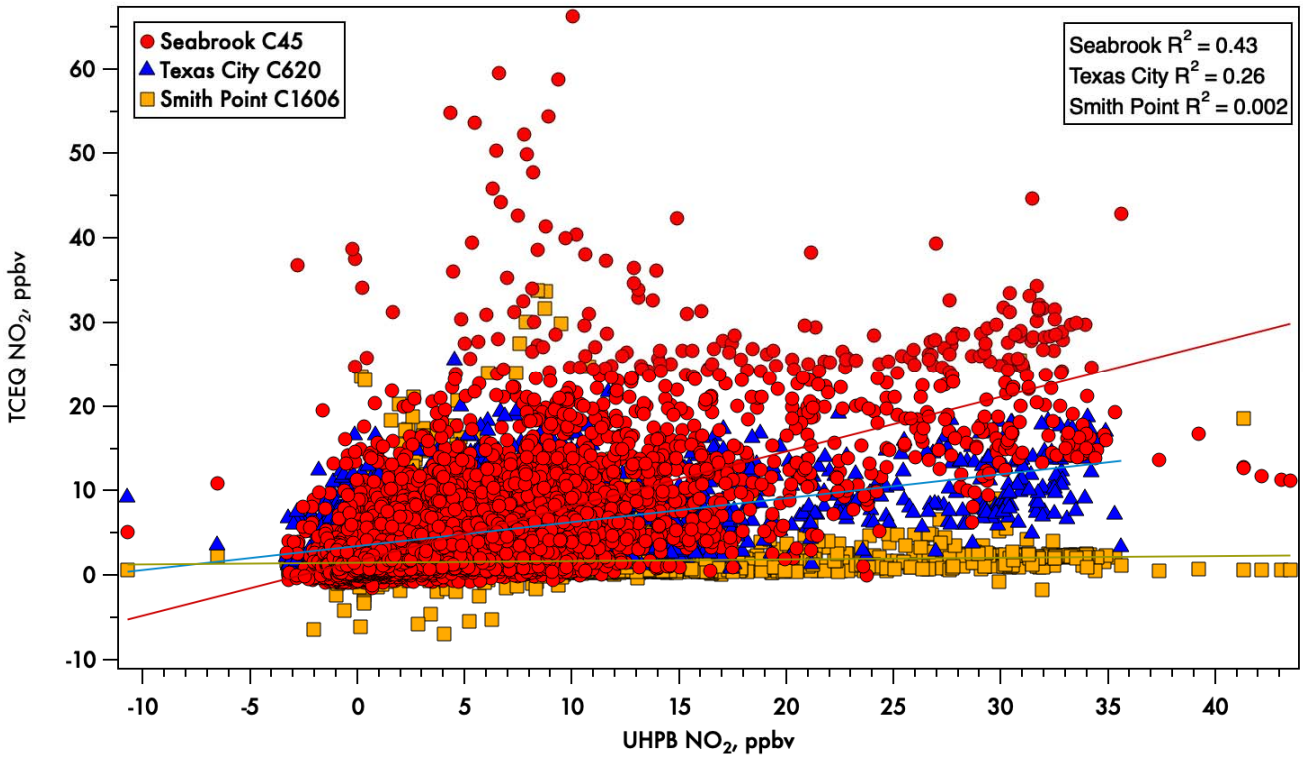

Figure 24. Scatter plot of 5-minute averaged nitrogen dioxide (NO_2) concentration from the UH Pontoon boat mobile monitor and other stationary monitors around Galveston Bay.

Comparisons between the UH Pontoon boats calculated NO_2 with the stationary NO_2 monitors around Galveston Bay are shown in Figure 24. Generally, the closest TCEQ monitor to the UH pontoon boat was the Seabrook (C45) monitor, which also showed the closest agreement (r^2 = 0.43) to the UH pontoon boat. The Texas City (C620) monitor located near-shore on the SW side of the Bay showed some agreement with the UH Pontoon boat (r^2 = 0.26), but significantly less than the closer Seabrook monitor. The Smith Point (C1606) monitor located on the East side of Galveston Bay showed no agreement (r^2 = 0.00) with the UH pontoon boat. This comparison indicates the significant spatial variability of NO_2 across Galveston Bay.

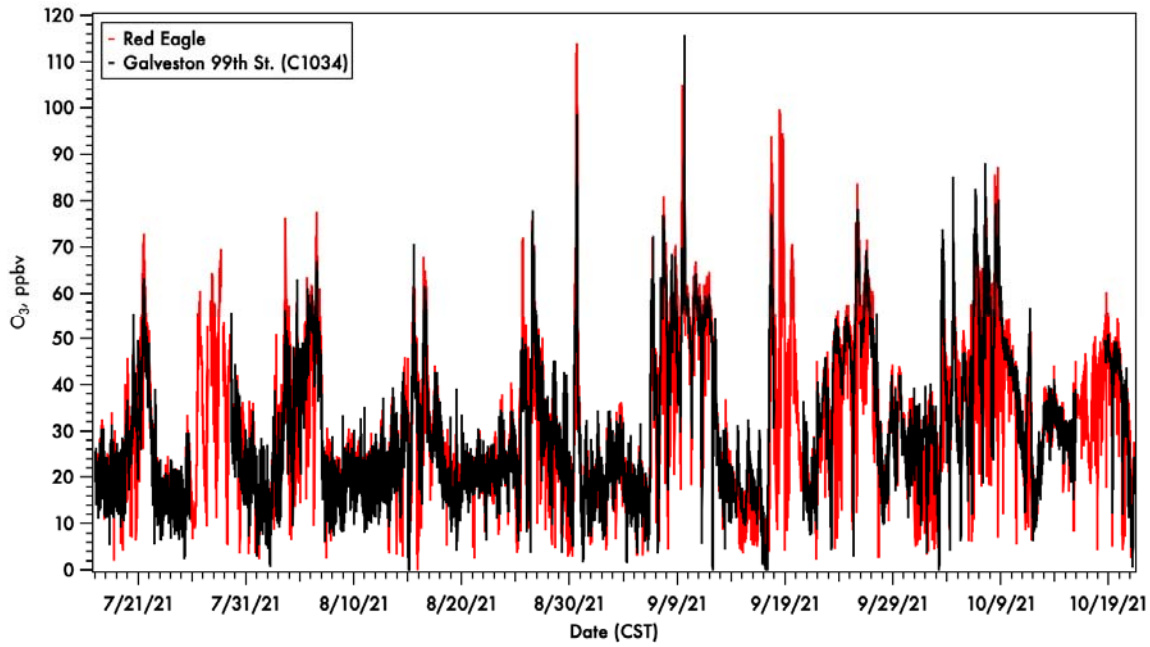

Figure 25. Time series of 5-minute averaged ozone concentration from the Red Eagle mobile monitor and the nearest TCEQ monitor, Galveston 99th St (C1034). Measurements are from July 17th – October 21st, 2021.

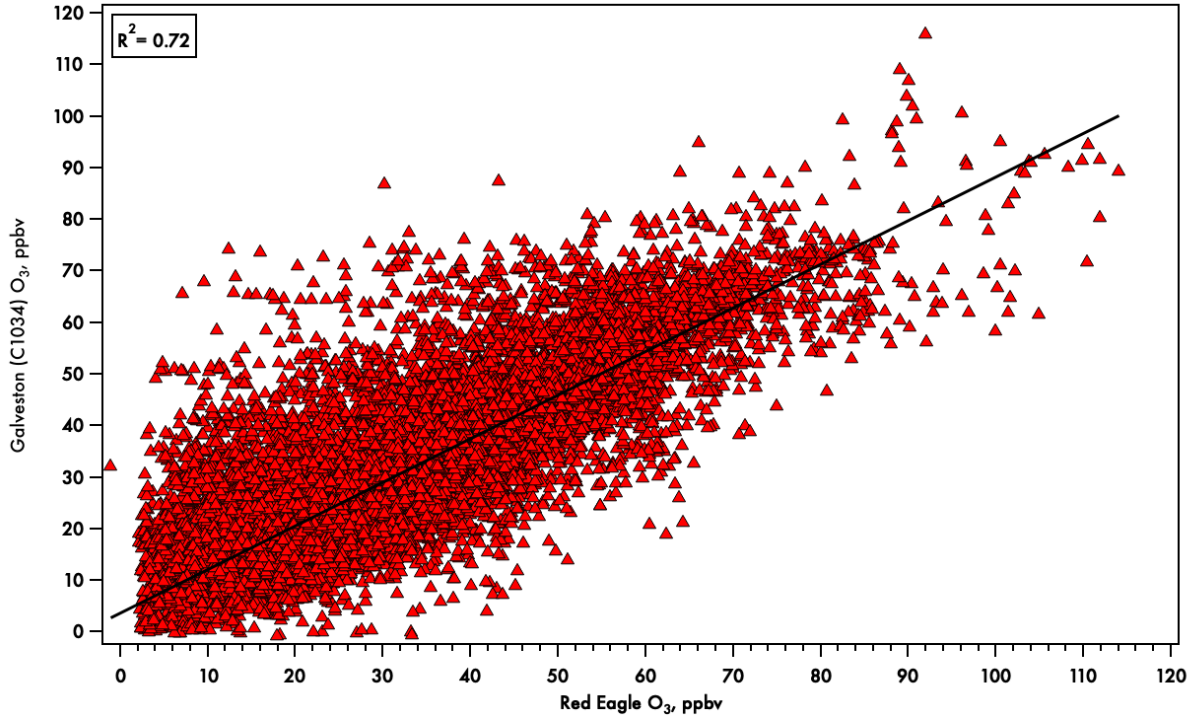

Figure 26. Scatter plot of 5-minute averaged ozone (O_3) concentration from the Red Eagle mobile monitor and the nearest TCEQ monitor, Galveston (C1034). Measurements are from July 7th, – October 21st, 2021.

The Red Eagle boat operating out of Galveston, TX, showed the weakest agreement between the nearest TCEQ monitor, Galveston 99th St. (C1034), as seen in Figure 26. In this case, the variability between the two monitors is likely exacerbated due to the locations of the monitors. The TCEQ monitor (C1034) is located on the Gulf side of Galveston Island and is not as likely to be impacted by titration due to local emissions. The Red Eagle, when at dock, is located on the Bay side of Galveston Island in a harbor that sees frequent ship traffic and is located adjacent to a moderately trafficked road (Harborside Dr.). Additionally, when maneuvering alongside the larger vessels that they service, the captain is not always able to position the Red Eagle in such a way as to avoid sampling the exhaust of the Red Eagle or other ships.

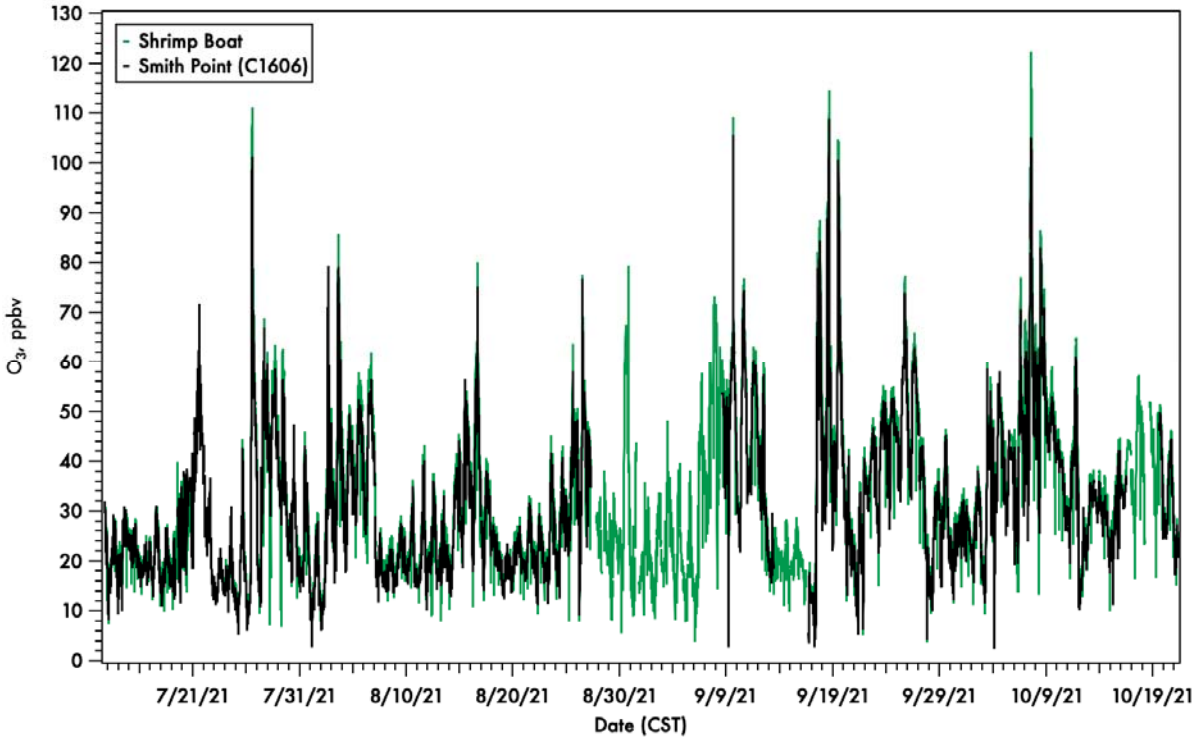

Figure 27. Time series of 5-minute averaged ozone concentration from the shrimp boat mobile monitor and the nearest TCEQ monitor, Smith Point (C1606). Measurements are from July 12th – October 24th, 2021.

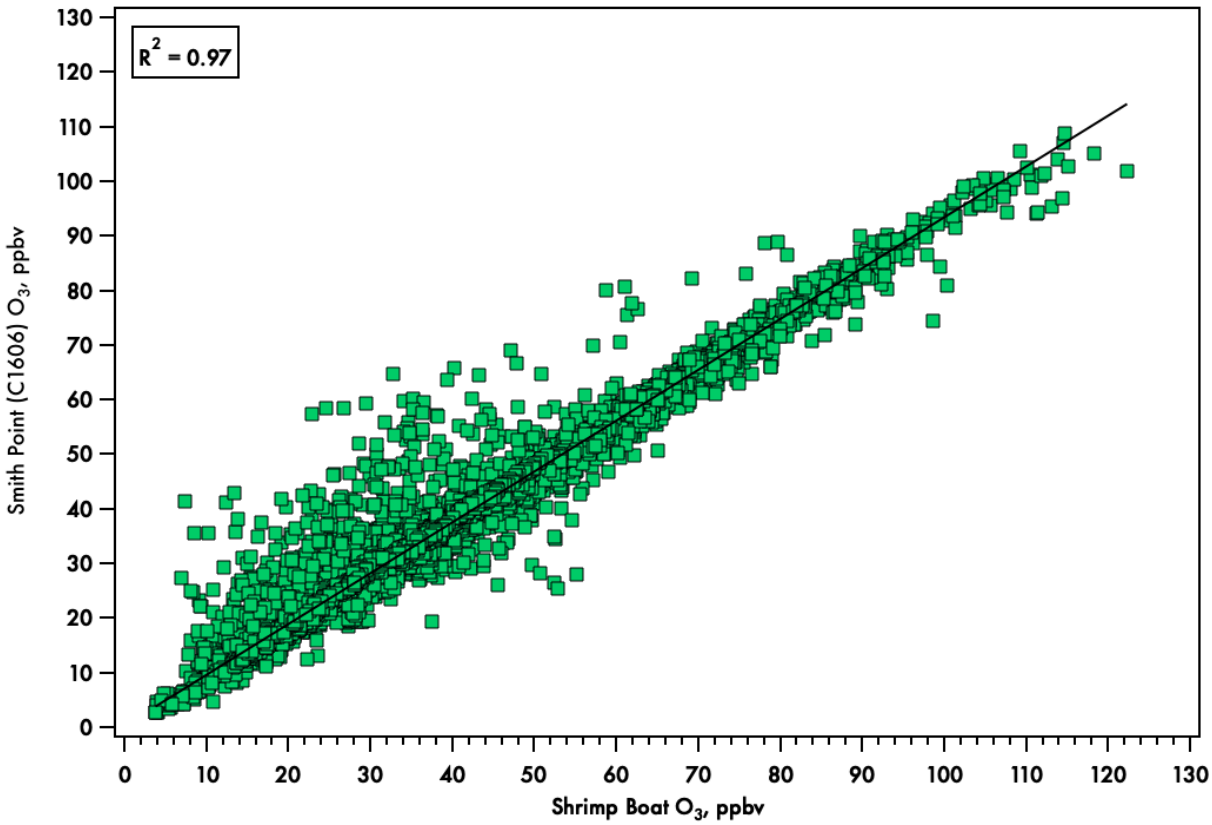

Figure 28. Scatter plot of 5-minute averaged ozone concentration from the shrimp boat mobile monitor and the nearest TCEQ monitor, Smith Point (C1606). Measurements are from July 12th – October 24th, 2021.

The closest agreement between measuring sites was between the Smith Point monitor (C1606) and the Shrimp Boat mobile platform (Figure 28). These two locations were approximately 230m apart when the shrimp boat was at dock. The shrimp boat also operated on a mobile basis the least frequently, due to a variety of reasons including poor shrimping due to the influence of fresh water from local rains and COVID-related recovery time. When the shrimp boat was operating, it also had the smallest spatial coverage of the three platforms, as seen in Figure 18. The strong correlation between these two measurements indicates that the C1606 monitor is representative of the O_3 conditions of the nearby Bay waters.

6.2.2 Are there indications that O_3 is higher over water due to a lack of titration from point and mobile sources?

While the interpretation of the Shrimp Boat and C1606 data seem to indicate relative homogeneity, at least over the area and limited frequency of the boat operations, there do appear to be some indications that over water O_3 may be higher than onshore measurements on the

western side of Galveston Bay. The comparison of the pontoon boat ozone data against observations from Seabrook C45 shows that the pontoon regularly observed slightly higher O_3 than at C45 even though the two sites are only 4 km apart and C45 is approximately 1.2 km inland from the Bay. While the slope of the correlation between the two monitors is ~0.95 (Figure 22) could be explained by slight differences in calibration, the scatter plot also shows that often the pontoon data (x-axis) could read as high as 50 ppbv while C45 was in the low single digit values. This is often a sign of local titration effects at night. An example of this is shown in the time series below (Figure 29); just after midnight on September 8th the pontoon boat was near 50 ppbv while C45 reported 30 ppbv, with the lower value at C45 likely due to local titration. While not as dramatic, the pontoon data consistently tracks higher than C45 during this period. However, the difference can be quite small, as seen around noon on September 10th. Additional measurements and modeling efforts already in the planning stages may help to further address this question in 2022. An additional feature in this time-series that is of note is the large spike of O_3 seen at the UH pontoon boat on September 9th but not seen at the C45 monitor. This day is discussed in further detail in Section 6.3.1.2, but the feature appears in part related to a bay breeze as identified by the KHGX radar (Figure 48).

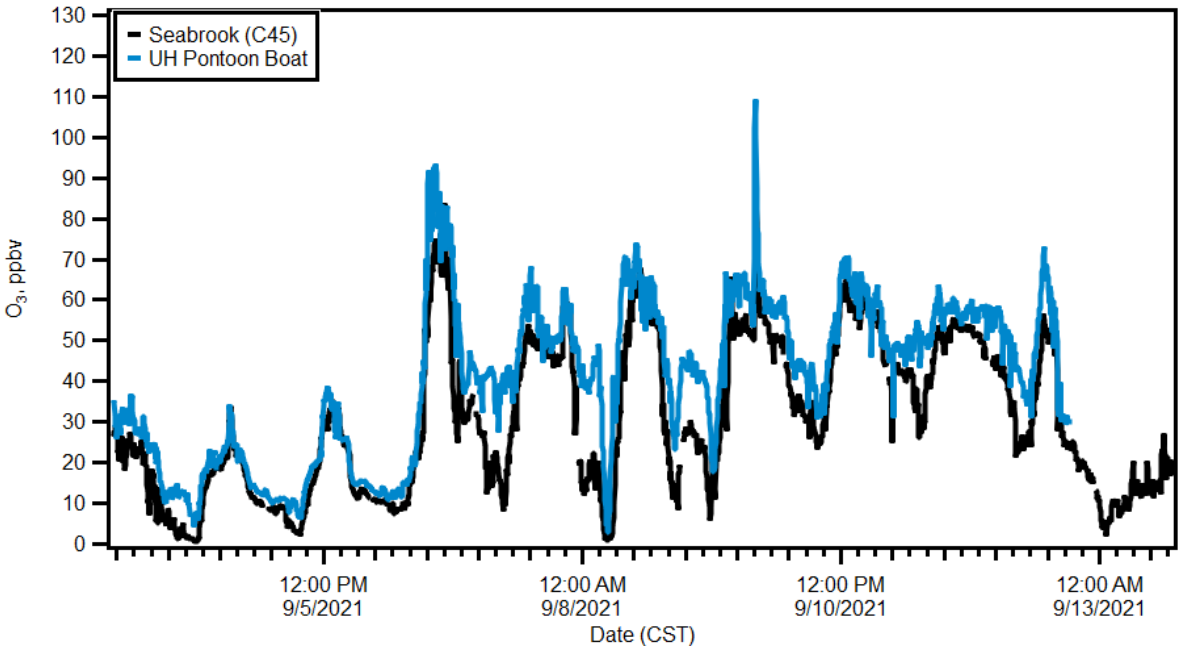

Figure 29. Time-series showing the UH Pontoon boat being consistently elevated relative to the Seabrook (C45) monitor

Although there are fewer mobile sources on the water than land, exhaust plumes from large ships were still encountered, mainly when operating the UH pontoon boat on Galveston Bay near the Houston Ship Channel. A clear example of one such plume is shown in Figure 30. This observation was made while the UH Pontoon boat was anchored in north Galveston Bay (Figure 31) in preparation for an ozonesonde launch. While at anchor, the UH science team on the pontoon boat smelled the distinctive smell of a ship exhaust from a passing ship, seen in Figure

31. Although this was prior to the addition of the NO_2 photocell, an approximately 50 ppbv titration of O_3 is a clear indicator of the ship plume.

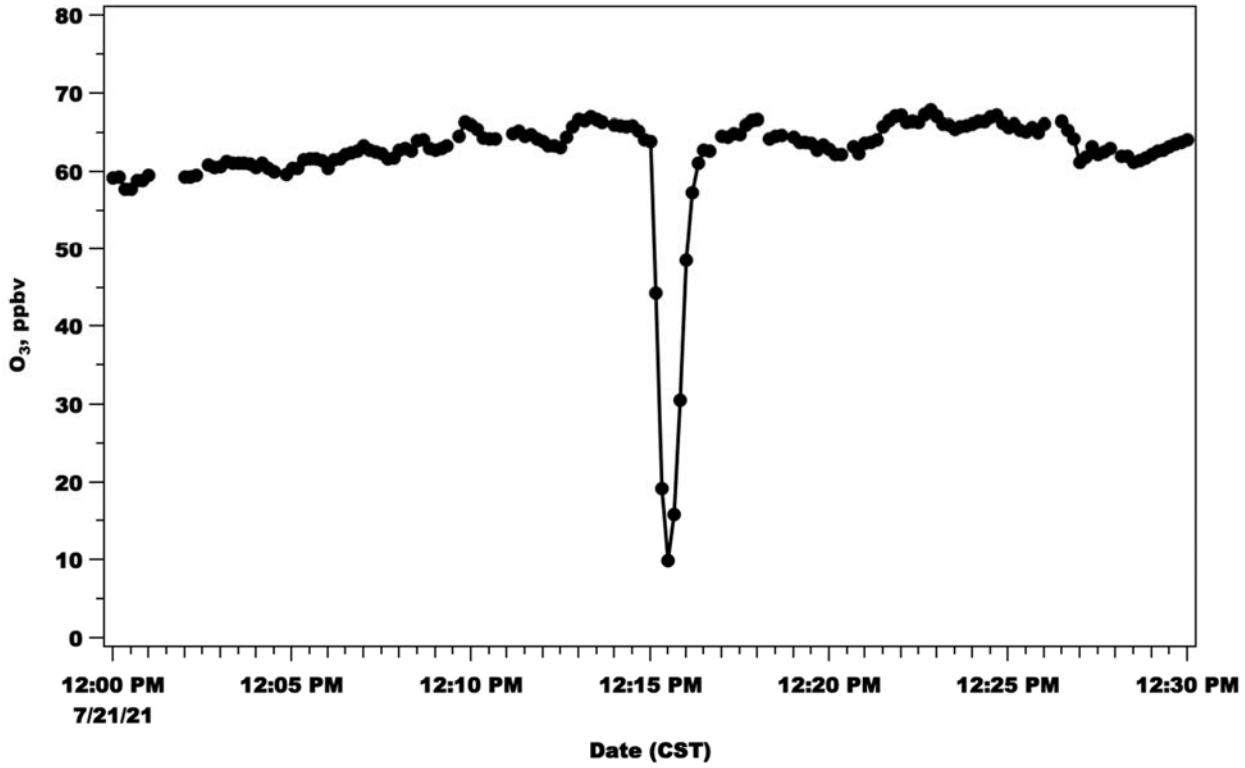

Figure 30. 10-second averaged ozone concentration while downwind of a ship emission plume.

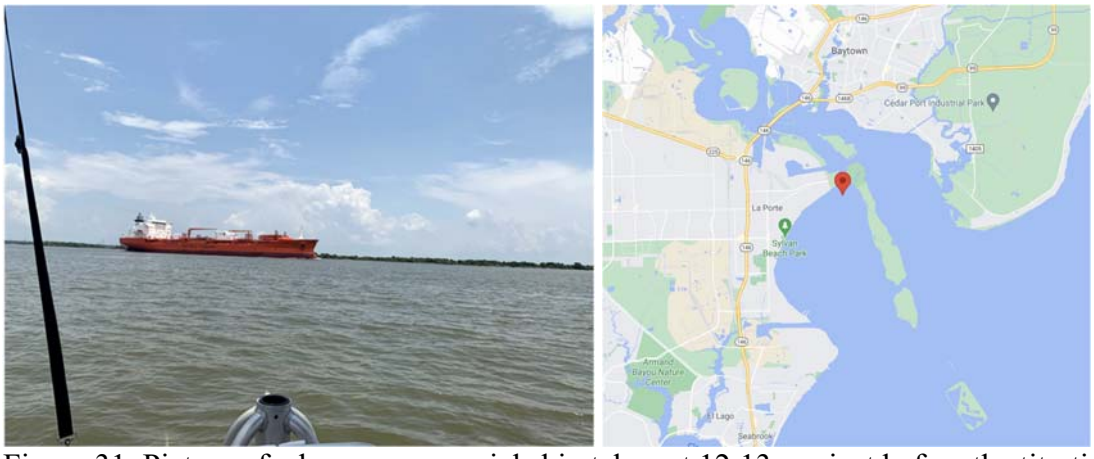

Figure 31. Picture of a large commercial ship taken at 12:13pm, just before the titration dip observed on the UH pontoon boat (left) and a map showing the location of the measurement as shown by the red pin in the map on the right.

6.2.3 Are the offshore O_3 values consistent with the findings from previous studies, including the coastal measurements at San Luis Pass in 2016 (Tuite et al., 2018)?

A day with low ozone was targeted for an ozonesonde launch to assess the vertical depth of low ozone for comparison of previous work done (Tuite et al., 2018) on the Texas coast near Galveston, TX. In 2016 a TCEQ study with UH, UCLA, and Environ (now Ramboll) to determine whether proposed halogen chemistry resulting from interactions with the ocean surface could be responsible for the observations of low O_3 reaching the Texas Gulf Coast during periods of onshore flow. The project found that there was evidence that halogen species were present in the onshore flow when O_3 values were low. Further, when binning the backward wind trajectories by the observed O_3 levels at the coast, the trajectories tended to show that the more time spent over water, the lower the O_3 readings were at the Texas coast (Figure 32). Iodine underestimation by the WRF-GC model could be one of the reasons for modeled ozone overestimation in comparison to the observations taken in this project. Iodine species emitted from the ocean surface photolyze and cycle between an I atom and IO, continuously destroying ozone catalytically (Tuite et al., 2018). The iodine species, including I and IO, are estimated to be a factor of 10 lower than measurements in Tuite et al. (2018), which could be one of the reasons for ozone overestimation over the Gulf in Figure 7.

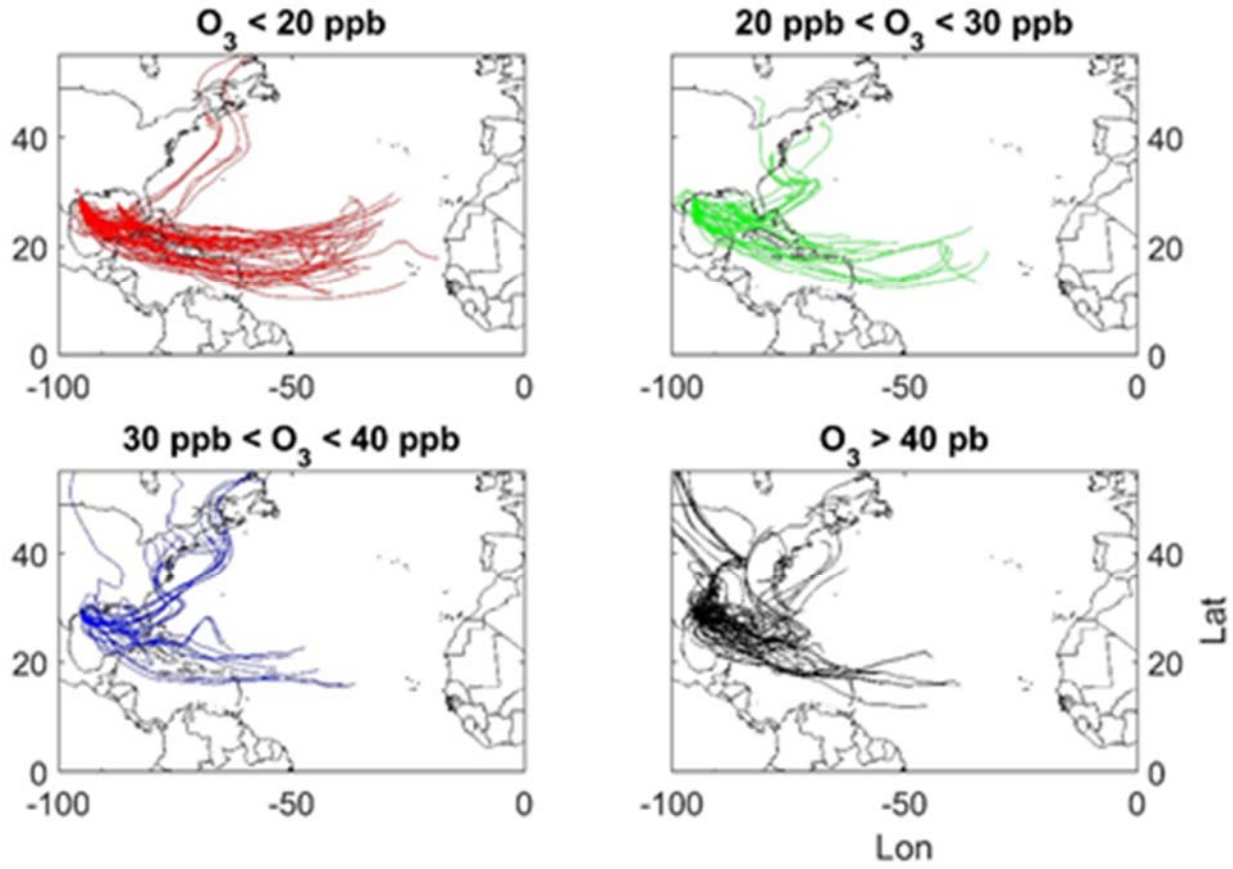

Figure 32. Ten-day back trajectories from San Luis Pass on the Texas Gulf Coast during summer 2016. Data are binned by observed O3 level at San Luis Pass. Adapted from Tuite, et al., 2018.

One outstanding question from this study was how the surface measurements compared to O_3 values aloft. Was the O_3 depletion from the halogen chemistry confined to the lowest portion of the boundary layer, or was it deeper? Ozonesondes were launched on a low O_3 day from the pontoon in southern Galveston Bay to help address this question. The vertical profile (Figure 33) from the launch on July 18th, a day where low O_3 was forecast (green category), shows that O_3 was between 20-30 ppbv from the surface to approximately 1,500 m (1.5 km), nearly 500 m above the boundary layer height as determined by the height of the inversion in the potential temperature profile. Figure 34 shows the ten-day back trajectory for the ozonesonde launch on July 18th, 2021, from three heights over the Bay, 500 m (red), 1,000 m (blue), and 1,500 m (green). These trajectories all originate in the central Atlantic and are comparable to the upper right panel in Figure 32. All three heights show that the airmass was located over the central Atlantic. This is consistent with the 10-day back trajectories found under these O_3 conditions in the previous work, as seen in the upper right panel in Figure 32. The altitude profiles for all three back trajectories experienced vertical transport where the three different heights mixed between 500-1,500 m. This is also consistent with the range of low O_3 in the vertical profile, indicating that at some point during the previous 10 days the air in the first 1,500 m may have mixed with the surface layer over the ocean, if not directly encountering the ocean surface. These results show that the layer of depleted O_3 is relatively deep and is not constrained to the boundary layer, much less the lowest portion of the boundary layer. These conditions may be targeted for additional launches in 2022 to allow for further study. A deeper analysis of the other launches in the Houston record, which date back more than 15 years, may yield additional results.

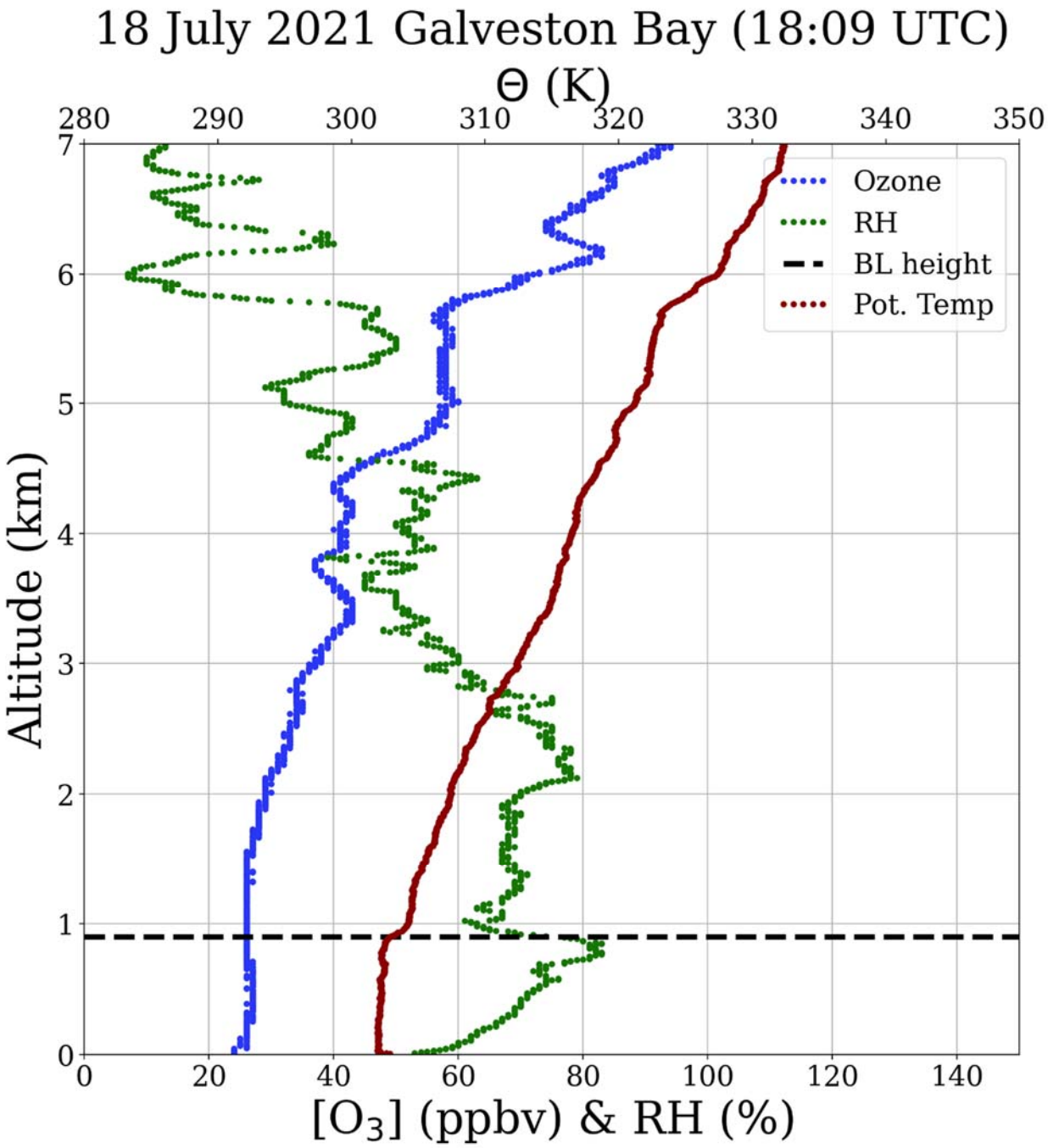

Figure 33. Vertical profiles of ozone (green), relative humidity (blue) and potential temperature (red). The derived boundary layer height is denoted by the horizontal dashed black line.

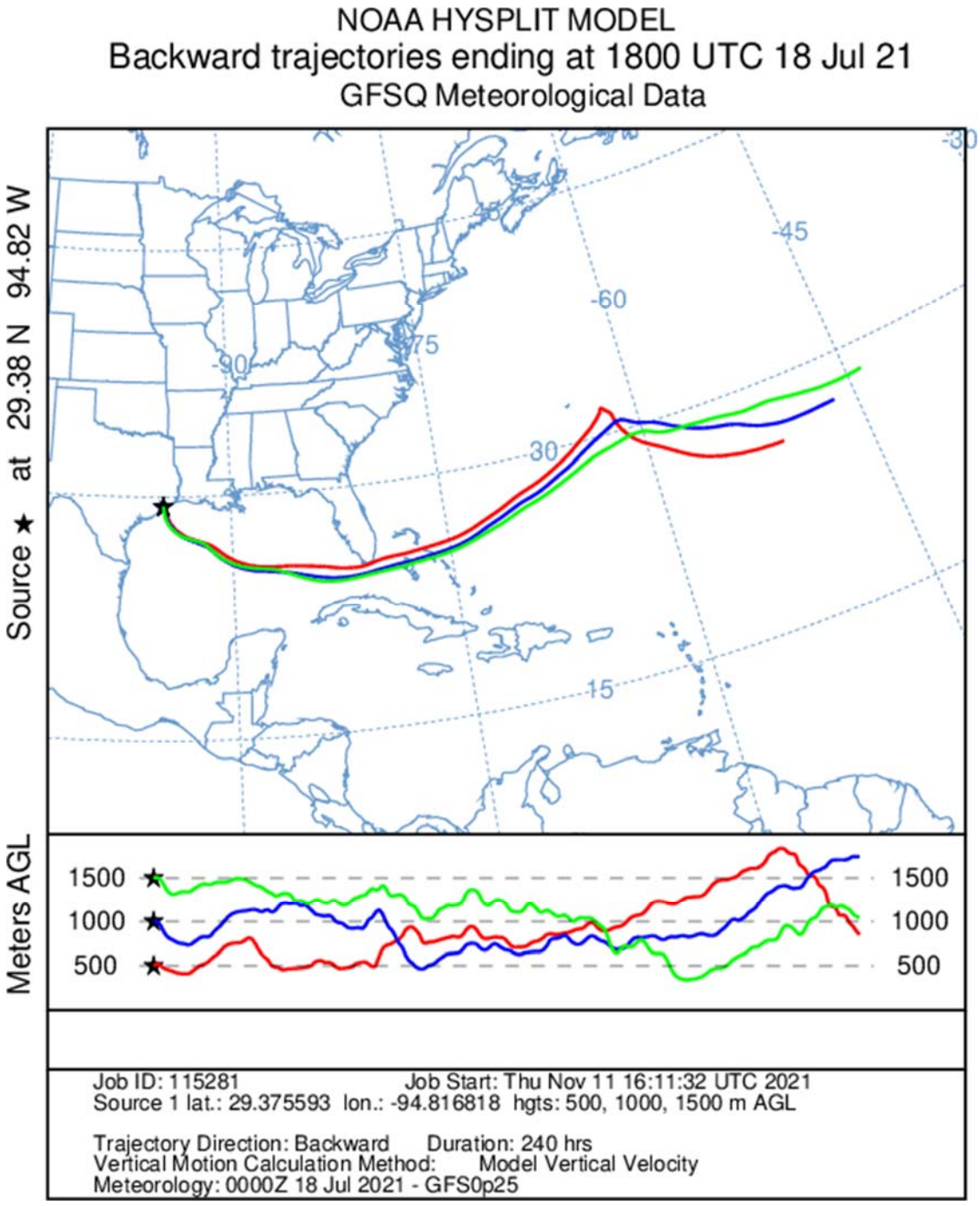

Figure 34. Ten-day back trajectory for the ozonesonde launch on July 18th, 2021, from three heights over the Bay, 500 m (red), 1,000 m (blue), and 1,500 m (green). These trajectories all originate in the central Atlantic and are comparable to the upper right panel in Figure 32 for the same O_3 conditions. Of note, at some point all three of the heights mix between 500-1,500 m, likely ensuring that all heights encountered the surface layer at some point.

6.3 Results Question 3: Impacts of local circulation on offshore O_3

6.3.1 How is O_3 formation over the water impacted by local circulation patterns?

The accepted conceptual model for most modern high ozone episodes in the Houston-Galveston-Brazoria region involves the recirculation of pollutants from the emission sources predominantly on the SE side of Houston, out over Galveston Bay and offshore waters and then brought back with the afternoon bay/sea breeze. Two time periods of interest during the study period were selected that demonstrate the potential for recirculation of a plume to the Houston area during a high ozone episode.

6.3.1.1 Case Study – July 26th, 2021

The UH pontoon boat operated July 26th, 2021, which the TCEQ forecast to be an ozone action day. The shrimp boat remained at port at Smith Point as did the Red Eagle (Gulf vessel) at Galveston Island (locations shown in Figure 35).

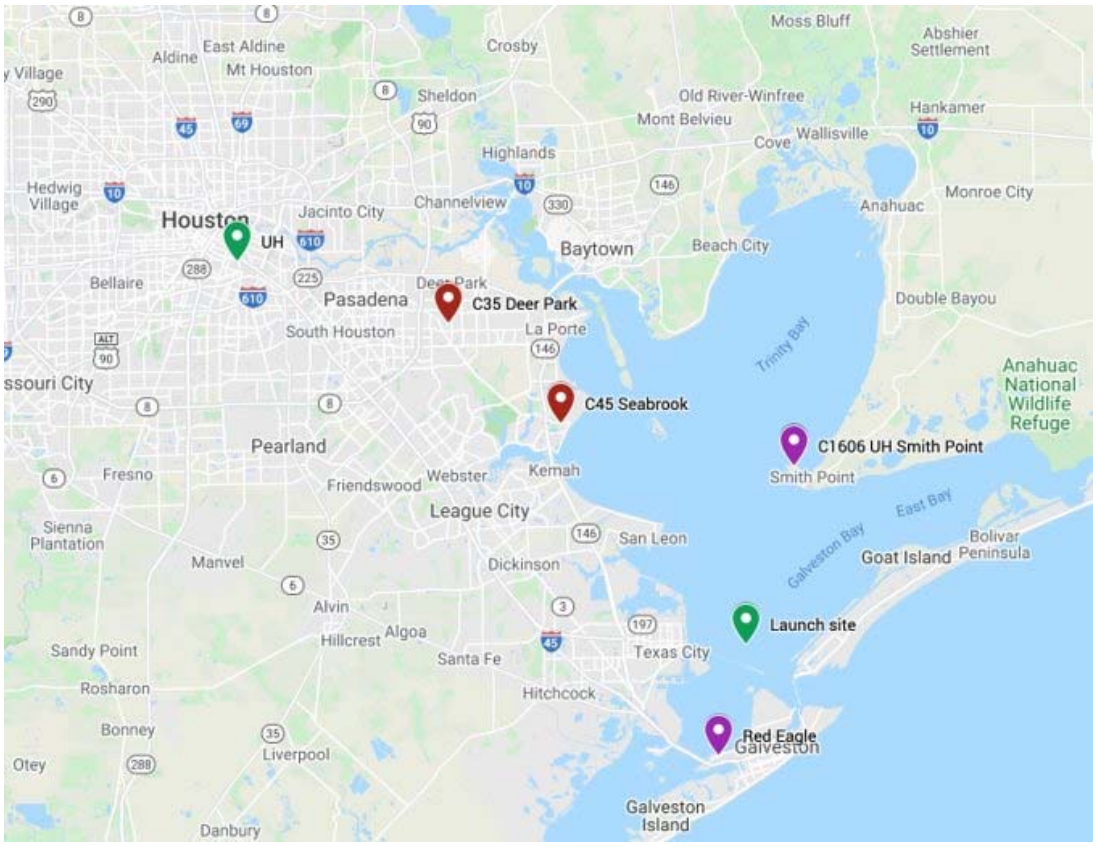

Figure 35. Map showing the TCEQ monitoring sites of interest (red), the docked shrimp boat and Red Eagle (purple) and the ozonesonde launch locations from Galveston Bay (pontoon) and the University of Houston- Main campus (green).

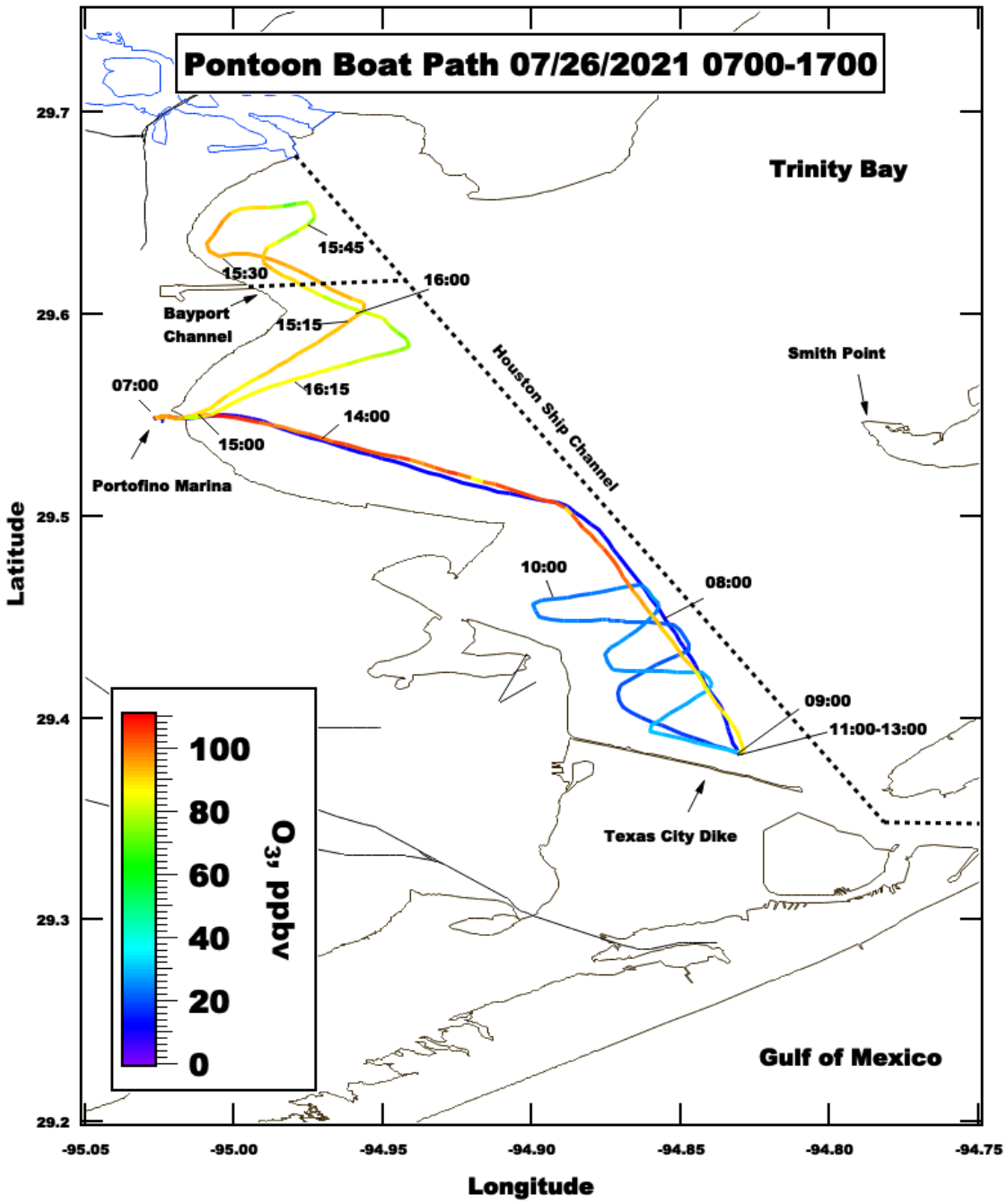

Figure 36. Spatial plot of surface ozone concentrations collected by the UH pontoon boat on July 26th, 2021.

The Red Eagle and shrimp boat were at dock on July 26th, 2021, but the UH pontoon boat was mobile, spatial pattern shown in Figure 36. Two sondes, one in the morning and the other in the afternoon, were launched from near the Texas City Dike (29.383° N, 94.831° W). The morning sounding (8:37 CST) on 26 July, shown in Figure 37, had missing data during the ascent from

0.57 - 1.13 km AMSL. The profile shows a marine layer height of 0.31 km AMSL, and an ozone enhancement of 66 ppbv above the surface at 1.13 km AMSL that would have the potential to mix down to the surface as the depth of the boundary layer grew throughout the day.

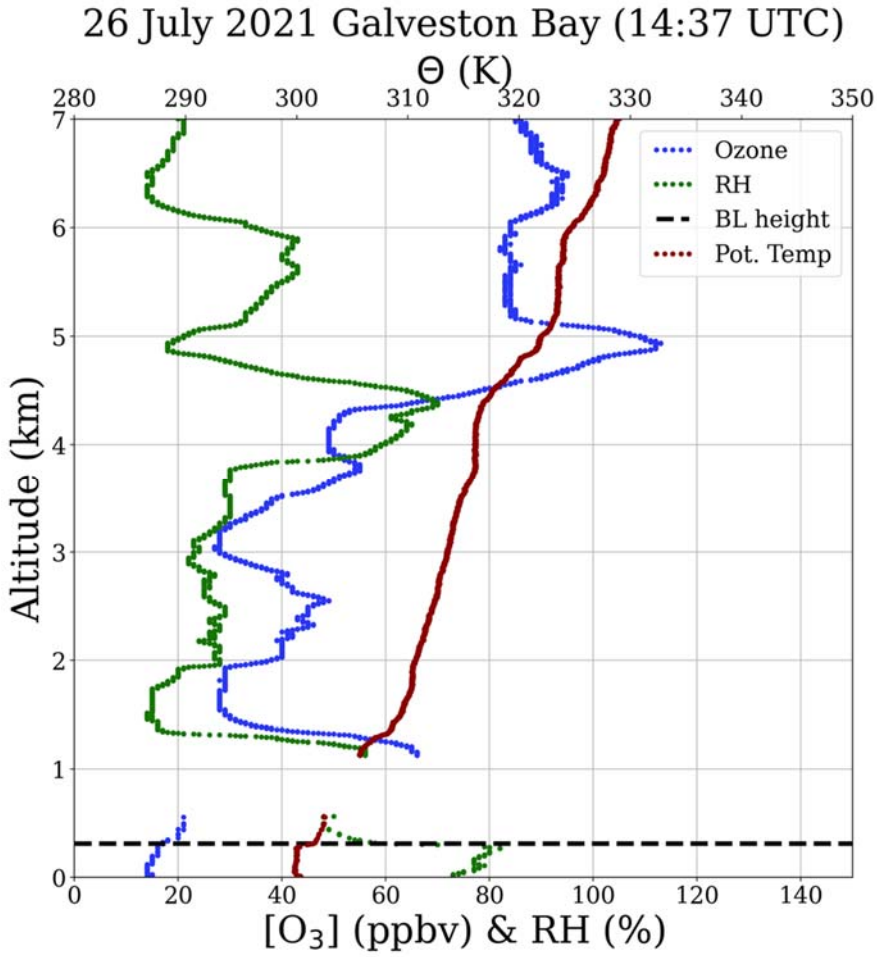

Figure 37. Ozonesonde profile from the morning launch in Galveston Bay at 9:37 local time (14:37 UTC).

The shrimp boat docked at Smith Point was the first location to show the rapid increase in surface ozone (Figure 38). The UH pontoon boat was in the SW quadrant of Galveston Bay near the Texas City Dike, approximately 18km southwest of Smith Point, observed an increase ~30 minutes later. The Red Eagle, docked at Galveston Island ~26km away, did not observe the rapid increase or high maximum surface ozone values observed by the other boats.

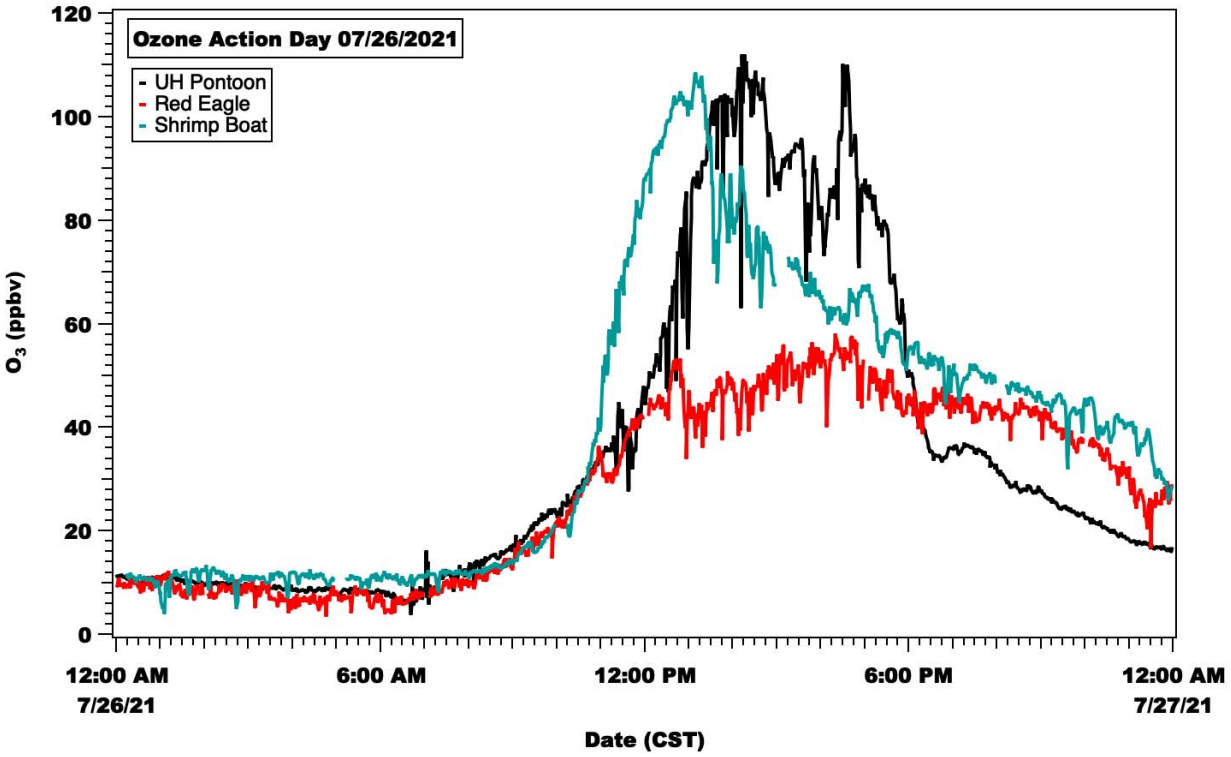

Figure 38. Time series of the three boats collecting surface ozone data around the Bay.

Comparisons of the ozone measurements taken aboard the shrimp boat showed good agreement (Figure 39) with the C1606 UH Smith Point monitor approximately 230 m away.

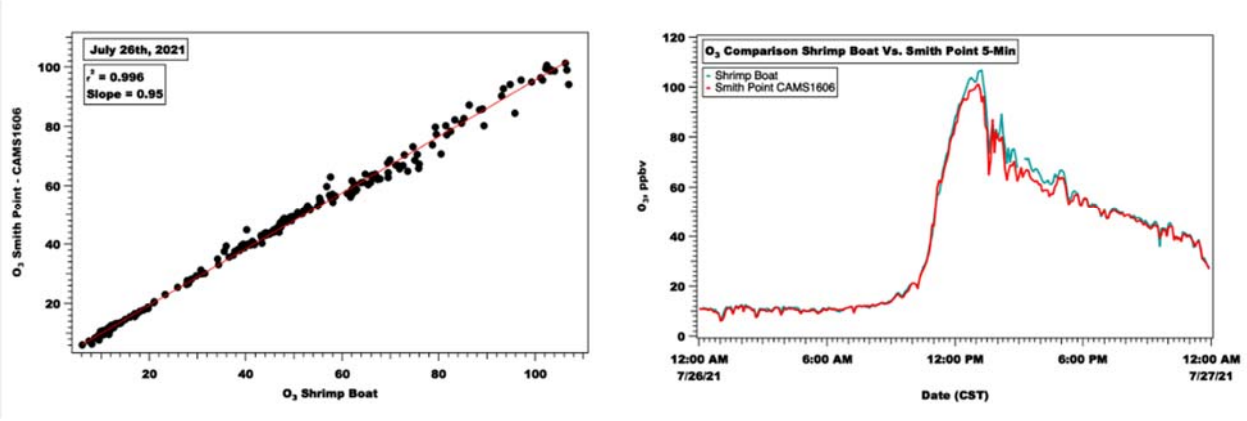

Figure 39. Comparison of the C1606 Smith Point monitor and the shrimp boat docked ~250m on July 26th, 2021.

A characteristic of this day was that the plume that was first seen at the shrimp boat worked its way WNW with the prevailing winds at the time. This feature can be seen in Figure 40, where the color gradient and legend are arranged from East to West (descending) across Houston. With the maximum value of more than 130 ppbv recorded at the C35 Deer Park site.

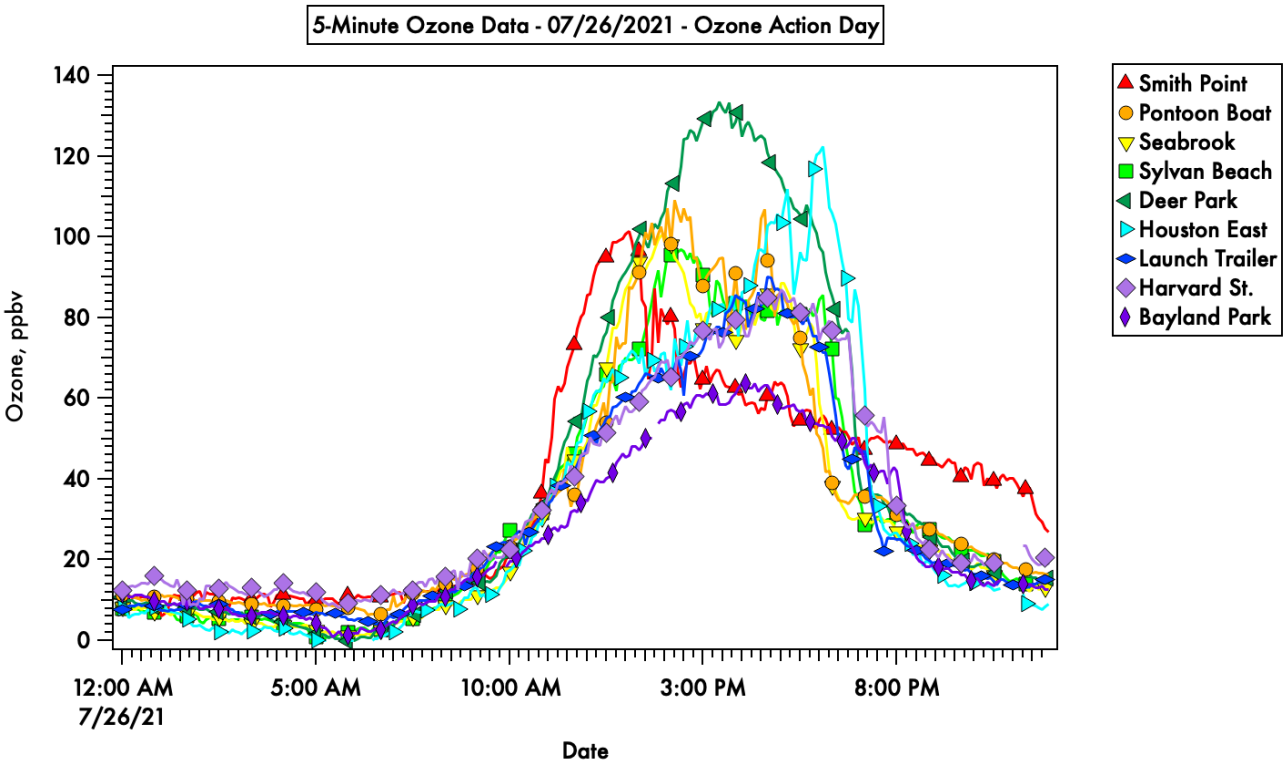

Figure 40. Time-series showing surface ozone concentrations at the UH pontoon boat and selected TCEQ monitoring sites. The sites are listed and colored from East to West in the legend.

The maximum daily 8-hour average (MDA8) [O_3] was 97 ppbv at C35 Houston Deer Park #2. Figure 41 shows the wind run for the C35 Deer Park #2 on July 26th. The wind run starts from the 00 CST hour, located at (0, 0) on the graph, and concludes on the 23 CST hour. The figures show wind vectors for each hour with distances in km. The color of the hourly wind vectors is based on the hourly ozone concentration, ranging from 0 ppbv (dark purple during the 5 am CST hour) to 130 ppbv (dark red during the 3 pm CST hour). The same scale is used for all wind runs shown in this report. The large black arrow represents the vector sum, and its length is the transport distance L. The total distance of all the hourly wind vectors (i.e., the sum of the magnitudes of the wind vectors) we denote S. The parameter related to the amount of potential recirculation is given by the ratio of 1 - L/S, which ranges from 0 (no recirculation) to 1 (much recirculation) (Levy, Dayan, and Mahrer 2008). Wind runs from different locations can show how much the wind pattern varies through the urban area for a given day. Quite often, ozone exceedance days exhibit distinctive wind run patterns (e.g., Li et al., 2020). Figure 41 shows a land breeze in the late morning changing to a bay breeze in the afternoon at the 2 pm CST hour at the C35 Deer Park #2 monitor.

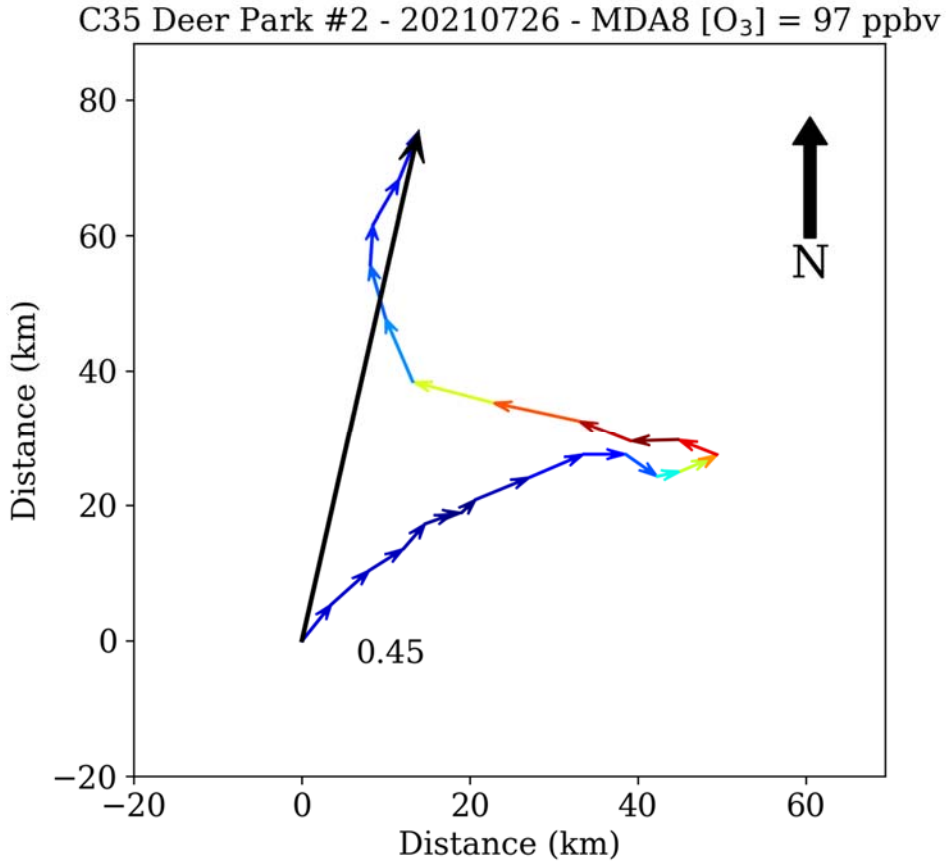

Figure 41. The 24-hour wind run for C35 Houston Deer Park #2 for 26 July 2021. Details described in text.

The 24-hour wind run for the C45 Seabrook monitor (left panel of Figure 42), located closer to Galveston Bay (see Figure 35), shows the transition from a land breeze to a bay breeze occurred earlier at the 11 am CST hour.

The morning winds at Smith Point (24-hour wind run shown in the right panel of Figure 42) suggest transport from Houston. The winds were nearly stagnant during the 12 pm CST hour when Smith Point reached [O_3] = 97 ppbv on the Shrimp Boat.

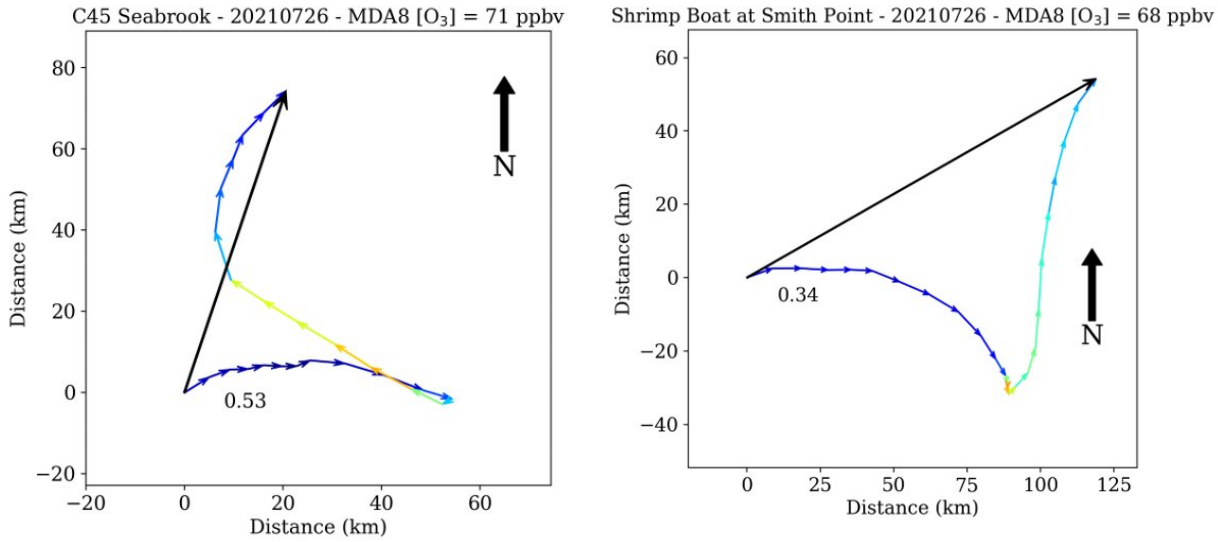

Figure 42. The 24-hour wind runs for C45 Seabrook (left) and the shrimp boat docked at Smith Point (right). Left: The change from a land breeze to a bay breeze occurred at Seabrook (11 am CST hour) before the transition occurred at Deer Park (2 pm CST hour). Right: The winds were nearly stagnant during the 12 pm CST hour when Smith Point reached [O_3] = 97 ppbv on the Shrimp Boat. The morning winds at Smith Point suggest transport from Houston.

6.3.1.2 Case Study – September 9th, 2021

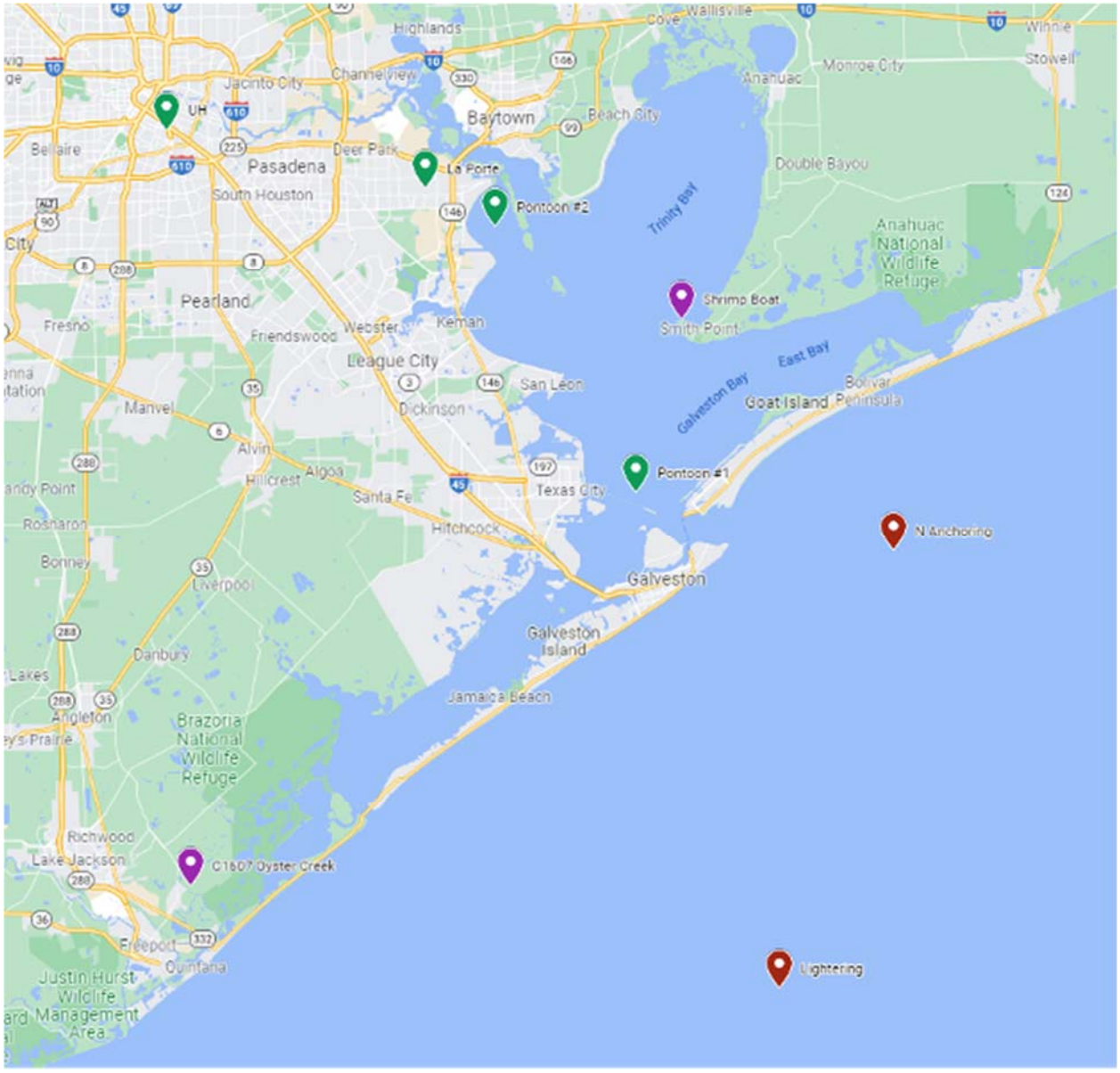

Figure 43. Map showing the TCEQ C1607 Oyster Creek monitor (purple) the ozonesonde launch locations from Galveston Bay (pontoon, green), La Porte (green), University of Houston - Main campus (green), and from aboard the Red Eagle (red) operating in the Gulf of Mexico.

The Red Eagle boat was chartered for the days operations to target both the anchorage and lightering areas offshore (Figure 43) during a suspected high ozone day. The spatial coverage and associated ozone concentrations are shown in Figure 44 below.

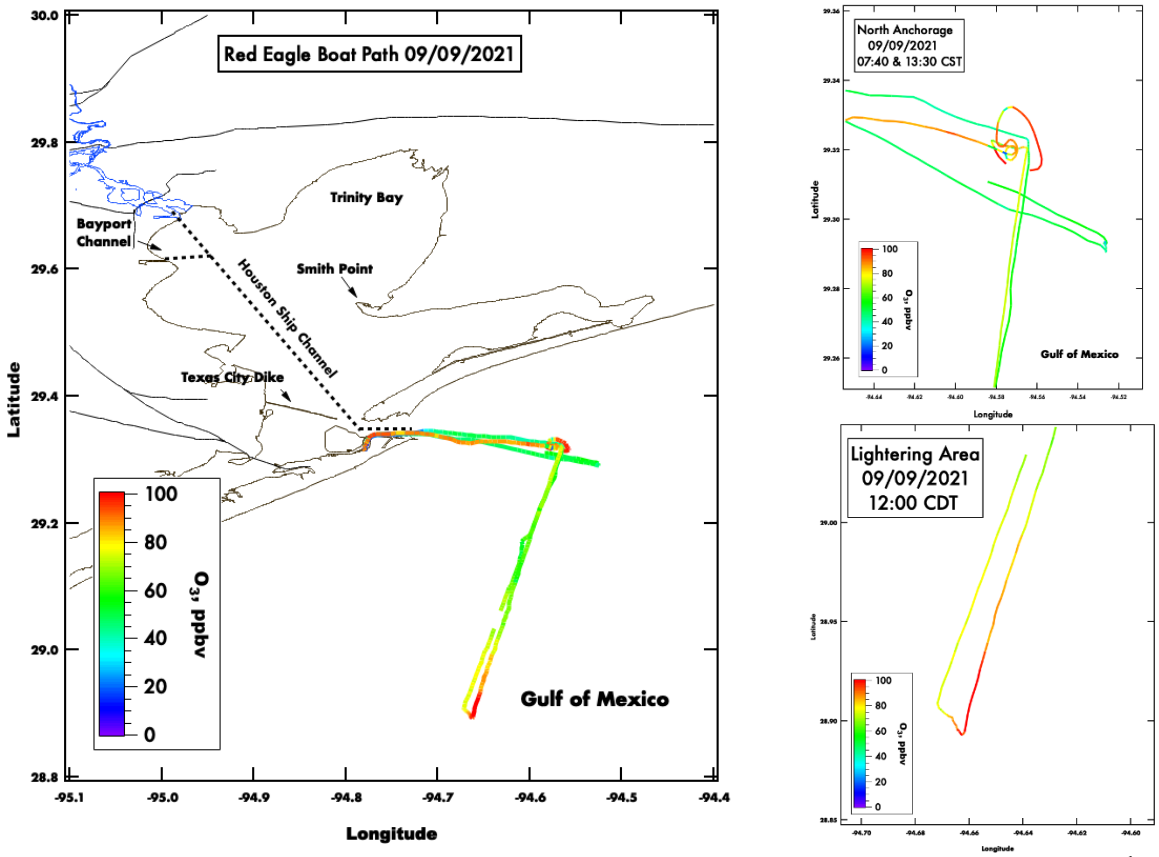

Figure 44. Left: Spatial plot of surface ozone collected by the Red Eagle on September 9th, 2021. Top-right: Zoomed in view of the N Anchorage area. Bottom-right: Zoomed in view of the Lightering area.

An overview of the surface data collected from the three mobile boat platforms on September 9th, 2021, is shown in figures 45-47 below. A feature of interest that appeared on this day was a rapid increase in surface ozone in the late afternoon, first observed by the Shrimp Boat docked at Smith Point, then subsequently observed at the UH pontoon boat, which was at dock in Kemah, TX. The shrimp boat was at 60ppb at 14:28 (CST) when the rapid increase in ozone concentration began. Four minutes later, the concentration had increased to 94 ppbv, ultimately peaking at 108 ppbv at 14:53 (CST). Across Galveston Bay, the UH pontoon boat was docking from the day's outing. Before seeing the spike in ozone, the pontoon boat was measuring 57ppb at 15:49 (CST). Eight minutes later, the ozone concentration had increased to 97 ppbv, and the increase continued until 16:13 (CST) when it peaked at 113 ppbv. The Red Eagle boat was offshore this afternoon and did not observe the same ozone spike feature. An explanation of the magnitude and timescale of these increases is not entirely clear but is likely the result of a changing air mass/plume being advected over the sites related to the bay breeze circulation.

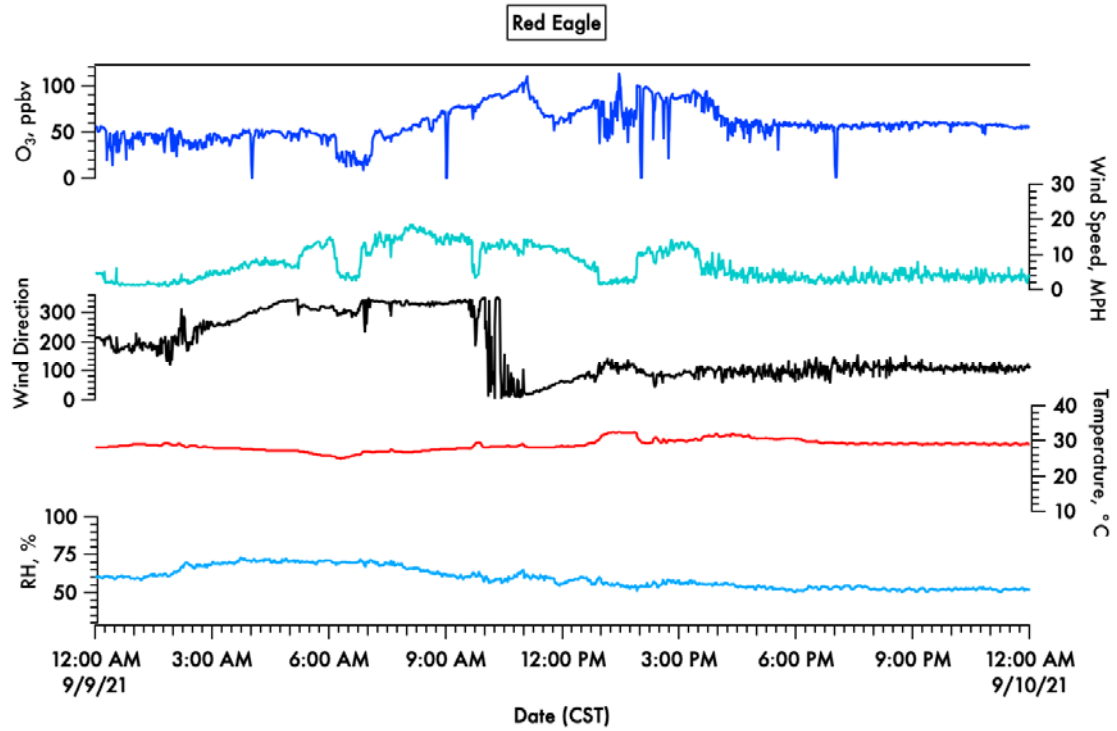

Figure 45. Time-series plot of surface ozone and meteorological parameters collected on the Red Eagle on September 9th, 2021.

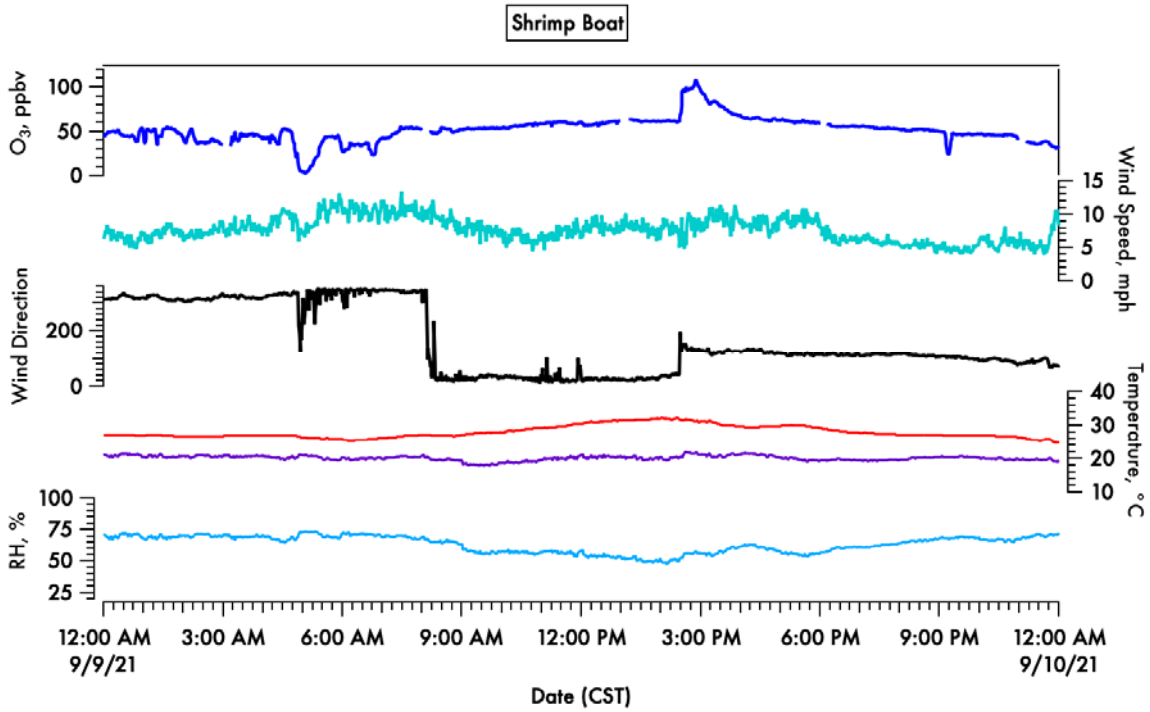

Figure 46. Time-series plot of surface ozone and meteorological parameters collected on the Shrimp boat on September 9th, 2021.

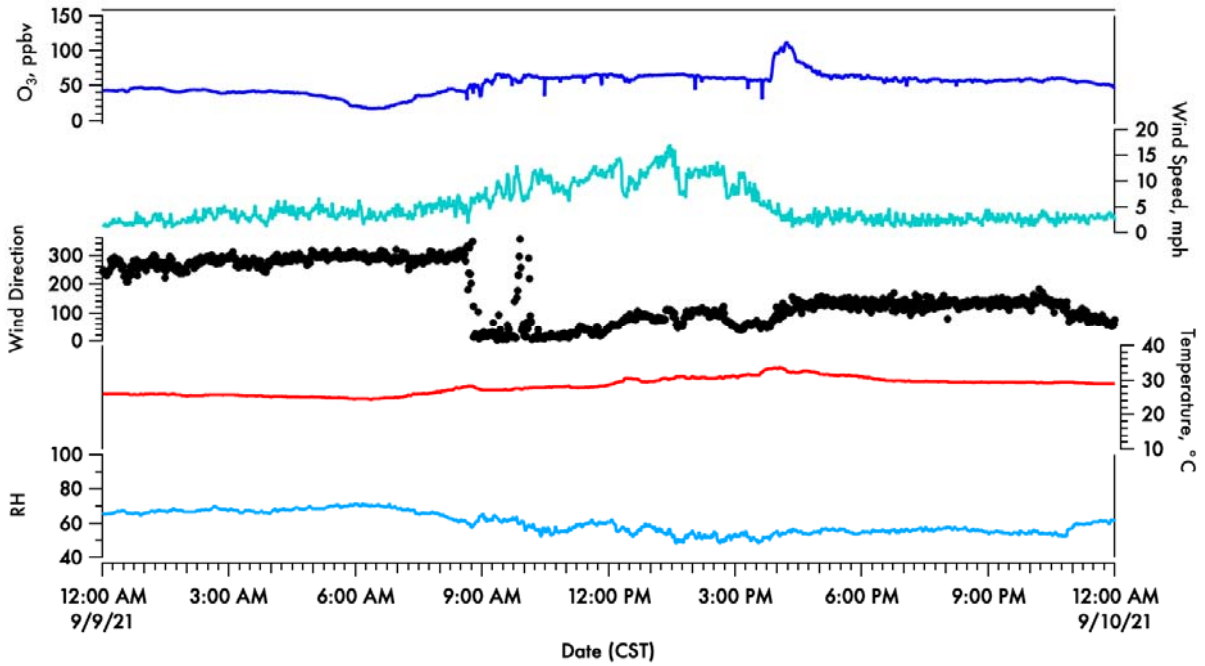

Figure 47. Time-series plot of surface ozone and meteorological parameters collected on the UH pontoon boat on September 9th, 2021.

The rapid increase of surface ozone at both the shrimp boat and the UH pontoon boat coincided with the passage of a bay breeze boundary which could be identified on the KHGX radar (Figure 48).

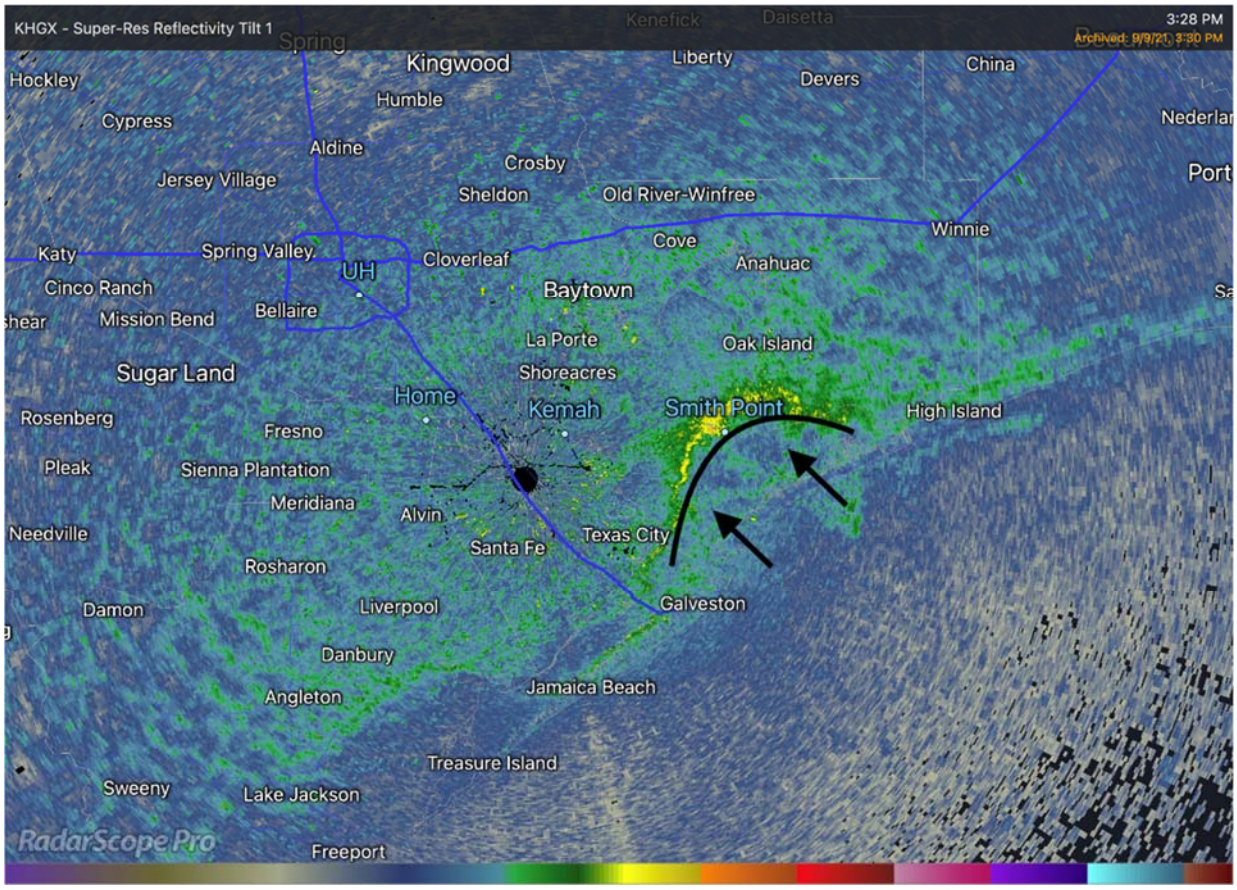

Figure 48. A frame from the KHGX doppler radar scan at 14:28 (CST) showing the passage of a bay breeze feature over Smith Point where the Shrimp boat was docked. The black line and arrows were added to highlight the direction and shape of the boundary.

The C1607 Oyster Creek monitor had the highest MDA8 [O_3] (81 ppbv) in the HGB area. The 24-hour wind run for that monitor is shown in Figure 49. In the morning, the winds were out the NNW before becoming easterly in the afternoon. That wind pattern is consistent with ozone and its precursors being transported from the Houston area to the Gulf in the morning. The Lightering area in the Gulf of Mexico, where measured ozone concentrations from the Red Eagle were observed to be 100 ppbv in the afternoon, is east of the C1607 Oyster Creek monitor. The afternoon wind speeds were high enough that it is unlikely that the higher ozone concentrations observed by the C1607 monitor were produced locally but were instead transported from nearby in the Gulf of Mexico.

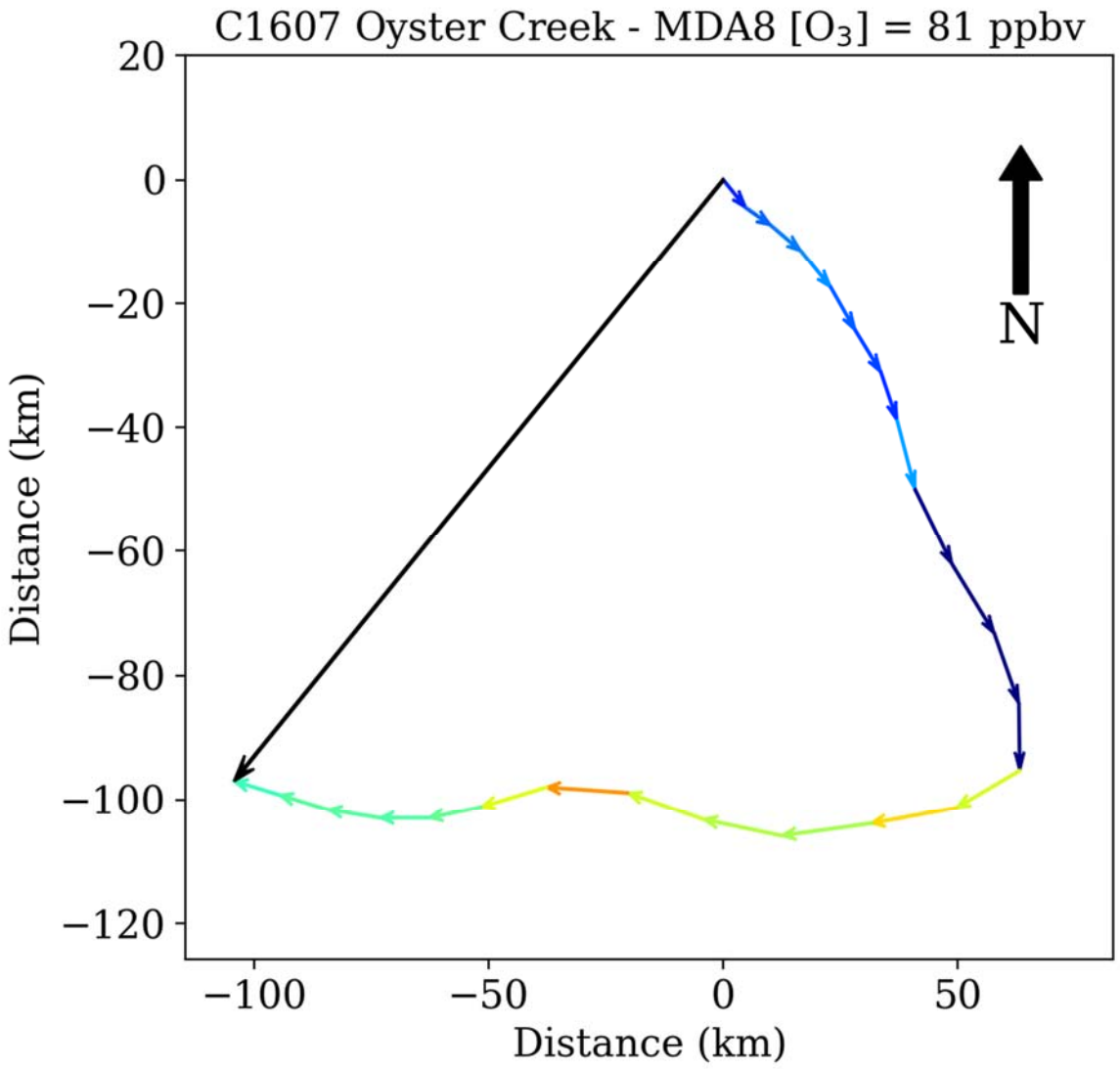

Figure 49. The 24-hour wind run for C1607 Oyster Creek for 9 September 2021.

6.3.2 How does the diurnal pattern over water differ from over land and from coastal measurement locations, such as Smith Point?

The diurnal pattern of ozone for the three instrumented boats has been analyzed for the study period. Observational differences for coastal and land-based sites were investigated directly with collected observations from the three boats and long-term stationary monitoring sites. However, comparison between of a diurnal pattern over water versus the land or coastal environment is not possible because the boats are not anchored on Galveston Bay, but rather on the coast of the Bay. Currently there is not a plan to establish an over water monitoring site.

The modeled diurnal patterns and differences between land and water are seen in Figure 50. Ozone and meteorological variables fluctuate largely over the course of the day. Over land, the

surface temperature is high, and strong heat fluxes drive high PBLs in the afternoon. High temperature and low relative humidity also tend to increase ozone in the afternoon over land. Low nighttime ozone results from vanishing photolysis, the nighttime chemistry of nitrate radical (NO_3) and N_2O_5, and changes in meteorology and PBL, etc. On the contrary, diurnal cycles over water are steadier on average, with generally smaller variations from minimum to maximum, as shown in Figure 50.

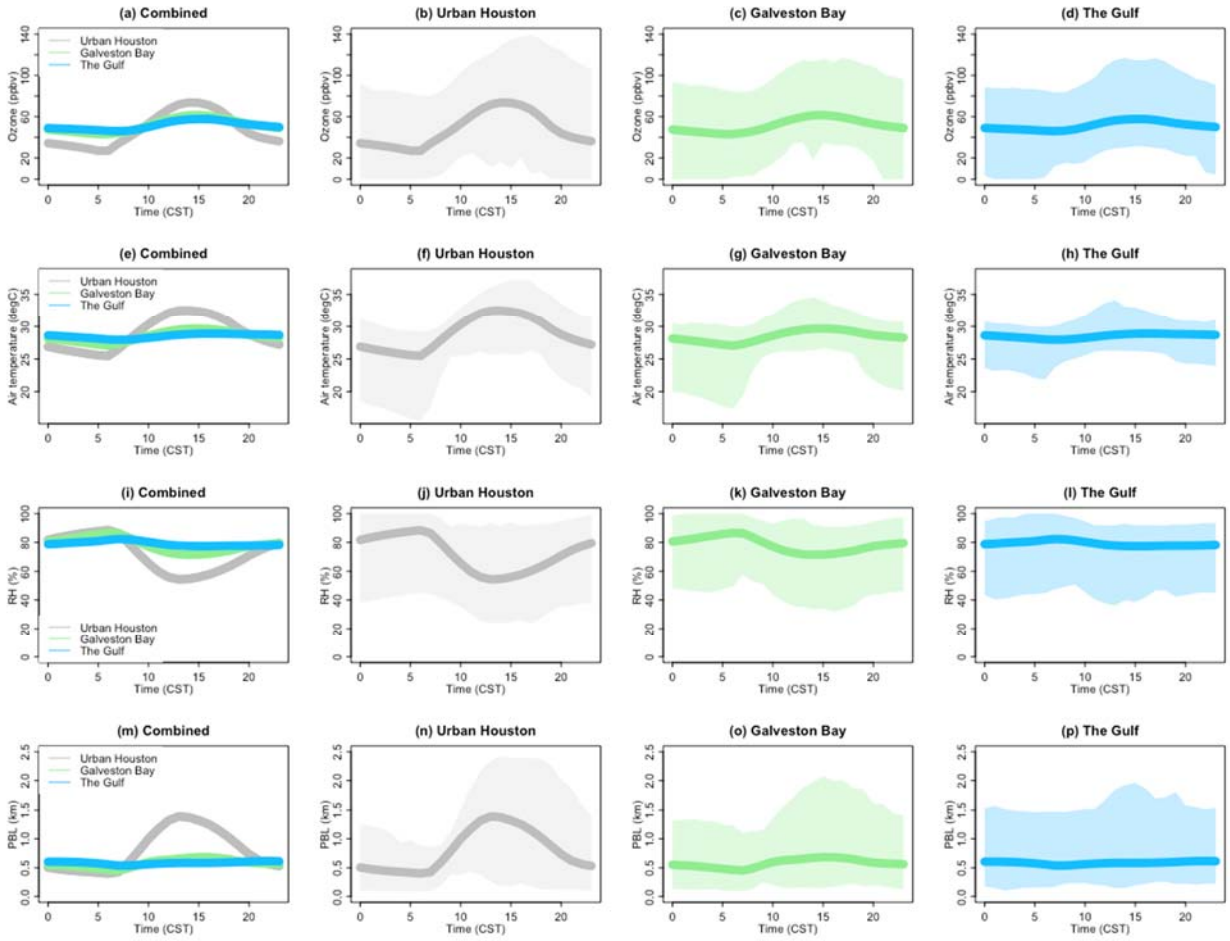

Figure 50. Diurnal cycles of ozone, temperature, relative humidity, and planetary boundary layer height at urban Houston (second column), Galveston Bay (third column), and the Gulf of Mexico (fourth column). The thick solid lines represent the mean, and the surrounding shadings represent ranges between minimum and maximum values. The first column shows the combined mean diurnal cycles from the three regions. The three regions are defined by black boxes in Figure 6a.

The O_3 diurnal pattern for all three boats averaged from July 17th- October 24th, 2021, is shown in Figure 51 below. Stationary monitors from nearby the boats and around Galveston Bay are also displayed. An inland location representative of urban Houston was also added to compare the differences between coastal and land-based measurements. The boat measurements include both stationary and mobile measurements. The three boats were docked most of the time, and

with the averaging over the entire study period, it is assumed the diurnal averages represent the coastal environment rather than an over water diurnal pattern.

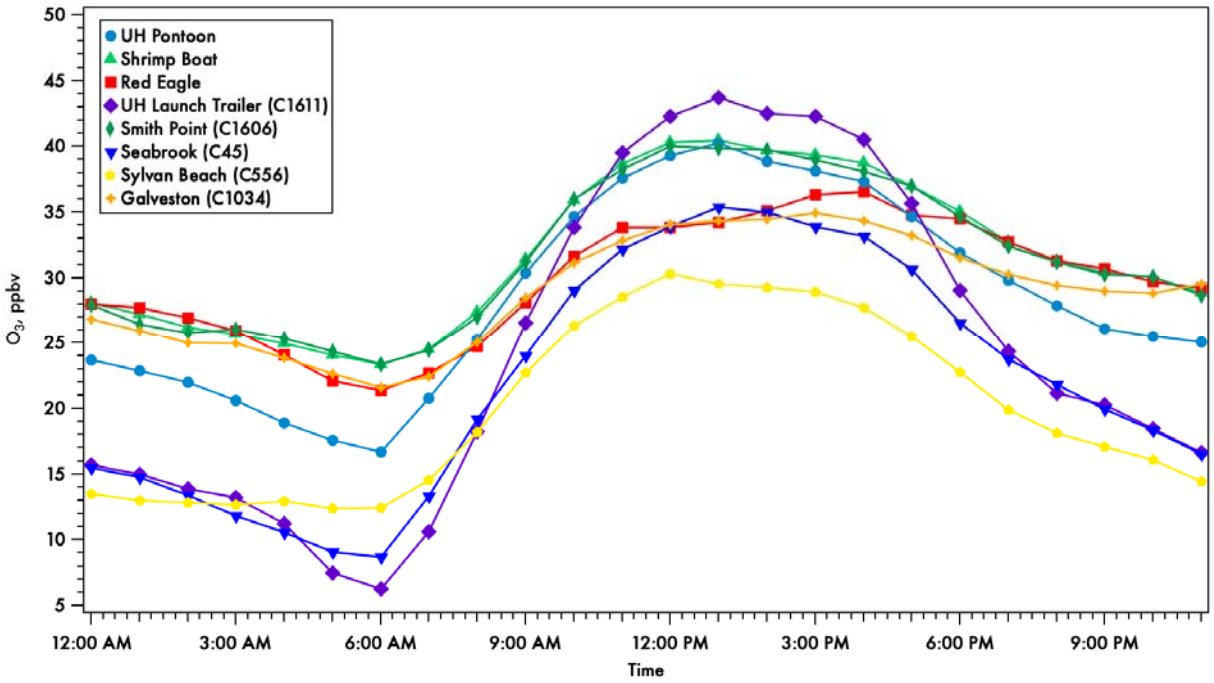

Figure 51. Diurnal pattern of O_3 for all three boats and a representative inland urban location. Ozone data was averaged from July 17th – October 24th, 2021.

The Red Eagle and the shrimp boat's diurnal ozone patterns were similar to their respective nearest stationary monitor during the study period. The shrimp boat revealed a near-identical diurnal pattern to the C1606 monitor located at Smith Point, TX. The Red Eagle showed some slight differences from the C1034 monitor on the Gulf side of Galveston Island, but despite the less favorable agreement in the scatter plot shown in Figure 26, the diurnal cycle is quite similar. The Galveston-based locations both show a delayed maximum daily value compared with all the other locations analyzed. Further differences in the diurnal ozone patterns around Galveston Bay are revealed at the locations on the west and north sides of the Bay. The UH pontoon boat, which docked in Kemah, TX, on the west side of Galveston Bay, showed lower minimum ozone concentrations before sunrise than the Red Eagle or Shrimp Boat although it reached similar maximums as the Shrimp Boat. Stationary near-coast monitors C45 and C556 north of the UH pontoon boat show a minimum daily value lower than the Kemah or Smith Point locations analyzed. The representative land-based stationary monitor C1611 (33 km inland) located at the University of Houston, SE of the urban center of Houston, showed the lowest minimum ozone value of the locations analyzed and the highest maximum value. The gradient of lower minimum diurnal ozone values occurring in the early morning closer to Houston's urban and industrial areas are likely reflecting the impact of increasing emission sources causing more ozone titration.

6.3.3 How frequently does the bay breeze result in a local circulation that brings urban plumes into Galveston Bay?

The local land/bay breeze has been identified as a potential factor in the transport of urban/industrial emissions over Galveston Bay that can be recirculated back to the urban center and lead to or exacerbate high ozone days in the HGB area (Banta et al., 2005). The C45 monitor in Seabrook, TX, near the NW coast of Galveston Bay, was investigated for wind flow direction change during the study period of July 17th – October 21st, 2021, to assess the frequency that a land/bay breeze circulates an urban plume over Galveston Bay. A wind direction change from N/NW overnight to S/SE during the daytime can indicate a flow reversal consistent with the land/bay breeze circulation. Of the 97 days that were analyzed, 32 days showed a bay breeze flow reversal (Table 6), 33% of the study period. Maximum 1-hour average O_3 and 5-minute NO_2 were also documented for each recirculation day to gauge the magnitude of an urban plume that the monitor observed. The 5-minute averaged NO_2 was used because of its propensity to chemically transform in a shorter time than O_3. Also, the NO_2 peaks seem to be associated with periods of high traffic on the nearby roadways. The C45 monitor is near high-trafficked roads, which can lead to high maximum values with favorable wind conditions, such as a N/NW wind during the pre-dawn rush hour. High O_3 time periods with a land-bay breeze circulation show a broader increase over the diurnal cycle.

Table 6. Days with a land/bay breeze as identified by a surface wind-flow reversal at the Seabrook (C45) monitor. Maximum daily surface 1-hour ozone concentration and daily maximum 5-minute NO_2 concentration are displayed as a tracer of an urban plume.

Date	**Observed 1-Hr Max. O_3**	**Observed 5-Minute Max. NO_2**
07/21/2021	60	22
07/22/2021	27	6
07/24/2021	35	7
07/25/2021	37	4
07/26/2021	94	19
07/27/2021	48	7
07/28/2021	52	27
07/29/2021	49	17
07/30/2021	38	7
07/31/2021	34	4
08/06/2021	52	30
08/12/2021	29	8
08/14/2021	40	15
08/15/2021	57	18
08/16/2021	63	29
08/22/2021	26	2
08/23/2021	40	13
08/24/2021	40	8

08/25/2021	49	17
08/26/2021	52	31
09/04/2021	31	4
09/05/2021	32	4
09/06/2021	73	15
09/08/2021	65	46
09/09/2021	70	36
09/17/2021	70	30
09/24/2021	49	20
09/25/2021	56	16
09/26/2021	55	20
10/06/2021	74	21
10/07/2021	102	45
10/08/2021	61	66

Figure 52 shows a five-day period with a land/bay breeze recirculation pattern. During this period, on July 26th, the second highest ozone day of the year was recorded at the site with a maximum hourly value of 94ppb. The NO_2 did see a peak in the morning of 19ppb, although it was not the highest observed value of NO_2 during the time period shown.

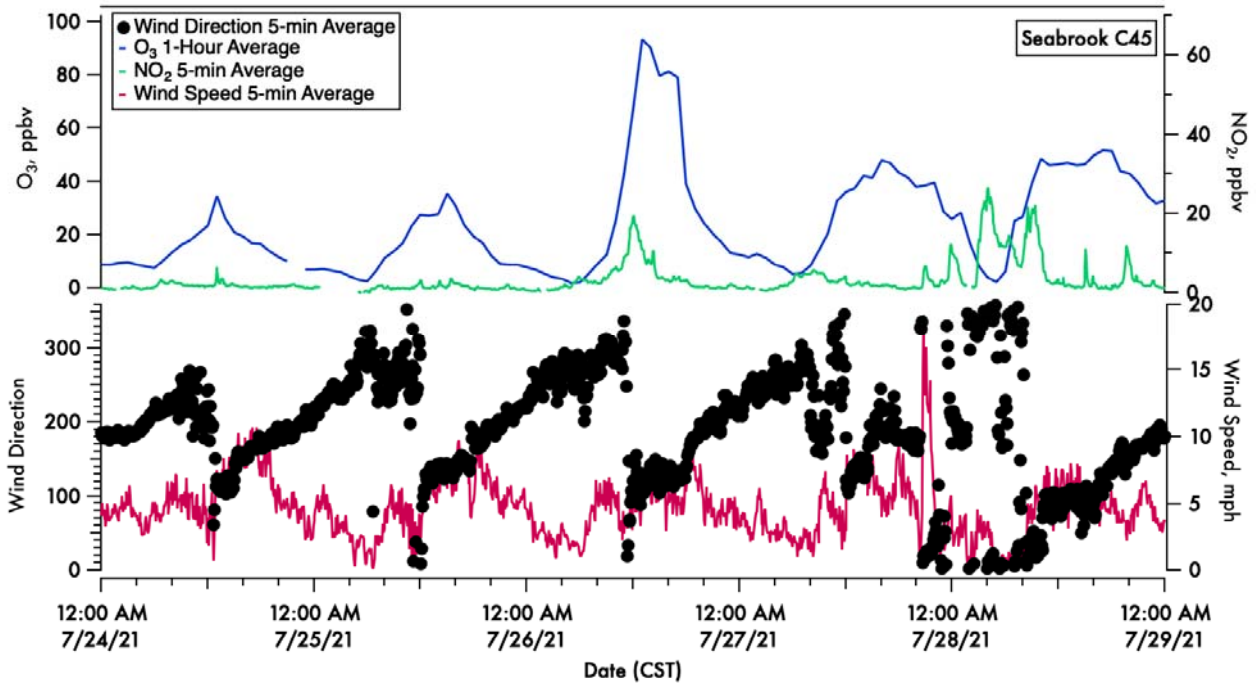

Figure 52. A 5-day period with several land/bay circulations at the C45 monitor in Seabrook, TX. In the top panel the blue line is 1-hour ozone concentration, and the green line is 5-minute NO_2 concentration. The bottom panel shows the wind direction in degrees.

Figure 53 shows a four-day period from the C45 monitor in Seabrook with consistent (southerly) onshore flow. This period was characterized by low O_3 and NO_2 as well as minimal intraday variability, consistent with a clean marine air mass being minimally impacted by local emissions.

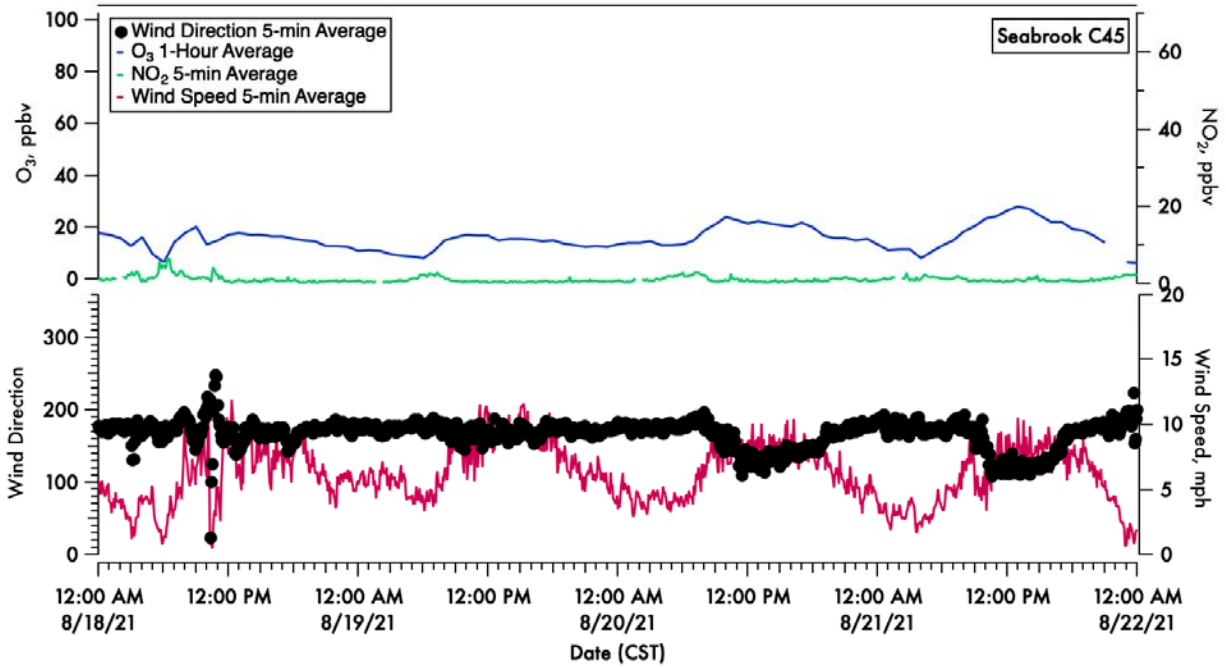

Figure 53. A 4-day period with no land/bay circulations at the C45 monitor in Seabrook, TX. In the top panel the blue line is 1-hour ozone concentration, and the green line is 5-minute NO_2 concentration. The bottom panel shows the wind direction in degrees.

6.3.4 What effect does this circulation have on O_3 in the Houston area in an era of reduced VOC emissions from the Houston Ship Channel area?

Between the lack of VOC measurements (not proposed or included in this project) and the shortened period allotted for analysis and modeling of the observations due to a one-year delay in response to the COVID pandemic (measurements did not conclude until October 24, 2021), this question cannot be properly answered at this time. Certainly, changes in VOCs in Houston have occurred, and previous work has shown that the total OH reactivity of VOCs measured at the UH campus during previous campaigns has been significantly reduced, with dramatic changes between 2006 and 2010. However, episodes of high O_3 still occur. One anecdotal observation during this campaign was that on most days, conditions over the Bay tended to be much more cloud-free than over the adjacent land. This lack of cloud cover coupled with a higher UV albedo from water than from grass (Renata and Girgždys, 2008) may increase the NO_2 photolysis rate over the water, leading to an increased potential for O_3 production over the water compared to over land (Flynn et al., 2009). This effect, combined with the land-bay breeze recirculation described in Banta et al. (2005), could result in elevated O_3 transported back into the Houston area. The inclusion of NO_2 photolysis rates over water and nearby land is being considered as part of the measurements planned for 2022. Moreover, fully addressing this question would require an in-depth modeling study and VOC measurements over the water that will be better suited for future work.

6.4 Results Question 4

6.4.1 What are the characteristics of the boundary layer over the water during high O_3 events, and how do the observed boundary layer heights compare to model predicted values?

Figure 54 shows that PBLs measured by ozonesonde are generally consistent with model estimates, except for launches over the Gulf of Mexico. High correlation (R=0.62-0.92) and low biases (<10%) suggest land and coastal PBLs variations are well captured over urban Houston, La Porte, and Galveston Bay. At urban Houston, modeled mean PBL of 1.08±0.57 km is slightly higher than the observed value of 1.02±0.74 km with correlation coefficient R = 0.73 and root mean square error RMSE = 0.50 km. At La Porte, modeled mean PBL of 0.98±0.43 km is relatively lower than the observed value of 1.07±0.62 km with correlation coefficient R = 0.92 and root mean square error RMSE = 0.29 km. At Galveston Bay, modeled mean PBL of 0.75±0.37 km is slightly higher than the observed value of 0.70±0.44 km with correlation coefficient R = 0.62 and root mean square error RMSE = 0.35 km. However, the model sees a large overestimation of mean PBL of 0.96±0.44 km compared to the observed value of 0.59±0.32 km. The model has PBL 61% higher than observations with correlation coefficient R = 0.25 and root mean square error RMSE = 0.55 km. Marine PBLs are always more complex than those over land, and double layers can sometimes appear. Despite the difficulties in capturing transient marine PBLs, the overestimation may indicate that the PBL scheme used in the current model has less performance over offshore waters than land.

Figure 55 shows continuous PBL measurements by ceilometers over Galveston Bay. Here, we adopted two layers of the ceilometer measurements. The modeled PBLs are ~20% lower than the lowest observed layer, as shown in Figure 54b,d. These ceilometer-to-model differences over Galveston Bay show the same direction as the ozonesonde-to-model differences in Figure 55d, but with relatively less correlation and larger biases. However, the continuity of ceilometer measurements provides potential possibilities to explore PBL diurnal evolution, which cannot be achieved by individual ozonesonde measurements. More analysis on the characteristics of PBL during high ozone episodes and PBL diurnal evolutions are down the road.

For ozonesonde profiles, the boundary layer height is determined by examining gradients in relative humidity (RH), O_3, temperature, and potential temperature (θ) and is identified as the height at which most (if not all of) these variables show a sharp change in their vertical gradients. Typically, for an afternoon potential temperature profile, just above the surface $\partial\theta/\partial z < 0$, the air is unstable (due to surface heating). After the initial negative gradient near the surface, the potential temperature is approximately constant ($\partial\theta/\partial z = 0$) to the top of the boundary layer near 3.9 km AMSL on this day. A near-zero gradient in potential temperature is common. The atmosphere is generally stable above the boundary layer, as indicated by the positive potential temperature gradient ($\partial\theta/\partial z > 0$). The larger a positive potential temperature gradient is, the stronger the atmospheres stability at that altitude. The potential temperature will reach the same value that it is at the surface at the top of the PBL (Haman, Lefer, and Morris 2012). As with

ceilometer data, when identifying the PBLH from ozonesonde profiles, in some cases, there are multiple possible layers present, and there is uncertainty based on which layer is chosen.

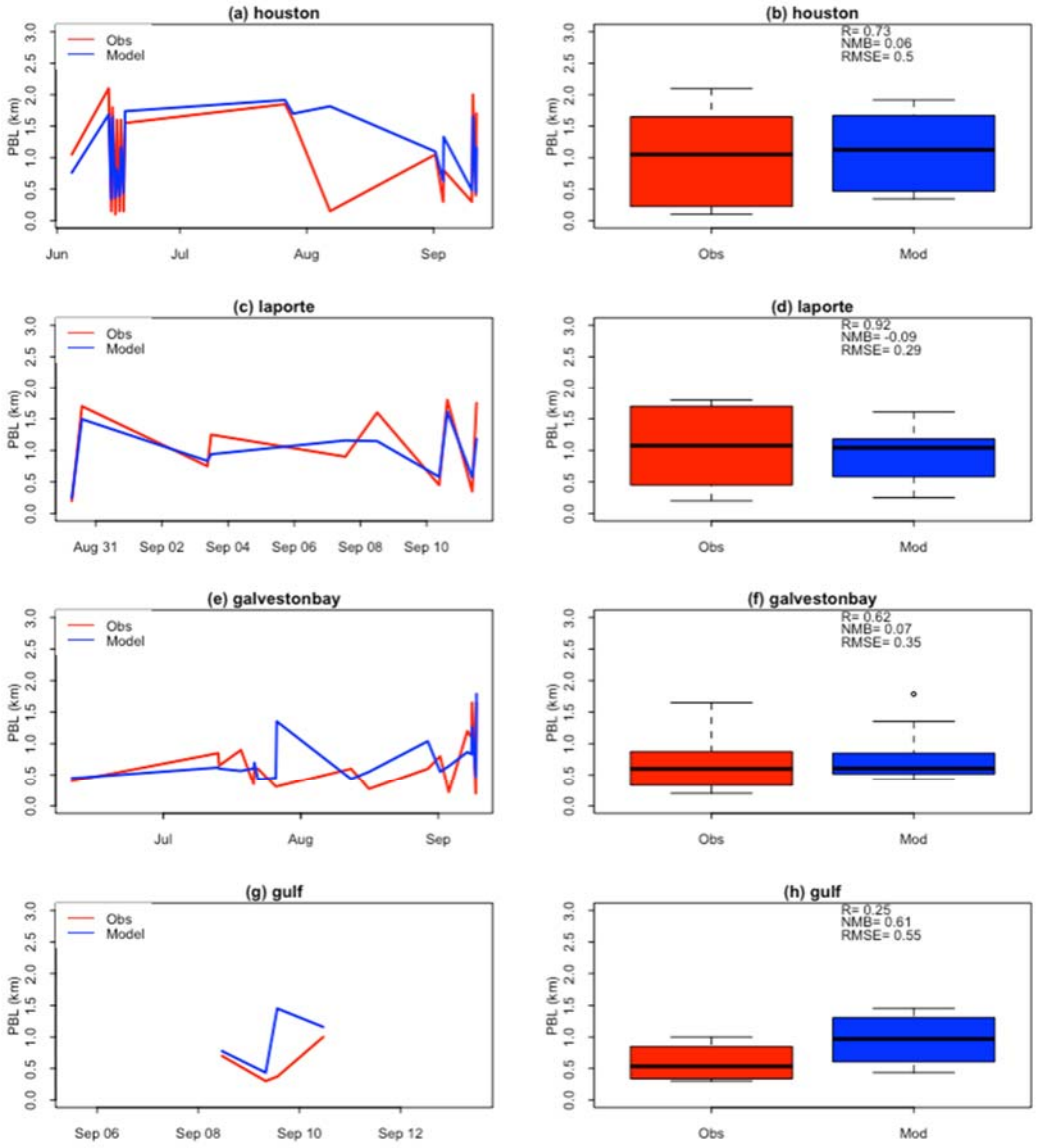

Figure 54. Ozonesonde observed and modeled planetary boundary layer height at urban Houston, La Porte, Galveston Bay, and the Gulf of Mexico. Left panel shows times series, and right panel shows overall temporal variability. In right panel, the horizontal line in each box shows the median, and the bottom and top of each box represent the first (Q1) and the third quartile (Q3) respectively. The dotted lines extending out of the box show the minimum and maximum values. The outliners are displayed as circles, whose values exceed 1.5 times the interquartile range (IQR; Q3–Q1). Correlation coefficient (R) normalized mean bias (NMB), and root mean square error (RMSE) are inserted.

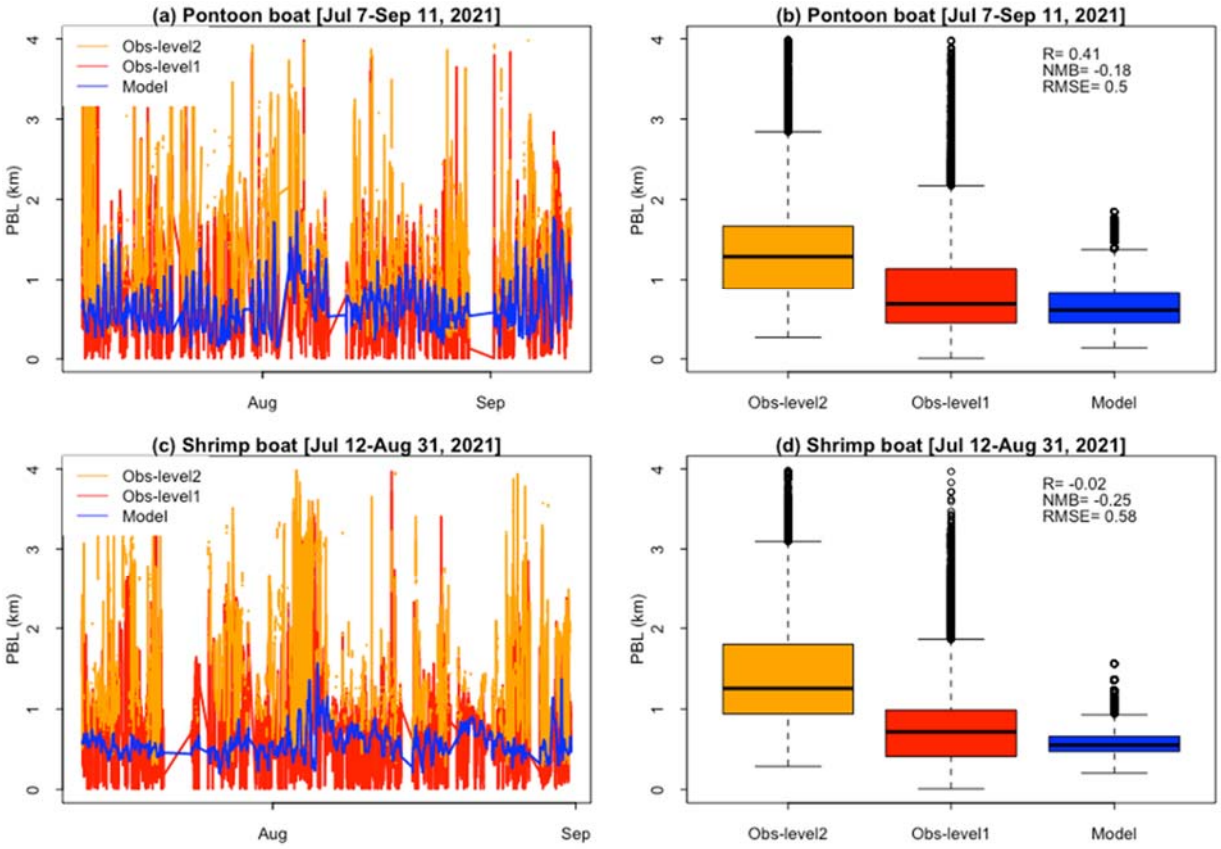

Figure 55. Ceilometer observed and modeled planetary boundary layer height. Left panel shows times series, and right panel shows overall temporal variability. In right panel, the horizontal line in each box shows the median, and the bottom and top of each box represent the first (Q1) and the third quartile (Q3) respectively. The dotted lines extending out of the box show the minimum and maximum values. The outliners are displayed as circles, whose values exceed 1.5 times the interquartile range (IQR; Q3–Q1). Correlation coefficient (R) normalized mean bias (NMB), and root mean square error (RMSE) between the lowest observed layer and modeled layer are inserted.

For ozonesonde launches that occurred from the UH Pontoon Boat, a comparison of the boundary layer heights from the ozonesonde profiles versus the Vaisala CL-51 ceilometer first identified boundary layer height is shown in Figure 56. The trendline has a slope of 0.58 ± 0.12 and a y-intercept of 223 ± 129 with an r^2 value of 0.45.

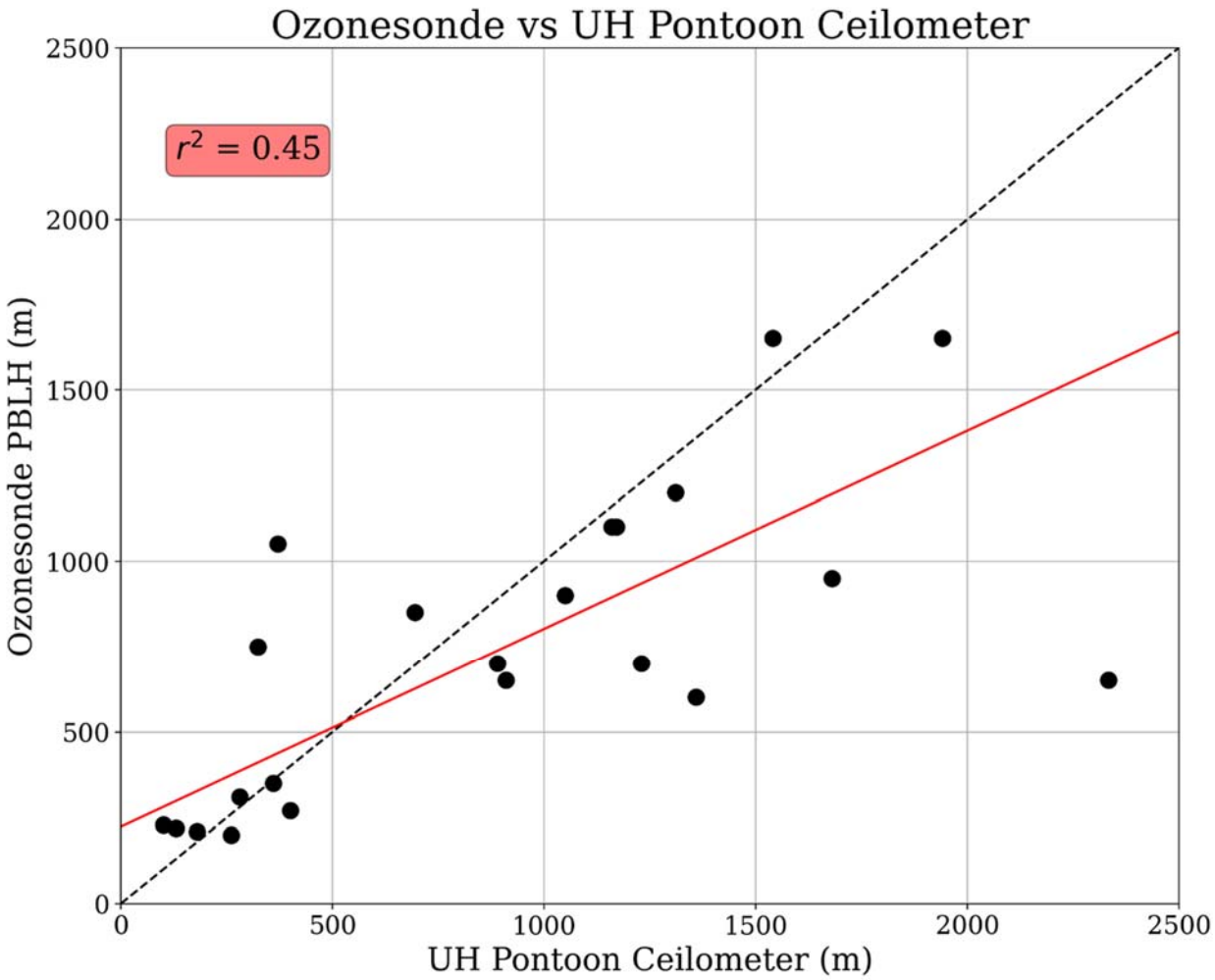

Figure 56. Comparison of boundary layer heights determined from profiles of collated ozonesonde launches versus the UH Pontoon boat Vaisala CL-51 ceilometer first identified boundary layer height. The red line shows a linear best fit with a slope of 0.58 ± .12 and a y-intercept of 223 ± 129. The dashed black line shows a 1-to-1 trendline.

6.4.2 Boundary layer heights over water are often parameterized and may not accurately represent reality, especially in areas with complex land-water interaction and circulation patterns, such as in Galveston Bay and the offshore waters (Dunker et al., 2019). How do the measured boundary layer heights compare to other land-based coastal measurements, such as those from Smith Point during DISCOVER-AQ Houston or from the Galveston 99th St. site (C1034)?

In addition to the observations of the boundary layer height from the pontoon boat described above, measurements were also collected on the Shrimp Boat during the first stages of the campaign. As reported in the monthly reports, a short circuit damaged the ceilometer on the pontoon boat system. The system from the Shrimp Boat was removed and subsequently installed

on the pontoon for the remainder of the campaign. This decision was largely based on the lack of movement in the Shrimp Boat. The CL-51 from the pontoon was returned to Vaisala for repair under warranty and was not returned before the conclusion of the campaign.

Data from the early portion of the project is shown below in Figures 56-59 as average diurnal profiles for the three layers identified by the instrument's software. Although the boats did operate out in the Bay to varying extents, the vast majority of the data was collected while in port. Therefore, these datasets are considered to be from either Smith Point (Shrimp Boat) on the east side of the Bay or Kemah (pontoon) on the western side. From Figure 57, we see significant differences in the two profiles, with the pontoon 200-400 m lower than the Shrimp Boat in the overnight hours but as much as 600-700 m higher than the Shrimp Boat in the afternoon. During the middle portion of the day, the two locations reported similar boundary layer heights. Aside from the clear differences in boundary layer height between the two sides of the Bay, each profile is interesting on its own. The profile from the Kemah location appears to be similar to other land-based boundary layer height measurements, with a minimum early in the morning and increasing throughout the day until shortly before sunset. On the other hand, the Smith Point profile shows a relatively stable boundary layer height near 1,000 m throughout the first half of the day and decreasing to around 500 m in the afternoon. The stability of the Smith Point profile in the first half of the day may be due to the relatively stable temperatures of the surrounding water. The decrease in boundary layer height in the afternoon period is interesting. An early hypothesis is that the effect seen here may be tied to the onset and retreat of a Gulf breeze moving in from the coast. However, at this time, a full analysis of this feature is beyond the scope of this project but may be included in future planned analyses. These features differ from those reported for Galveston at the C1034 site during DISCOVER-AQ in September 2013 (Figure 58), which found that the first layer was often around 200 m with a second layer near 700 m. Given the proximity of the Galveston measurements to the Gulf, the measurements here are likely more sensitive to the conditions over the Bay. In addition to the difference in year, season (September 2013 for Galveston and July-August 2021 for Smith Point and Kemah) may play a role in the observed differences. Both layers two (Figure 59) and three (Figure 60) for Kemah and Smith Point differ from layer 1 in that they are quite similar to each other despite being separated by over 20 km of water on opposite sides of the Bay. This seems to indicate that the lofted features may be regional in scale and less impacted by Bay or Gulf driven dynamics.

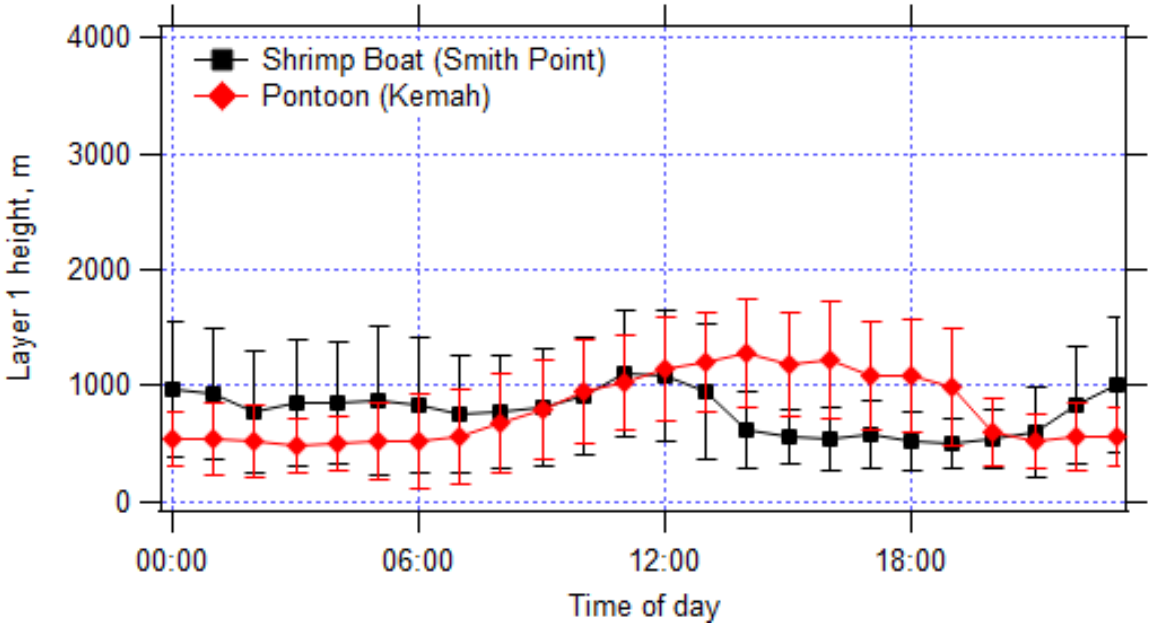

Figure 57. Diurnal profile (± one standard deviation) of the first identified layer height from the Shrimp Boat at Smith Point and the pontoon boat in Kemah. This layer is often considered the boundary layer height. Significant differences are seen between these two profiles, indicating variability in the boundary layer height over the Bay.

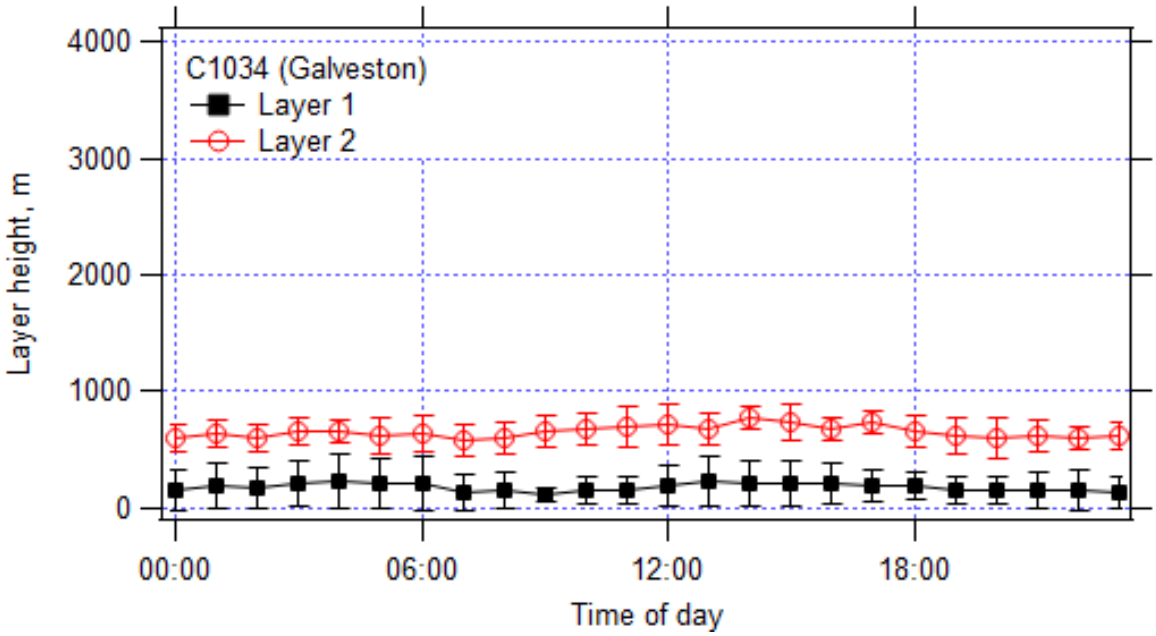

Figure 58. Diurnal profile of Layers 1 and 2 for Galveston (C1034) during DISCOVER-AQ in September 2013.

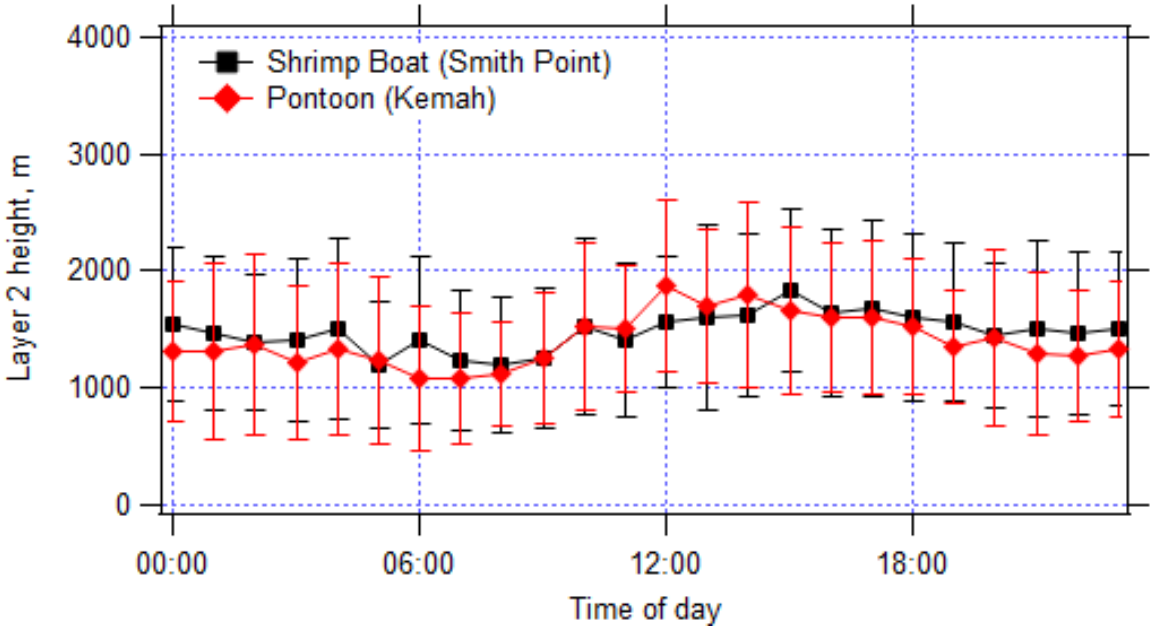

Figure 59. Diurnal profile (± one standard deviation) of the second identified layer height from the Shrimp Boat at Smith Point and the pontoon boat in Kemah. This elevated layer compares quite well between the two over the Bay.

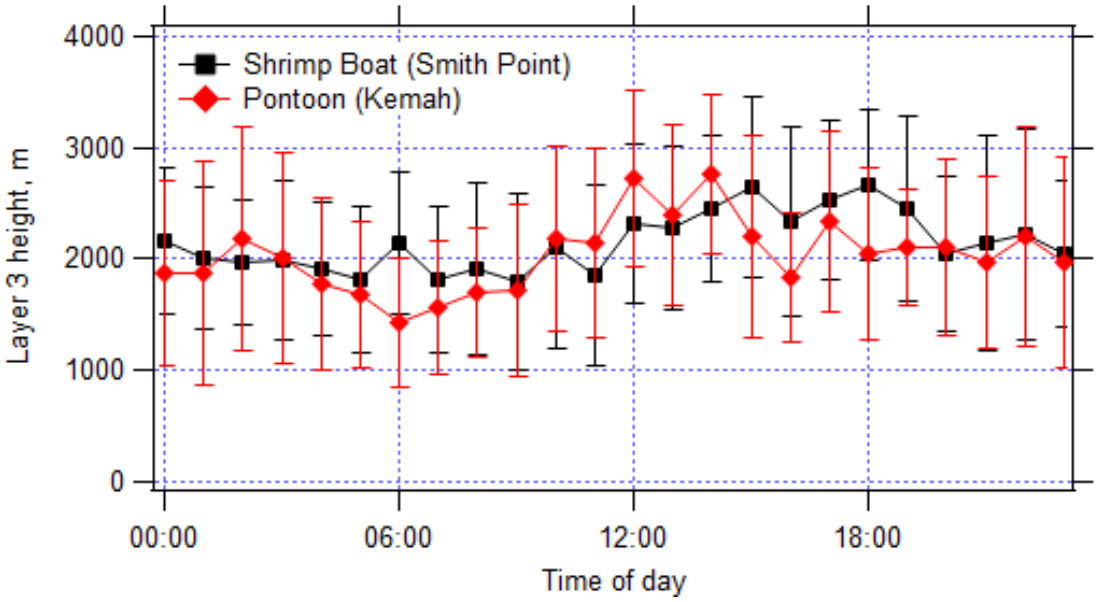

Figure 60. Diurnal profile (± one standard deviation) of the third identified layer height from the Shrimp Boat at Smith Point and the pontoon boat in Kemah. Like the second layer above, the third layer is consistent between the two platforms, indicating a uniform feature over the Bay.

6.4.2.1 Case Study – July 26th, 2021

The ceilometer data from the UH pontoon boat (Figure 61) and the shrimp boat (Figure 62) both show structure of multiple aerosol layers below an altitude of 2 km. The shrimp boat ceilometer data shows a more persistent lower layer than the UH pontoon boat which was on the west side of Galveston Bay near the Texas City Dike in the morning then traversing to the NW quadrant of the bay in the afternoon.

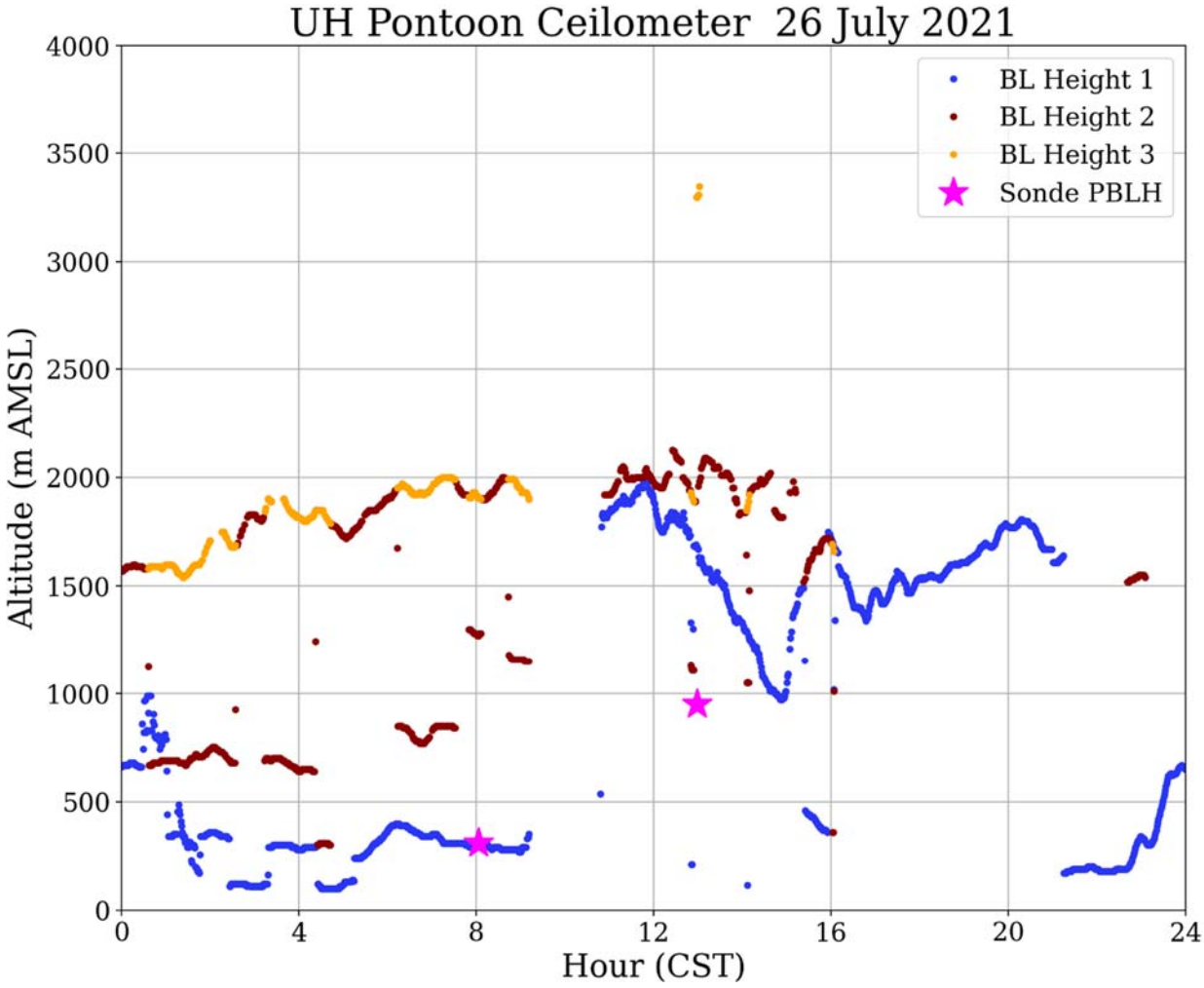

Figure 61. UH Pontoon Vaisala CL-51 ceilometer returned boundary layer heights and boundary layer heights from the ozonesonde profiles on 26 July 2021.

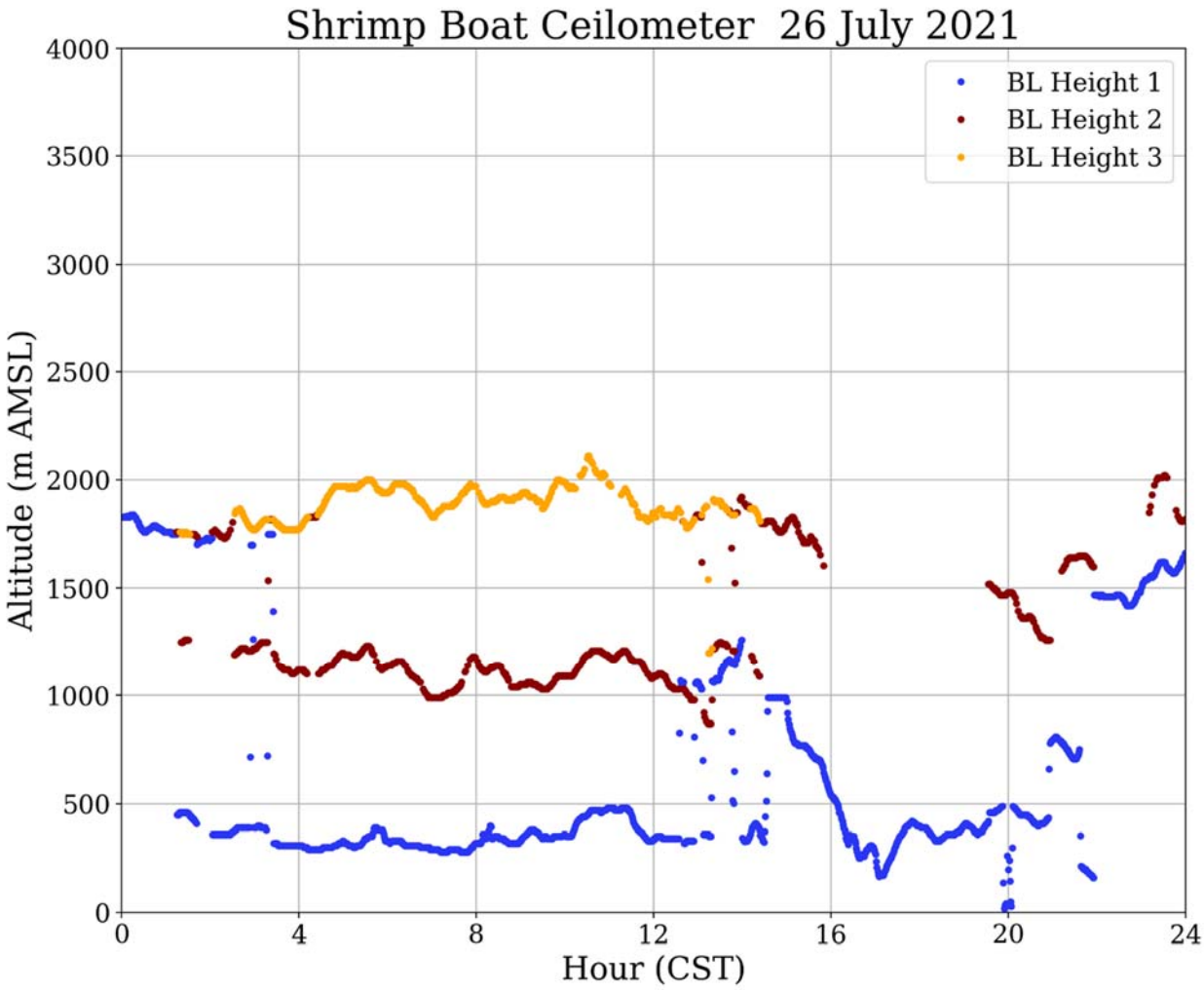

Figure 62. Shrimp Boat Vaisala CL-51 ceilometer returned boundary layer heights on 26 July 2021.

In Figure 63, the morning ozonesonde profile shows possible layers at 0.31 km, 1.4 km, and 1.9 km, which may be consistent with the locations of aerosol layers measured by the ceilometers. At 0.31 km, there is a sharp change in the gradient of the potential temperature as well as the relative humidity. Near 1.4 km, the potential temperature, relative humidity, and ozone concentration undergo fairly abrupt changes. Near 1.9 km, we again see rapid changes (albeit smaller in magnitude) in the potential temperature, relative humidity, and ozone concentration. The ozone enhancement observed in the morning profile at 1.1 km AMSL was above the marine surface layer but below the second aerosol layer. At the altitude of the ozone enhancement, winds were out of the NE where just above the enhancement the winds shifted to being out of the N.

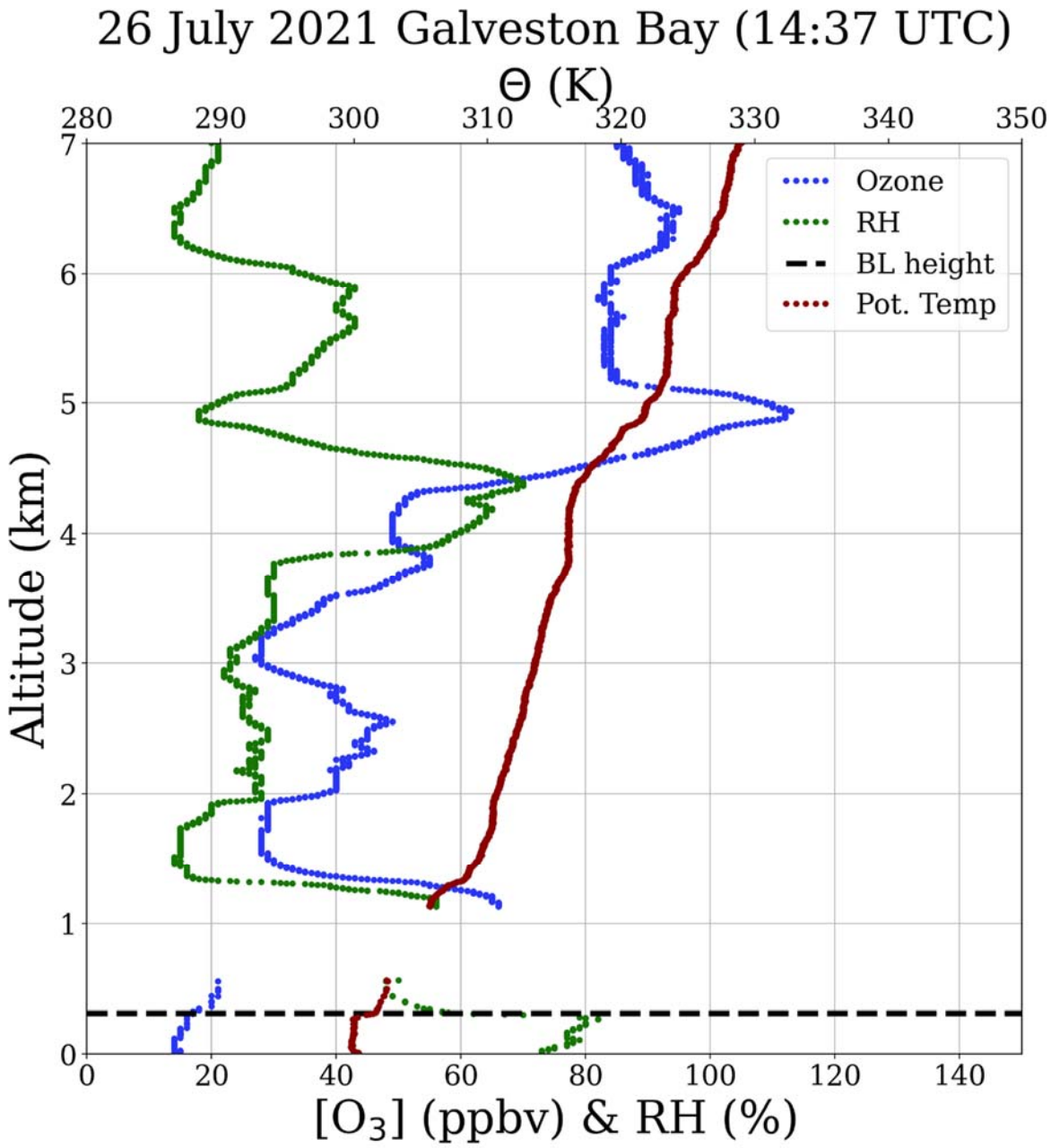

Figure 63. Vertical profiles of ozone (blue), RH (green) and potential temperature (red) for a sounding on 26 July 2021 at 8:37 am CST from near the Texas City Dike in Galveston Bay.

In the afternoon (12:59 CST), a sonde was launched from Galveston Bay near the Texas City Dike (Figure 64). The potential temperature profile (red) shows signs of a complex structure with possible layers at 0.95 km, 1.5 km, and 1.9 km based on the changes in the vertical gradients at those altitudes. At each of those altitudes, the vertical gradient changes from $\partial\theta/\partial z \sim 0$ (unstable air allowing for convective mixing) to $\partial\theta/\partial z > 0$ (stable air preventing convective mixing). The UH pontoon boat ceilometer data shows aerosol layers at 1.4 km and 2 km at the same time.

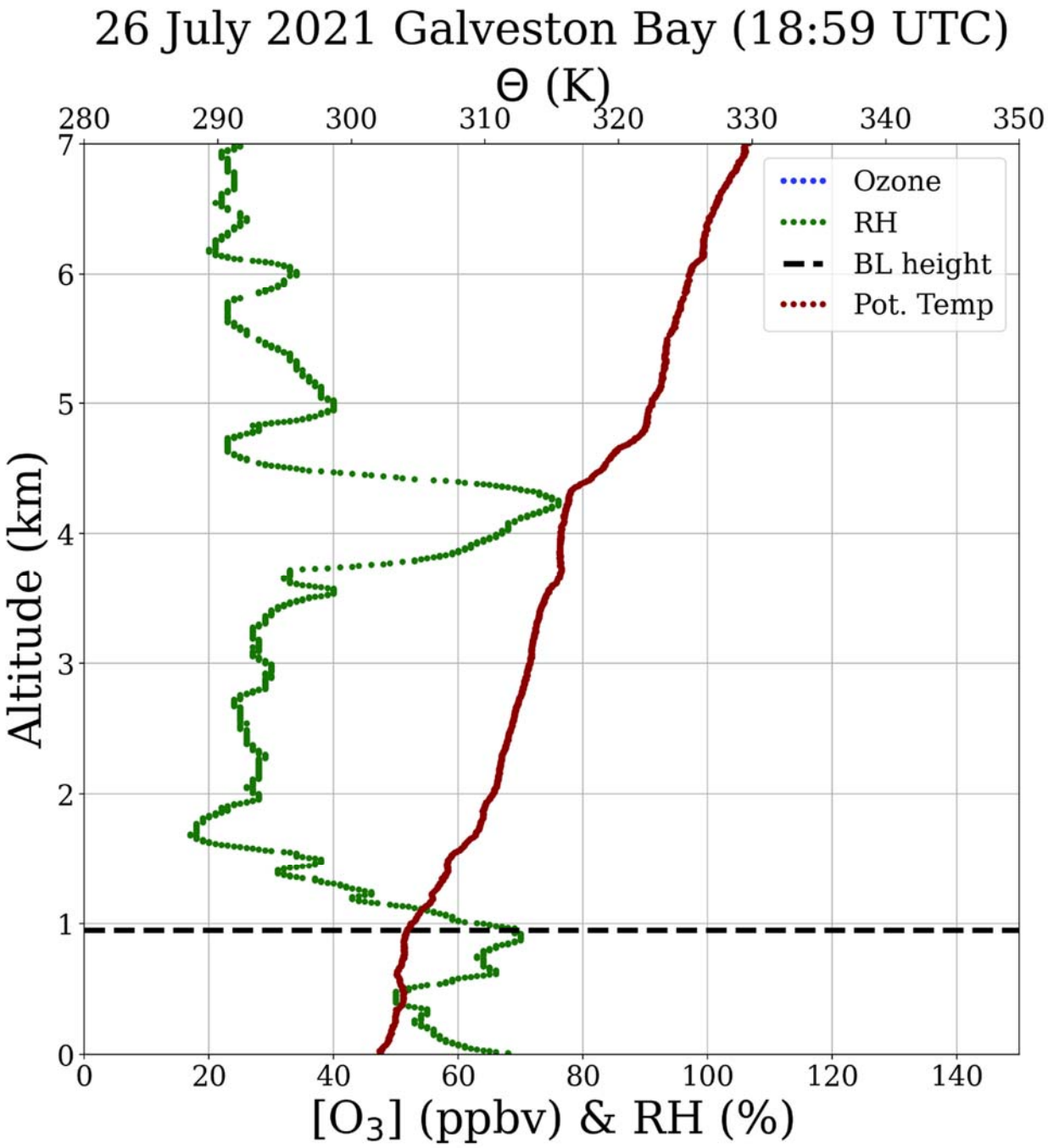

Figure 64. Vertical profiles of RH (green) and potential temperature (red) for a sounding on 26 July 2021 at 12:59 pm CST from near the Texas City Dike in Galveston Bay.

6.4.2.2 Case Study – September 9th, 2021

Nine ozonesondes were launched on 9 September 2021: 2 from the pontoon boat in Galveston Bay, 2 from La Porte, 2 from the University of Houston, and 3 from the Gulf of Mexico. The four profiles from Galveston Bay and La Porte are shown in Figure 65.

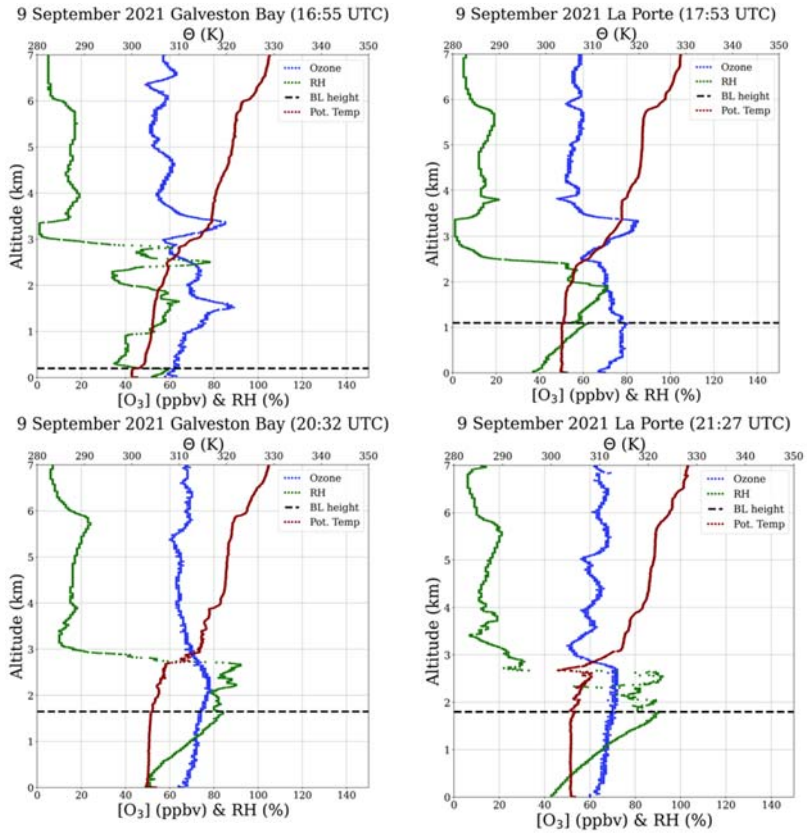

Figure 65. Ozonesonde profiles on 9 September 2021 from the pontoon boat in Galveston Bay (top-left and bottom-right panels), La Porte (top-right and bottom-right panels).

The first ozonesonde profile (launched near the Texas City Dike at 10:55 am CST; top-left panel of Figure 65) from Galveston Bay shows a marine layer at 0.2 km. Ceilometer data from the pontoon boat (Figure 66) shows general agreement with an aerosol layer at 0.25 km at the same time. The ceilometer data shows a second layer at 1.8 km, just above an ozone enhancement observed in the ozonesonde profile.

The second ozonesonde profile from the pontoon boat in Galveston Bay (launched in the NW quadrant of Galveston Bay at 2:32 pm CST; the bottom-left panel of Figure 65) shows features between 1.7 km and 2.8 km AMSL that are also observed in the pontoon boat ceilometer data (Figure 66). The ozonesonde launch occurred approximately 10 km east of La Porte, where an ozonesonde was also launched an hour later at 3:27 pm CST (profile shown in the bottom-right panel of Figure 65).

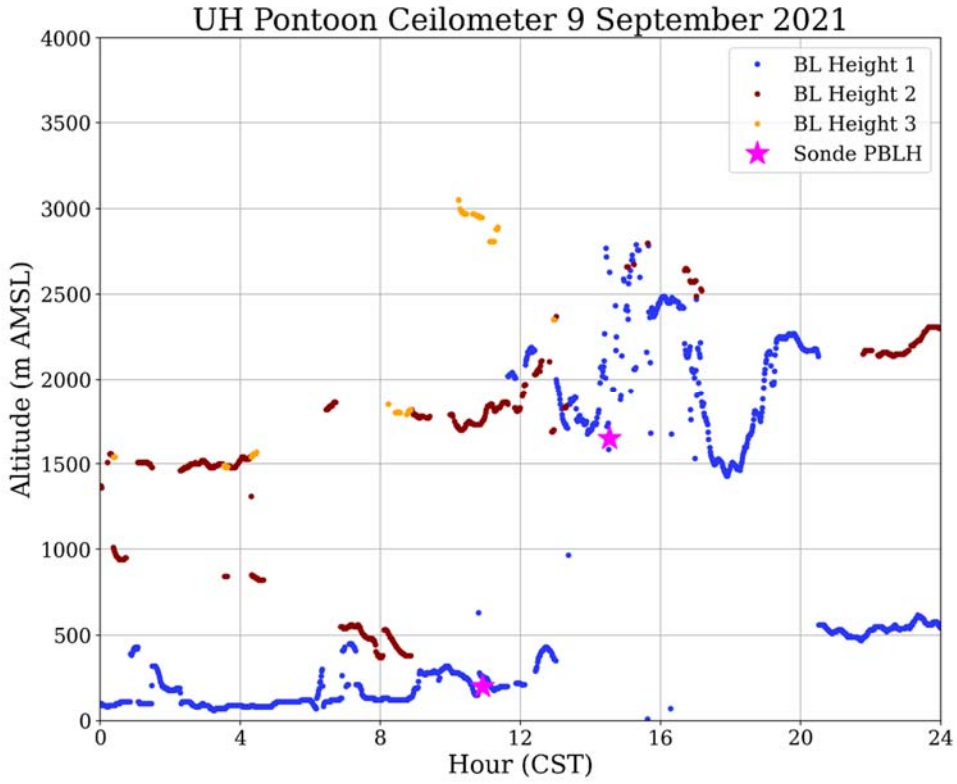

Figure 66. Ceilometer data from the pontoon boat on 9 September 2021.

6.5 Question 5

6.5.1 How do small O_3, O_X, and meteorology sampling systems installed on commercial vessels help us better understand O_3 and O_X in Galveston Bay and the Gulf of Mexico?

Air quality measurements over the water are sparse and often associated with intensive campaigns that may only operate for short periods. There are many challenges with continuous over-water measurements such as initially securing a site and access for maintenance, power, and data transfer. During projects such as TexAQS II / GoMACCS 2006, NOAA operated the R/V Ron Brown in the Gulf of Mexico in August and September of 2006. With a draft of 17' and a typical depth of Galveston Bay less than 10', the Brown was confined to the shipping lanes and commercial berths, and required scheduling to utilize the main channel, just as all large commercial vessels do. Measurements on offshore platforms have also been conducted, such as the radar wind profiler on a platform in the Gulf during the same campaign. Negotiating access to these platforms can be difficult as there are significant liability issues to be addressed, and accessing the equipment requires a helicopter or crew boat. Smaller unattended platforms do exist in Galveston Bay, but power availability would likely require a large solar panel system and significant battery supply for cloudy days.

For this project, commercial boat operators were selected based on their typical operating area, frequency of operations, power availability, and of course, willingness to work with the science team for a reasonable price. The use of these boats, combined with a small unobtrusive sampling package, allowed the team to collect measurements of O_3 in the Gulf of Mexico and parts of Galveston Bay with a frequency not seen before. The data, as described in the sections above, show a unique view of the O_3, Ox, and meteorology over the Bay, and as shown in the July 26th case study, can demonstrate the transport of high O_3 over the Bay into the Houston metro area's monitoring network, and yield clues as to the sources of this transported O_3.

6.5.2 Measurements of O_3 and meteorological parameters have been installed on commercial aircraft, such as in the MOZAIC project (Marenco et al., 1998). Do the vessels operating in Galveston Bay and the offshore coastal areas provide appropriate spatial coverage to investigate O_3 over water under a variety of weather conditions?

One of the lessons learned during this project was that smaller, single boat, single operator enterprises are potentially less likely to cover the area advertised. Initially, our Shrimp Boat operator described his typical operating pattern of shrimping in one section of the Bay for a few days at a time before moving onto another area. This was enticing such that a given area would be repeated several times and still cover a significant portion of the Bay. Unfortunately, for both COVID and weather-related impacts on the shrimp harvest, this boat's operations did not live up to the team's expectations. However, the commercial crew boat in the Gulf went out just as hoped and even made trips into the industrialized portion of the Houston Ship Channel and Trinity Bay on one occasion. The spatial coverage of this type of operation yielded significant amounts of data in previously unsampled areas, and as a commercial operator supporting oceangoing shipping, the Red Eagle operated in all weather conditions short of hurricanes and strong tropical storms. This vessel utilizes electric power for steering and is kept powered 24/7, even while in port. Future projects should consider using commercial vessels from larger operations that will not be dependent on a single individual or industry, such as fishing, which can be variable in activity level based on the weather and harvest.

6.5.3 Can a small sampling system be designed such that it operates with little to no impact on the routine vessel operations?

As demonstrated with the data and findings in the previous sections, it is possible to design a small sampling system that can be operated routinely with little to no intervention from the commercial boat operators. Careful selection of components such as high-efficiency power supplies and energy-efficient instruments and computers to reduce internal heat buildup, light-colored waterproof cases with insulation, and radiant barriers to reduce the impact of solar/ambient heating. A high-capacity thermoelectric air cooler was used to regulate the internal temperature to ~30 °C, sufficient to maintain instrument operating parameters while also avoiding condensation in the sample lines. The cooling systems rarely exceeded 60% of the cooler's capacity, even when the ambient temperatures exceeded 95 °F on the hottest days of the year. Watertight connectors, bulkhead fittings, large desiccant bags, and exhausting the sample back outside the case helped to prevent moisture build up inside the case, which could lead to corrosion. Internally the 2B instruments were upgraded with fresh dew lines to regulate humidity in the sample and redundant long-life sample pumps to reduce the likelihood of pump failure.

The sample flows of the 2Bs were regulated to ~1 standard liters per minute (slpm) to increase the residence time in the NO2 photocells and increase the conversion efficiency. The combination of flow rate and large surface area of the 90 mm filters allowed the team to reduce filter changes to once a month.

These cases were installed on the roofs of the pilot houses, as shown in Figure 2 and Figure 3 in Section 4.1 above. The cases were constructed such that an exterior button to force a reboot of the system was easily within reach of the crews if we were unable to contact or reboot the system remotely. The single power cord was then routed to the interior of the boat and plugged into a standard 120V wall outlet. The inlet used an extended Teflon rain shield to prevent rain and sea spray from entering the 90 mm filter collocated with the AirMar meteorological and GPS sensor at an elevated point to reduce impacts of the boat itself on the measurements (i.e. exhaust or turbulence). On the Shrimp Boat, the CL-51 ceilometer was positioned next to the O_3 sampling system to avoid issues with the rigging for the nets and to keep the cable lengths short.

The only contact between the Red Eagle crew and the science team was to notify the team that the mounting method specified by the boat's captain was beginning to come loose. The team quickly visited the boat, replaced the failing attachments, and significantly increased the number of attachment points, resolving the problem for the remainder of the project. The Shrimp Boat also operated quite well but did suffer one electrical failure on a wire segment with a blocking diode to isolate the thermoelectric cooler from the computer power. Due to changes in the wiring prior to deployment this diode was not needed, and a straight wire section was installed in the field, correcting the problem.

Other than the single maintenance visits to each boat, no unscheduled visits were required for either system over the course of the deployment (mid-July – October). The automated small sampling instrumentation worked quite well and proved a viable approach to collecting unattended measurements on commercial boats.

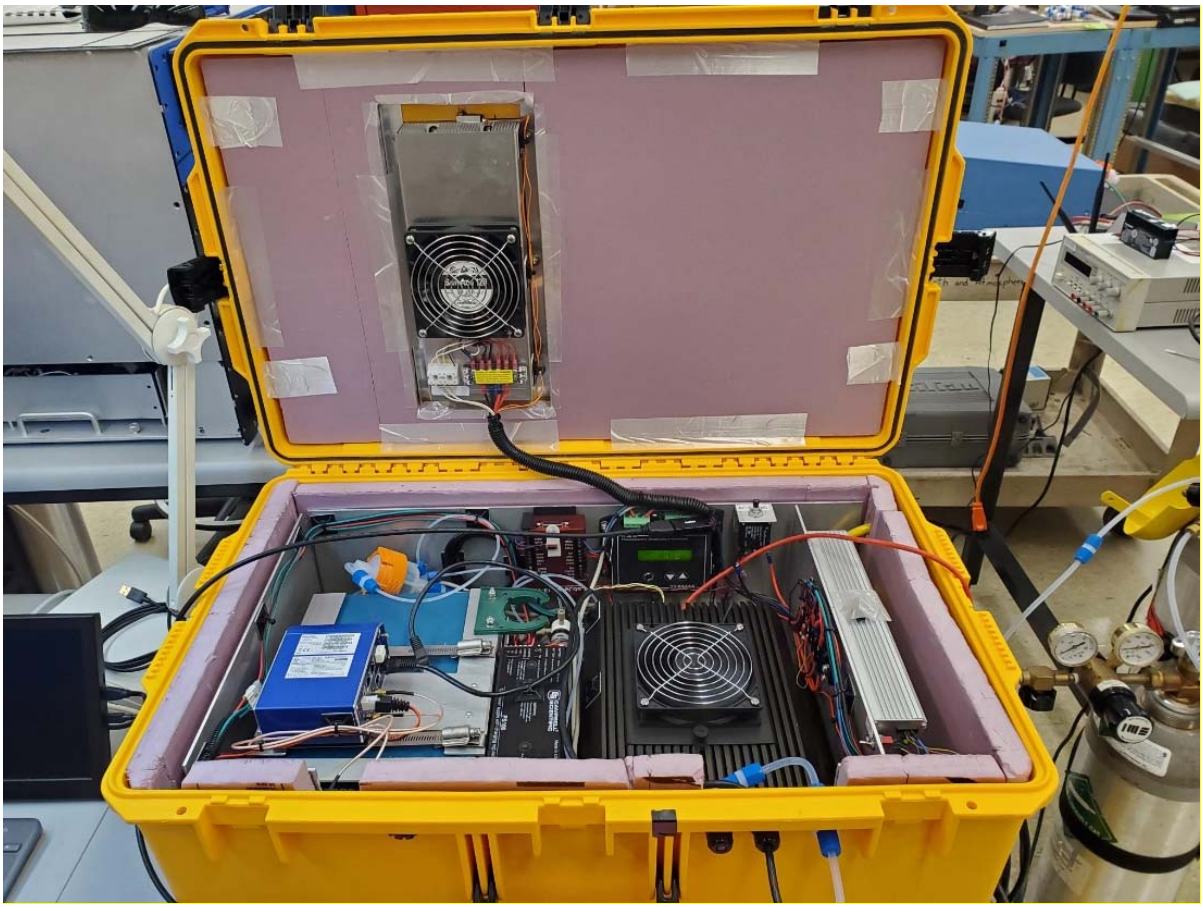

Figure 67. Instrumented weatherproof enclosure installed on the two commercial boats showing the 2B Tech O_3 monitor (blue box, bottom left), dual-sim cellular router (small blue box above 2B), backup battery (black box, center), zeroing cartridge (orange and clear, left rear), rugged industrial computer (black box with fan on top, right), high efficiency 24VDC power supply (silver box, far right). The rear panel of the chassis provides space for the LabJack U3 data card (red, center rear), thermoelectric temperature controller (black with green screen, rear behind computer), and circuit breaker for the thermoelectric cooler system (black button on silver tab, right of temperature controller). Space for mounting the NO_2 photocells is reserved on top of the O_3 analyzer, near the cellular router and will be installed for future campaigns.

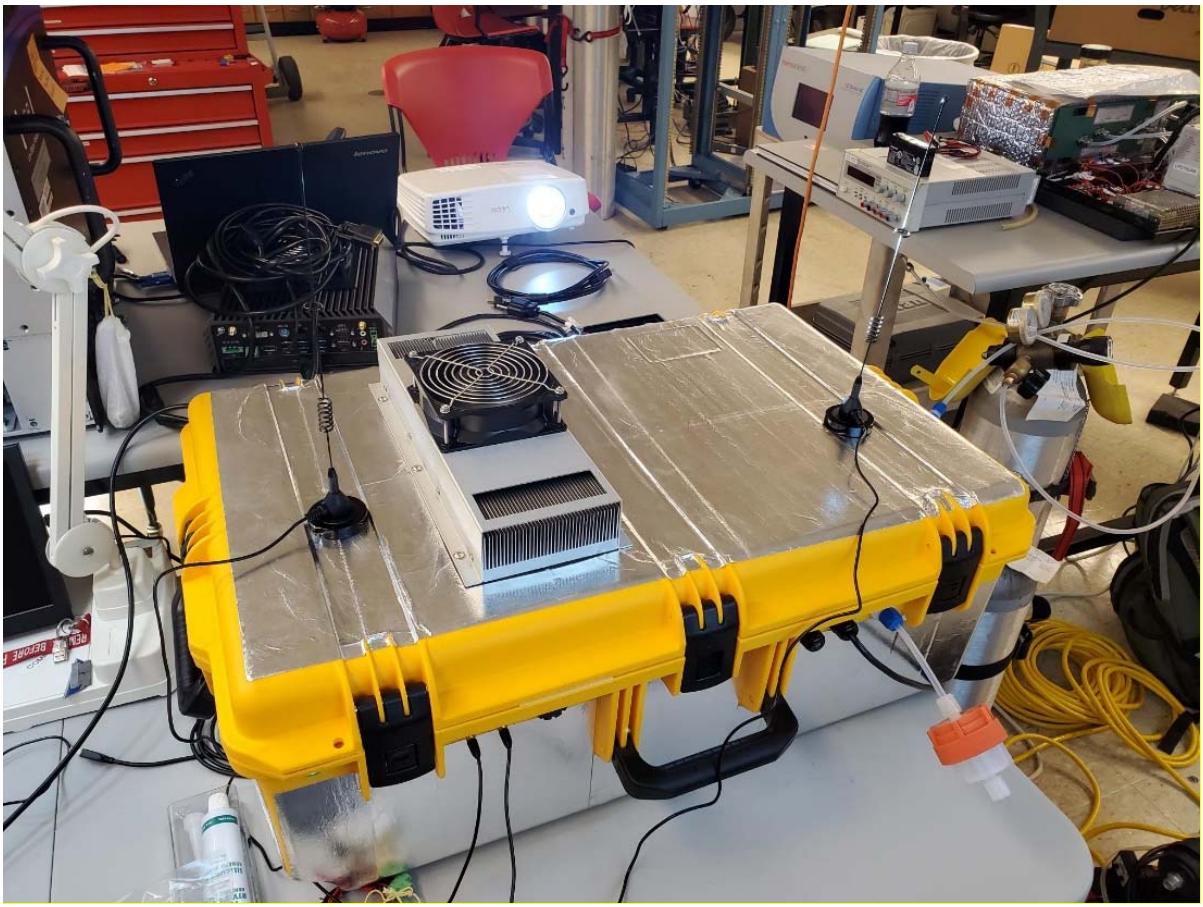

Figure 68. System closed for testing in the lab showing the radiant barrier applied to the exterior as well as the hot exhaust side of the thermoelectric cooler and dual cellular antennas.

7 Conclusions and Recommendations for Future Work

This project was highly successful, collected a robust set of data, and demonstrated that small sampling systems can be reliably deployed on commercial boats. Furthermore, traditional instrumentation can be deployed on a dedicated research boat and operated safely in Galveston Bay to collect O_3, Ox, boundary layer height, meteorological data, and serve as a platform for launching radiosondes and ozonesondes. Although delayed and limited to the UH pontoon boat, the addition of an NO_2 photocell to an O_3 monitor allowed for a measurement of Ox. Through careful calibration of the Ox and O_3 instruments, an estimate of NO_2 was possible, revealing that in addition to discrete plumes from passing boats and ships, broad areas of NO_2 were occasionally present over the Bay. Changes in the partitioning of O_3 and NO_2 resulted in apparent gradients in O_3 that were not as pronounced when examining Ox and would have otherwise been misrepresented. This further underscores the importance of understanding O_3 and NO_2, particularly in and around urban areas where titration can play a significant role.

WRF-GC model data predicted high O_3 (hourly O_3 over 70 ppbv) over Galveston Bay on 30-50% of the days during this project; O_3 over 70 ppbv was found on 23% (6 out of 26) trips into the Bay. WRF-GC did capture all the forecast high O_3 days; however, because of operational restrictions on the pontoon boat, such as water conditions, under-sampling by the pontoon boat may have occurred. Additionally, due to speed, fuel, and time limitations, only sections of the Bay could be sampled on any given day. High O_3 over the Gulf of Mexico was less frequent, modeled roughly 20% of the time. However, observations of O_3 over the Gulf did occur several times, including late at night and on occasion was as much as 110 ppbv (September 9, 2021). The modeled values were found to over predict O_3 over the Bay under most conditions, and vertical profiles of O_3 over Galveston Bay were also consistently overpredicted by 10-20 ppbv.

Ozone over the water did vary spatially and was not always uniform based on the observations from the UH pontoon and Red Eagle boats. High O_3 was rarely seen in the southern portions of Galveston Bay but was more frequently found in the northwestern portion. Some parts of the Bay, such as northern Galveston Bay between the Ship Channel and Baytown, were too shallow or populated with too many gas wells to safely navigate, so measurements in those sections were not attempted. Others like Trinity Bay tended to be rougher than our comfort level and operational limits for the pontoon typically allowed, in part due to the ability for uninterrupted winds on the Bay to create choppier conditions. Observations from the Red Eagle in the Gulf frequently found relatively low O_3 levels. However, O_3 over 70, and occasionally over 100 ppbv were encountered during this project and typically were not uniform throughout the trip.

The Ox measurements that were collected in the second half of September from the UH pontoon, along with the longer record of O_3 measurements, indicates that even coastal measurements such as those in Kemah showed fewer effects from local emissions resulting in the titration of O_3 relative to nearby monitors such as C45 in Seabrook. When compared to NO_2 measurements from Texas City and Smith Point, there was little agreement with the pontoon, an indication of both the local impacts on the measurements and the variability across and around the Bay. While it is unsurprising that ship plumes would titrate O_3 to NO_2, the frequency, strength, and reliable nature of plume encounters in the Bay is remarkable and could be exploited in future projects if shipping emissions are of interest.

Targeted ozonesonde launches, such as on July 18th, shed additional light on the potential depth of the layer in which O_3 may be depleted due to catalytic losses from halogen reactions near the surface of the water. Ten-day back trajectories were consistent with the O_3 levels and trajectory clusters found during the 2016 TCEQ halogen study at San Luis Pass, and the vertical motion of the lowest 1,500 m showed parcel movement that would cause air in that mass to potentially encounter lower layers which would be more directly influences by air-water interactions.

Several case studies during this campaign showed how local circulation patterns over and around the Bay could influence measured O_3 values. On July 26th, measurements from the Shrimp Boat and UH pontoon encountered a plume that moved from east to west and ultimately into the HGB monitoring network. Interestingly, this plume did not seem to impact measurements on the Red Eagle while docked in northern Galveston. Impacts from Gulf breezes were also observed on several occasions, notably September 9th, where the evening breeze caused a rapid (minutes) increase of 40-50 ppbv of O_3 at both the Smith Point and UH pontoon boat monitors. Other

periods in September, in conjunction with other programs supported by NASA and the TCEQ, also show multi-day episodes where local and regional circulation patterns affected O_3 over the Gulf, Bay, and Houston metro area. These results will be more thoroughly addressed in separately funded work as it incorporates numerous other datasets which have yet to be finalized.

During this project, a land-bay breeze reversal was noted roughly 1/3 of the time when examining data from C45 in Seabrook. Not all days resulted in hourly O_3 over 70 ppbv; however, 6 days, or 20% of the land-bay breeze events, did report hourly O_3 of 70 ppbv or greater. One anecdotal observation by the UH pontoon crew was that conditions over the Bay tended to be more cloud-free than over the surrounding land. This, combined with a potential higher UV albedo of water compared to grass-covered ground, could increase O_3 production over Galveston Bay relative to nearby land. While it is often discussed whether an airmass is NOx or VOC limited, the formation of ozone is photon limited across all regimes.

Measured boundary layer heights over the Bay differed from the model and between the two measurement locations on the east and west sides of the Bay. While the second and third measured layers agreed quite well, the lowest layer did not and interestingly portrayed nearly opposite diurnal profiles. On the western side, the pontoon boat measured from a marina in Kemah presented a more traditional diurnal profile of boundary layer height, lowest overnight and in the early morning with a peak in mid-late afternoon before decreasing again with the loss of solar heating. In contrast, the Smith Point site on the east side showed a consistent and higher boundary layer between midnight and noon, with a significant decrease in the afternoon. The current hypothesis is that this could be related to the onset of the Gulf breeze. However more study is needed before any definitive conclusions can be drawn.

Data from this project collected by the Red Eagle, Shrimp Boat, and the UH pontoon boat over the Gulf of Mexico and Galveston Bay could inform future modeling studies by providing measurements to compare model boundary conditions. It could also be used to determine the proper parameters to use in CAMx in order for the model results to better represent the observations. Additionally, to better represent coastal ozone and meteorology in the WRF-GC model, two major improvements could be implemented for the current model settings. One is to adopt fine resolution (e.g. 1–4 km) emissions with detailed emission patterns for major roads and the Shipping Channel for Houston-Galveston region, replacing the current 10 km-resolution emissions in the model. The second is to test the best practice for model physics schemes, particularly PBL schemes, that may work best over land vs. water. Additional sensitivity tests employing results from this and the prior halogen study results may allow for additional improvements in the modeling of O_3 over water on the Texas coast.

With the successful deployment of the instrument packages, continued measurements over the Gulf of Mexico and Galveston Bay with these systems would be useful to follow up on the trends and spatial patterns observed in O_3, Ox, and boundary layer heights. The incorporation of NO_2 photocells into the small sampling packages are planned over the winter (2021-2022), making it possible to deploy the measurements for a full ozone season (April – October 2022) and potentially capture different patterns in the spring ozone peak as well as provide comparisons to the 2021 summer/fall ozone season measurements.

Because the pontoon boat is owned and operated by UH researchers, it is also possible to include more traditional measurement equipment than would be realistic to automate on a commercial vessel. These measurements could include trace gases such as NO, NOx, NOy, CO, and SO_2 in addition to O_3 to better characterize the photochemical age of the plume and emission sources. VOC measurements, such as resin tube sampling, could help to better understand potential sources influencing chemistry over the water as well as aiding photochemical modeling. Measuring the photolysis rate of NO_2 from the pontoon boat and nearby inland location, such as the UH trailer collocated at the La Porte airport C243 site, would allow for quantifying the relative impact of clouds on photochemistry and O_3 production over the water. Additional measurements on the commercial boats could include boundary layer height measurements so that all boats have ceilometers. It may also be possible to set up a small VOC sampling system to either operate when certain conditions are met (i.e. latitude/longitude boundaries, forward motion, O_3 levels, etc.) or on a fixed schedule. Similarly, the addition of small optical particle spectrometers may identify periods when increased aerosol loadings are present, such as transported dust and biomass burning smoke events. With respect to the two commercial boat operators used this year, the Red Eagle was much more active than the Shrimp Boat for reasons described previously. Future projects may benefit from choosing to partner with commercial operations that service industry and transportation and are less dependent on weather, fishing, or single individuals, which can have more disruptions to their operations. For instance, the Red Eagle is just one of many crew and service boats operated by the same company, and certain boats tend to operate in more defined areas than others, such as the industrialized and controlled portion of the Houston Ship Channel.

8 References

- Banta, R., Senff, C., Nielsen-Gammon, J., Darby, L., Ryerson, T., Alvarez, R., Sandberg, S., Williams, E., Trainer, M., 2005. A bad air day in Houston. Bulletin of the American Meteorological Society 86, 657-670.
- Berlin, S.R., Langford, A.O., Estes, M., Dong, M., Parrish, D.D., 2013. Magnitude, decadal changes, and impact of regional background ozone transported into the Greater Houston, Texas, area. Environmental science & technology 47, 13985-13992.
- Caicedo, V., Rappenglueck, B., Cuchiara, G., Flynn, J., Ferrare, R., Scarino, A., Berkoff, T., Senff, C., Langford, A., Lefer, B., 2019. Bay and sea-breeze circulations impacts on the planetary boundary layer and air quality from an observed and modeled DISCOVER-AQ Texas case study. Journal of Geophysical Research: Atmospheres.
- Dunker, A., Koo, B., Yarwood, G., 2019. Standard and alternative procedures for projecting future ozone in the Houston area using relative reduction factors, Atmospheric Environment: X, 2, 2590-1621, https://doi.org/10.1016/j.aeaoa.2019.100029.
- Flynn, J., et al. (2010), Impact of clouds and aerosols on ozone production in Southeast Texas, Atmospheric Environment, 44(33), 4126-4133, doi:10.1016/j.atmosenv.2009.09.005.
- Goldberg, D.L., Loughner, C.P., Tzortziou, M., Stehr, J.W., Pickering, K.E., Marufu, L.T., Dickerson, R.R., 2014. Higher surface ozone concentrations over the Chesapeake

Bay than over the adjacent land: Observations and models from the DISCOVER-AQ and CBODAQ campaigns. Atmospheric environment 84, 9-19.

- Jacob, D.J. and Winner, D.A., 2009. Effect of climate change on air quality. *Atmospheric environment*, *43*(1), pp.51-63.
- Langford, A., Senff, C., Banta, R., Hardesty, R., Alvarez, R., Sandberg, S.P., Darby, L.S., 2009. Regional and local background ozone in Houston during Texas Air Quality Study 2006. Journal of Geophysical Research: Atmospheres 114.
- Li, L., Chen, C., Huang, C., Huang, H., Zhang, G., Wang, Y., Wang, H., Lou, S., Qiao, L., Zhou, M., 2012. Process analysis of regional ozone formation over the Yangtze River Delta, China using the Community Multi-scale Air Quality modeling system. Atmospheric Chemistry and Physics 12, 10971-10987.
- Liu, X., Tai, A. P. K., and Fung, K. M.: Responses of surface ozone to future agricultural ammonia emissions and subsequent nitrogen deposition through terrestrial ecosystem changes, Atmos. Chem. Phys. Discuss., https://doi.org/10.5194/acp-2021-492, accepted, 2021.
- Loughner, C.P., Allen, D.J., Pickering, K.E., Zhang, D.-L., Shou, Y.-X., Dickerson, R.R., 2011. Impact of fair-weather cumulus clouds and the Chesapeake Bay breeze on pollutant transport and transformation. Atmospheric environment 45, 4060-4072.
- Mazzuca, G.M., Pickering, K.E., Clark, R.D., Loughner, C.P., Fried, A., Zweers, D.C.S., Weinheimer, A.J., Dickerson, R.R., 2017. Use of tethersonde and aircraft profiles to study the impact of mesoscale and microscale meteorology on air quality. Atmospheric environment 149, 55-69.
- Mellor, G.L. and Yamada, T., 1982. Development of a turbulence closure model for geophysical fluid problems. Reviews of Geophysics, 20(4), pp.851-875.
- Murphy, C.F., Allen, D.T., 2005. Hydrocarbon emissions from industrial release events in the Houston-Galveston area and their impact on ozone formation. Atmospheric Environment 39, 3785-3798.
- Nakanishi, M. and Niino, H., 2006. An improved Mellor–Yamada level-3 model: Its numerical stability and application to a regional prediction of advection fog. Boundary-Layer Meteorology, 119(2), pp.397-407.
- Nakanishi, M. and Niino, H., 2009. Development of an improved turbulence closure model for the atmospheric boundary layer. Journal of the Meteorological Society of Japan. Ser. II, 87(5), pp.895-912.
- Nielsen-Gammon, J., Tobin, J., McNeel, A., Li, G., 2005. A conceptual model for eight-hour ozone exceedances in Houston, Texas Part I: Background ozone levels in eastern Texas.
- Osthoff, H.D., Roberts, J.M., Ravishankara, A., Williams, E.J., Lerner, B.M., Sommariva, R., Bates, T.S., Coffman, D., Quinn, P.K., Dibb, J.E., 2008. High levels of nitryl chloride in the polluted subtropical marine boundary layer. Nature Geoscience 1, 324.
- Parrish, D., Allen, D.T., Bates, T., Estes, M., Fehsenfeld, F., Feingold, G., Ferrare, R., Hardesty, R., Meagher, J., Nielsen-Gammon, J., 2009. Overview of the second Texas air quality study (TexAQS II) and the Gulf of Mexico atmospheric composition and climate study (GoMACCS). Journal of Geophysical Research: Atmospheres 114.

- Renata Chadyšiene & Aloyzas Girgždys (2008) Ultraviolet radiation albedo of natural surfaces, Journal of Environmental Engineering and Landscape Management, 16:2, 83-88, DOI: 10.3846/1648-6897.2008.16.83-88
- Sadiq, M., Tai, A. P. K., Lombardozzi, D., and Val Martin, M.: Effects of ozone-vegetation coupling on surface ozone air quality via biogeochemical and meteorological feedbacks, Atmos. Chem. Phys., 17, 3055–3066, doi.org/10.5194/acp-17- 3055-2017, 2017.
- Schulze, B.C., Wallace, H.W., Bui, A.T., Flynn, J.H., Erickson, M.H., Alvarez, S., Dai, Q., Usenko, S., Sheesley, R.J., Griffin, R.J., 2018. The impacts of regional shipping emissions on the chemical characteristics of coastal submicron aerosols near Houston, TX. Atmospheric Chemistry and Physics 18, 14217-14241.
- Stauffer, R.M., Thompson, A.M., 2015. Bay breeze climatology at two sites along the Chesapeake bay from 1986–2010: Implications for surface ozone. Journal of atmospheric chemistry 72, 355-372.
- Tanaka, P.L., Riemer, D.D., Chang, S., Yarwood, G., McDonald-Buller, E.C., Apel, E.C., Orlando, J.J., Silva, P.J., Jimenez, J.L., Canagaratna, M.R., 2003. Direct evidence for chlorine-enhanced urban ozone formation in Houston, Texas. Atmospheric Environment 37, 1393-1400.
- Vizuete, W., Kim, B.-U., Jeffries, H., Kimura, Y., Allen, D.T., Kioumourtzoglou, M.-A., Biton, L., Henderson, B., 2008. Modeling ozone formation from industrial emission events in Houston, Texas. Atmospheric Environment 42, 7641-7650.
- Wallace, H.W., Sanchez, N.P., Flynn, J.H., Erickson, M.H., Lefer, B.L., Griffin, R.J., 2018. Source apportionment of particulate matter and trace gases near a major refinery near the Houston Ship Channel. Atmospheric environment 173, 16-29.
- Wang, L., Tai, A.P., Tam, C.Y., Sadiq, M., Wang, P. and Cheung, K.K.,: Impacts of future land use and land cover change on mid-21st-century surface ozone air quality: distinguishing between the biogeophysical and biogeochemical effects, Atmos. Chem. Phys., 20, 11349–11369, doi.org/10.5194/acp-20-11349-2020, 2020.
- Wang, Y., Jia, B., Wang, S.-C., Estes, M., Shen, L., Xie, Y., 2016. Influence of the Bermuda High on interannual variability of summertime ozone in the Houston–Galveston–Brazoria region. Atmospheric Chemistry and Physics 16, 15265-15276.
- Williams, E., Lerner, B., Murphy, P., Herndon, S., Zahniser, M., 2009. Emissions of NOx, SO2, CO, and HCHO from commercial marine shipping during Texas Air Quality Study (TexAQS) 2006. Journal of Geophysical Research: Atmospheres 114.
- Yerramilli, A., Challa, V.S., Dodla, V.B.R., Myles, L., Pendergrass, W.R., Vogel, C.A., Tuluri, F., Baham, J.M., Hughes, R., Patrick, C., 2012. Simulation of surface ozone pollution in the Central Gulf Coast region during summer synoptic condition using WRF/Chem air quality model. Atmospheric Pollution Research 3, 55-71.

9 Appendix

9.1 7 October 2021:

Travis Griggs (UH) and Ryan Salazar (UH) met at Portofino Harbor Marina at 8:00 am CST and pushed off at 8:40am CST. High ozone (~60 ppb) was observed from morning onward. The pontoon initially went South towards San Leon, then east across the Houston Ship Channel (HSC) at the south cut. The pontoon then worked North and crossed back west over the HSC at the north cut. Ozone concentrations exceeded 100 ppb at approximately 10:30 am (CST) near the intersection of the Bayport channel and the main ship channel. The science team decided to anchor and launch an ozonesonde (GB030 launched at 11:27 pm CST) north of the Bayport Channel. The ozone concentration was at 100 ppb on the pontoon boat at the time of release. After the launch a gradient pattern in the NW quadrant where the highest observed ozone of the year was recorded, with max concentrations exceeding 130 ppb in the afternoon. When fuel was approaching reserve levels, course was set to Kemah for refuel and to dock.

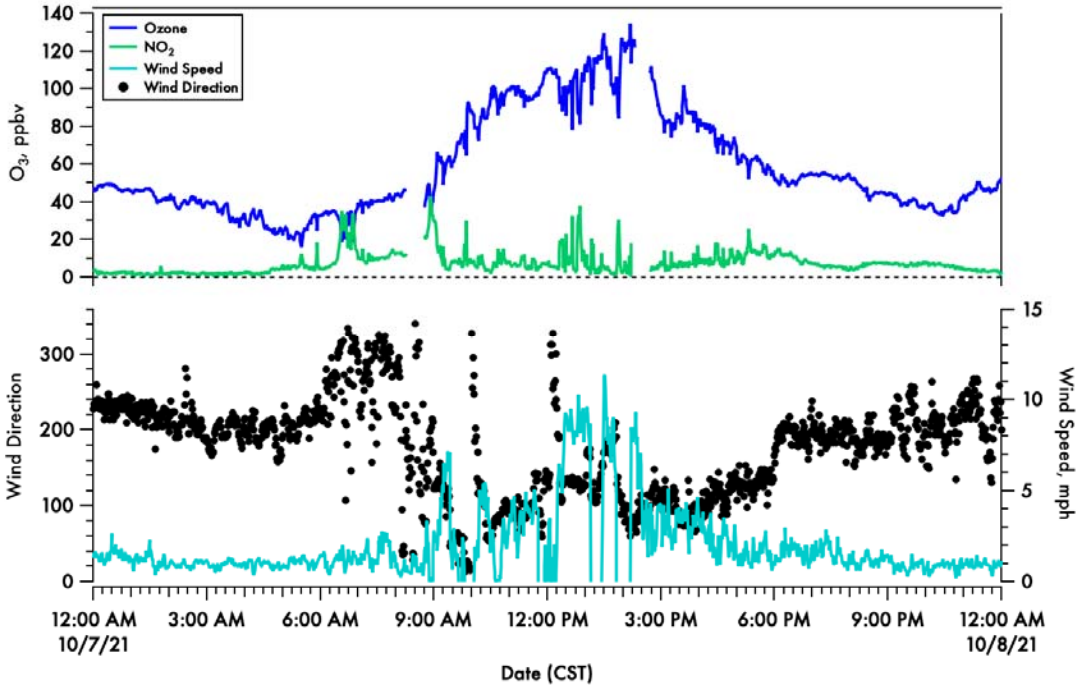

Figure 69. A time-series of 1-minute averaged ozone (blue) and calculated NO_2 (green) on the top panel and wind speed (light blue) and direction (black dots) in the bottom panel.

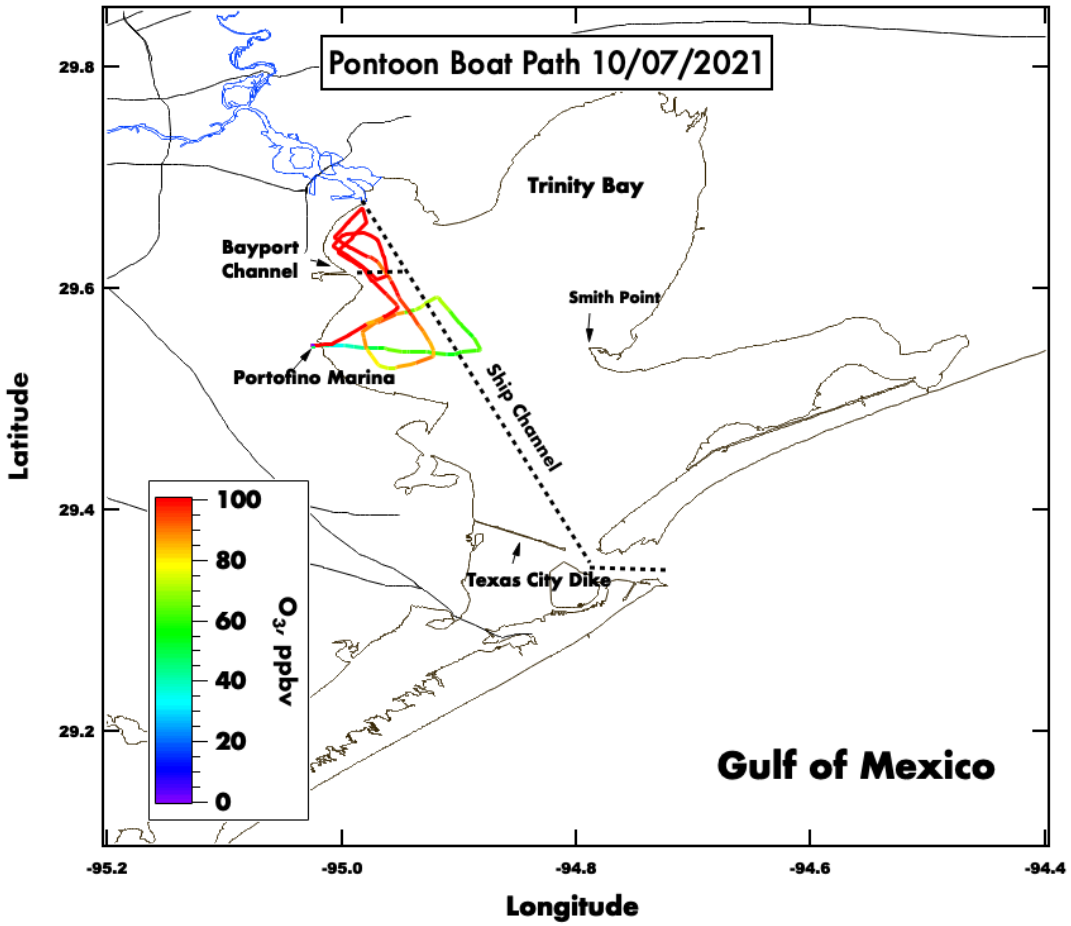

Figure 70. Spatial plot of surface ozone collected from the UH pontoon boat on October 7th, 2021.

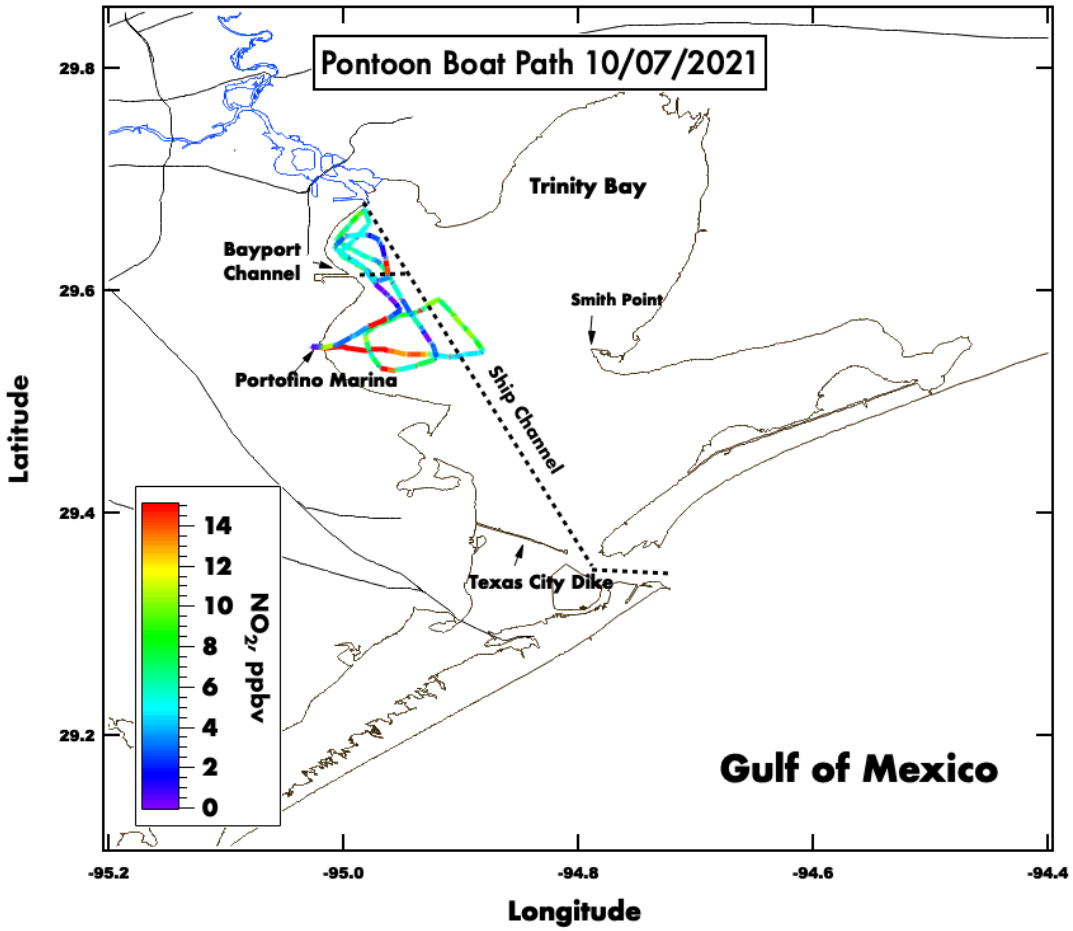

Figure 71. Spatial plot of surface NO_2, calculated from observed Ox, collected from the UH pontoon boat on October 7th, 2021.

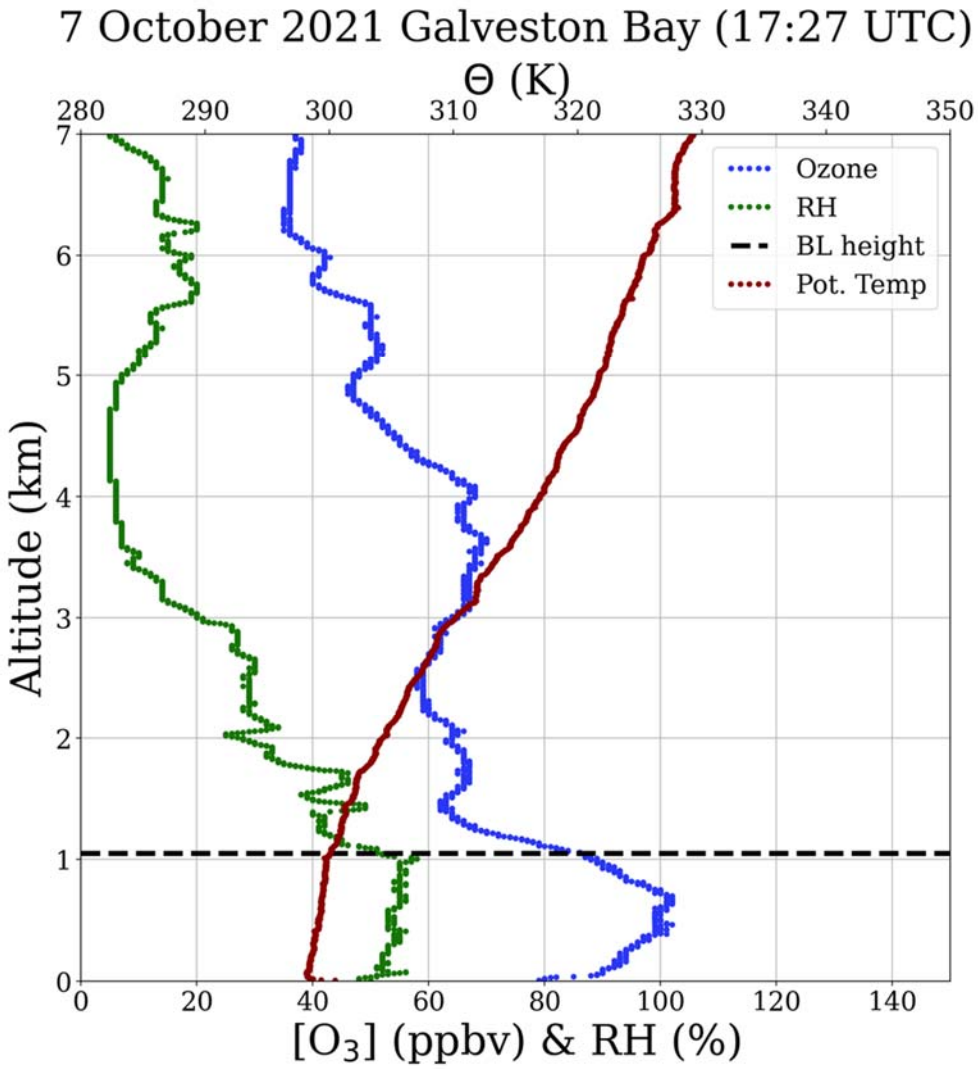

Figure 72. Vertical profiles of ozone (blue), relative humidity (green) and potential temperature (red). The derived boundary layer height is denoted by the horizontal dashed black line.

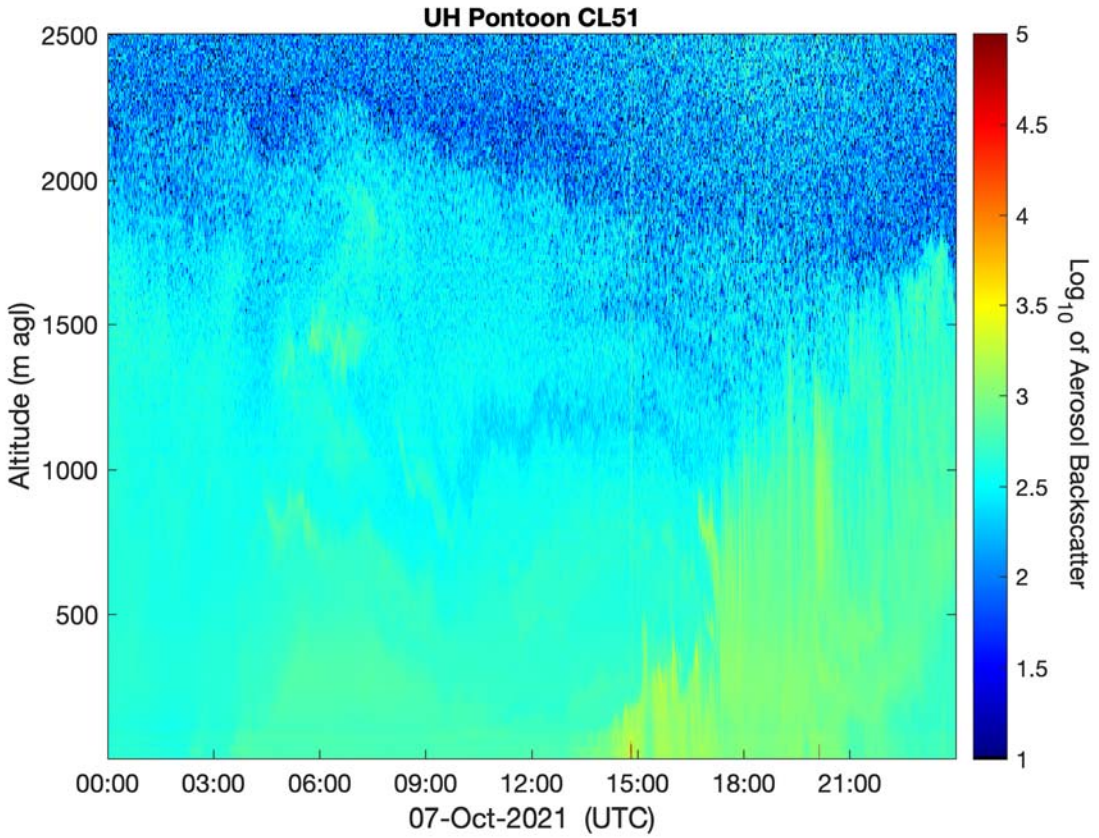

Figure 73. Vertical profile of the aerosol backscatter collected from a Vaisala CL-51 ceilometer mounted on the UH Pontoon boat.

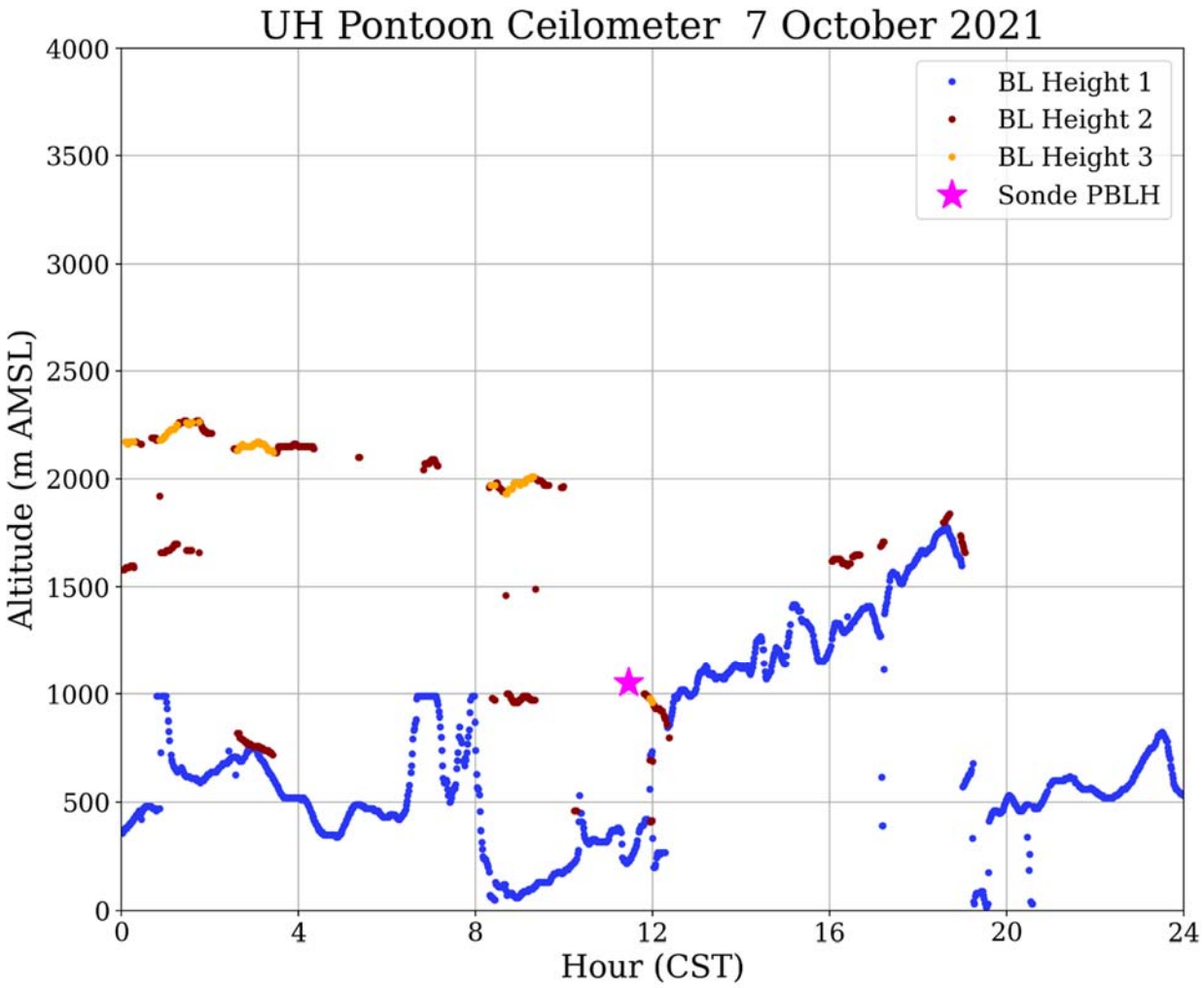

Figure 74. UH Pontoon Vaisala CL-51 ceilometer returned boundary layer heights and boundary layer heights from the ozonesonde profile.

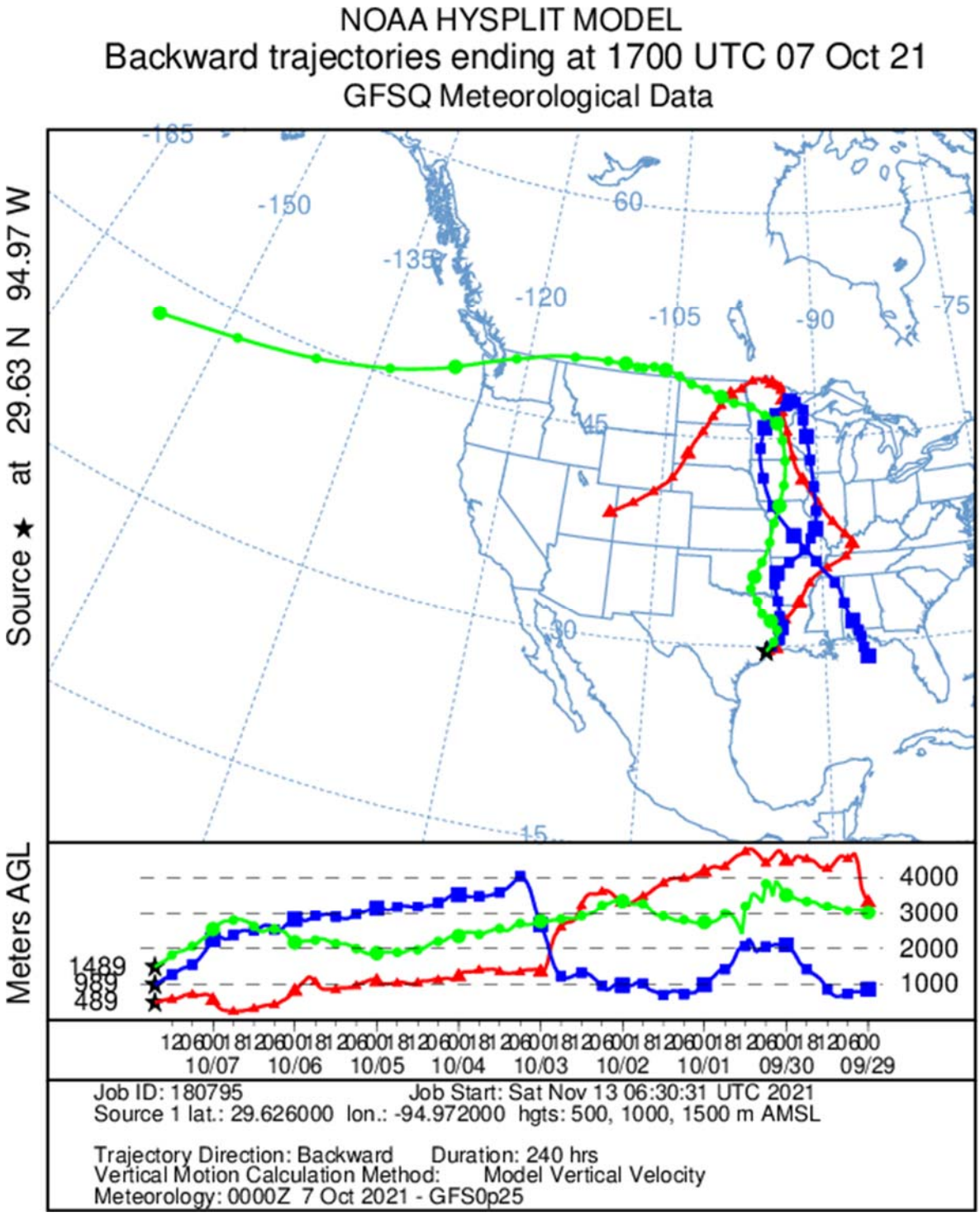

Figure 75. Ten-day HYSPLIT back trajectory for the ozonesonde launch on 7 October 2021 from three heights over the Bay: 500 m (red), 1,000 m (blue), and 1,500 m (green). Each data point is 6 hours apart.

9.2 6 October 2021:

Travis Griggs and Luke Griggs met at the marina at 9:00am CST. The day's plan was to go South towards Texas City and then circle back to the N/NW portion of the Bay in the afternoon. Ozone was moderate in the south, ~50ppb at 11:00am CST, but began to increase on the transit North, getting up to 75-80ppb by 1:00pm CST, in the NW area of the Bay. On the way back to the Marina another uptick to nearly 100ppb ozone was observed. It was decided to launch the ozonesonde (GB029) that was prepared. A successful launch occurred at 2:00pm CST, just outside of the Clear Lake Channel. Fuel was exhausted for the day and the pontoon boat was refueled and docked at ~ 3:00pm CST.

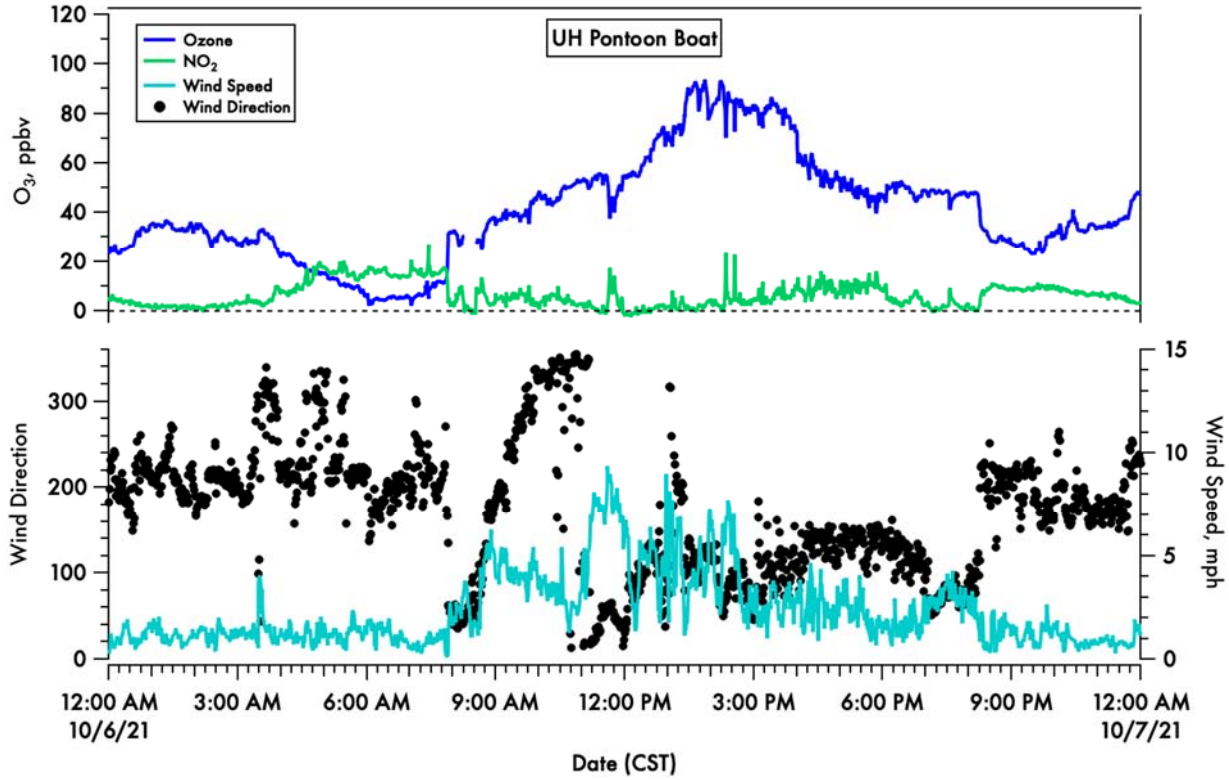

Figure 76. A time-series of 1-minute averaged ozone (blue) and calculated NO_2 (green) on the top panel and wind speed (light blue) and direction (black dots) in the bottom panel.

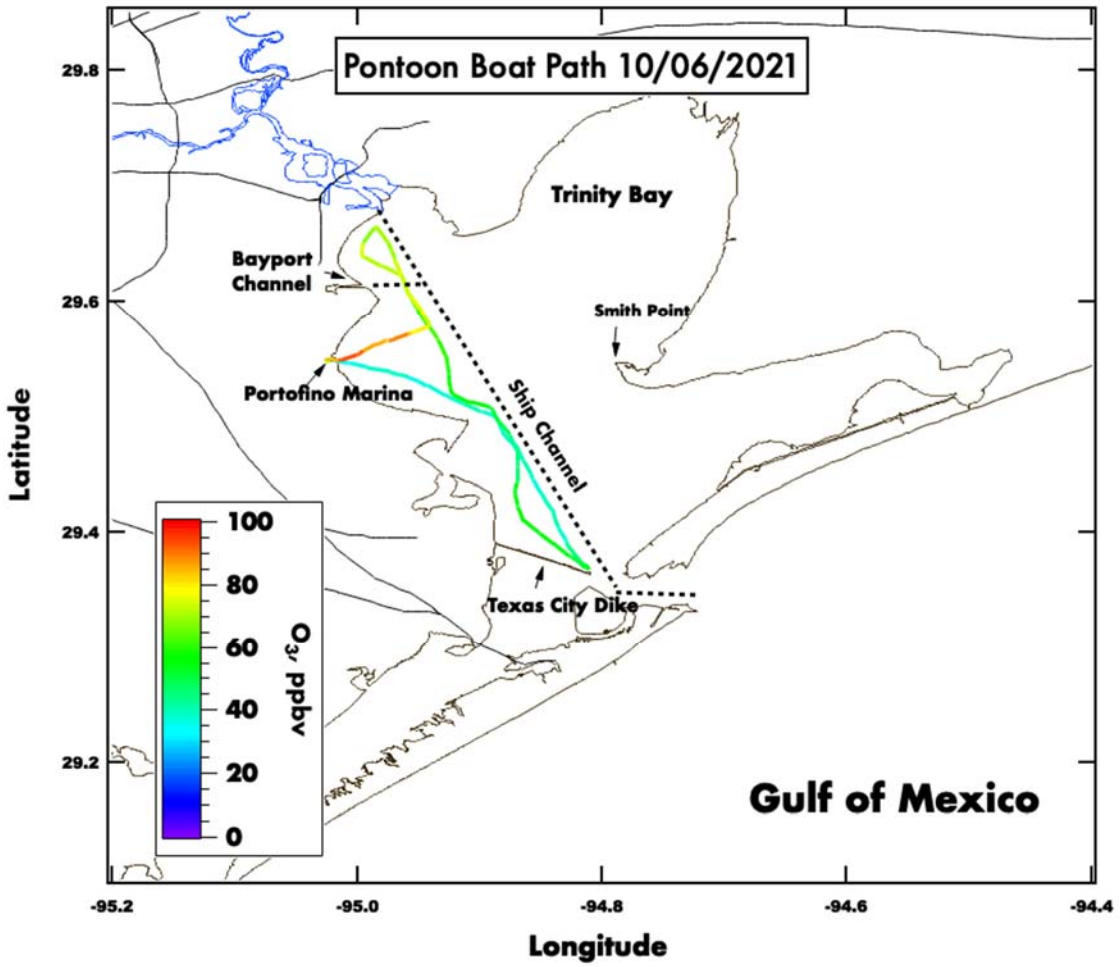

Figure 77. Spatial plot of surface ozone collected from the UH pontoon boat on October 6th, 2021.

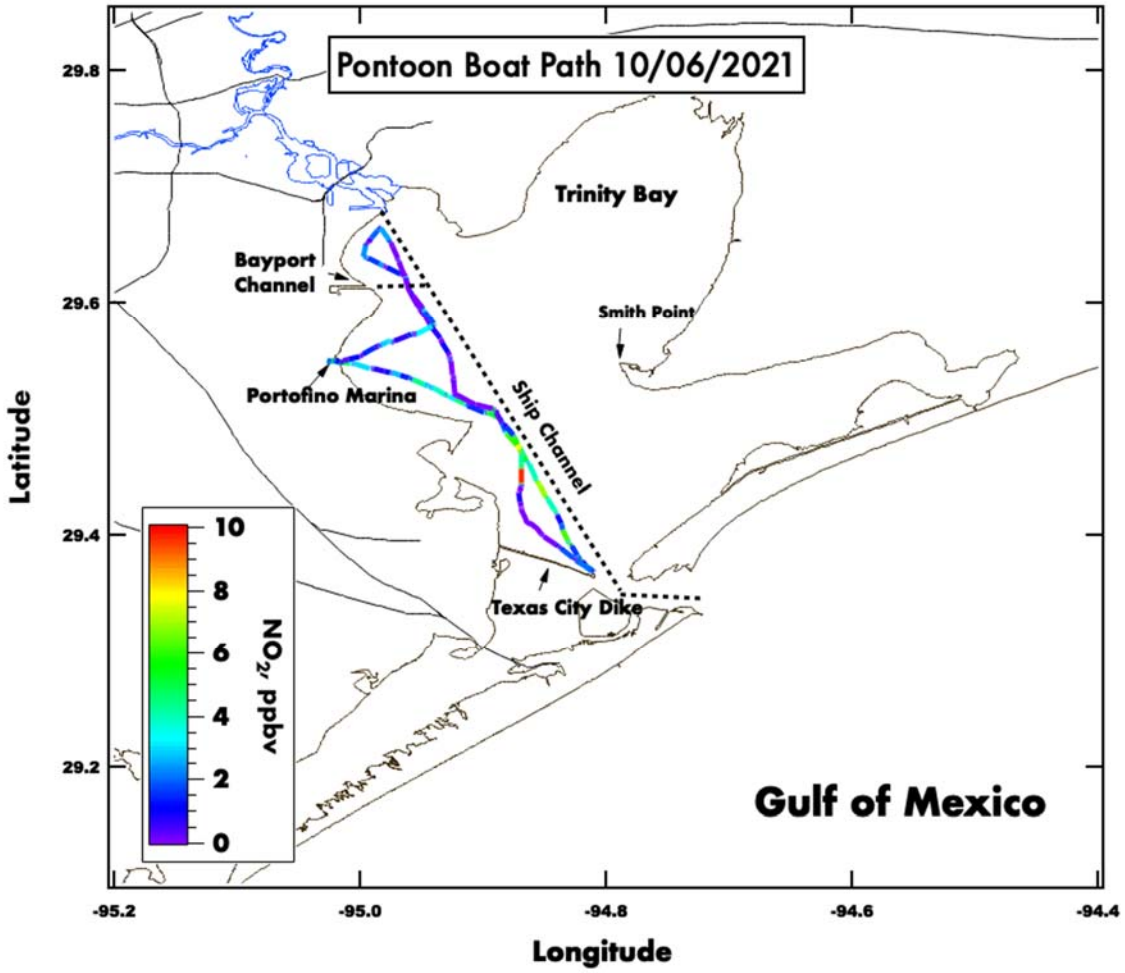

Figure 78. Spatial plot of surface NO_2, calculated from observed Ox, collected from the UH pontoon boat on October 6th, 2021.

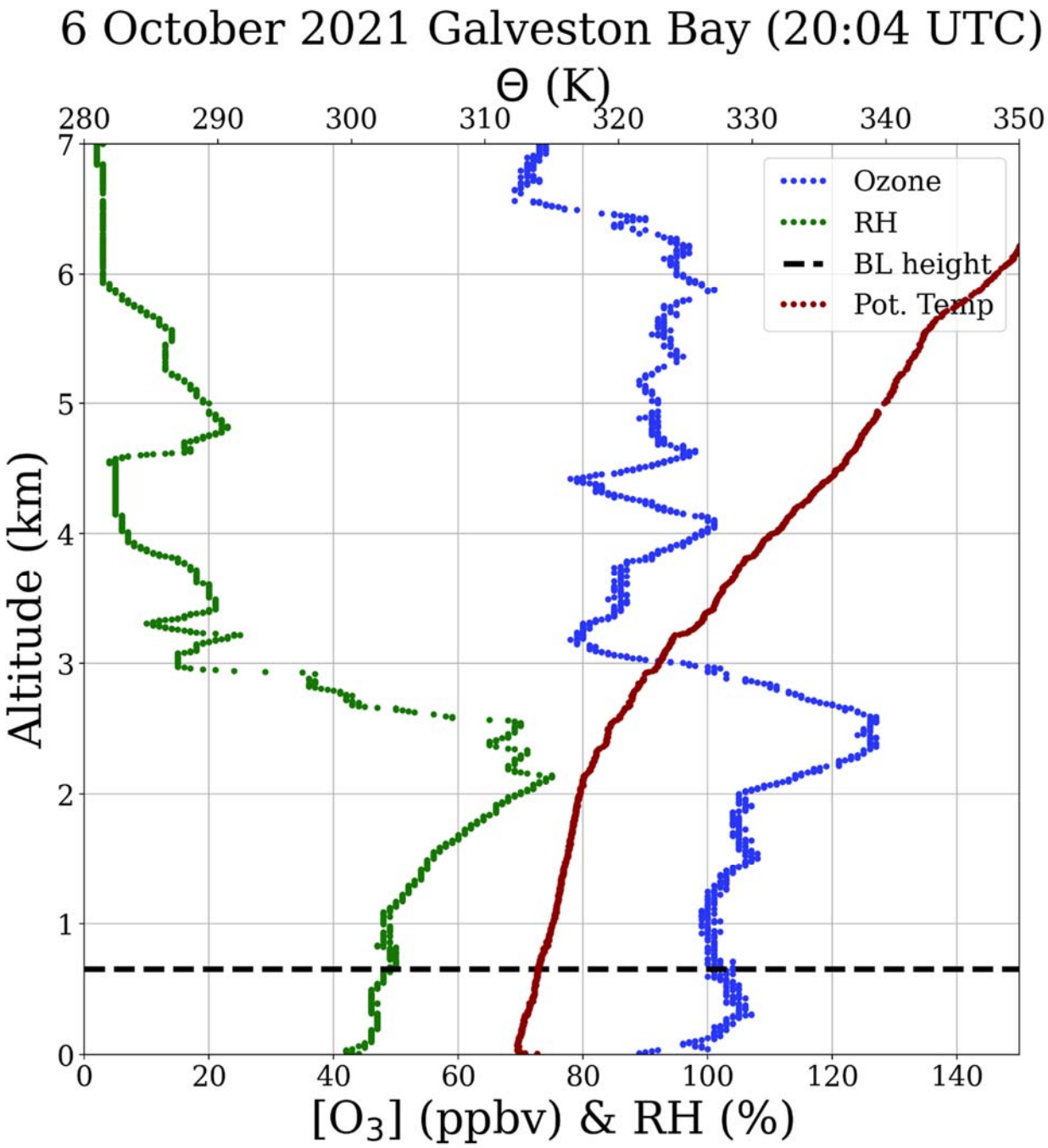

Figure 79. Vertical profiles of ozone (blue), relative humidity (green) and potential temperature (red). The derived boundary layer height is denoted by the horizontal dashed black line.

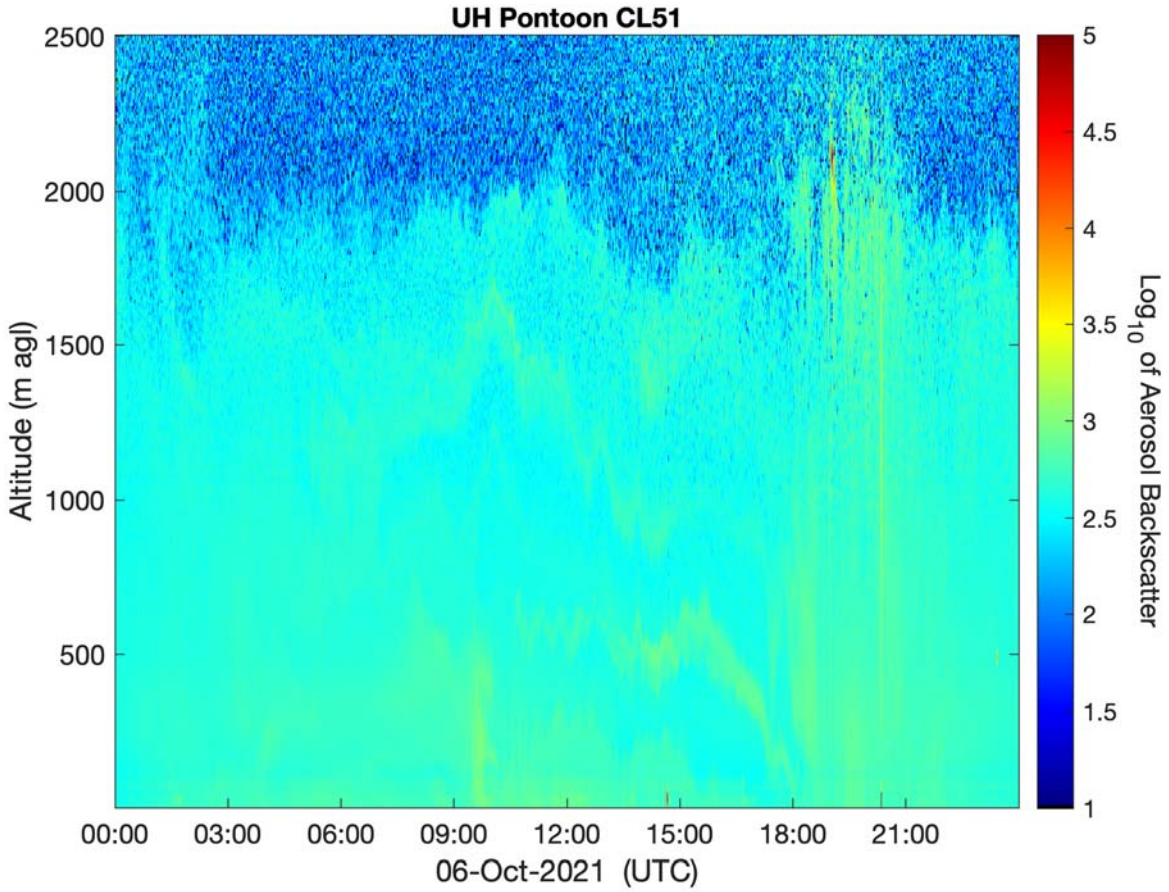

Figure 80. Vertical profile of the aerosol backscatter collected from a Vaisala CL-51 ceilometer mounted on the UH Pontoon boat.

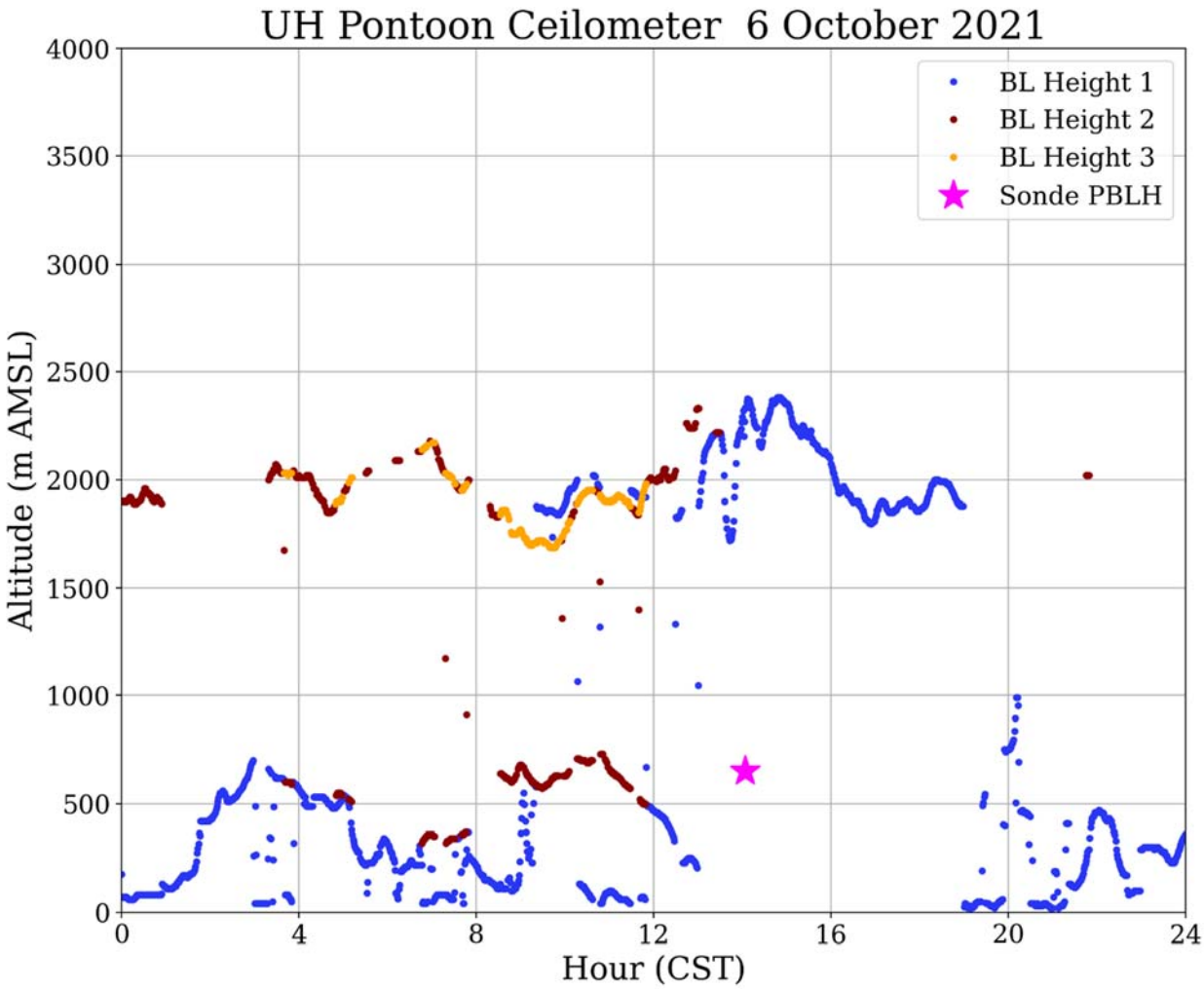

Figure 81. UH Pontoon Vaisala CL-51 ceilometer returned boundary layer heights and boundary layer heights from the ozonesonde profile.

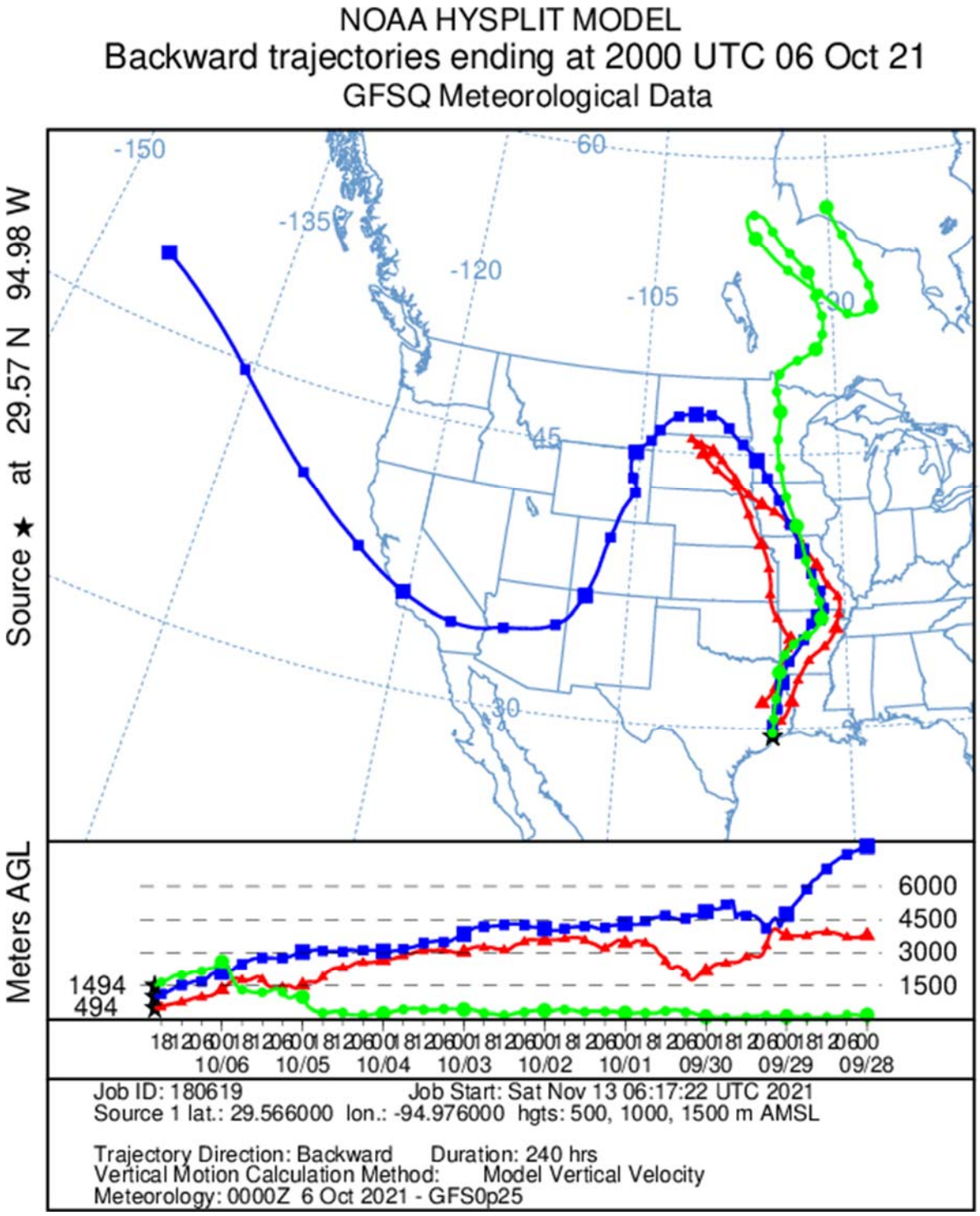

Figure 82. Ten-day HYSPLIT back trajectory for the ozonesonde launch on 6 October 2021 from three heights over the Bay: 500 m (red), 1,000 m (blue), and 1,500 m (green). Each data point is 6 hours apart.

9.3 26 September 2021:

Travis Griggs (UH), Angelique Demitillo (UVA) and Hieu (NASA Fellow) met at the marina at 8:30am. The days plan was to launch 2 ozonesondes in the NW quadrant of the Bay to coincide with the NASA aircraft (last flight day). The first launch was at 9:00am CST(coincided with the Raster 1 flyover) and the second launch was at 1:00pm CST(Not a coordinated flyover launch). Ozone was not observed at high levels over the Bay in the daily observations. There was a noticeable uptick in recreational boat traffic (Nice day/Sunday). Pontoon was refueled and docked at ~2:30pm CST.

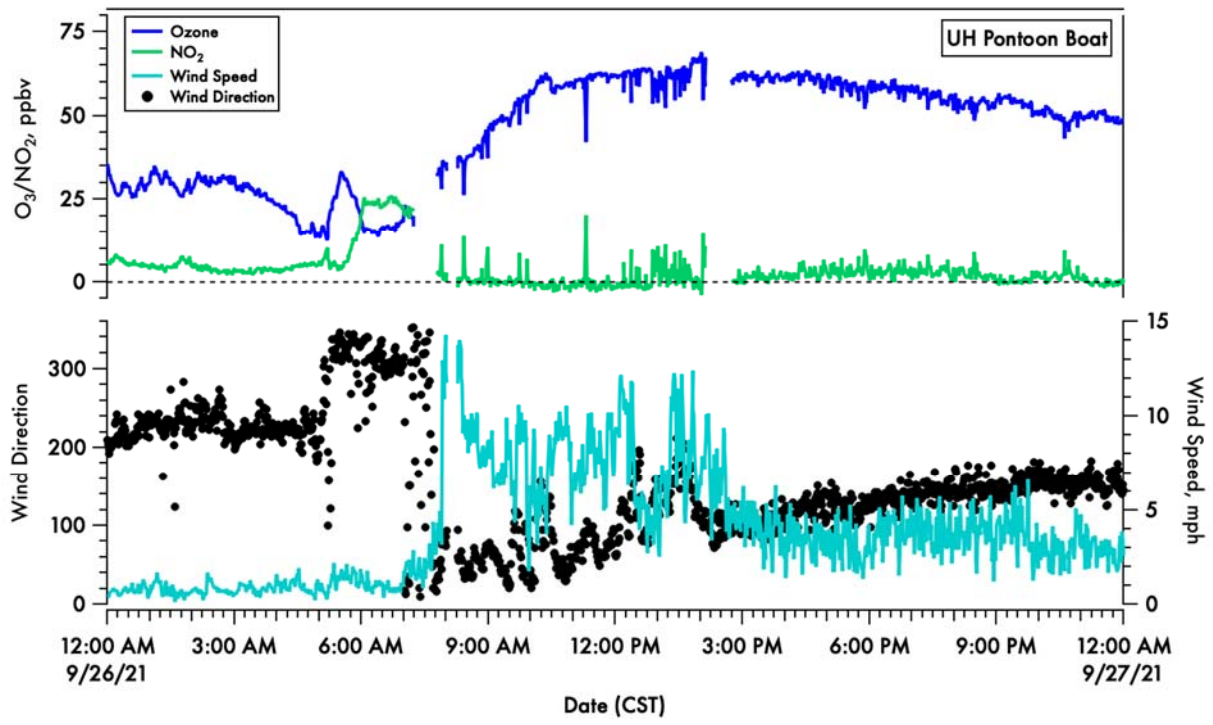

Figure 83. A time-series of 1-minute averaged ozone (blue) and calculated NO_2 (green) on the top panel and wind speed (light blue) and direction (black dots) in the bottom panel.

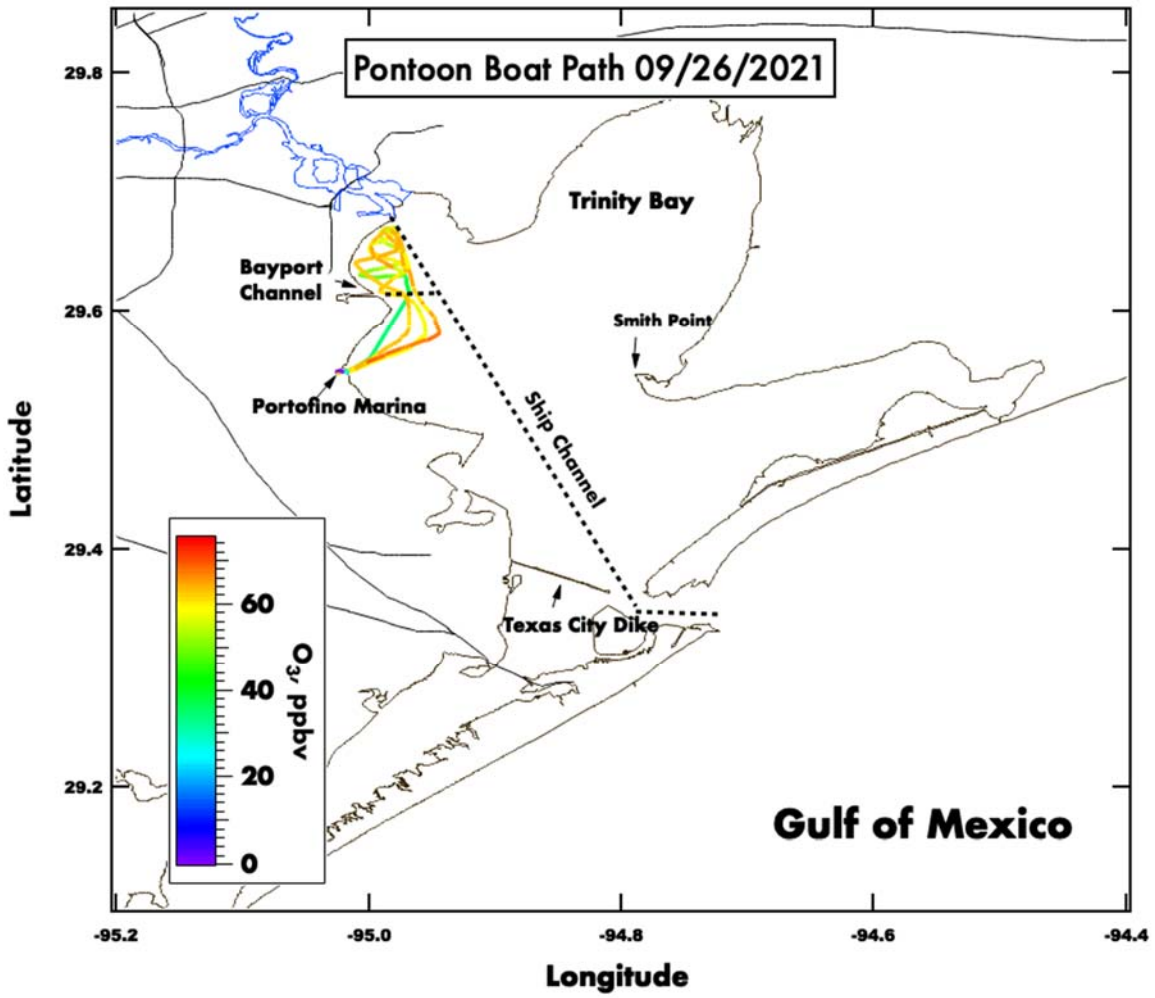

Figure 84. Spatial plot of surface ozone collected from the UH pontoon boat on September 26th, 2021.

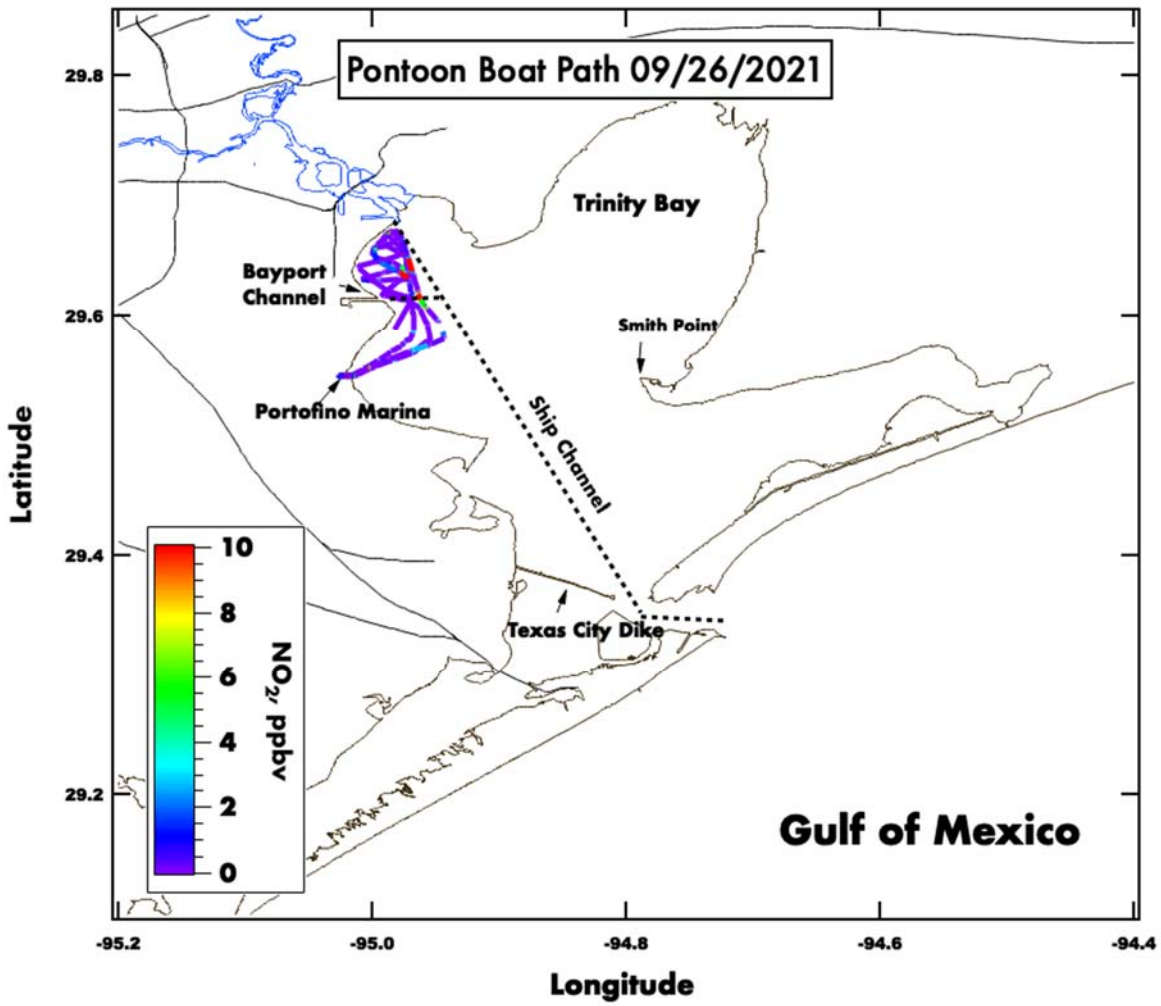

Figure 85. Spatial plot of surface NO_2, calculated from observed Ox, collected from the UH pontoon boat on September 26th, 2021.

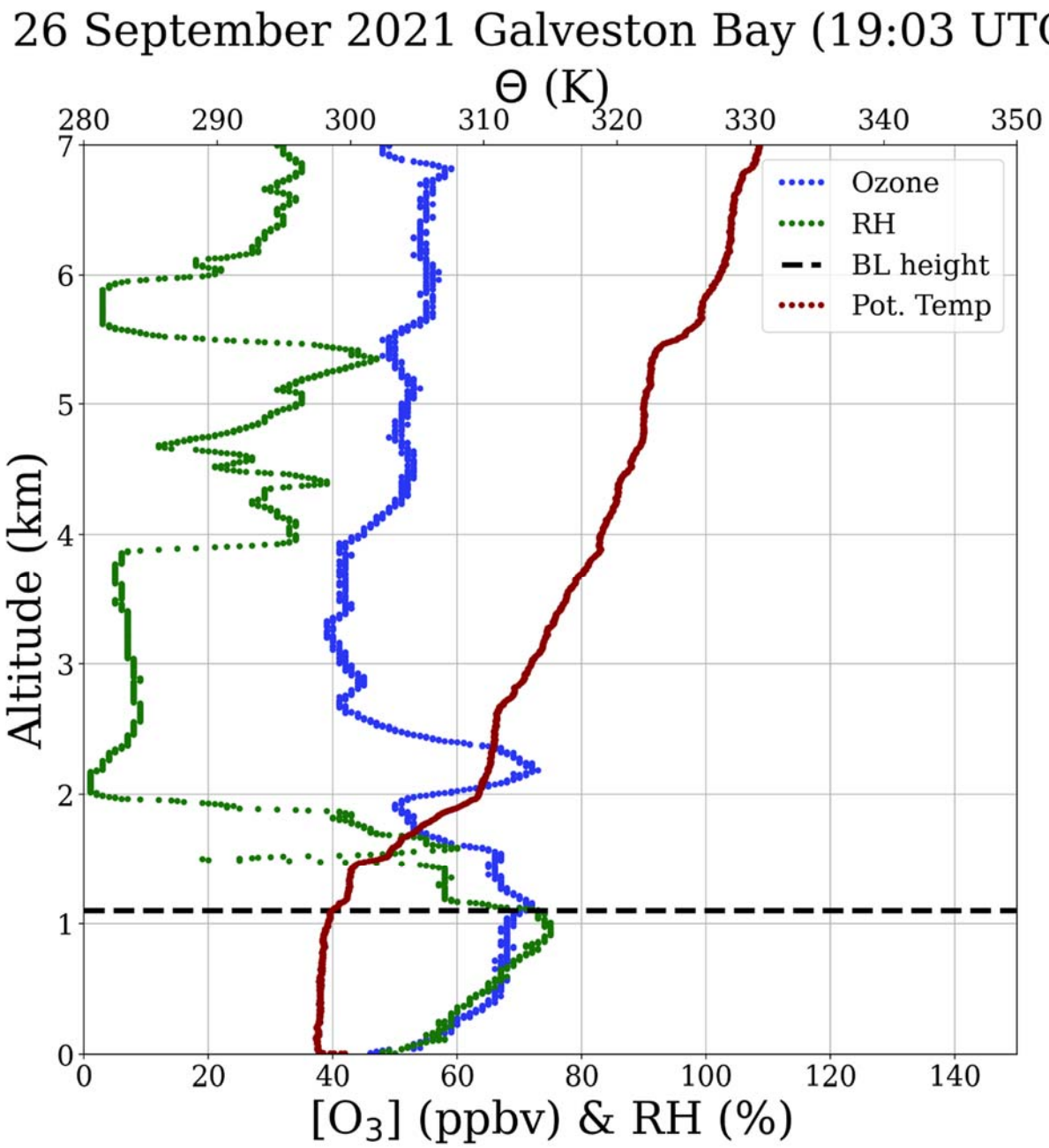

Figure 86. Vertical profiles of ozone (blue), relative humidity (green) and potential temperature (red). The derived boundary layer height is denoted by the horizontal dashed black line.

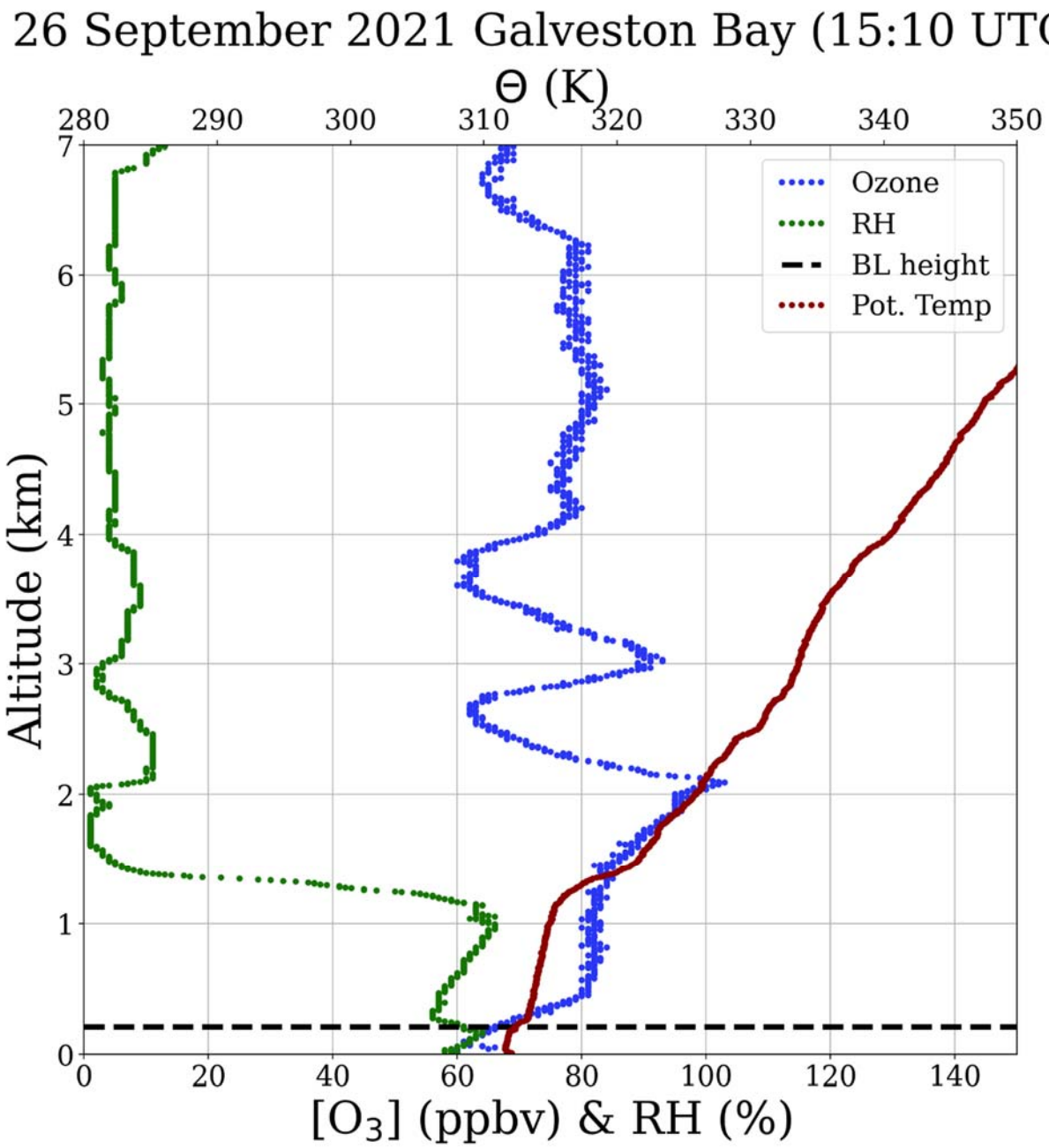

Figure 87. Vertical profiles of ozone (blue), relative humidity (green) and potential temperature (red). The derived boundary layer height is denoted by the horizontal dashed black line.

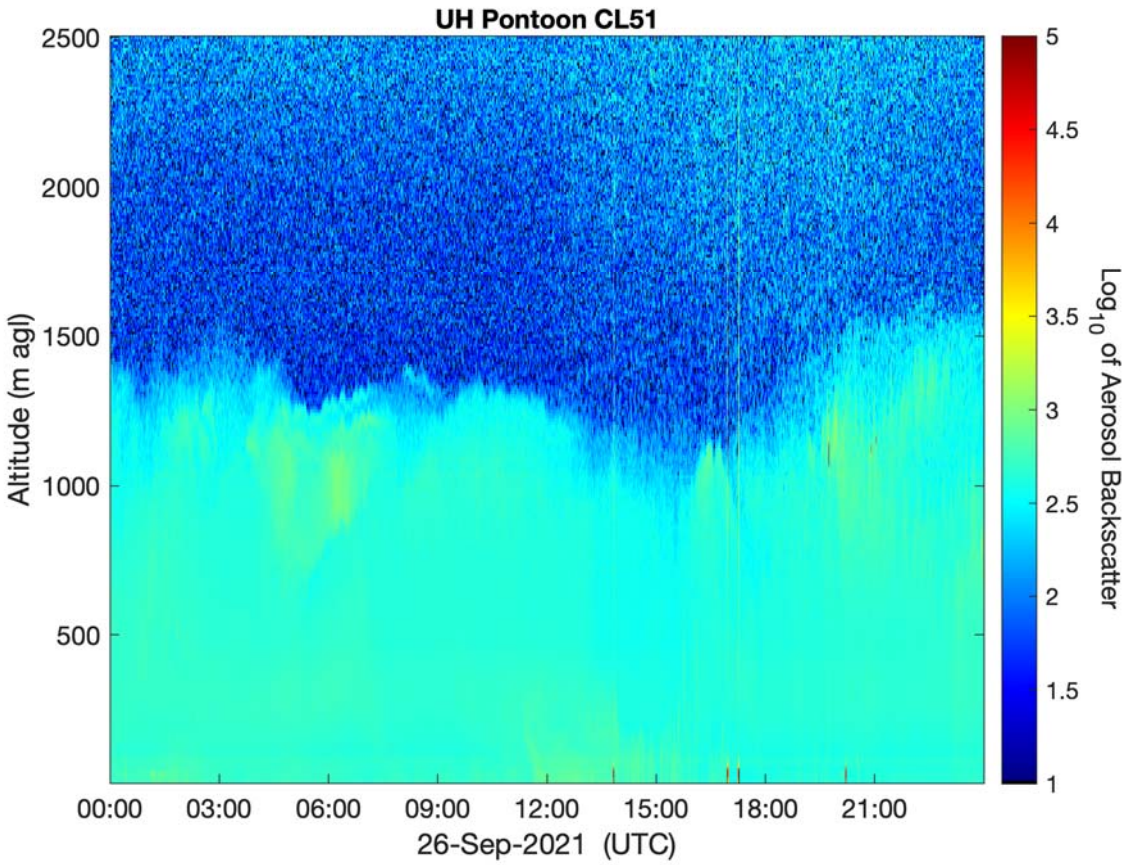

Figure 88. Vertical profile of the aerosol backscatter collected from a Vaisala CL-51 ceilometer mounted on the UH Pontoon boat.

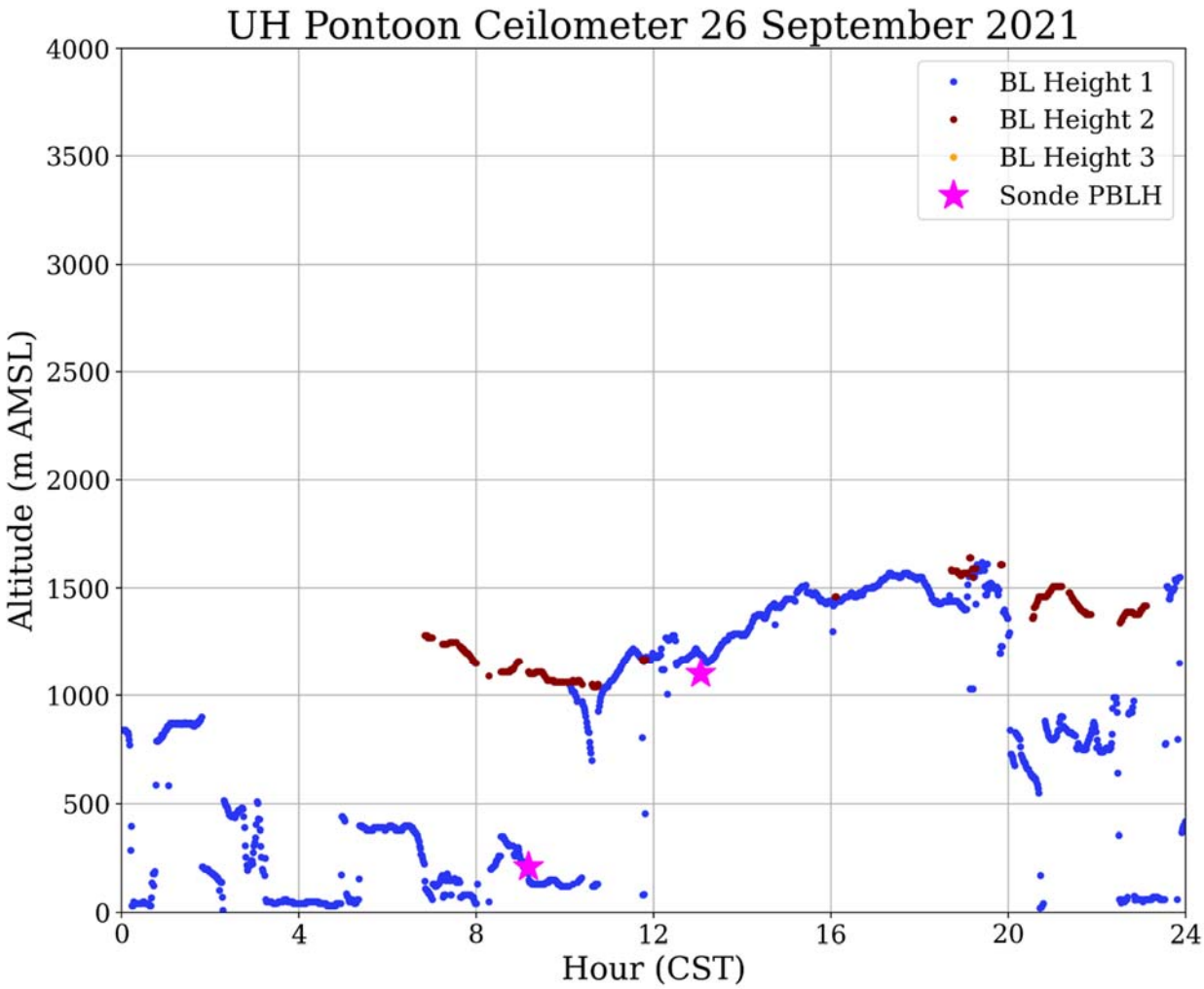

Figure 89. UH Pontoon Vaisala CL-51 ceilometer returned boundary layer heights and boundary layer heights from the ozonesonde profile.

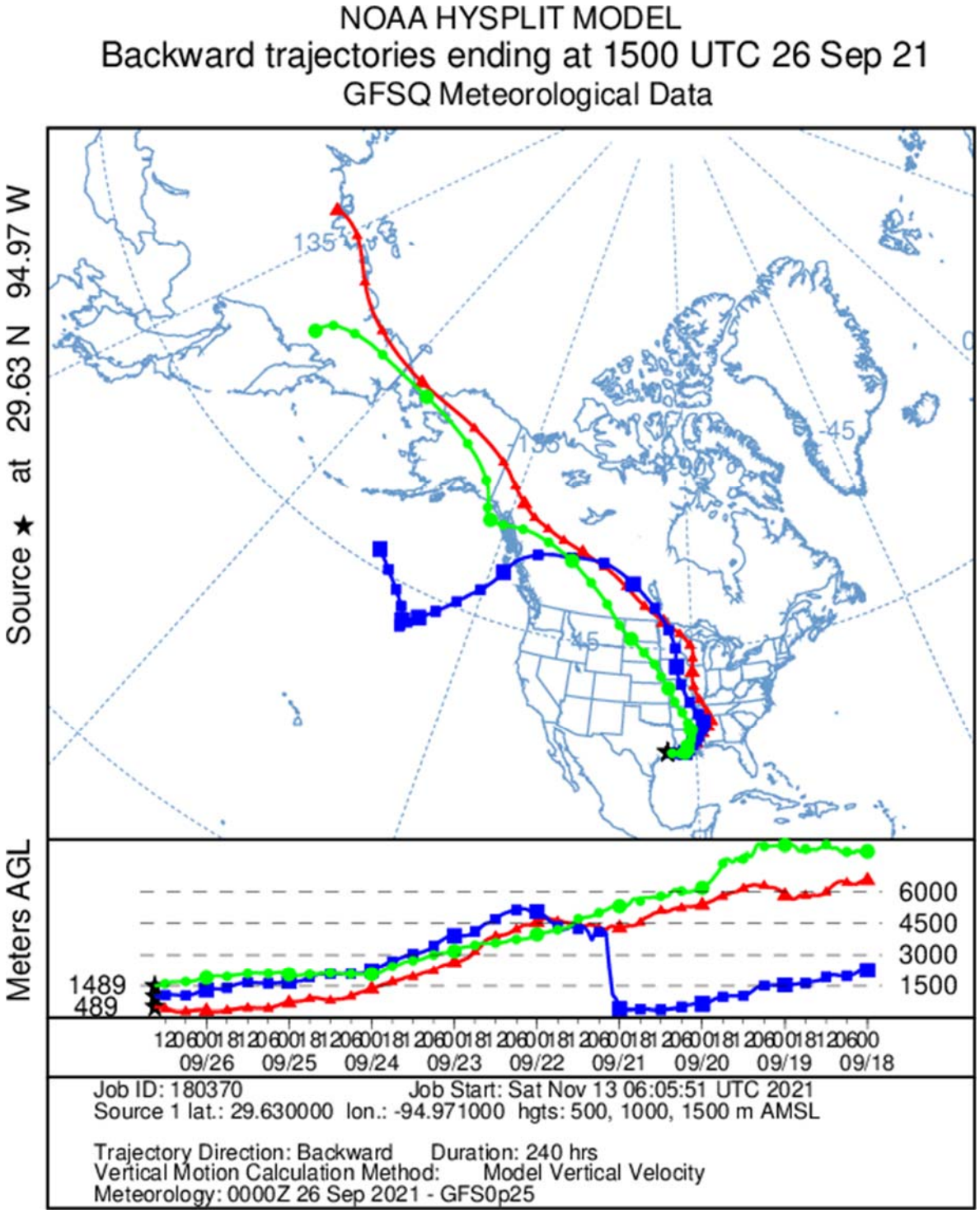

Figure 90. Ten-day HYSPLIT back trajectory for the first ozonesonde launch on 26 September 2021 from three heights over the Bay: 500 m (red), 1,000 m (blue), and 1,500 m (green). Each data point is 6 hours apart.

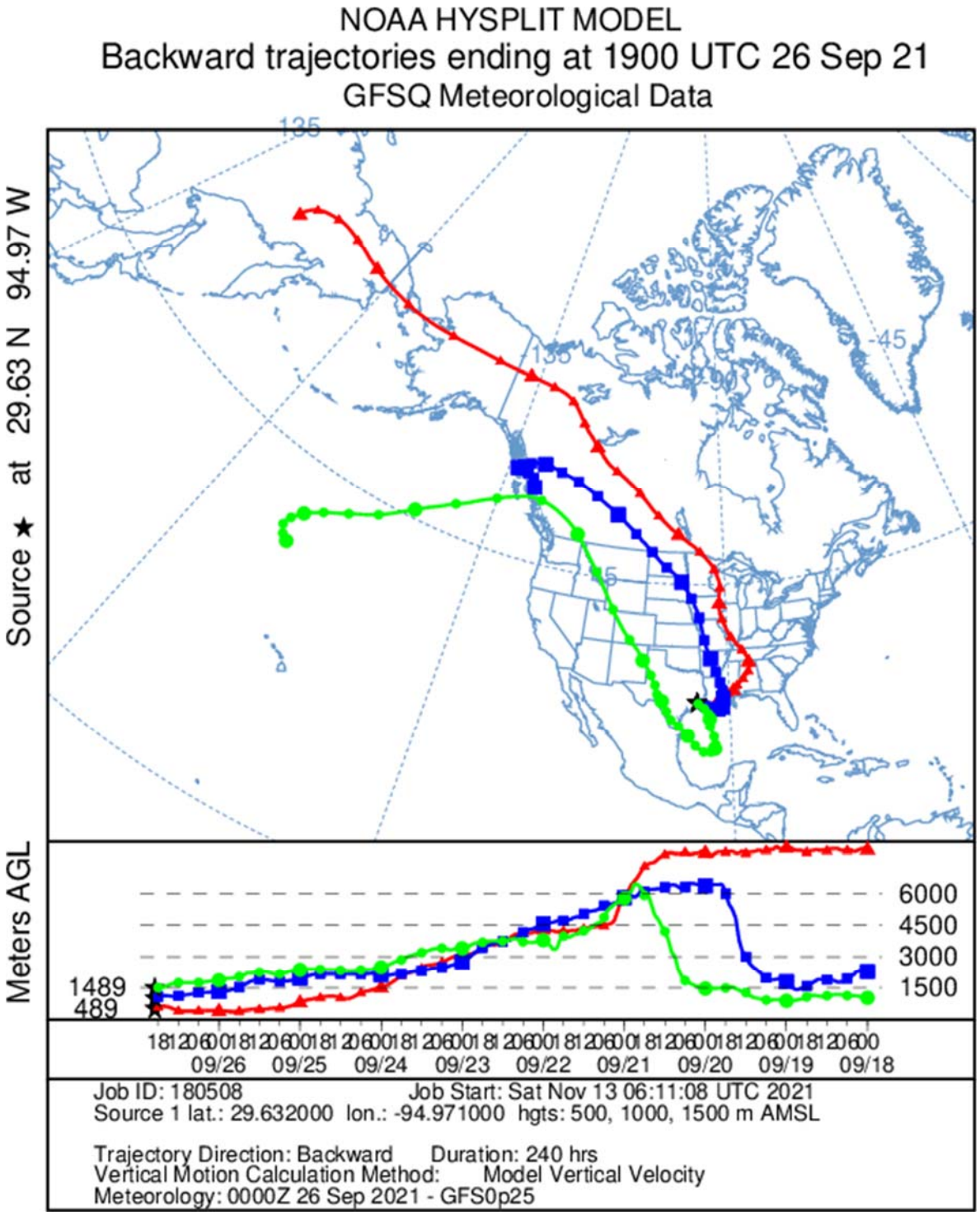

Figure 91. Ten-day HYSPLIT back trajectory for the second ozonesonde launch on 26 September 2021 from three heights over the Bay: 500 m (red), 1,000 m (blue), and 1,500 m (green). Each data point is 6 hours apart.

9.4 25 September 2021:

Travis Griggs (UH) and Michael Comas (UH) met at the marina at 7:15am CST. Bay conditions were smooth to slightly choppy with an ENE wind of around 7 knots. The daily plan was to head NW for the 1st Raster then go SW for the 3rd Raster to release ozonesonde launches coordinated with the NASA aircraft. After the first ozonesonde launch, which was released at 9:01am CST near the Bayport channel, resin tube samples for Baylor were collected near the Bayport and Houston Ship channel intersection. After the first launch a gradient pattern in the North Bay was executed. The pontoon was taken back to Kemah, TX for refueling. A second ozonesonde was launched in the afternoon in the SW area of the bay near the Texas City Dike coordinated with the 3rd raster pattern flyover of the NASA aircraft flyover. The Pontoon was refueled and docked at ~5:00pm CST.

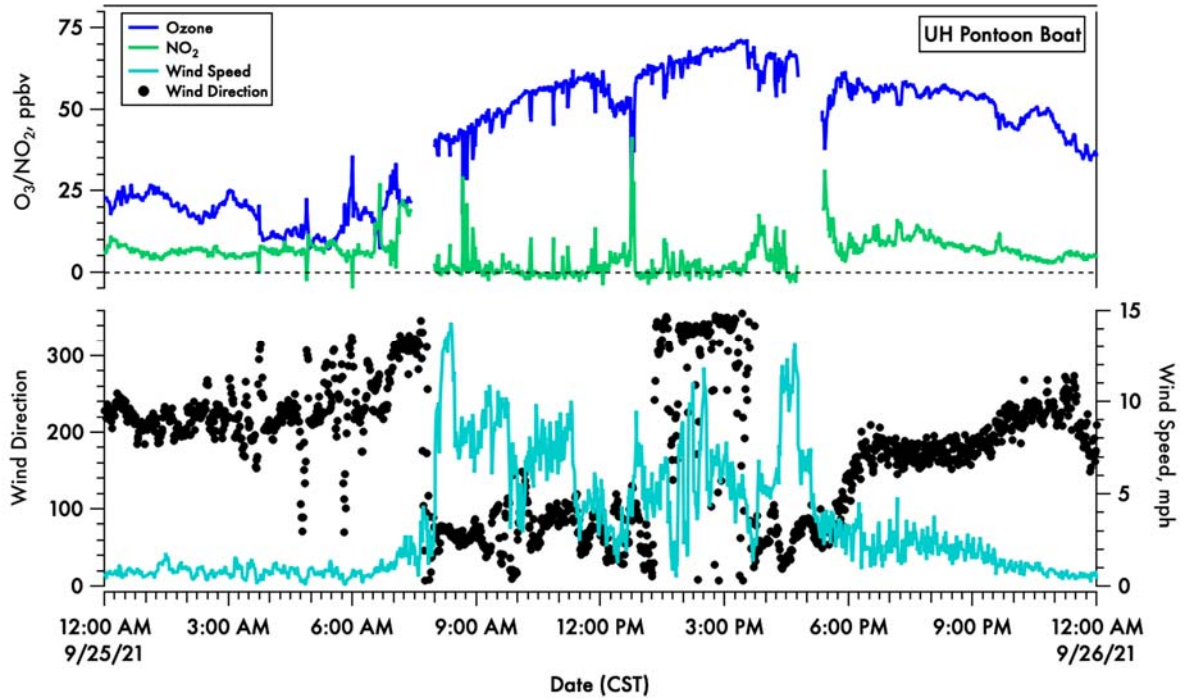

Figure 92. A time-series of 1-minute averaged ozone (blue) and calculated NO_2 (green) on the top panel and wind speed (light blue) and direction (black dots) in the bottom panel.

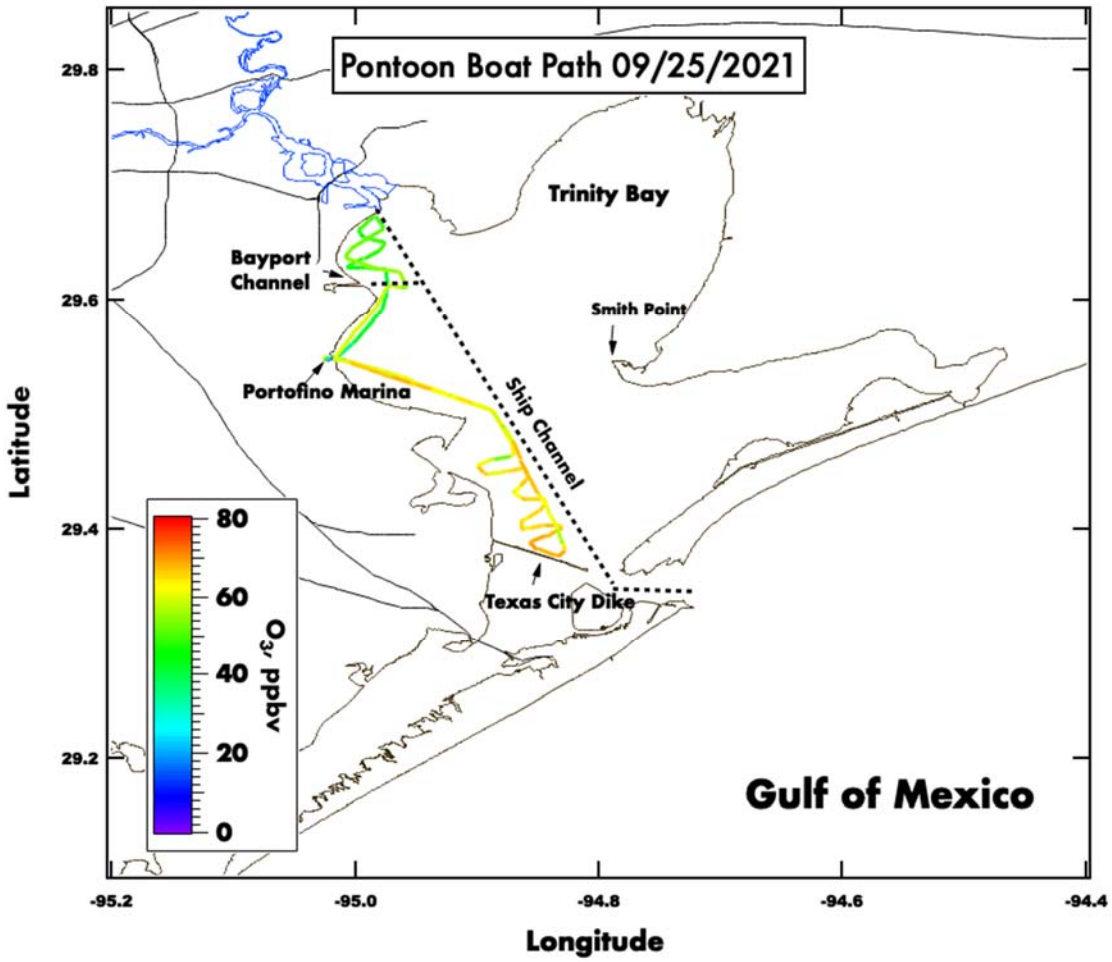

Figure 93. Spatial plot of surface ozone collected from the UH pontoon boat on September 25th, 2021.

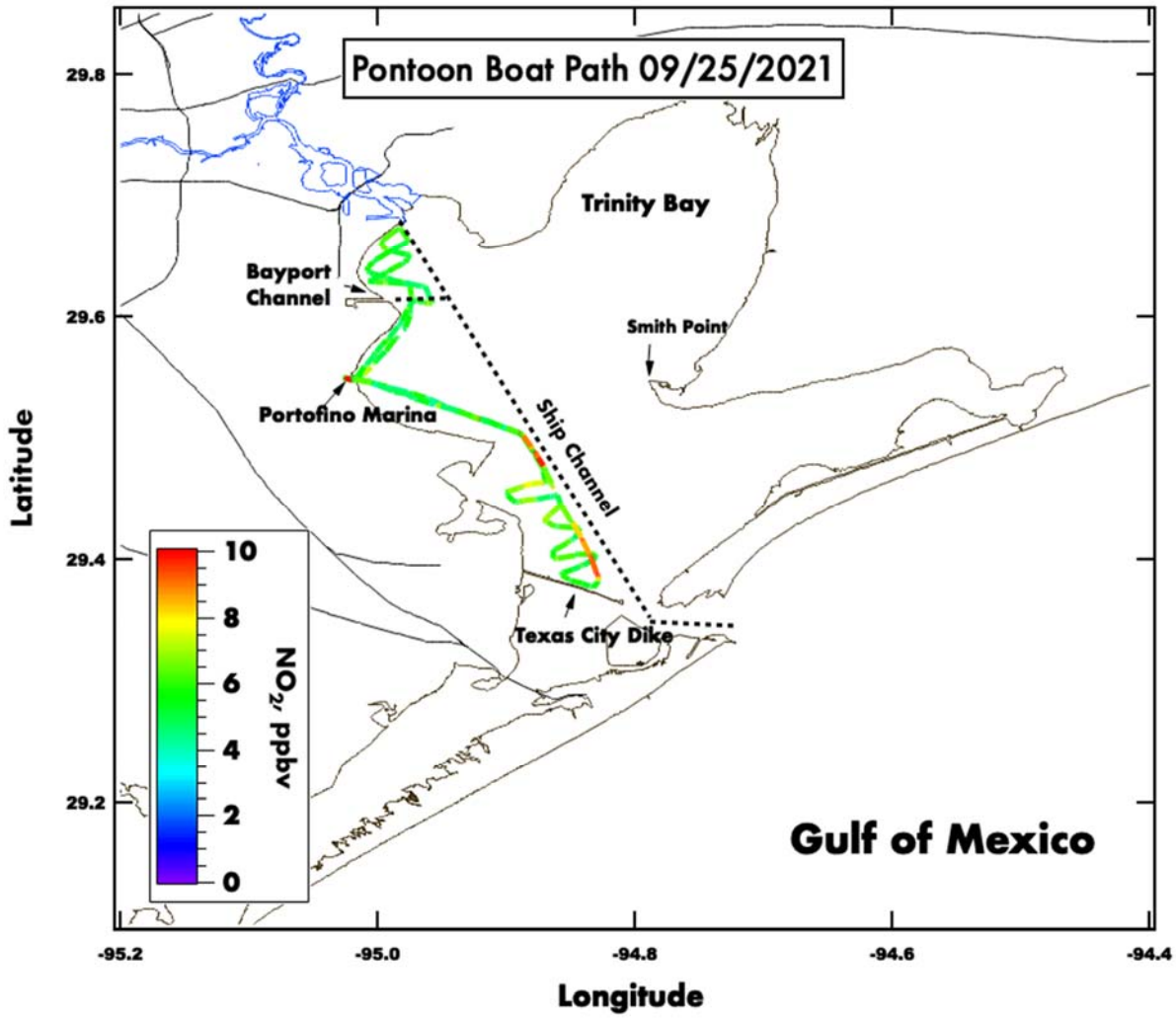

Figure 94. Spatial plot of surface NO_2, calculated from observed Ox, collected from the UH pontoon boat on September 25th, 2021.

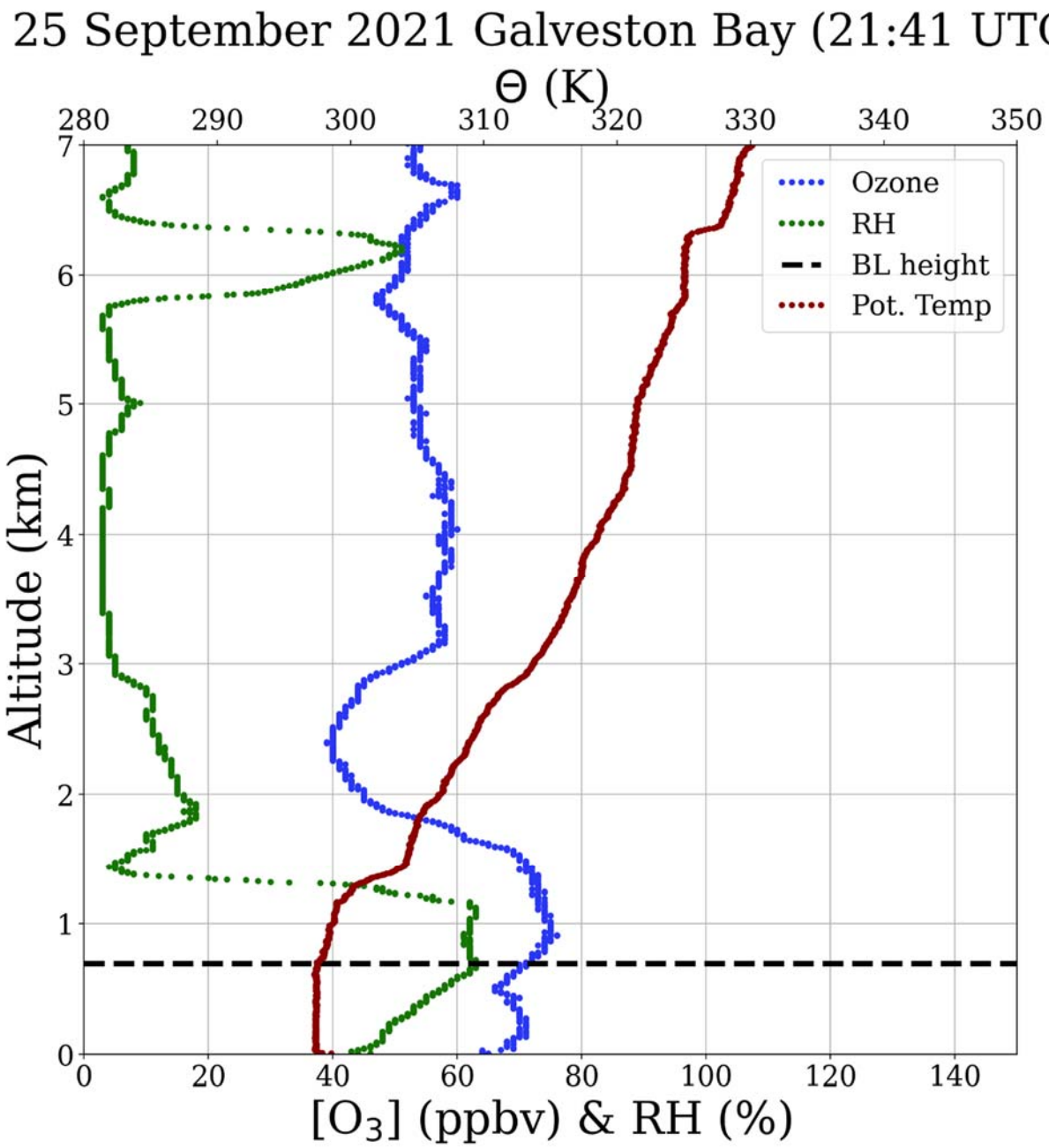

Figure 95. Vertical profiles of ozone (blue), relative humidity (green) and potential temperature (red). The derived boundary layer height is denoted by the horizontal dashed black line.

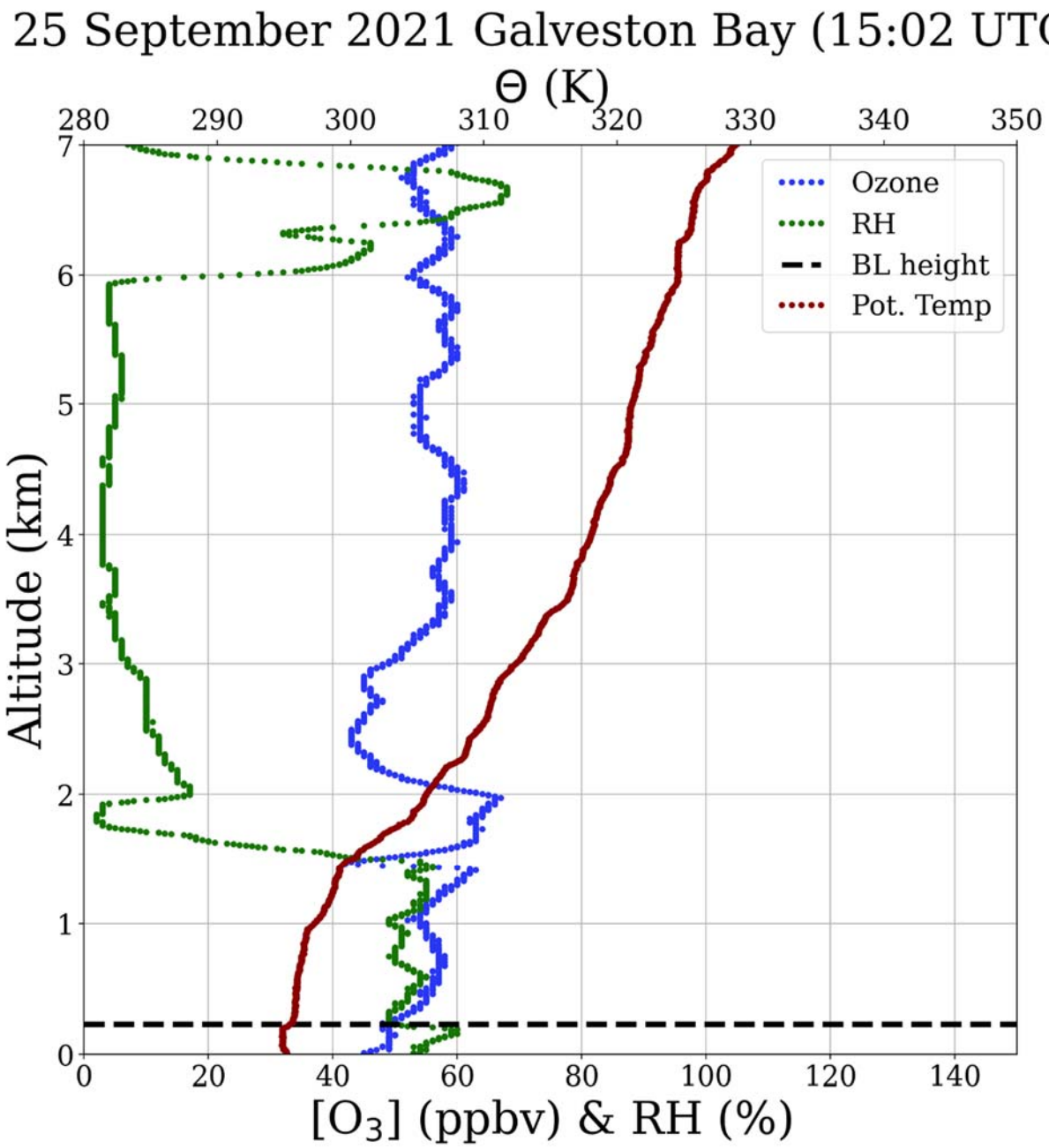

Figure 96. Vertical profiles of ozone (blue), relative humidity (green) and potential temperature (red). The derived boundary layer height is denoted by the horizontal dashed black line.

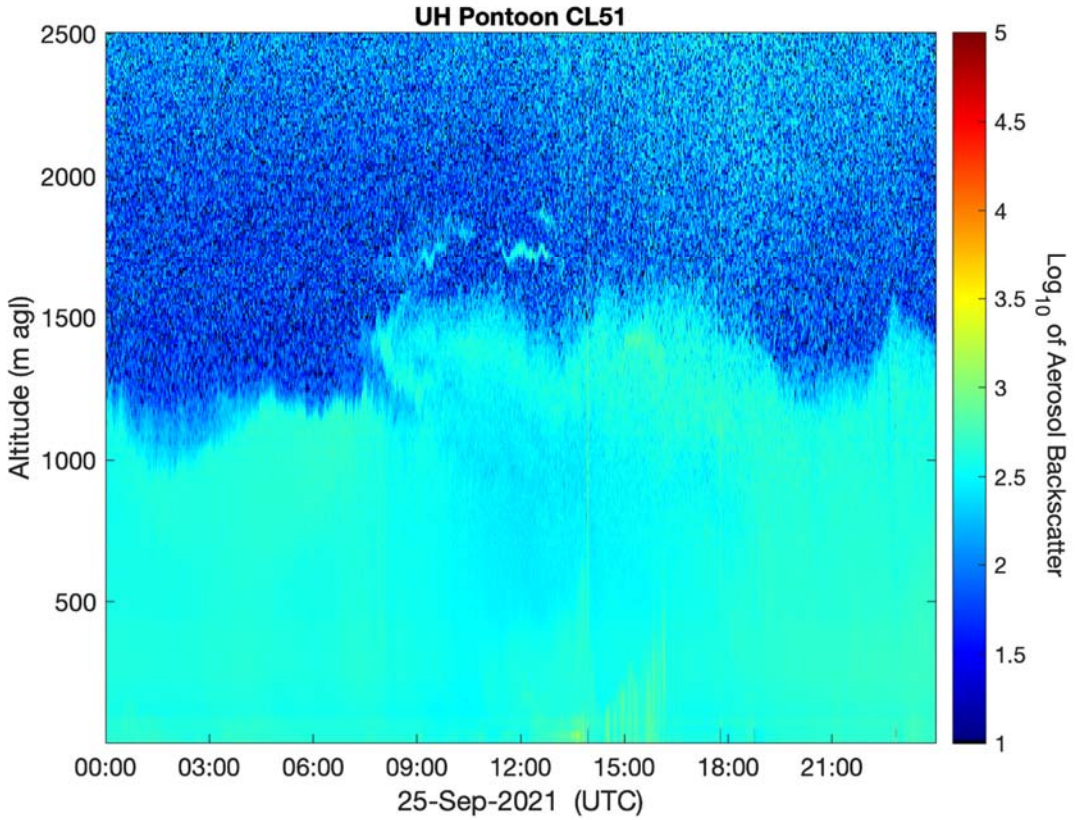

Figure 97. Vertical profile of the aerosol backscatter collected from a Vaisala CL-51 ceilometer mounted on the UH Pontoon boat.

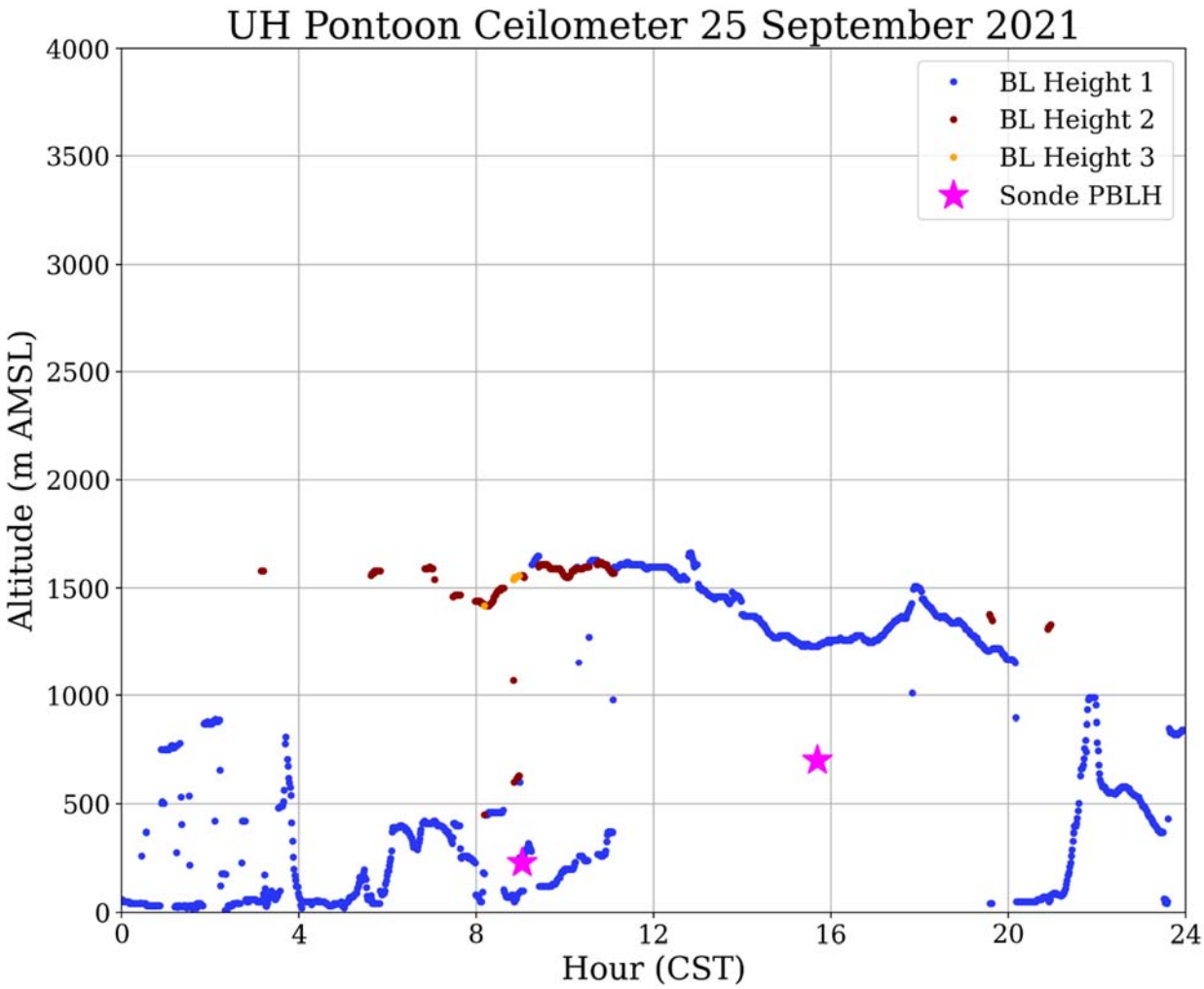

Figure 98. UH Pontoon Vaisala CL-51 ceilometer returned boundary layer heights and boundary layer heights from the ozonesonde profile. In the afternoon ozonesonde profile, a layer may be present at 1.1 km AMSL as well.

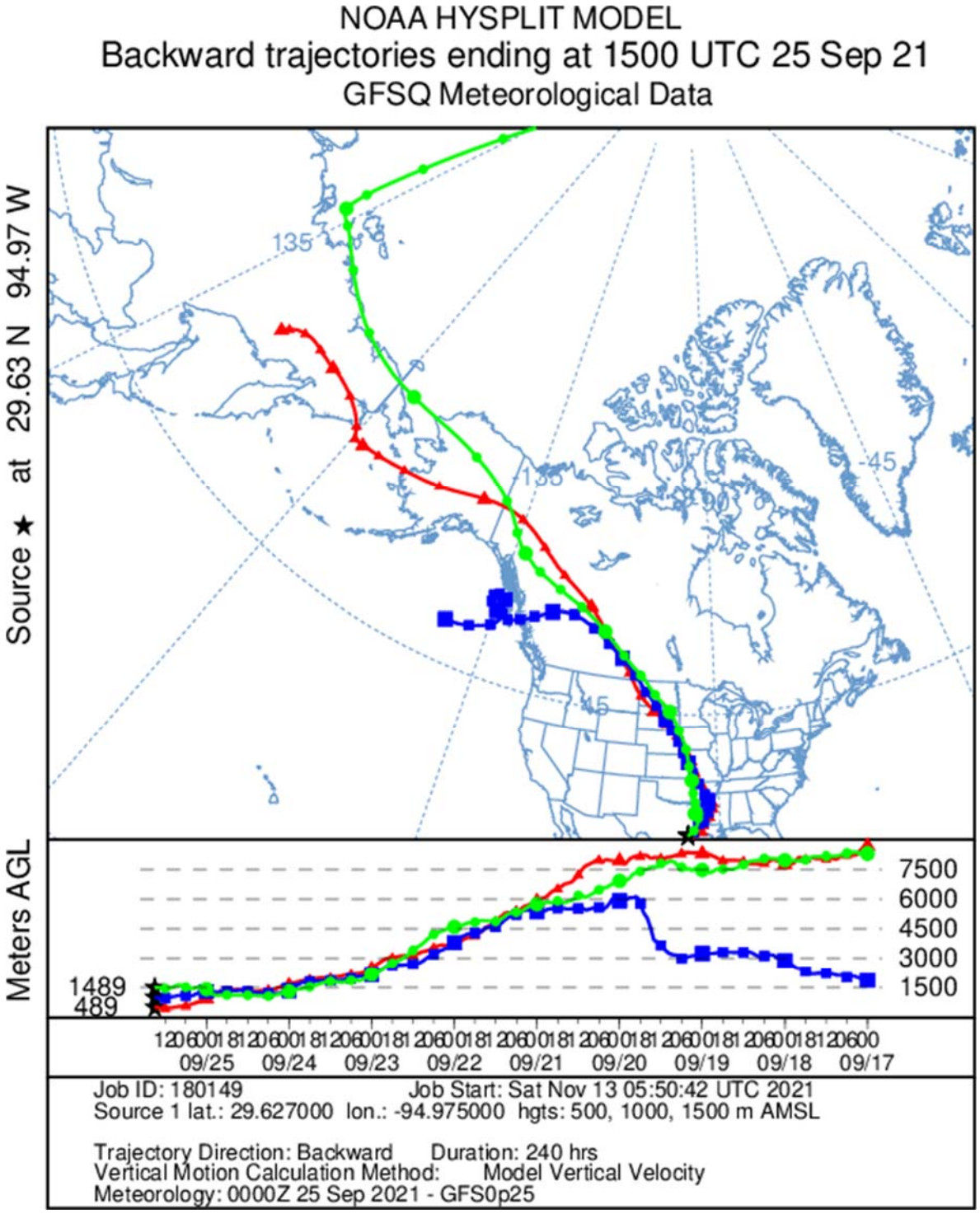

Figure 99. Ten-day HYSPLIT back trajectory for the first ozonesonde launch on 25 September 2021 from three heights over the Bay: 500 m (red), 1,000 m (blue), and 1,500 m (green). Each data point is 6 hours apart.

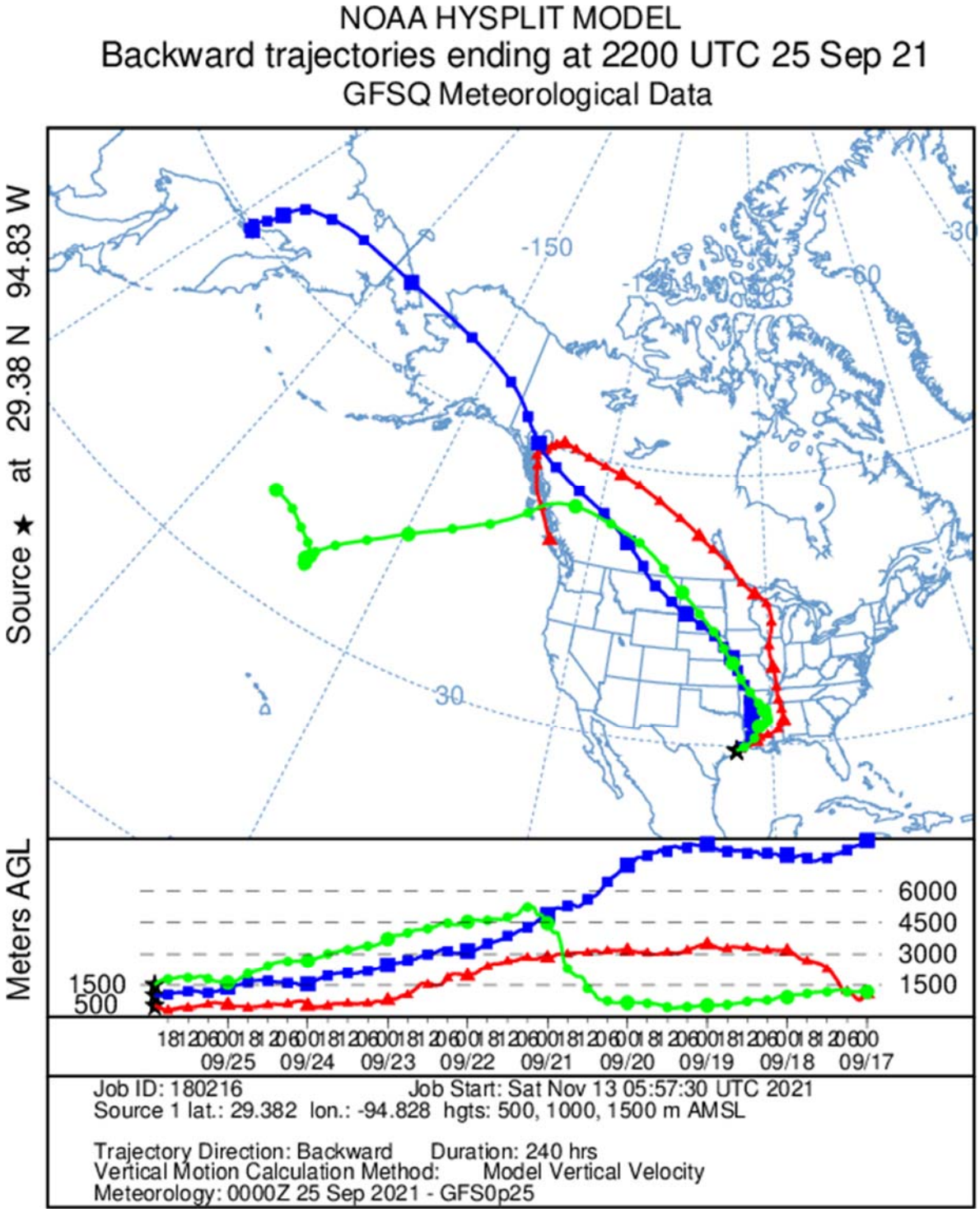

Figure 100. Ten-day HYSPLIT back trajectory for the second ozonesonde launch on 25 September 2021 from three heights over the Bay: 500 m (red), 1,000 m (blue), and 1,500 m (green). Each data point is 6 hours apart.

9.5 21 September 2021:

Travis Griggs (UH), Michael Comas (UH) and Angelique Demitillo (UVA) met at the Portofino Harbor Marina at 7:10am CST. The daily plan was to go South towards the Texas City Dike to compare measurements with the UH Mobile Air Quality Lab (MAQL-1). Successful stationary co-sampling occurred with MAQL-1from ~10:10-10:40am CST. After stationary co-sampling both labs did a down and back parallel pass on the Texas City Dike from ~10:45am - 11:20pm CST. After sampling in the SW bay, the pontoon boat was taken back to Kemah, TX to be refueled and then taken back out to the NW area of the Bay for surface sampling. The pontoon boat was docked and refueled at ~3:15pm CST.

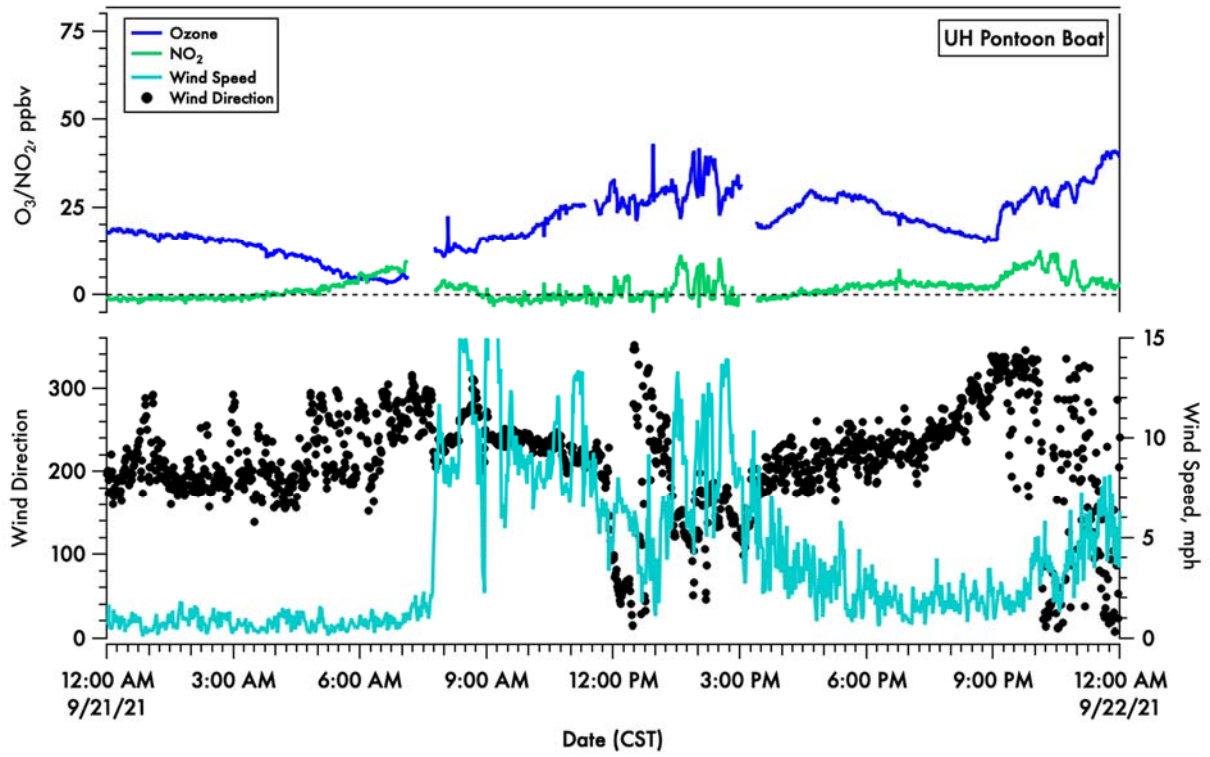

Figure 101. A time-series of 1-minute averaged ozone (blue) and calculated NO_2 (green) on the top panel and wind speed (light blue) and direction (black dots) in the bottom panel.

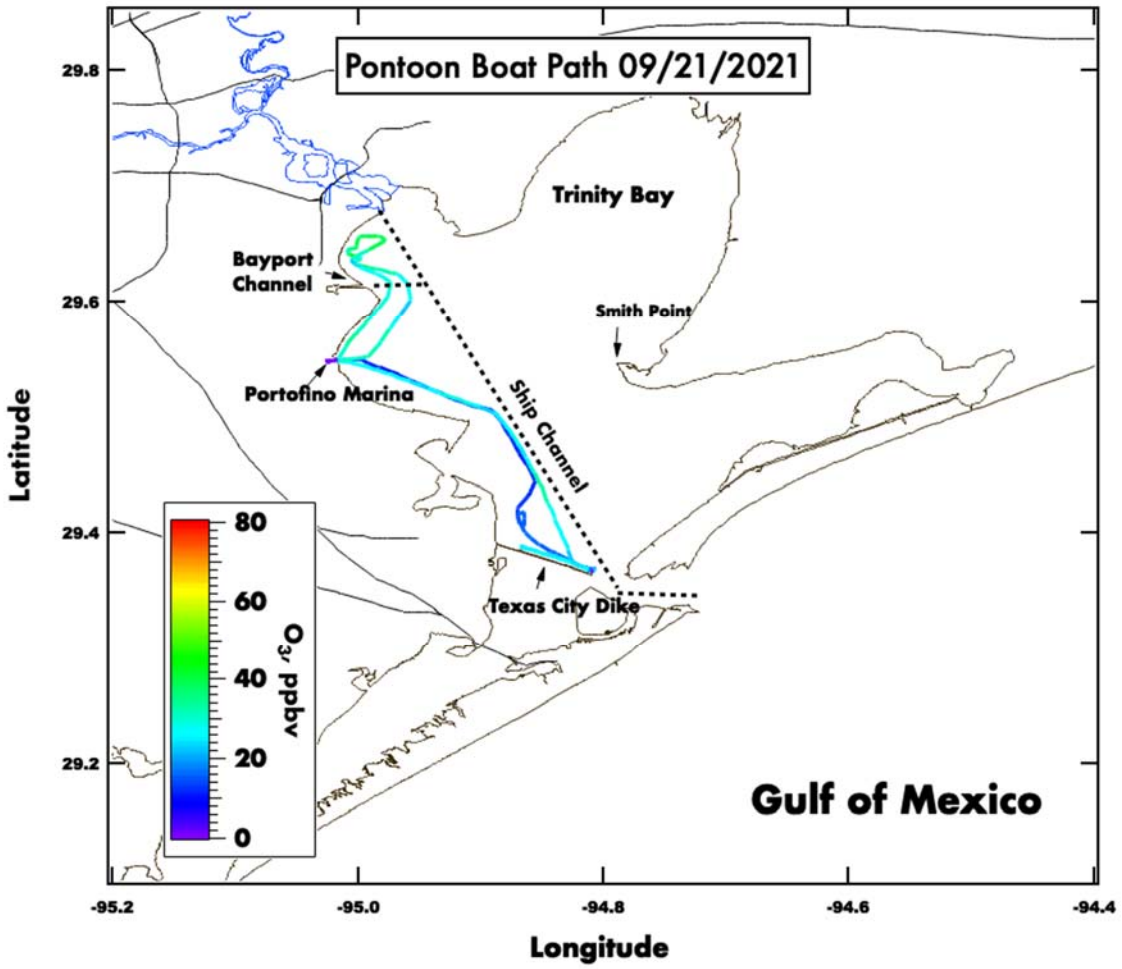

Figure 102. Spatial plot of surface ozone collected from the UH pontoon boat on September 21st, 2021.

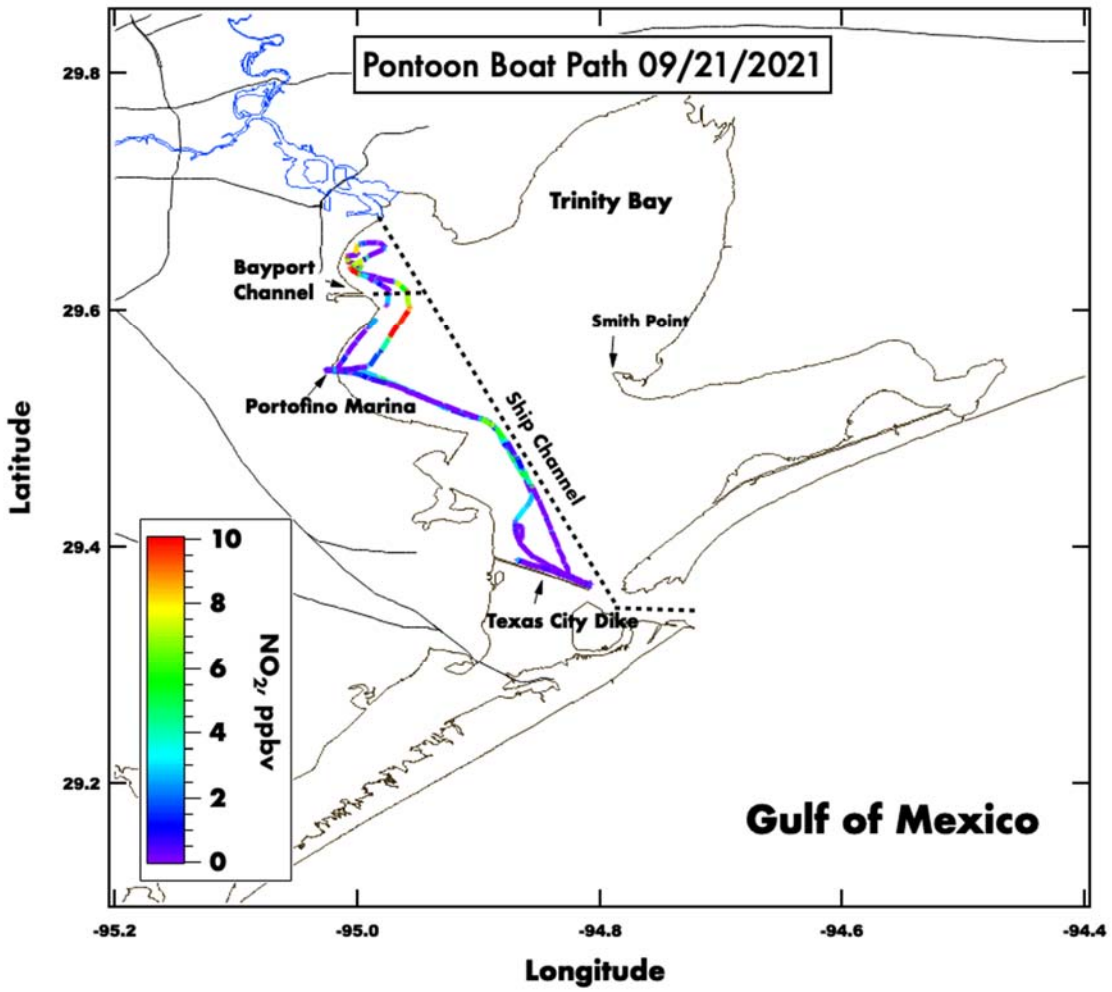

Figure 103. Spatial plot of surface NO_2, calculated from observed Ox, collected from the UH pontoon boat on September 21st, 2021.

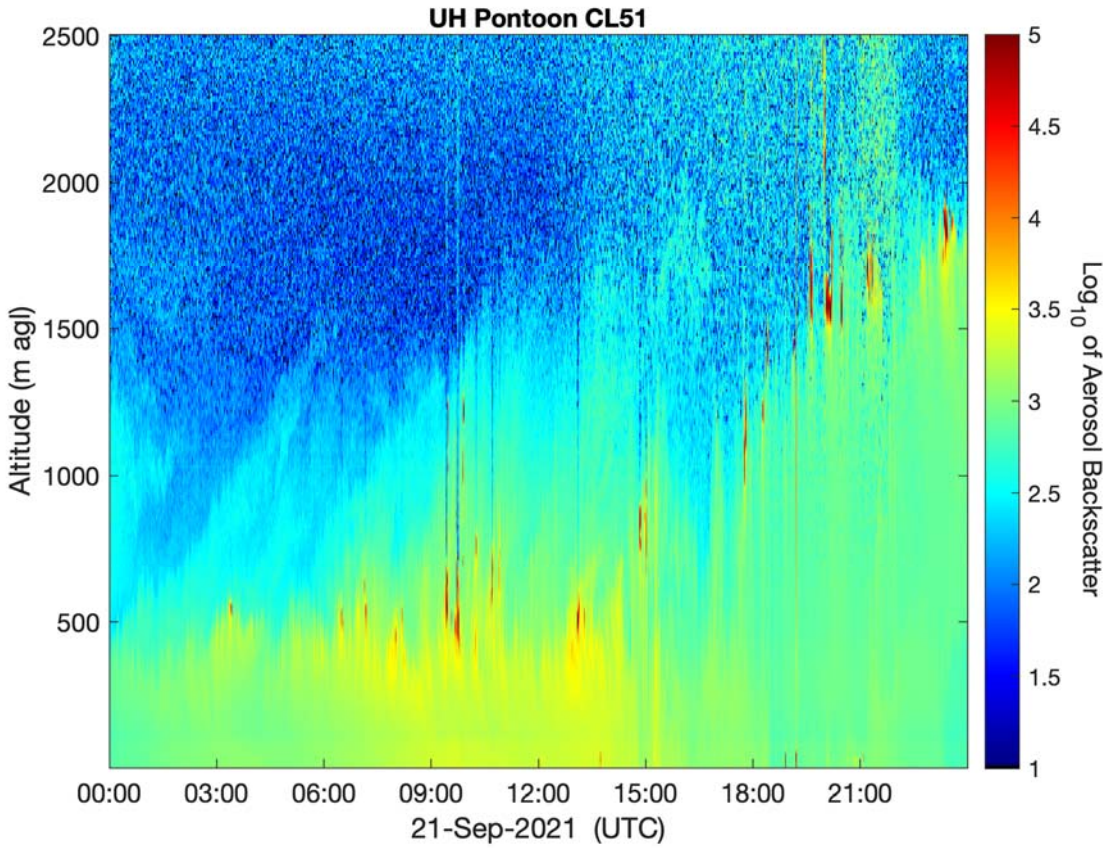

Figure 104. Vertical profile of the aerosol backscatter collected from a Vaisala CL-51 ceilometer mounted on the UH Pontoon boat.

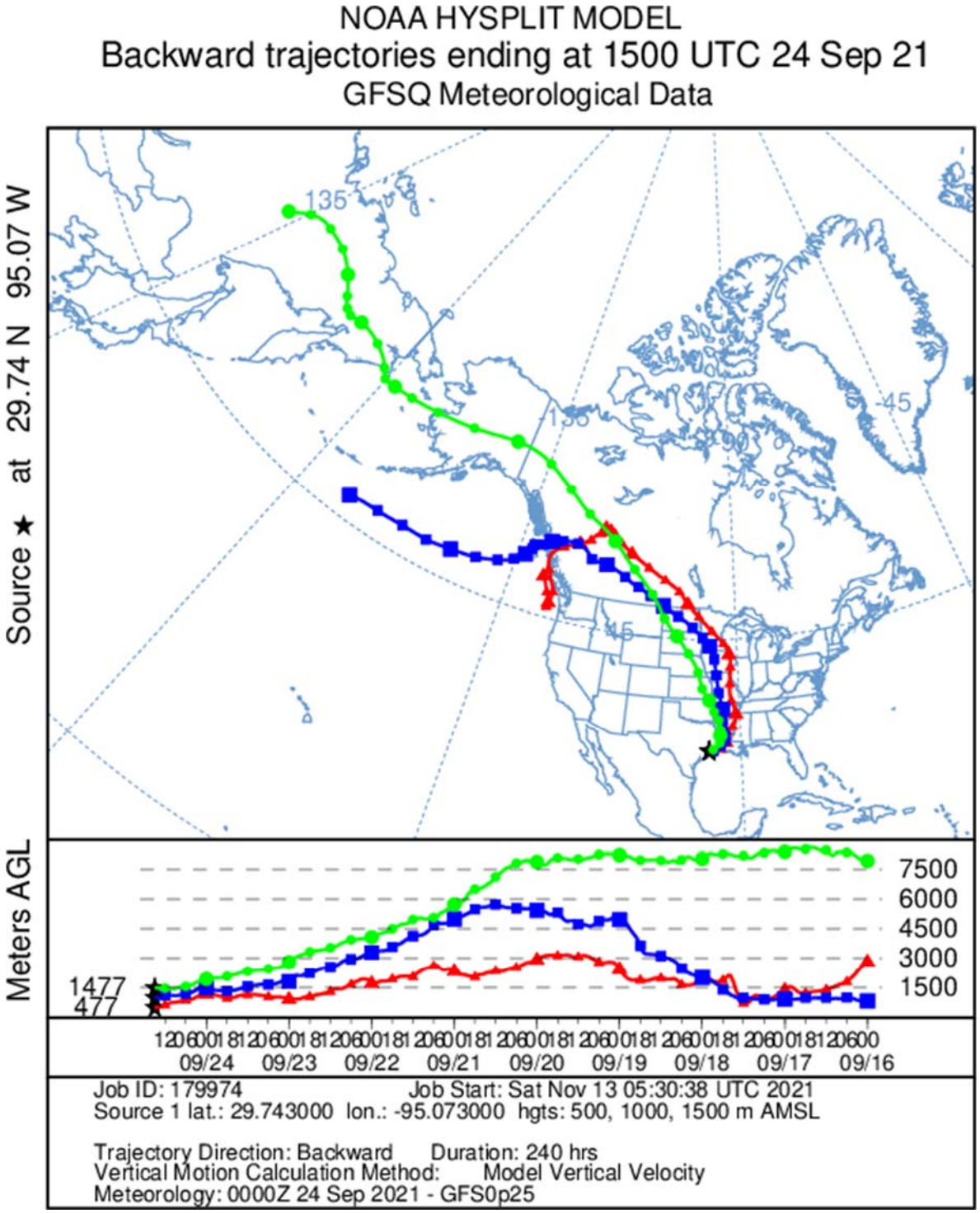

Figure 105. Ten-day HYSPLIT back trajectory for the first ozonesonde launch on 24 September 2021 from three heights over the Bay: 500 m (red), 1,000 m (blue), and 1,500 m (green). Each data point is 6 hours apart.

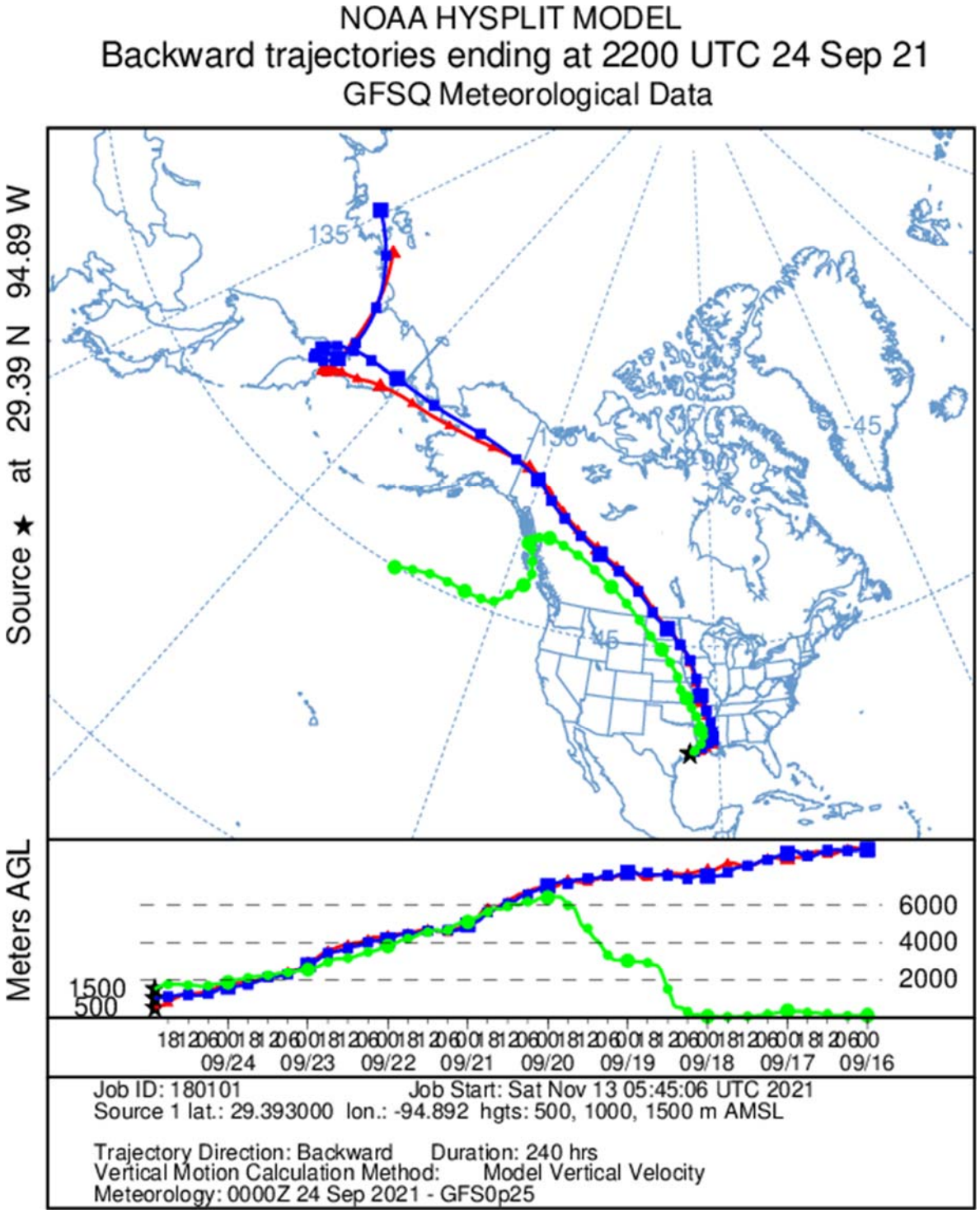

Figure 106. Ten-day HYSPLIT back trajectory for the second ozonesonde launch on 24 September 2021 from three heights over the Bay: 500 m (red), 1,000 m (blue), and 1,500 m (green). Each data point is 6 hours apart.

9.6 20 September 2021:

Travis Griggs (UH) and Michael Comas (UH) met at the marina at 7:45am CST. The daily plan was to survey the NW portion of the Bay using one fuel tank. Only surface sampling was completed on this day. There was an interesting Bay Breeze feature observed on the KHGX radar at approximately 1:00 pm CST. Ozone jumped from ~40ppb to ~60ppb near the Bayport Channel in the wake of this feature. The pontoon was refueled and docked in the afternoon at ~1:40pm CST.

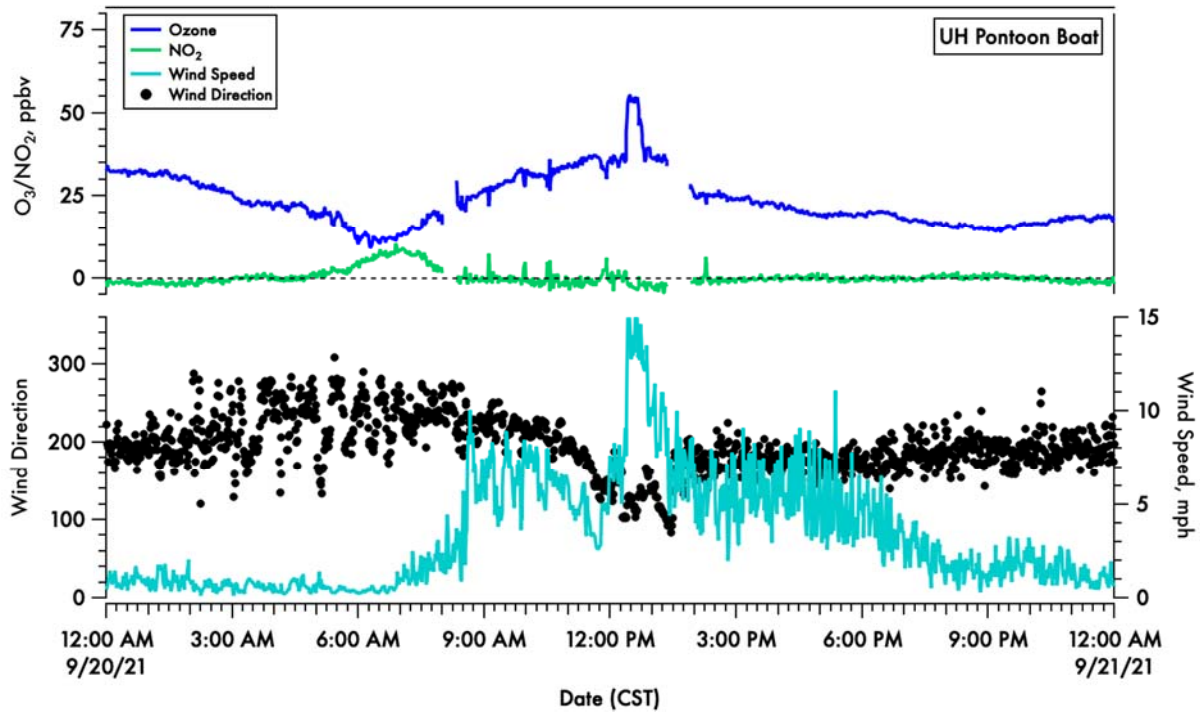

Figure 107. A time-series of 1-minute averaged ozone (blue) and calculated NO_2 (green) on the top panel and wind speed (light blue) and direction (black dots) in the bottom panel.

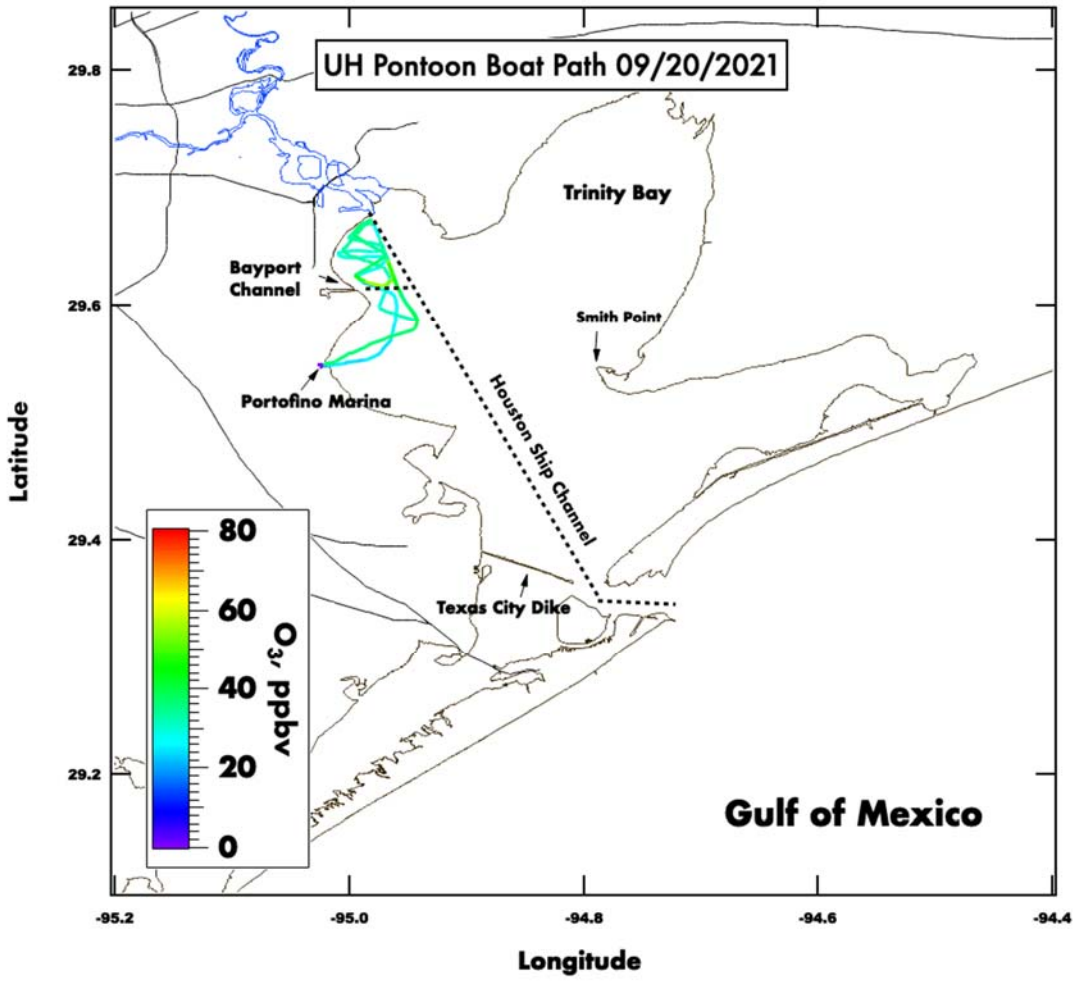

Figure 108. Spatial plot of surface ozone collected from the UH pontoon boat on September 20th, 2021.

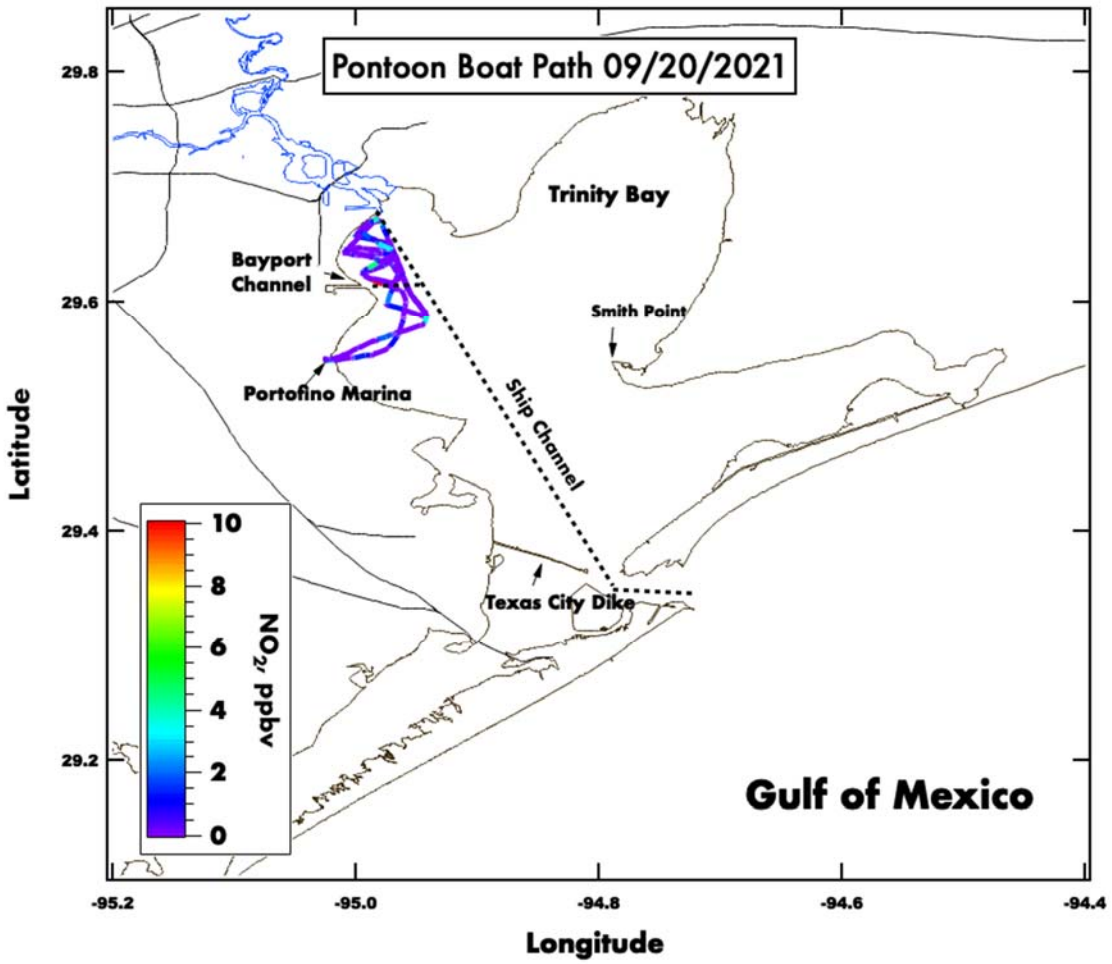

Figure 109. Spatial plot of surface NO_2, calculated from observed Ox, collected from the UH pontoon boat on September 20th, 2021.

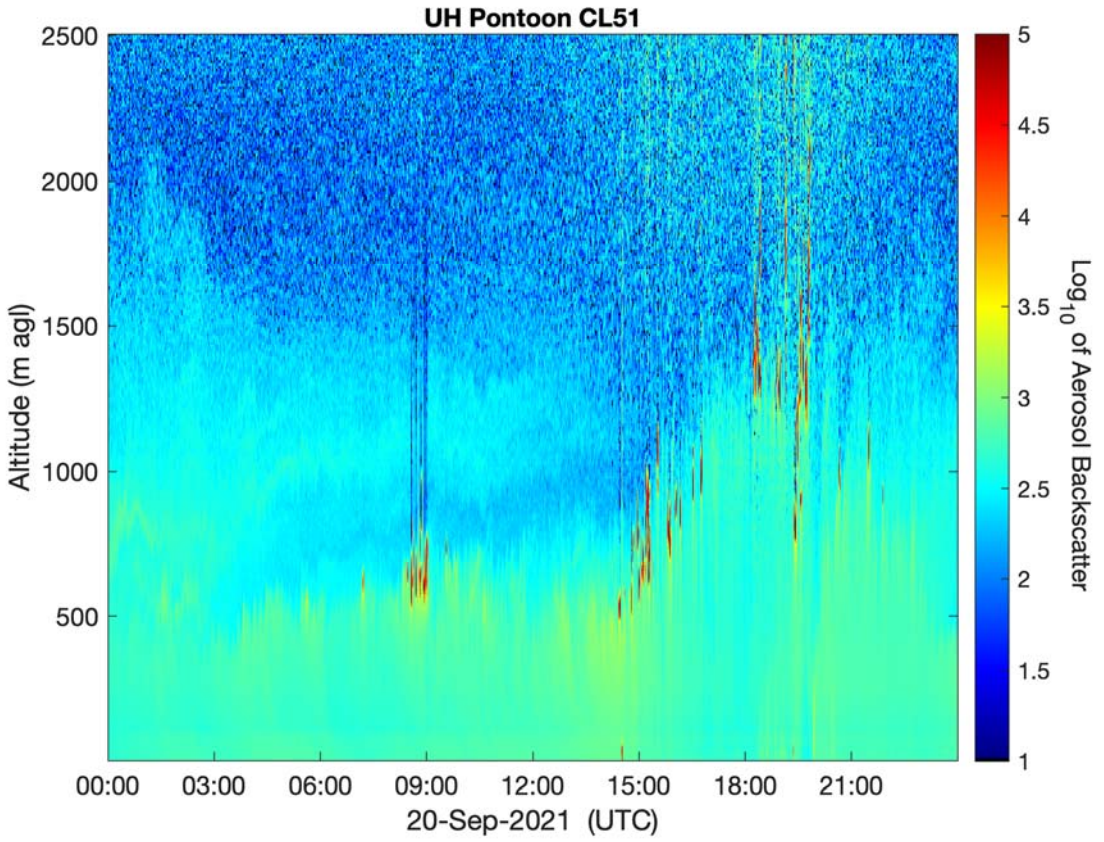

Figure 110. Vertical profile of the aerosol backscatter collected from a Vaisala CL-51 ceilometer mounted on the UH Pontoon boat.

9.7 17 September 2021:

Travis Griggs (UH), Jimmy Flynn (UH) and Sergio Alvarez (UH) redeployed the UH pontoon to Galveston Bay via Sylvan Beach Park after the passing of TS Nicholas (Briefly a Cat 1 Hurricane). The UH pontoon underwent repairs/maintenance/cleaning while in the warehouse for storage. Also, an additional instrument was added to the package to capture an NO_2 concentration with a Blue Light Converter (BLC) in a 49i Thermo. Once launched, ozone was observed in the 70ppb range and increased rapidly, peaking at ~ 105ppb on the W/NW side of the Bay. High ozone had not been forecast to the extent that was observed, so the UH pontoon science team decided to make a loop around the W/NW sector of the Bay. The pontoon was refueled and docked at ~4:40pm CST.

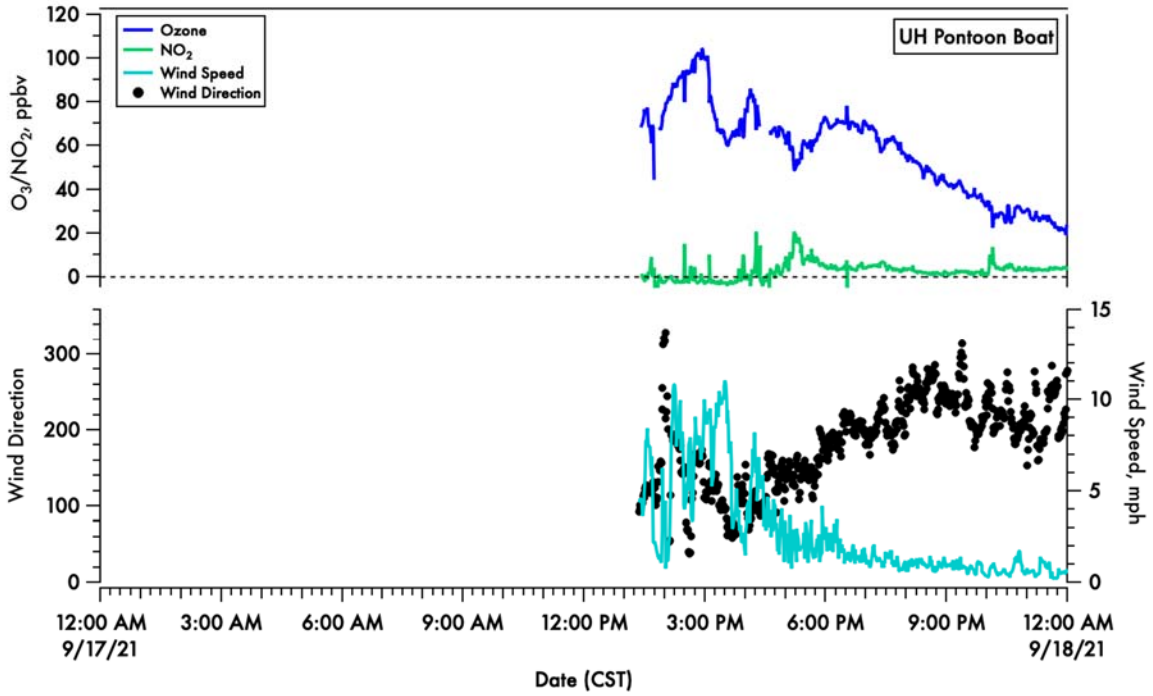

Figure 111. A time-series of 1-minute averaged ozone (blue) and calculated NO_2 (green) on the top panel and wind speed (light blue) and direction (black dots) in the bottom panel.

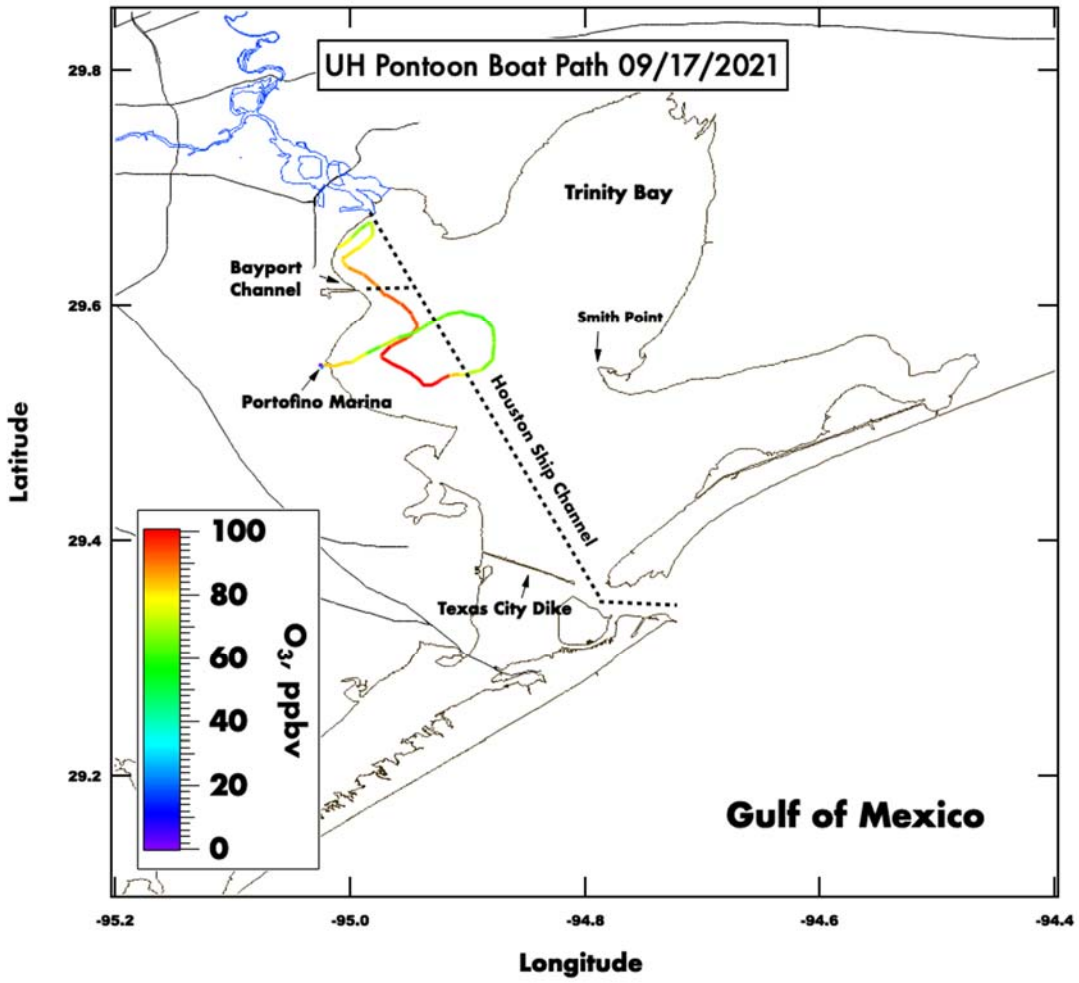

Figure 112. Spatial plot of surface ozone collected from the UH pontoon boat on September 17th, 2021.

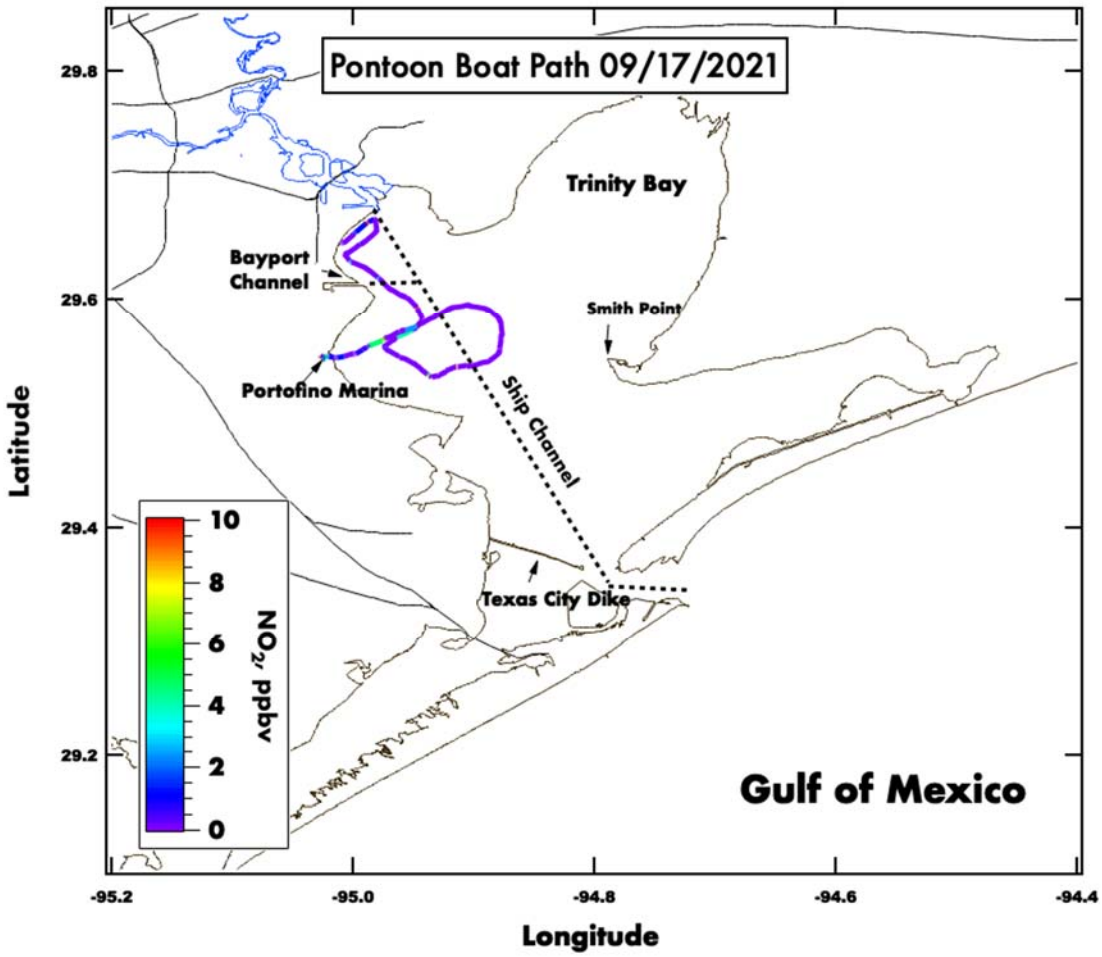

Figure 113. Spatial plot of surface NO_2, calculated from observed Ox, collected from the UH pontoon boat on September 17th, 2021.

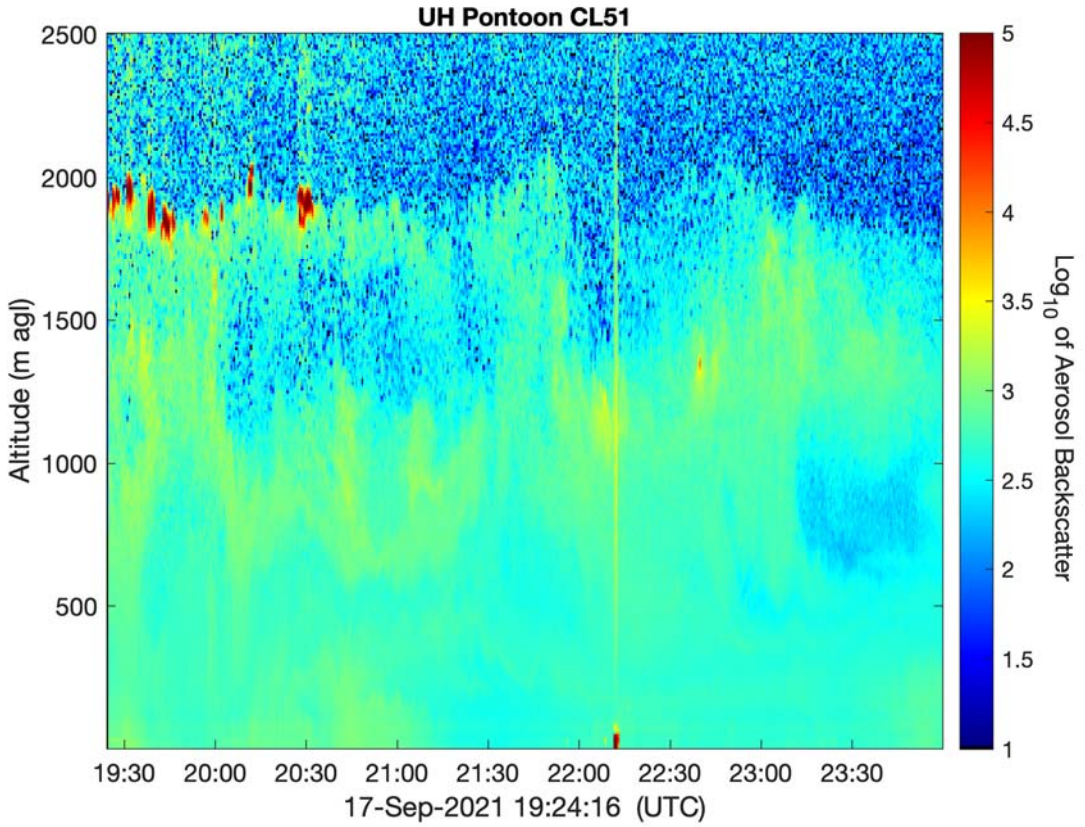

Figure 114. Vertical profile of the aerosol backscatter collected from a Vaisala CL-51 ceilometer mounted on the UH Pontoon boat.

9.8 9 September 2021:

Travis Griggs (UH) and Michael Comas (UH) met at the marina at 7:00am CST. The daily plan was to replace the starter on the boat motor before deploying. Unfortunately, the wrong part had been shipped out. The original starter was reinstalled, and the pontoon was deployed at 8:20am CST. The pontoon went south towards the Texas City Dike and launched the first ozonesonde at 10:55am CST. There was a noticeable haze layer near the surface on this morning. After the first launch the pontoon was taken back to Kemah to refuel. Afterwards the UH pontoon boat went to the NW section of the Bay and launched a second ozonesonde near Morgan's Point. At 2:30pm CST. The pontoon was refueled and docked at approximately 3:30pm CST.

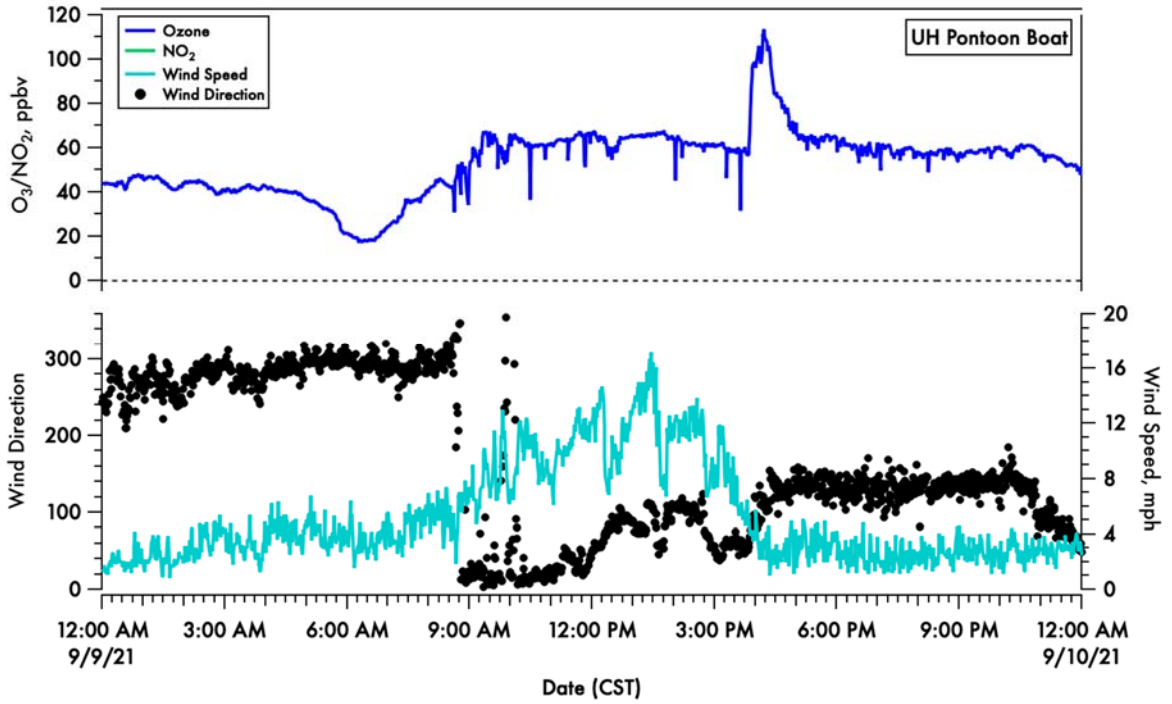

Figure 115. A time-series of 1-minute averaged ozone (blue) on the top panel and wind speed (light blue) and direction (black dots) in the bottom panel.

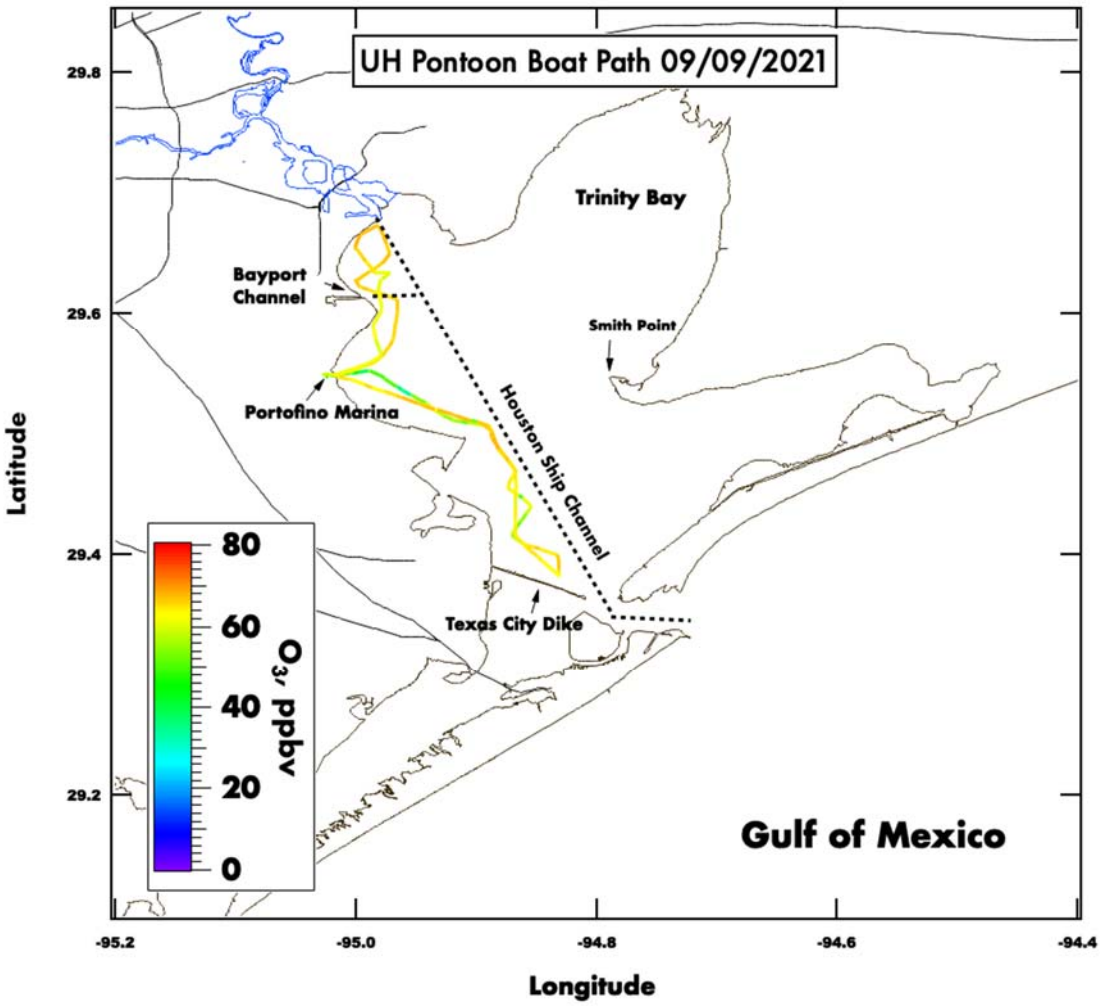

Figure 116. Spatial plot of surface ozone collected from the UH pontoon boat on September 9th, 2021.

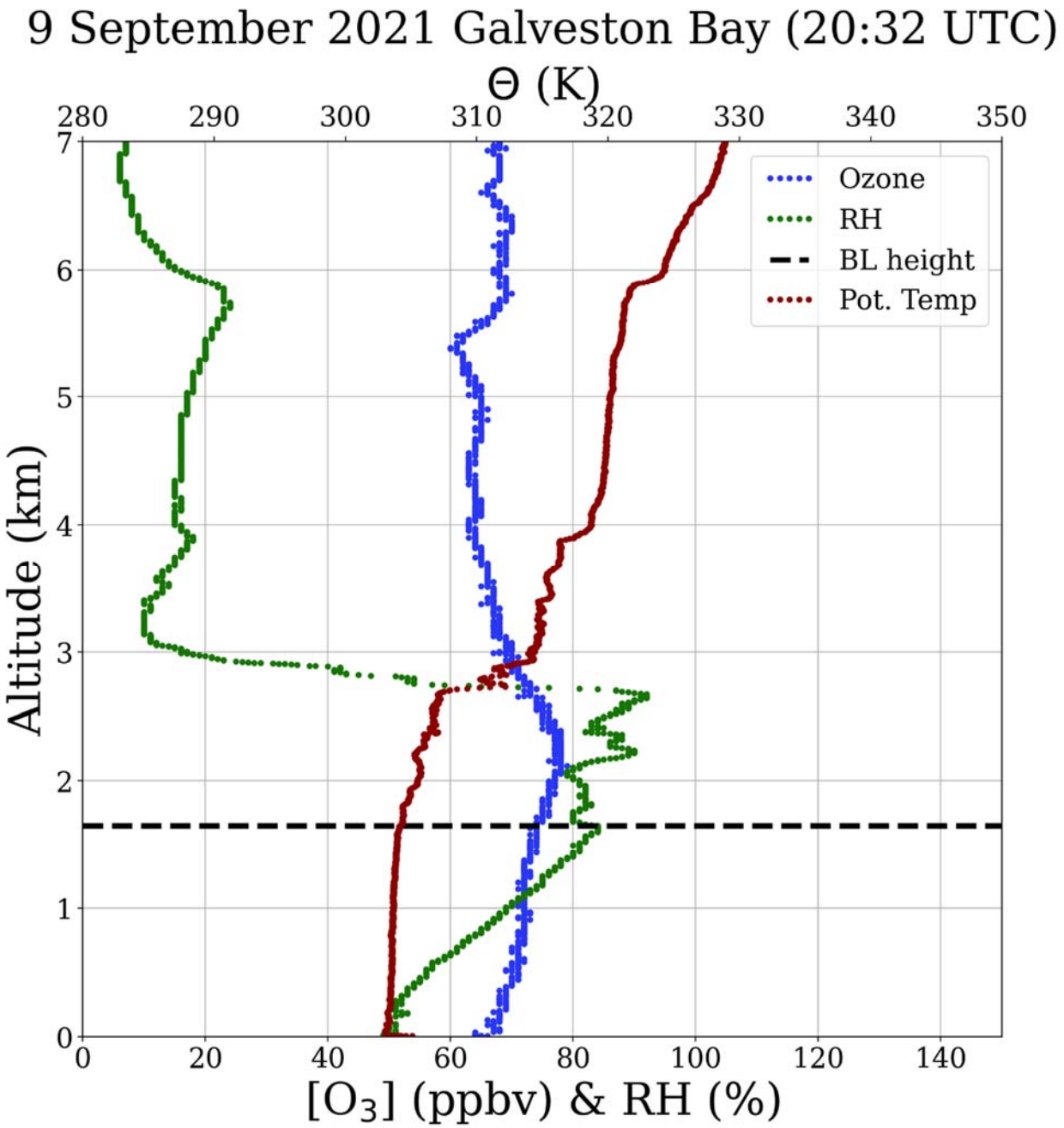

Figure 117. Vertical profiles of ozone (blue), relative humidity (green) and potential temperature (red). The derived boundary layer height is denoted by the horizontal dashed black line.

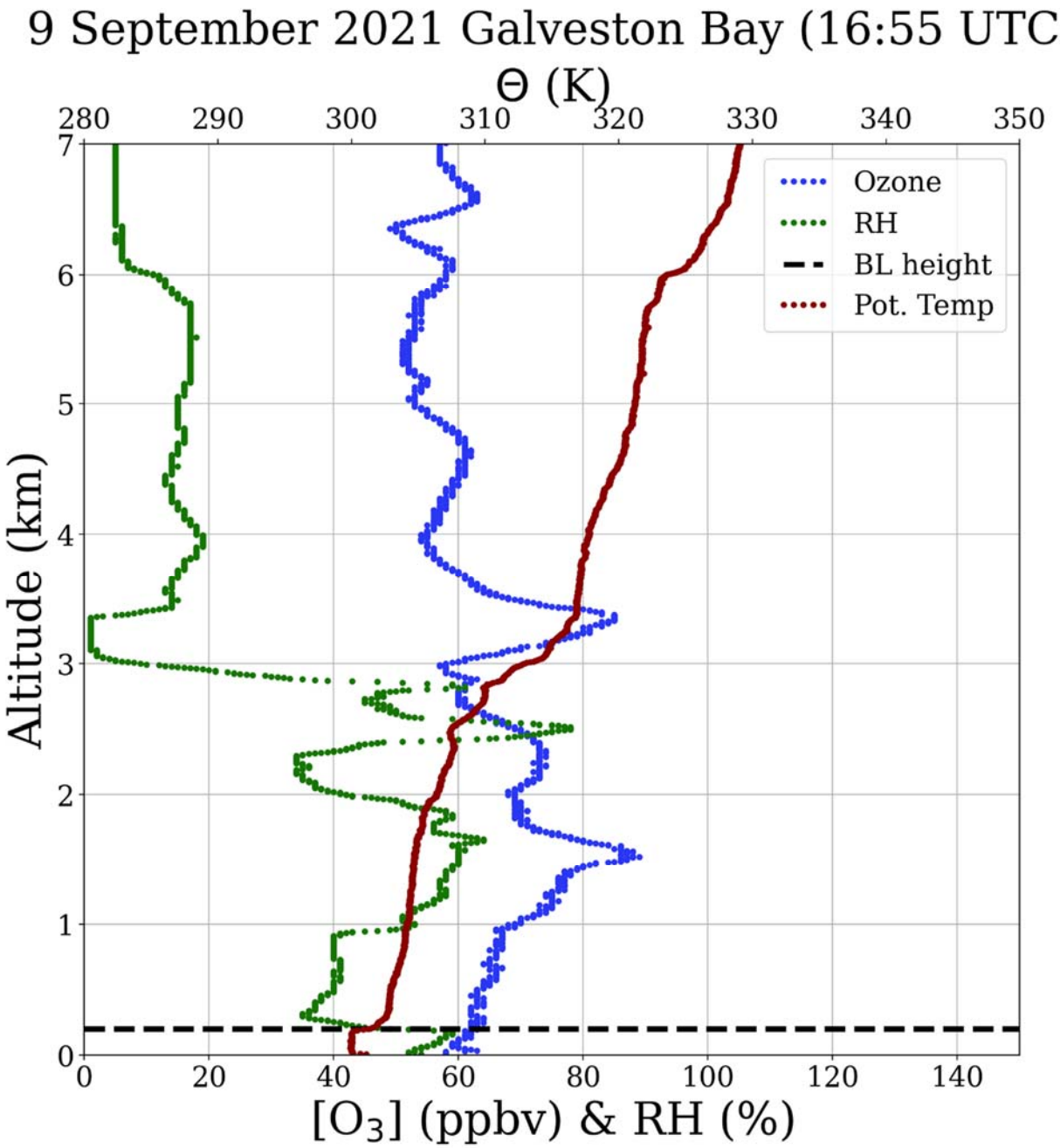

Figure 118. Vertical profiles of ozone (blue), relative humidity (green) and potential temperature (red). The derived boundary layer height is denoted by the horizontal dashed black line.

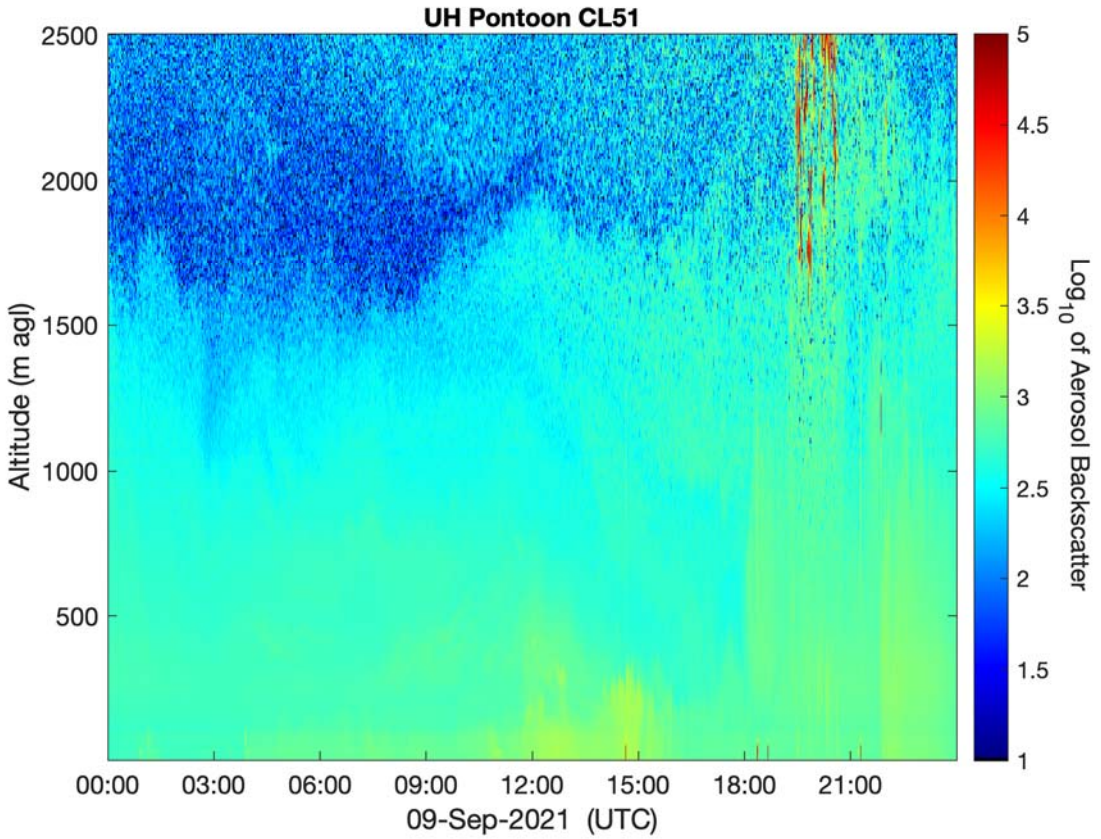

Figure 119. Vertical profile of the aerosol backscatter collected from a Vaisala CL-51 ceilometer mounted on the UH Pontoon boat.

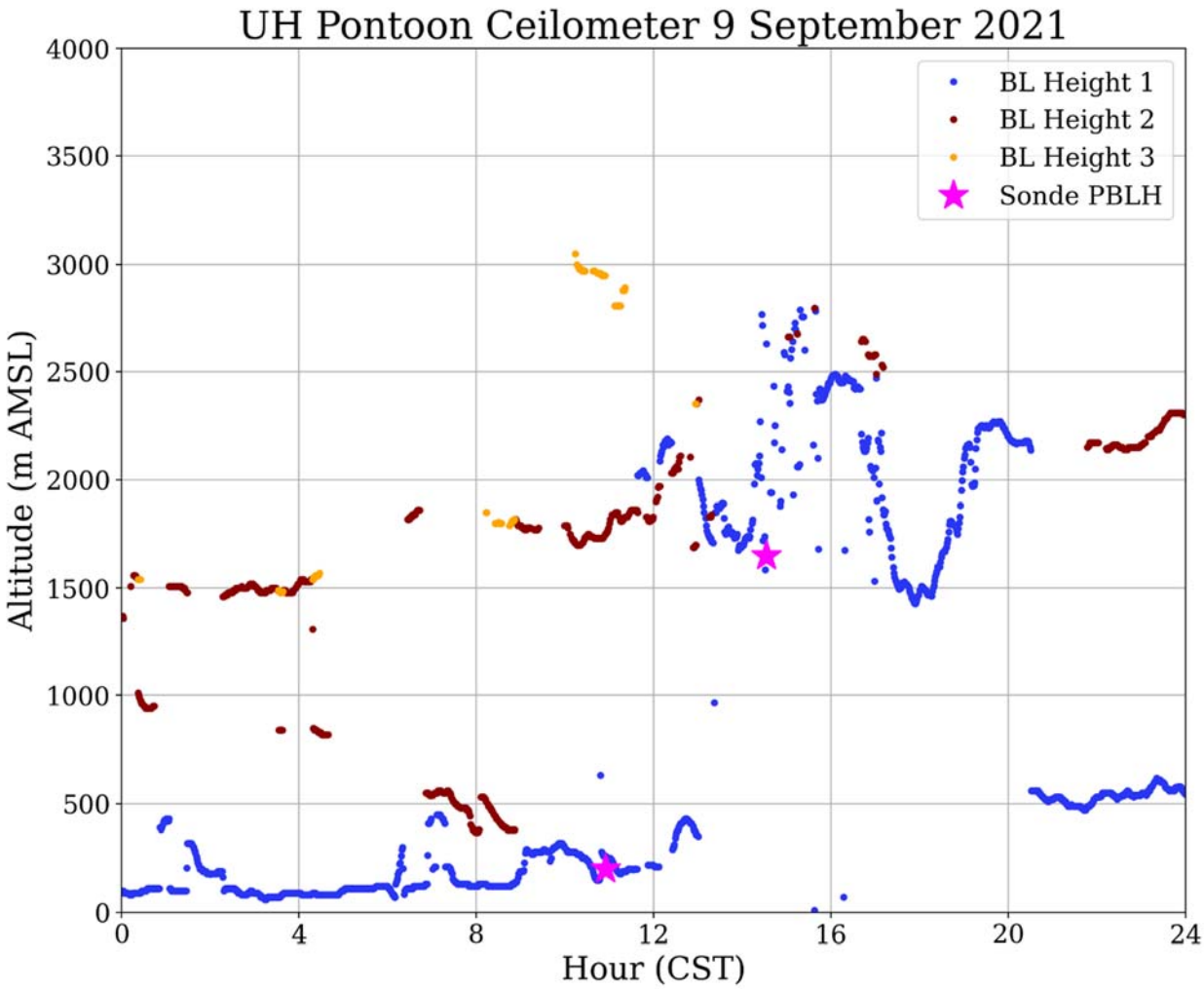

Figure 120. UH Pontoon Vaisala CL-51 ceilometer returned boundary layer heights and boundary layer heights from the ozonesonde profile.

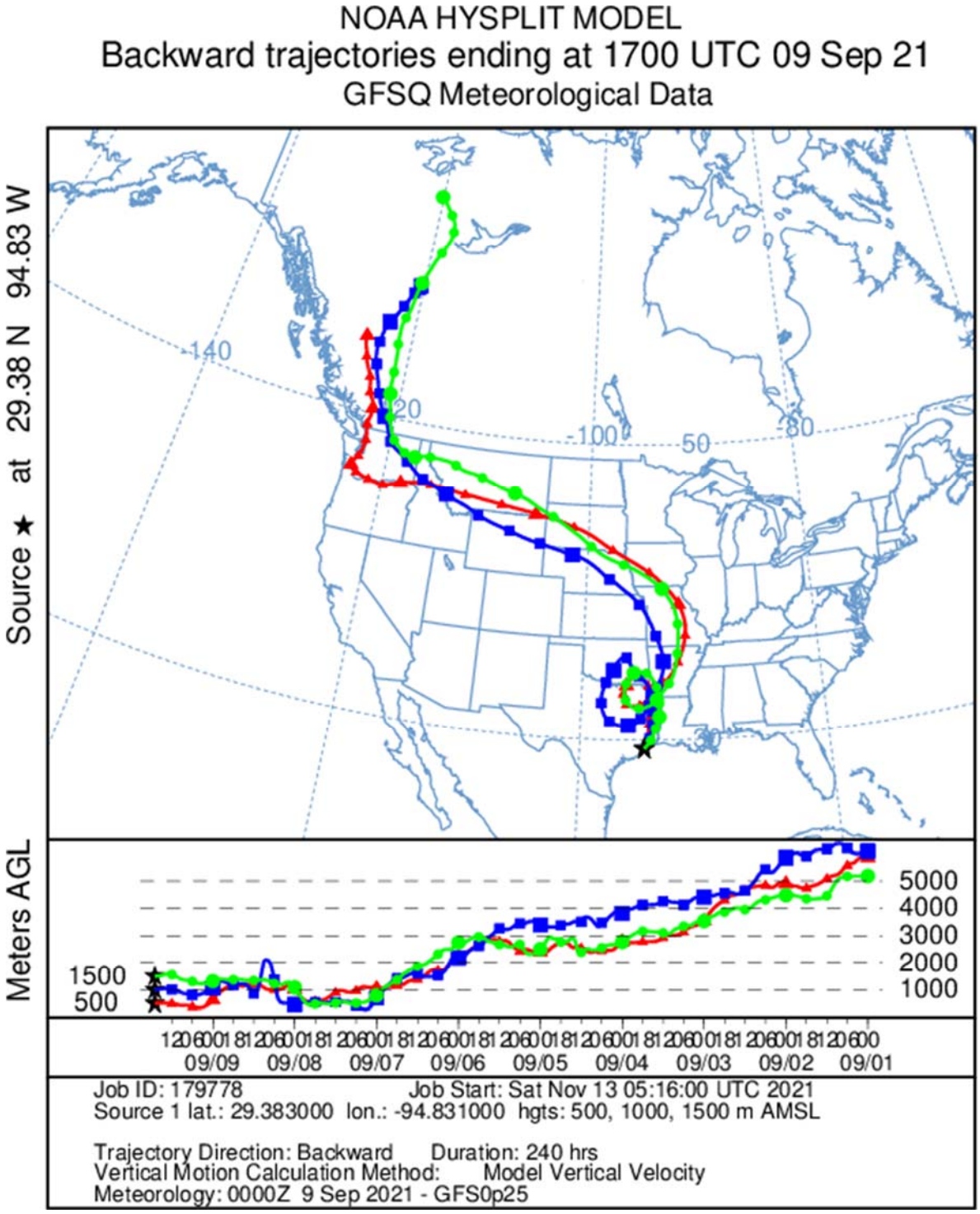

Figure 121. Ten-day HYSPLIT back trajectory for the first ozonesonde launch on 9 September 2021 from three heights over the Bay: 500 m (red), 1,000 m (blue), and 1,500 m (green). Each data point is 6 hours apart.

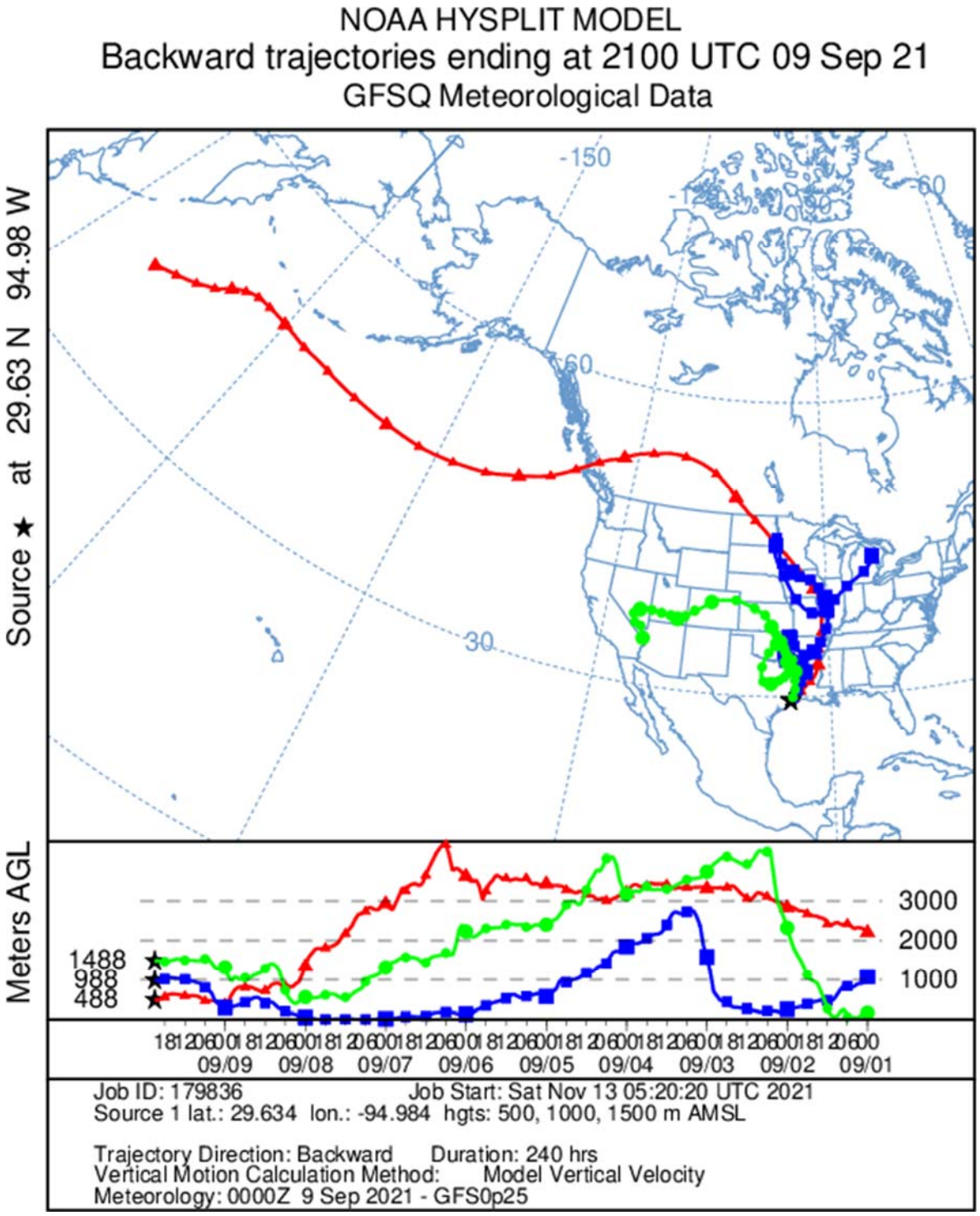

Figure 122. Ten-day HYSPLIT back trajectory for the second ozonesonde launch on 9 September 2021 from three heights over the Bay: 500 m (red), 1,000 m (blue), and 1,500 m (green). Each data point is 6 hours apart.

9.9 8 September 2021:

Travis Griggs (UH) and Michael Comas (UH) met at the marina at 7:00am CST. The daily plan was to go south towards the Texas City Dike. The Bay conditions were a little rougher than expected and the trip to the Texas City Dike took longer than expected. The first ozonesonde was launched near the Texas City Dike at ~11:45pm CST. After the launch the pontoon was taken back to Kemah to be refueled and then redeployed to the NW section of the Bay for afternoon sampling and a second ozonesonde launch. The second ozonesonde launch was successfully released at ~2:22pm CST near Morgan's point. The pontoon boat was refueled and docked at approximately 4:45pm CST.

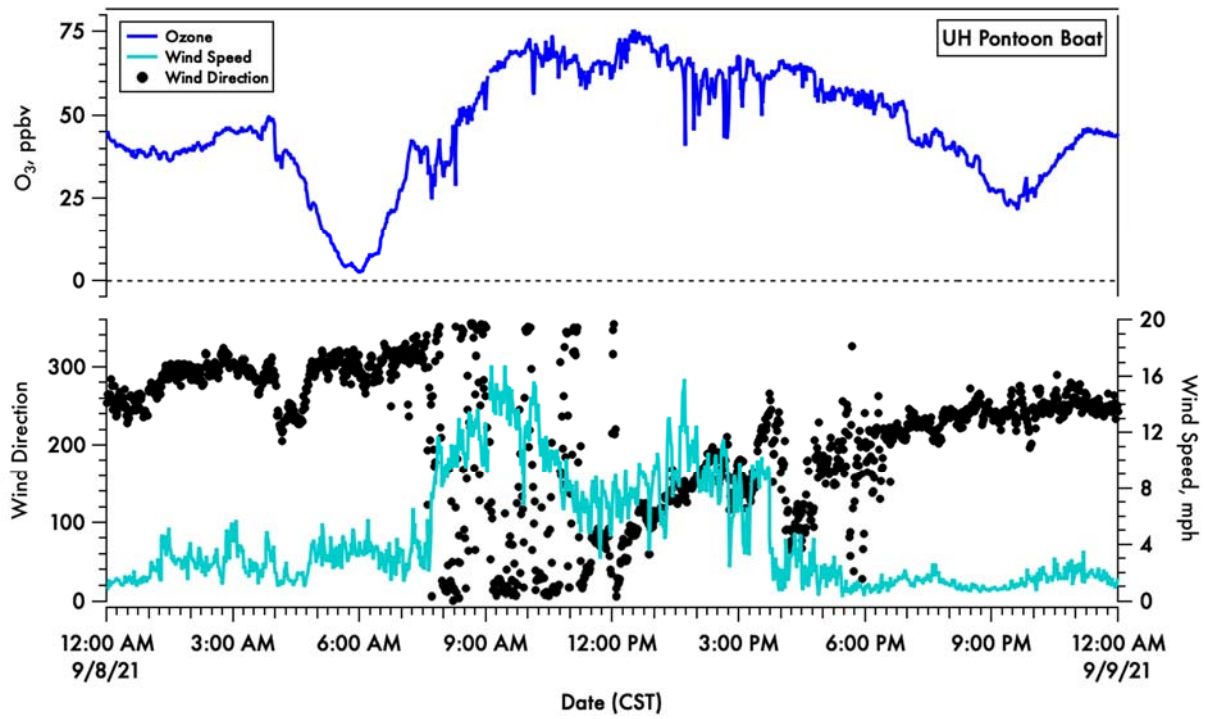

Figure 123. A time-series of 1-minute averaged ozone (blue) on the top panel and wind speed (light blue) and direction (black dots) in the bottom panel.

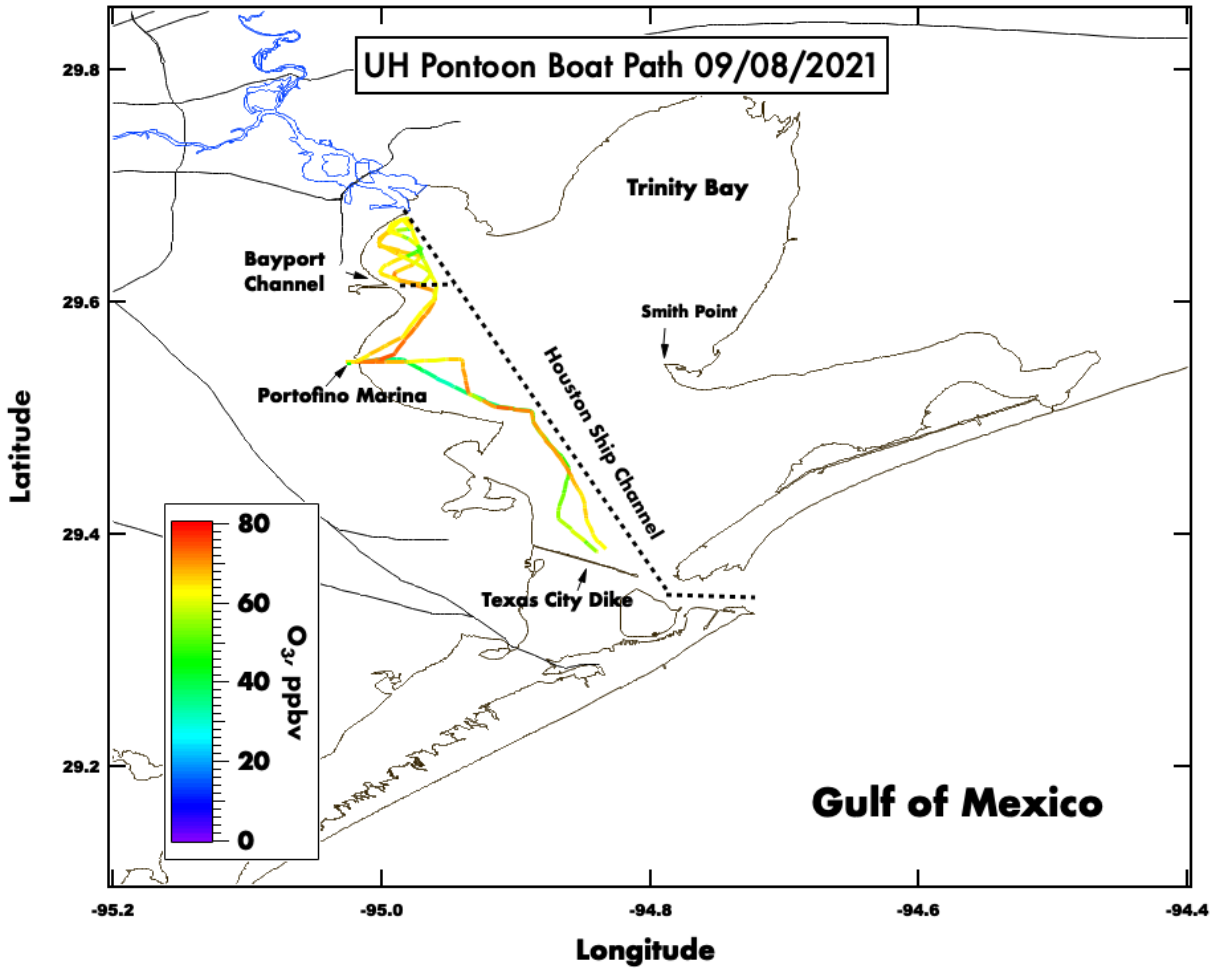

Figure 124. Spatial plot of surface ozone collected from the UH pontoon boat on September 9th, 2021.

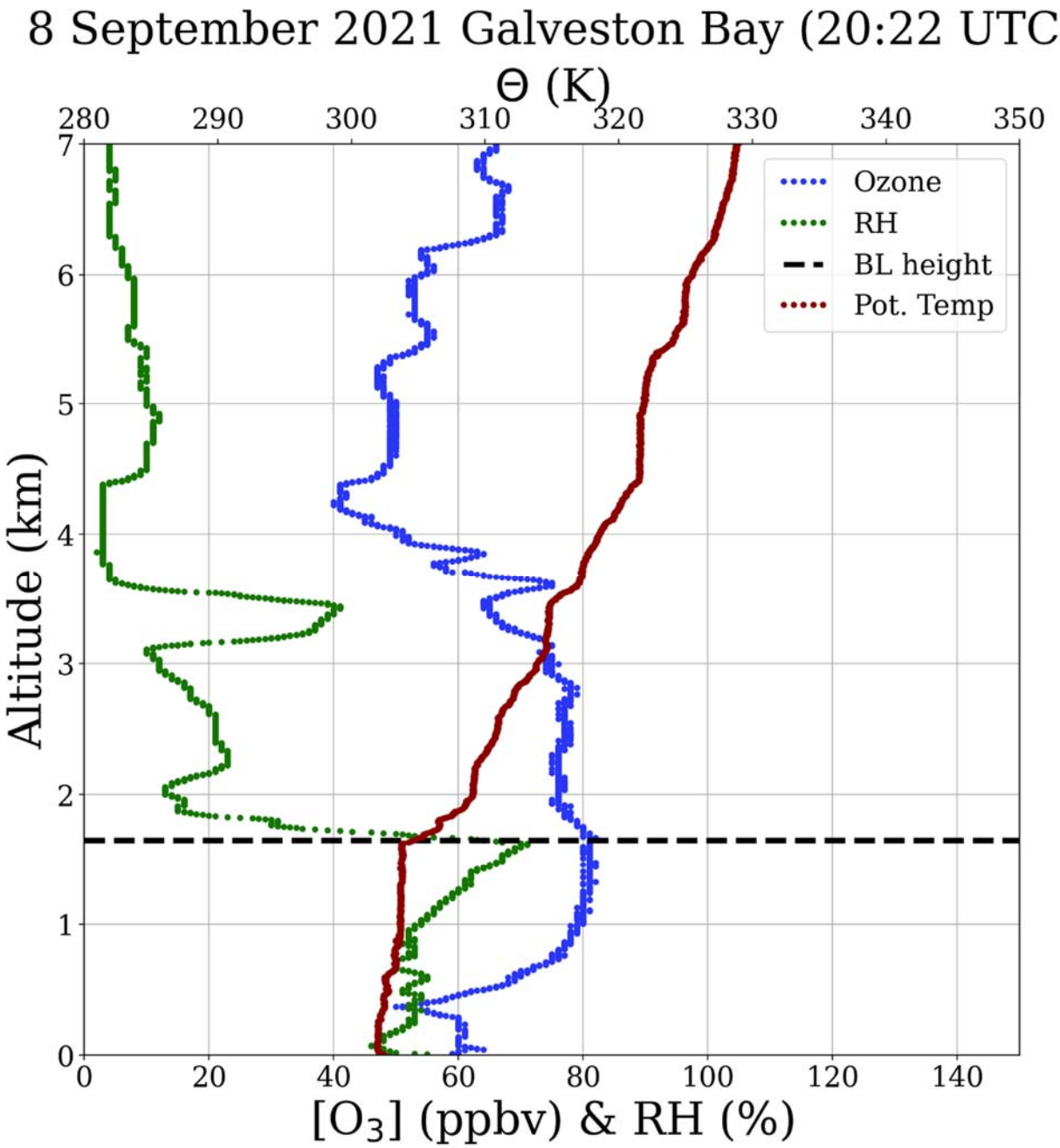

Figure 125. Vertical profiles of ozone (blue), relative humidity (green) and potential temperature (red). The derived boundary layer height is denoted by the horizontal dashed black line.

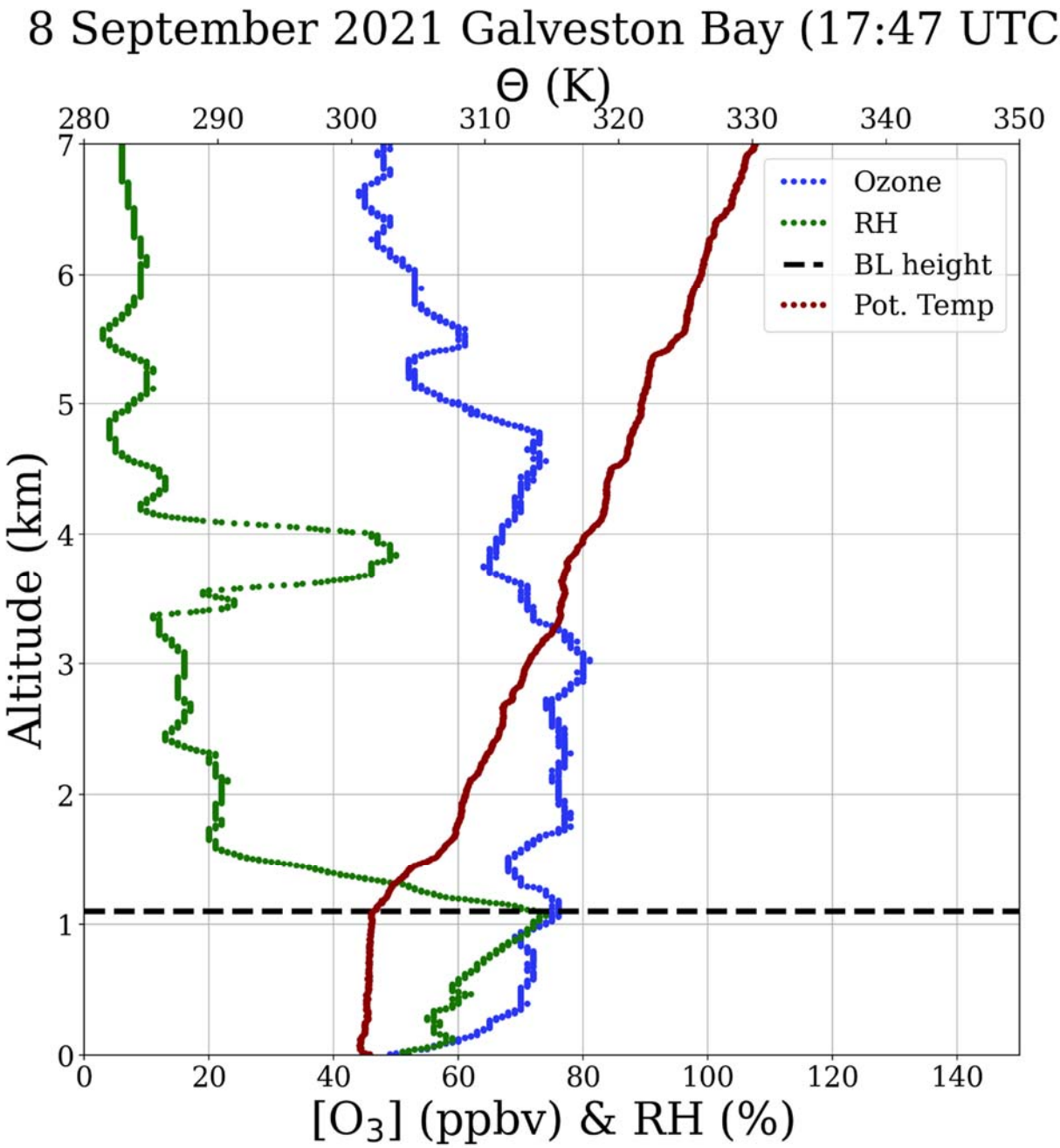

Figure 126. Vertical profiles of ozone (blue), relative humidity (green) and potential temperature (red). The derived boundary layer height is denoted by the horizontal dashed black line.

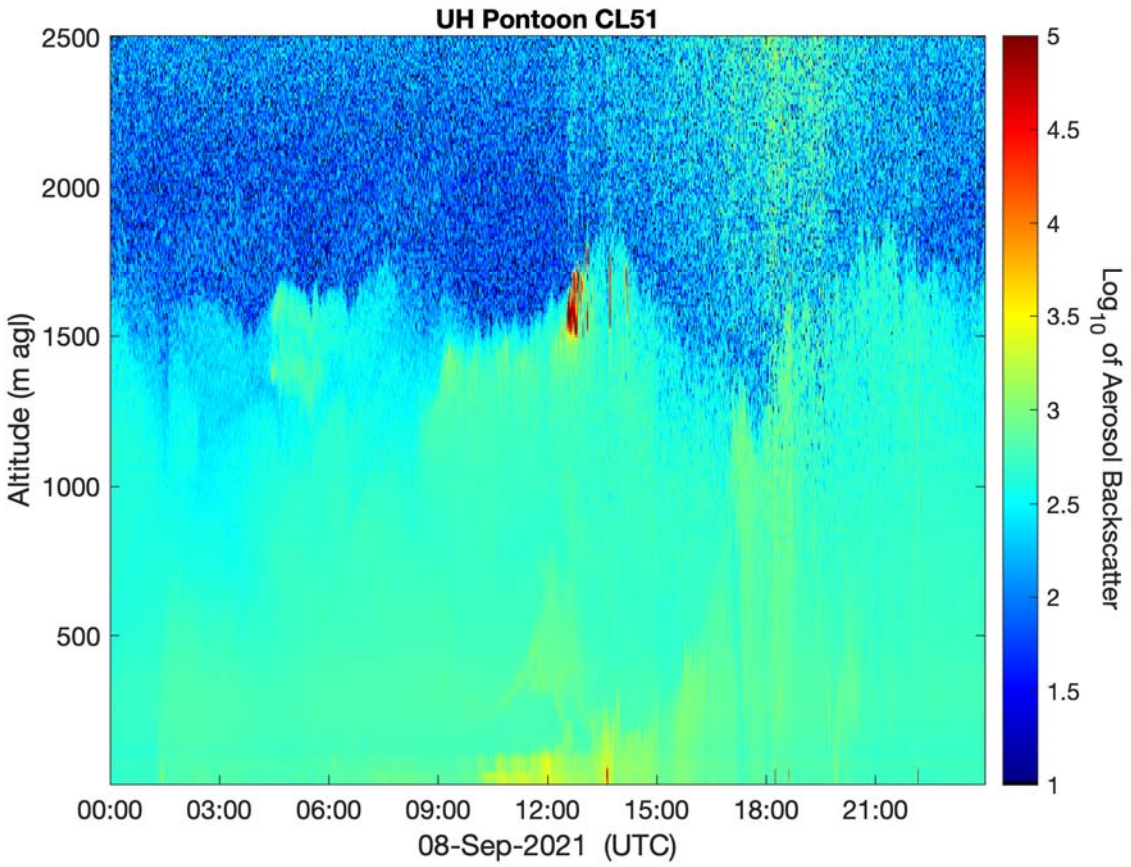

Figure 127. Vertical profile of the aerosol backscatter collected from a Vaisala CL-51 ceilometer mounted on the UH Pontoon boat.

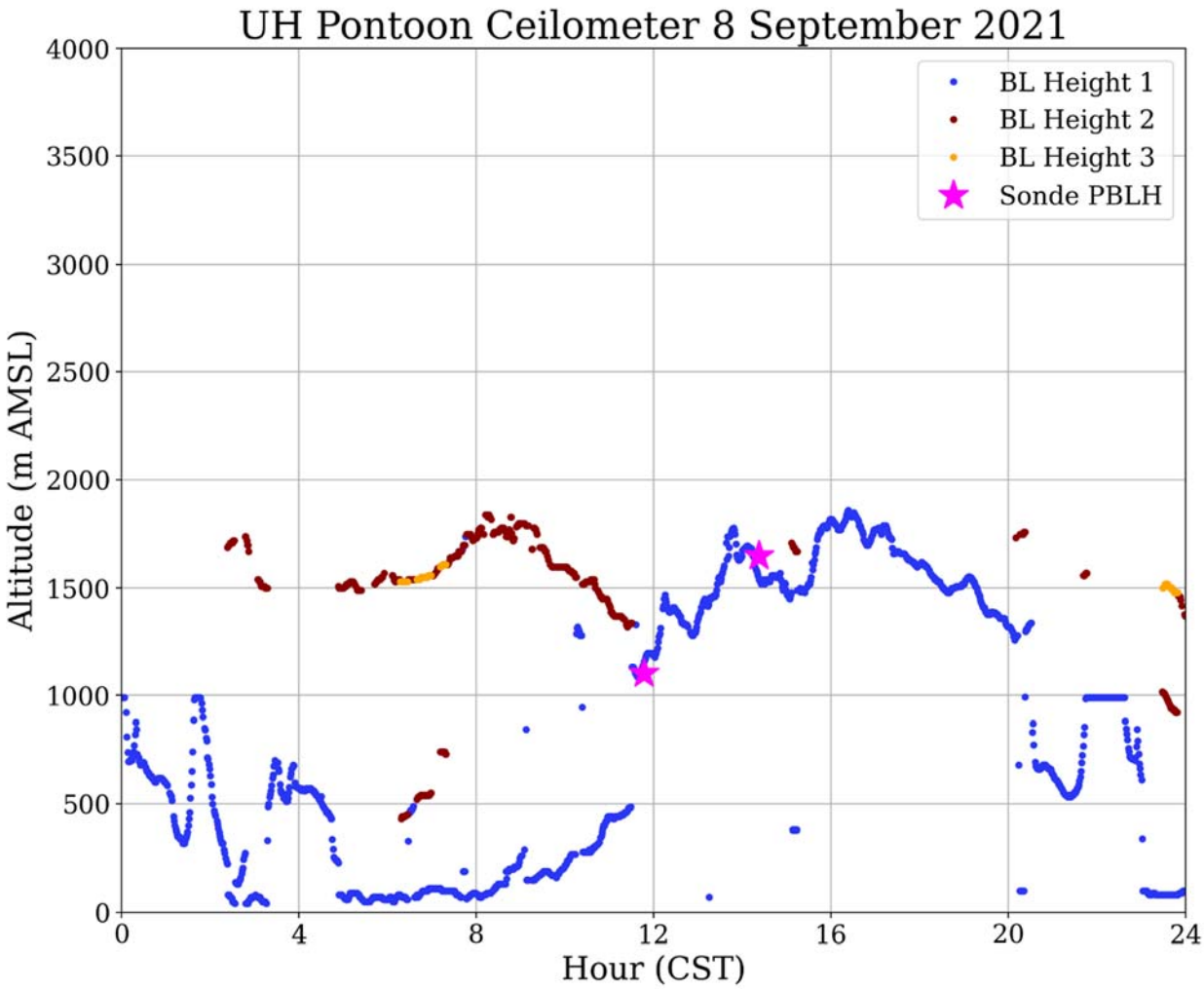

Figure 128. UH Pontoon Vaisala CL-51 ceilometer returned boundary layer heights and boundary layer height from the ozonesonde profile.

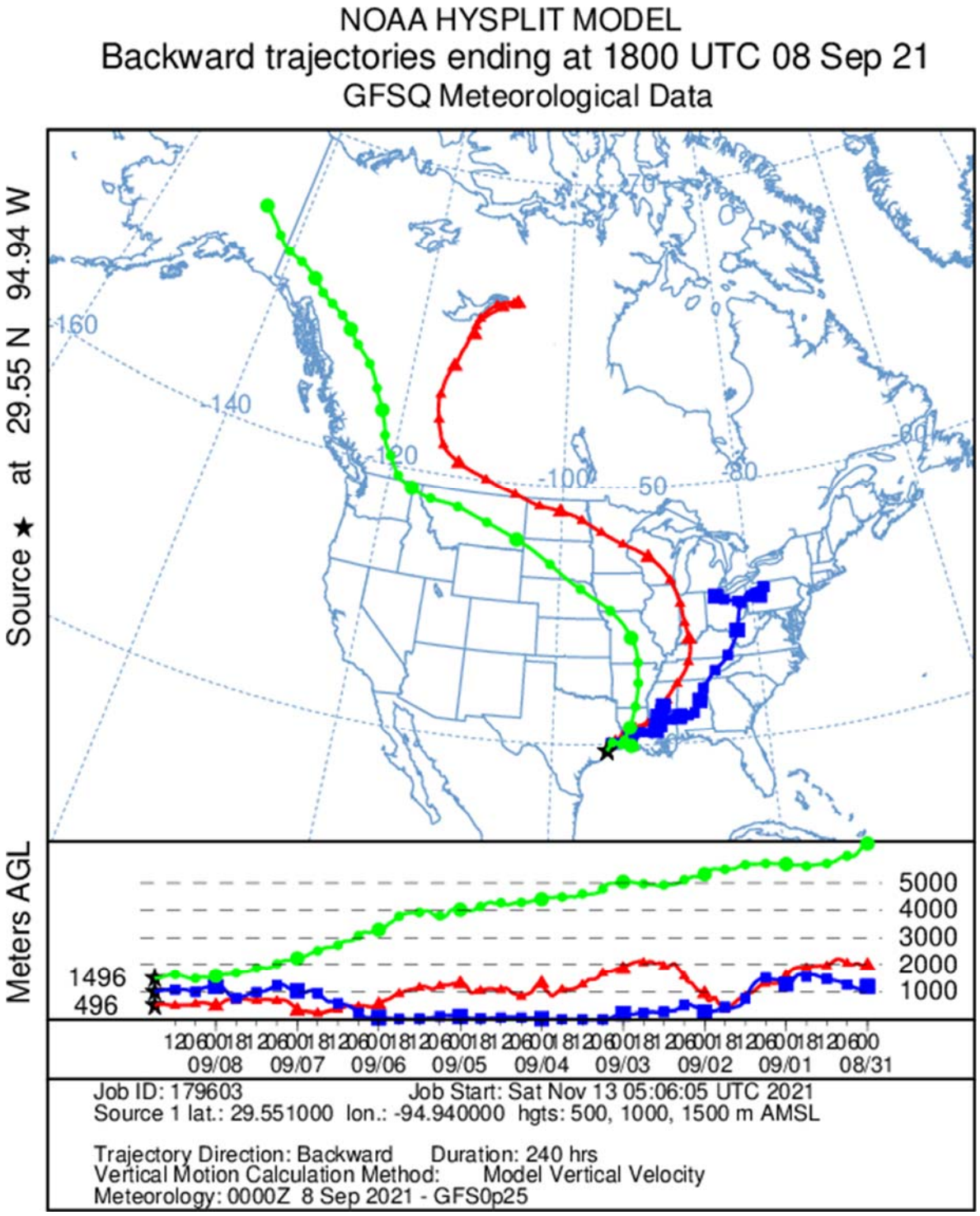

Figure 129. Ten-day HYSPLIT back trajectory for the first ozonesonde launch on 8 September 2021 from three heights over the Bay: 500 m (red), 1,000 m (blue), and 1,500 m (green). Each data point is 6 hours apart.

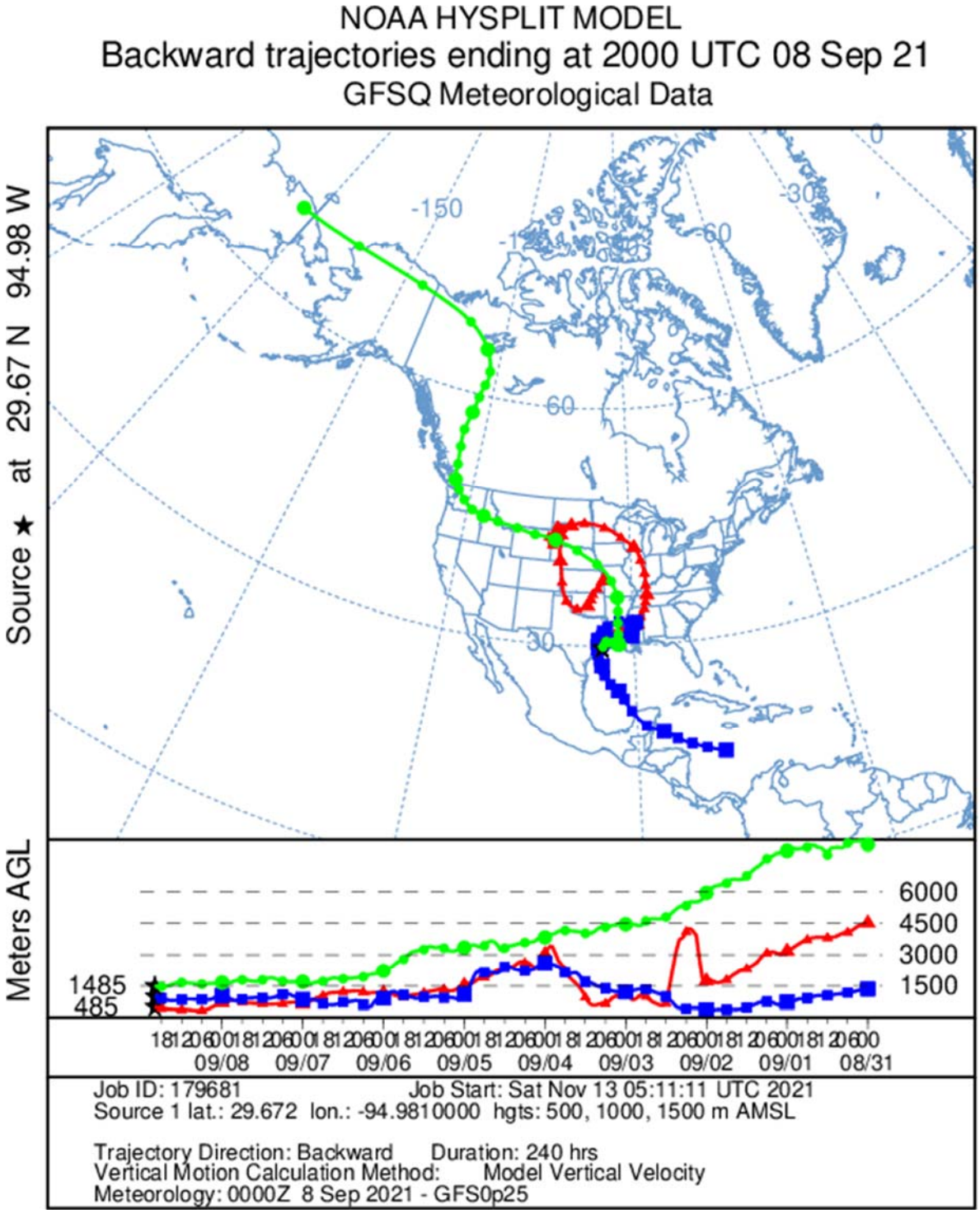

Figure 130. Ten-day HYSPLIT back trajectory for the second ozonesonde launch on 8 September 2021 from three heights over the Bay: 500 m (red), 1,000 m (blue), and 1,500 m (green). Each data point is 6 hours apart.

9.10 7 September 2021:

Travis Griggs (UH) and Michael Comas (UH) met at the marina at 7:30am CST. The daily plan was to go north towards Morgan's Point and launch an ozonesonde with The NASA aircraft overpass. The sonde was successfully launched at approximately 1:00pm CST. The pontoon was refueled and docked in Kemah at approximately 2:00pm CST.

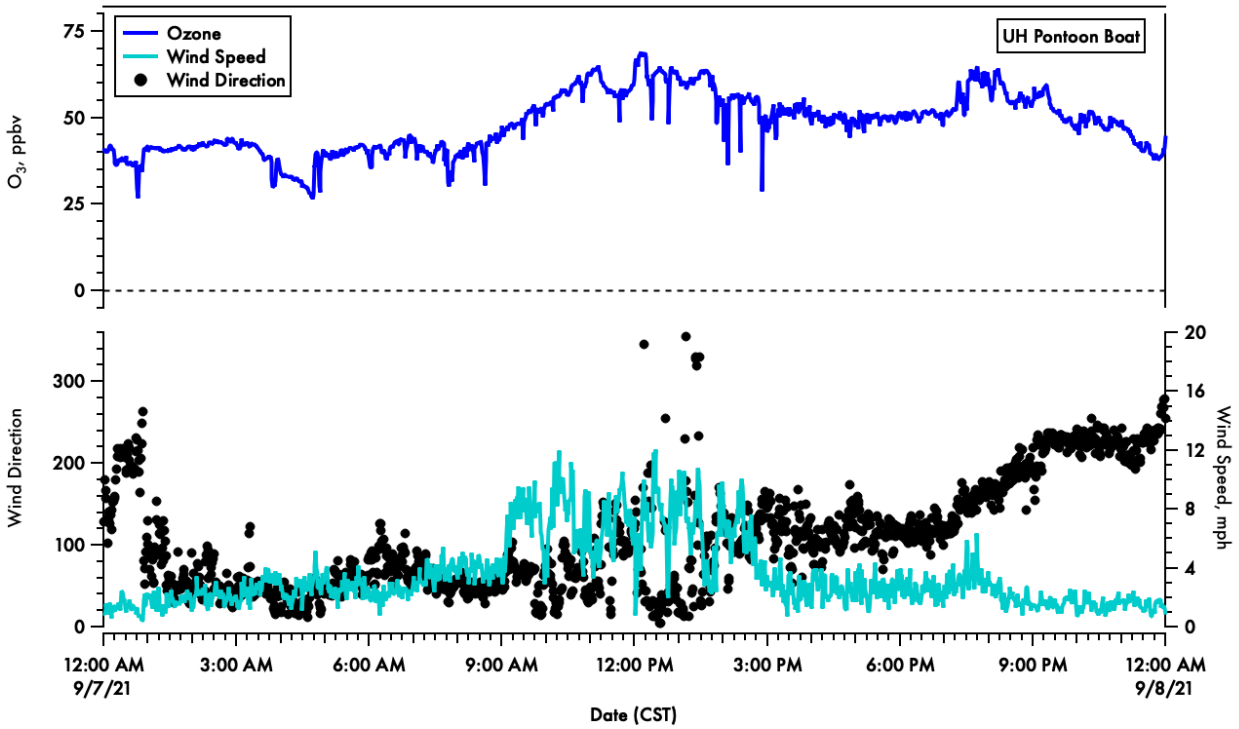

Figure 131. Time-series of 1-minute averaged ozone (blue) on the top panel and wind speed (light blue) and direction (black dots) in the bottom panel.

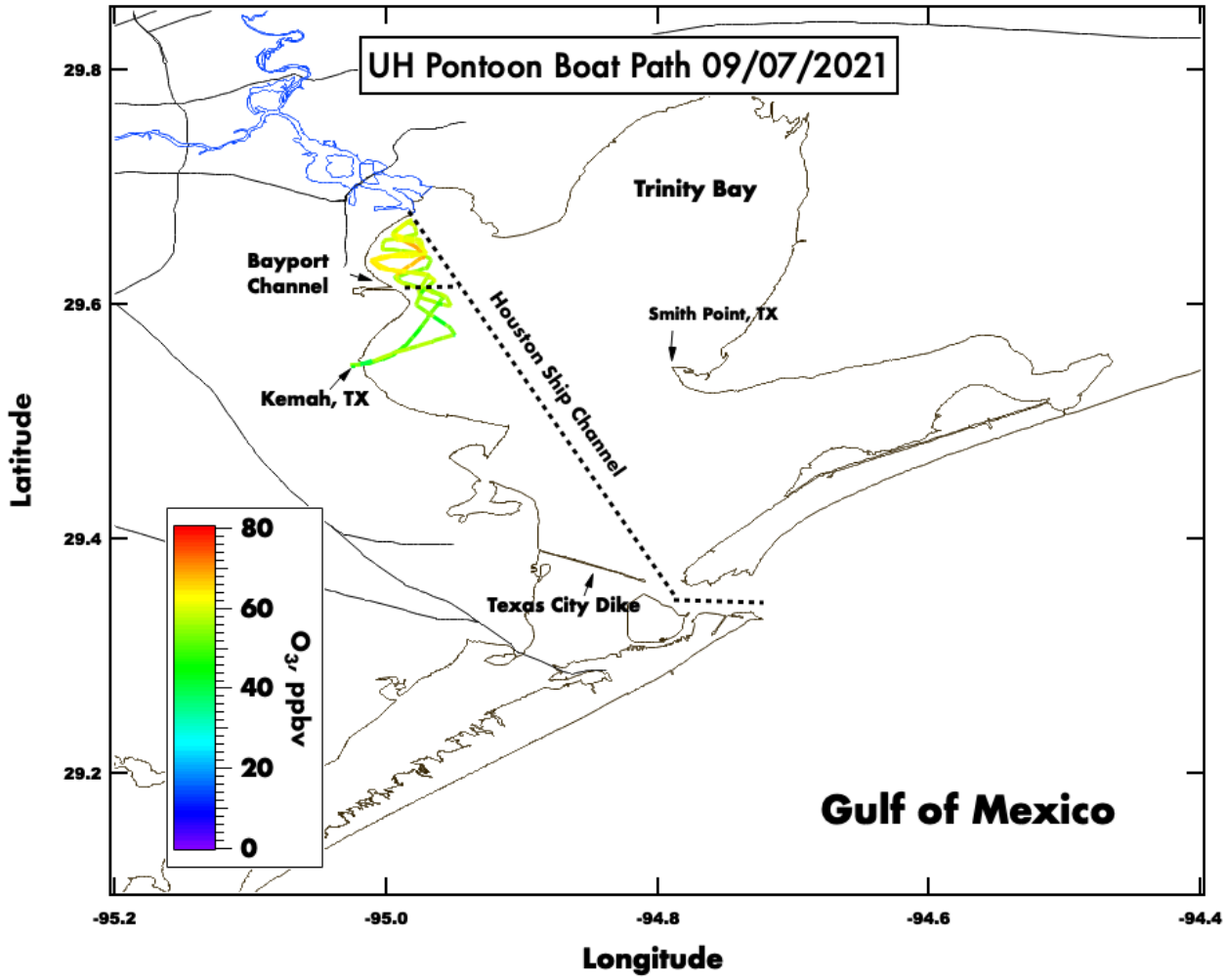

Figure 132. Spatial plot of surface ozone collected from the UH pontoon boat on September 7th, 2021.

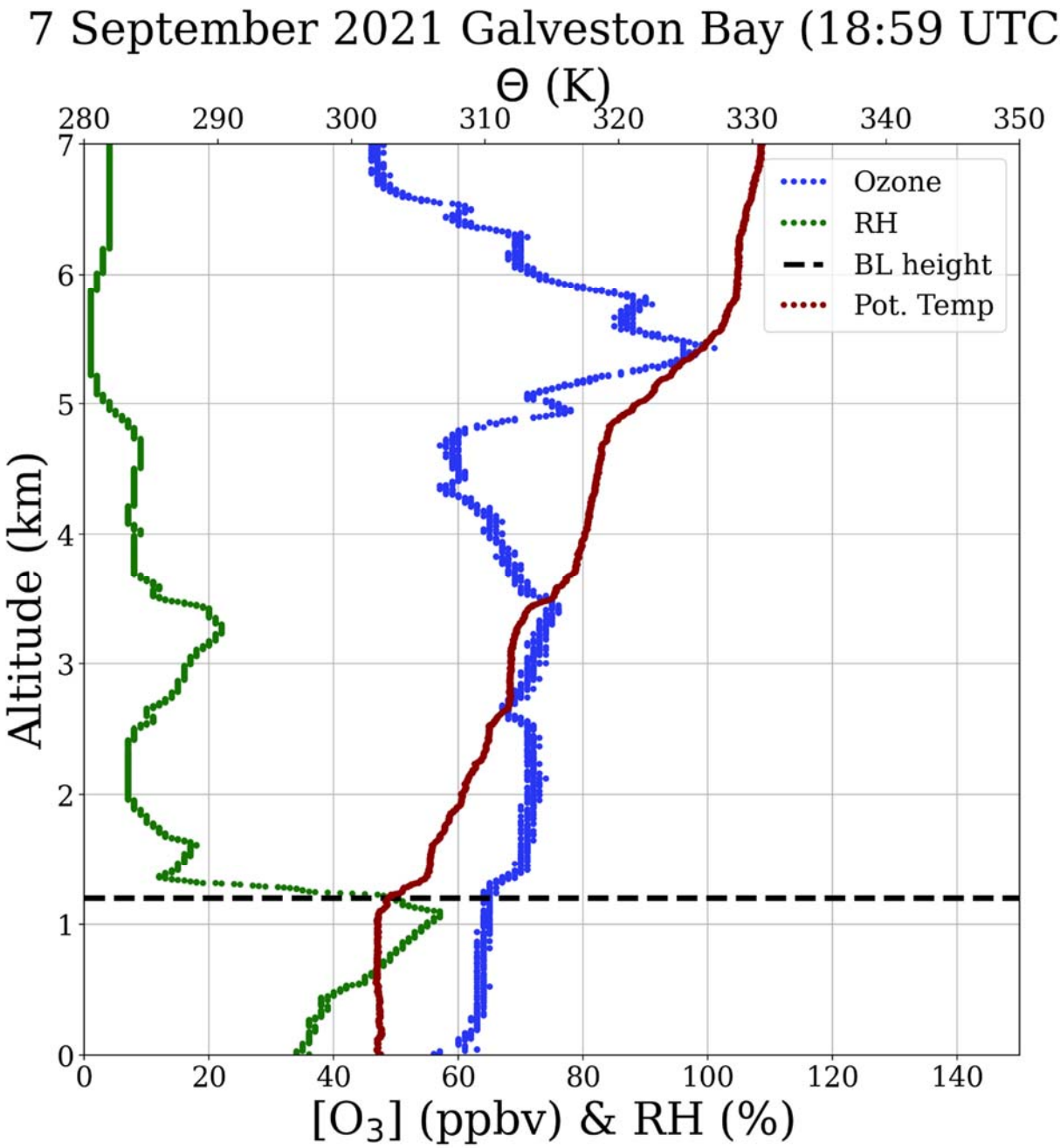

Figure 133. Vertical profiles of ozone (blue), relative humidity (green) and potential temperature (red). The derived boundary layer height is denoted by the horizontal dashed black line.

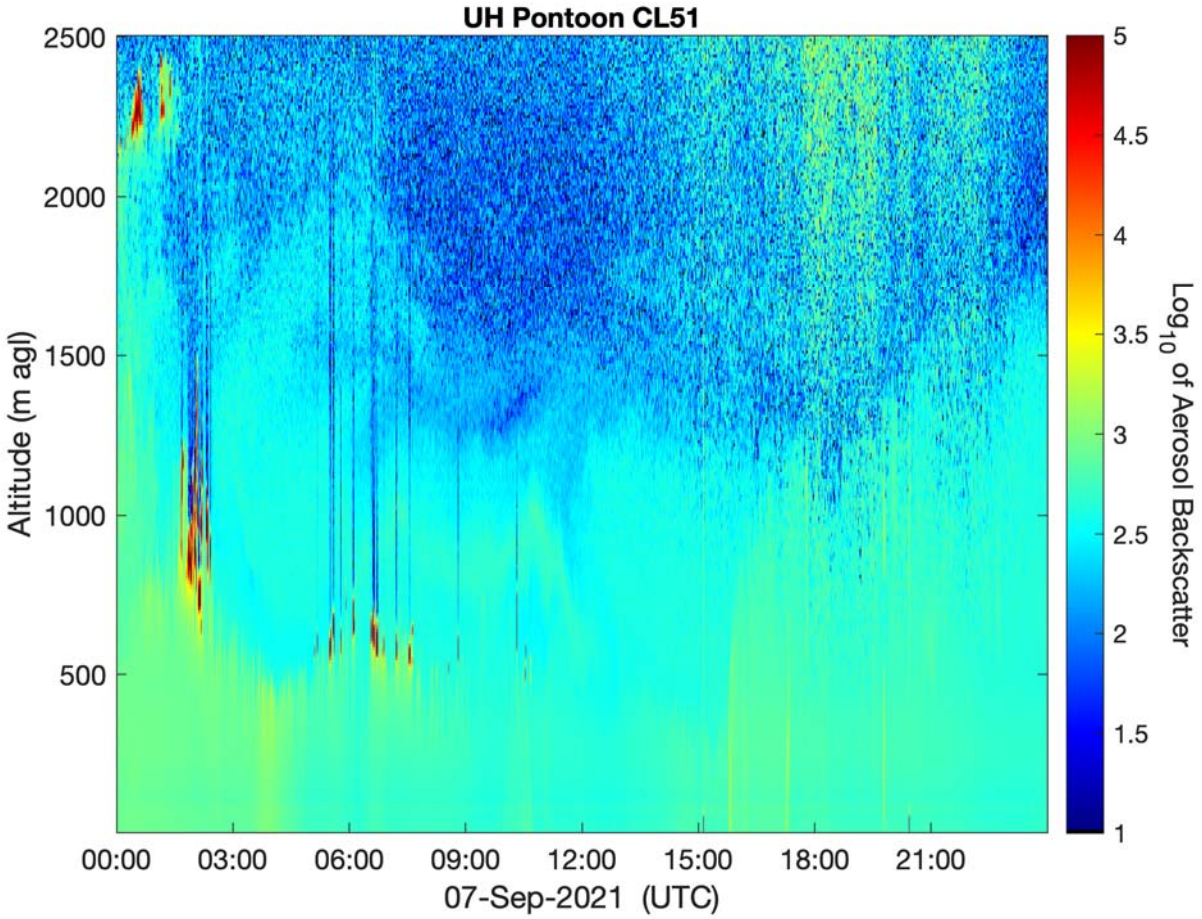

Figure 134. Vertical profile of the aerosol backscatter collected from a Vaisala CL-51 ceilometer mounted on the UH Pontoon boat.

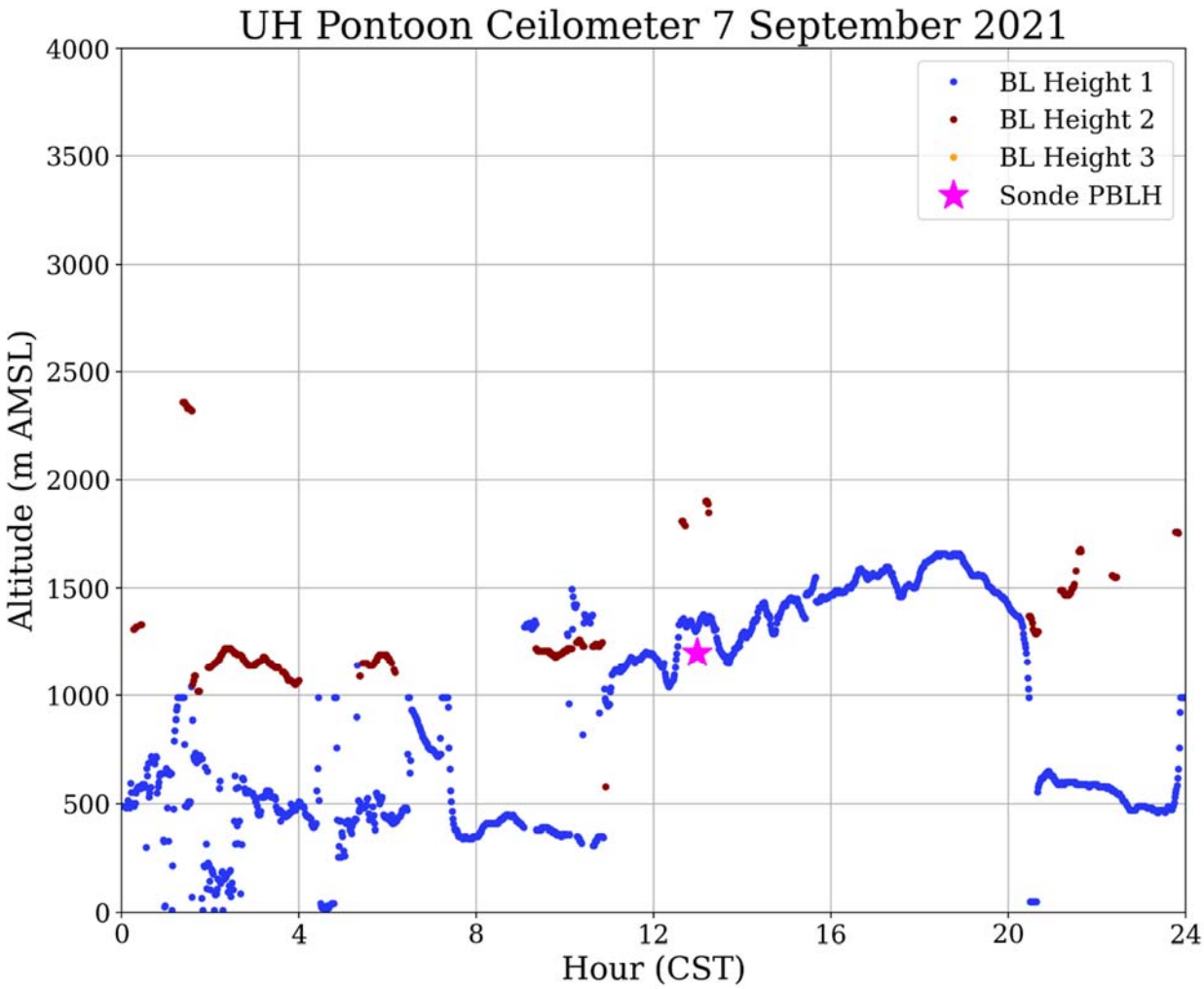

Figure 135. UH Pontoon Vaisala CL-51 ceilometer returned boundary layer heights and boundary layer height from the ozonesonde profile.

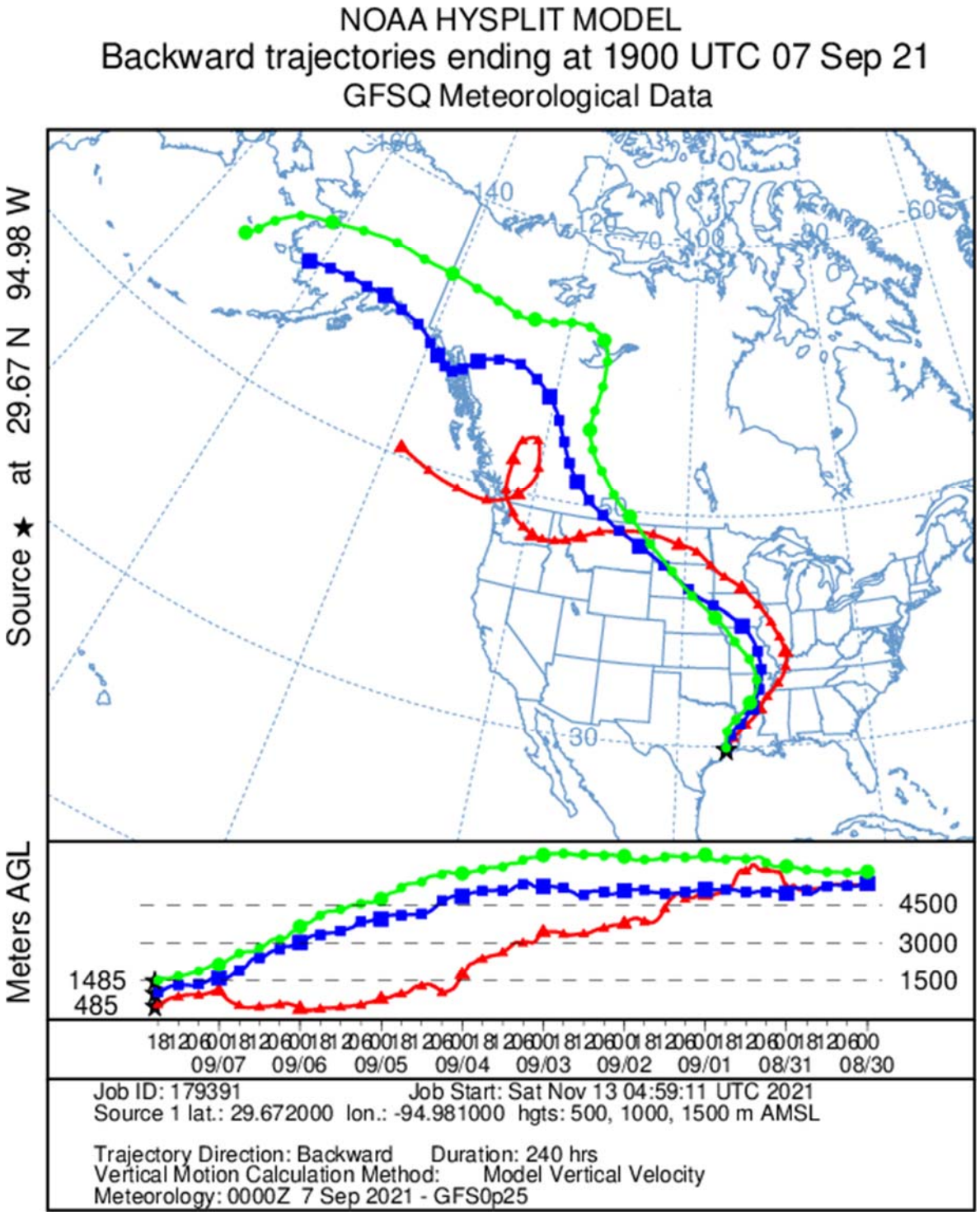

Figure 136. Ten-day HYSPLIT back trajectory for the ozonesonde launch on 7 September 2021 from three heights over the Bay: 500 m (red), 1,000 m (blue), and 1,500 m (green). Each data point is 6 hours apart.

9.11 3 September 2021:

Travis Griggs (UH) and Michael Comas (UH) met at the Portofino Harbor Marina at 7:00am - pushed off at 7:25am CST. Headed to the western portion of the Bay for an ozonesonde launch coinciding with the NASA aircraft flyover. Ozonesonde was launched at 8:30am CST. The pontoon conducted surface sampling in the NW section of the Bay after the launch. The pontoon made a pass into Trinity Bay before heading back to the marina. The afternoon NASA raster patterns were cancelled, and the pontoon headed back to refuel and dock at ~10:50am CST.

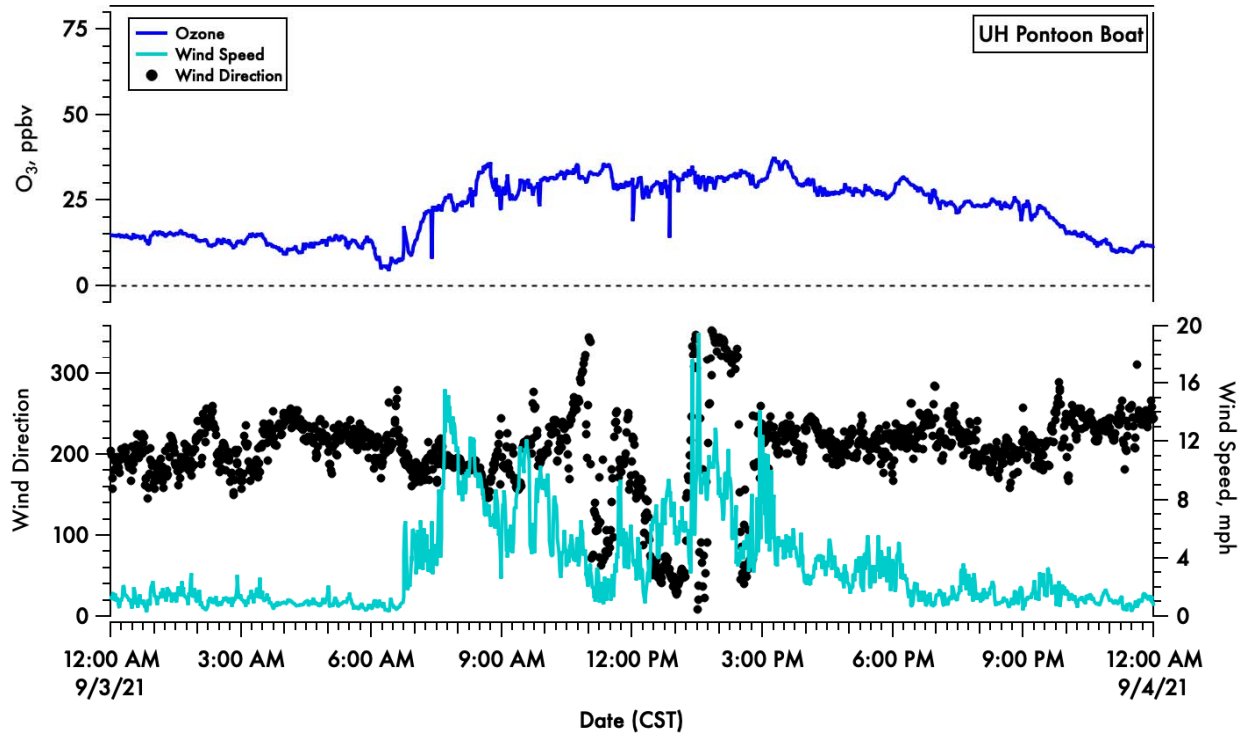

Figure 137. Time-series of 1-minute averaged ozone (blue) on the top panel and wind speed (light blue) and direction (black dots) in the bottom panel.

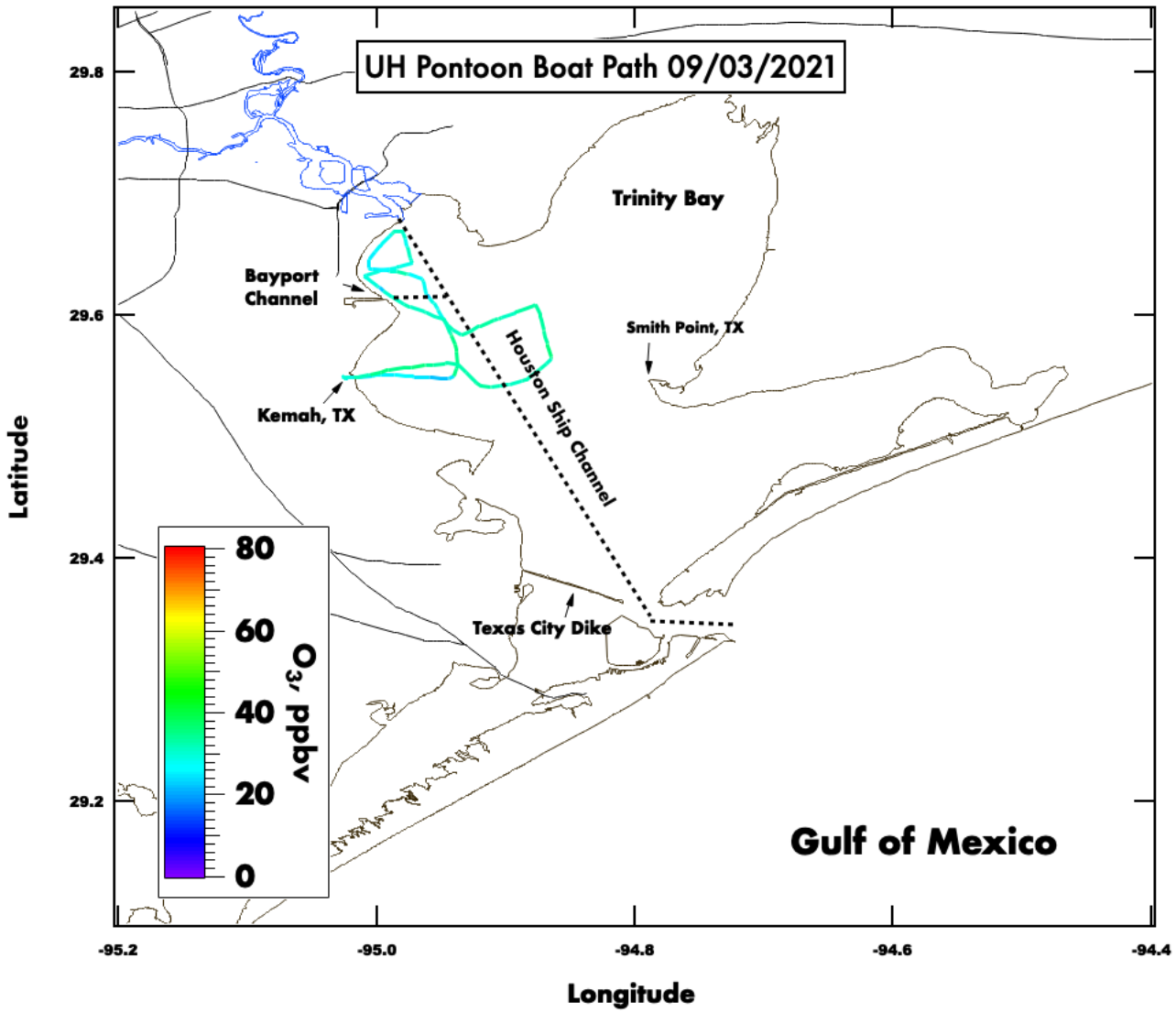

Figure 138. Spatial plot of surface ozone collected from the UH pontoon boat on September 3rd, 2021.

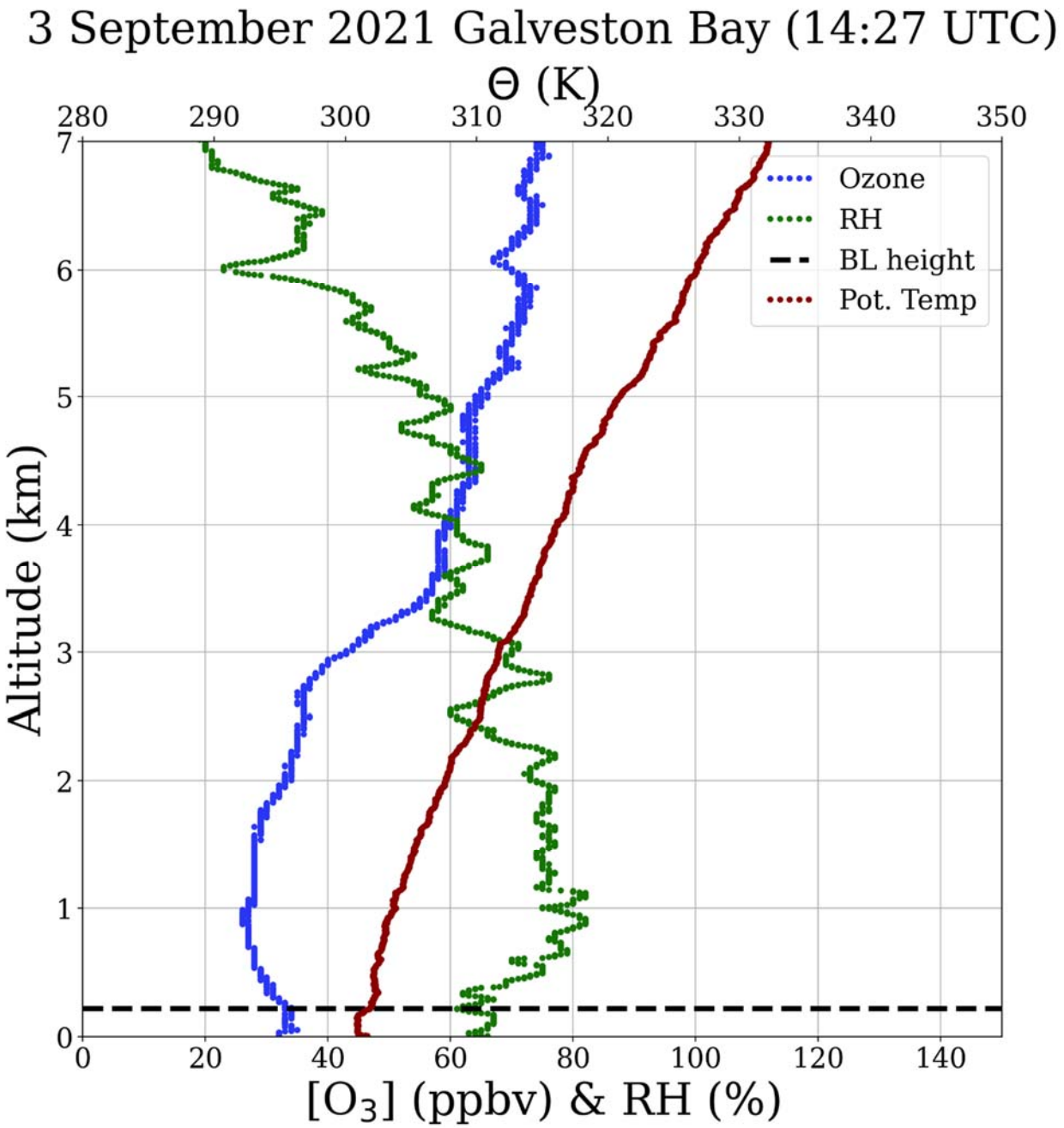

Figure 139. Vertical profiles of ozone (blue), relative humidity (green) and potential temperature (red). The derived boundary layer height is denoted by the horizontal dashed black line.

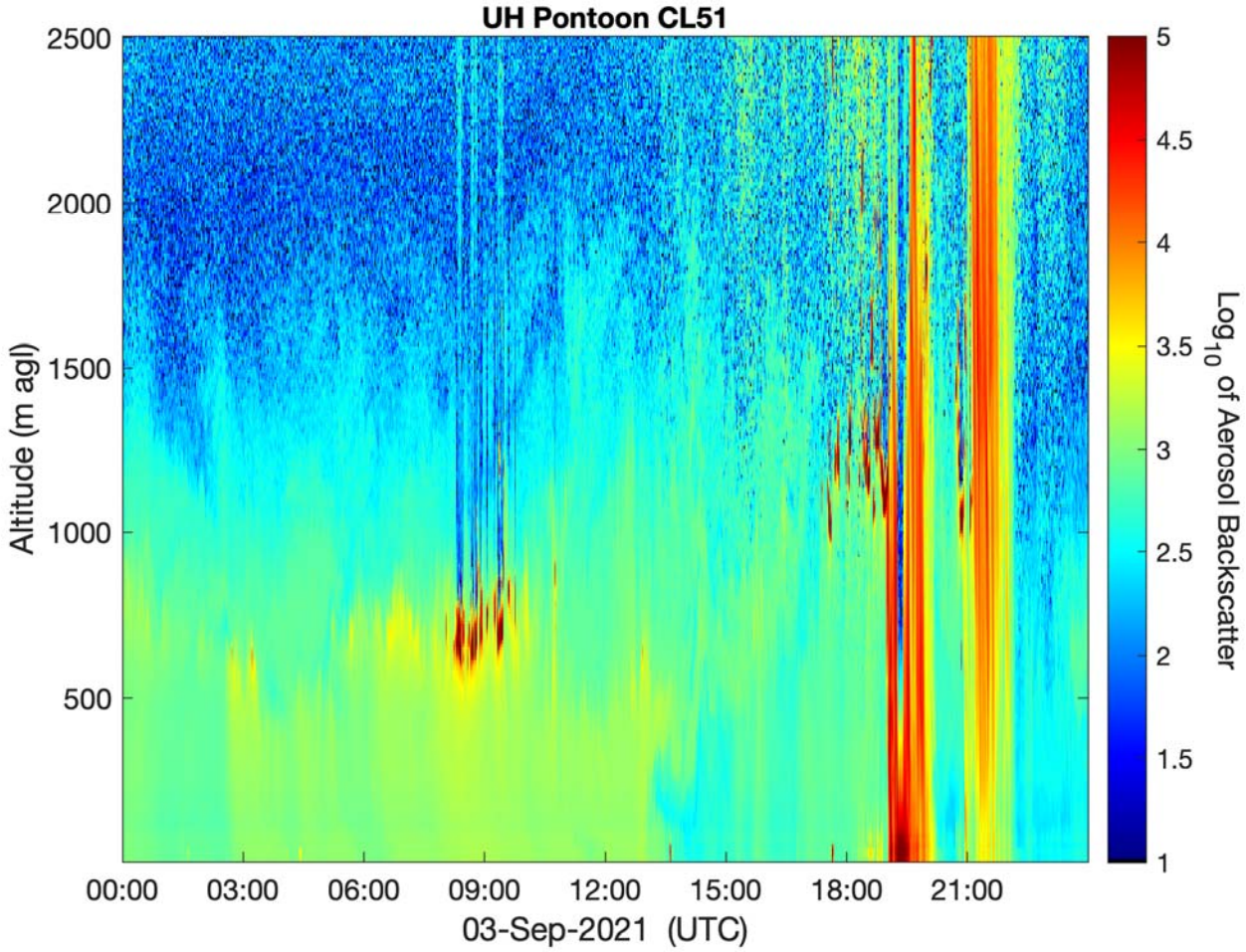

Figure 140. Vertical profile of the aerosol backscatter collected from a Vaisala CL-51 ceilometer mounted on the UH Pontoon boat.

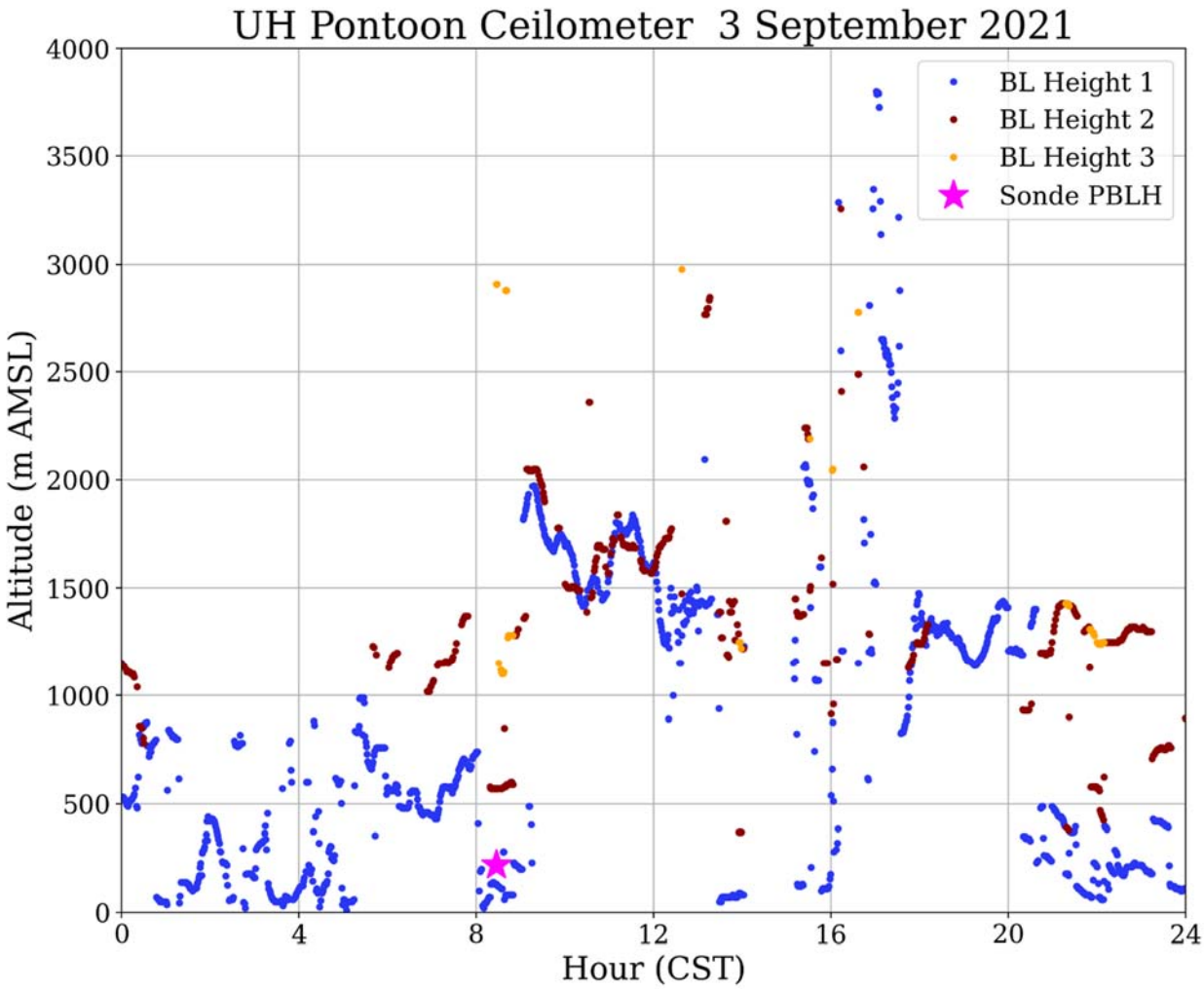

Figure 141. UH Pontoon Vaisala CL-51 ceilometer returned boundary layer heights and boundary layer height from the ozonesonde profile.

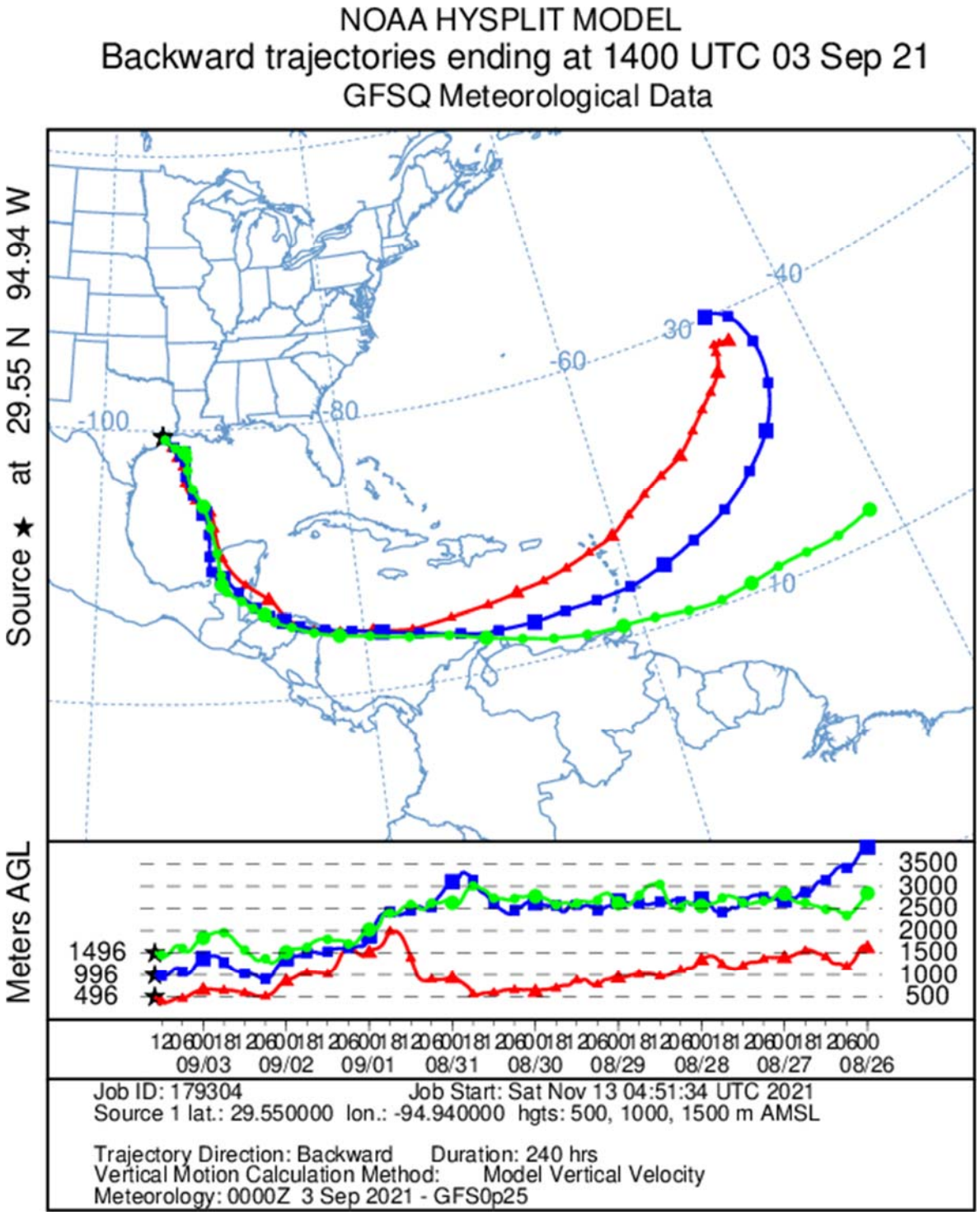

Figure 142. Ten-day HYSPLIT back trajectory for the ozonesonde launch on 3 September 2021 from three heights over the Bay: 500 m (red), 1,000 m (blue), and 1,500 m (green). Each data point is 6 hours apart.

9.12 1 September 2021:

Travis Griggs (UH), Michael Comas (UH) and Claudia Bernier (UH) met at the Portofino Marina at 7:00am CST. First day of the TRACER-AQ campaign. The UPS died overnight; the instruments had to be reconfigured which caused a small delay in deployment. The pontoon initially headed north towards Morgan's Point for surface sampling and launched a 10:00am CST ozonesonde. The NASA aircraft cancelled the afternoon rasters because of cloudy conditions. The pontoon continued surface sampling until it was taken back to Kemah to be refueled and docked at 2:00pm CST.

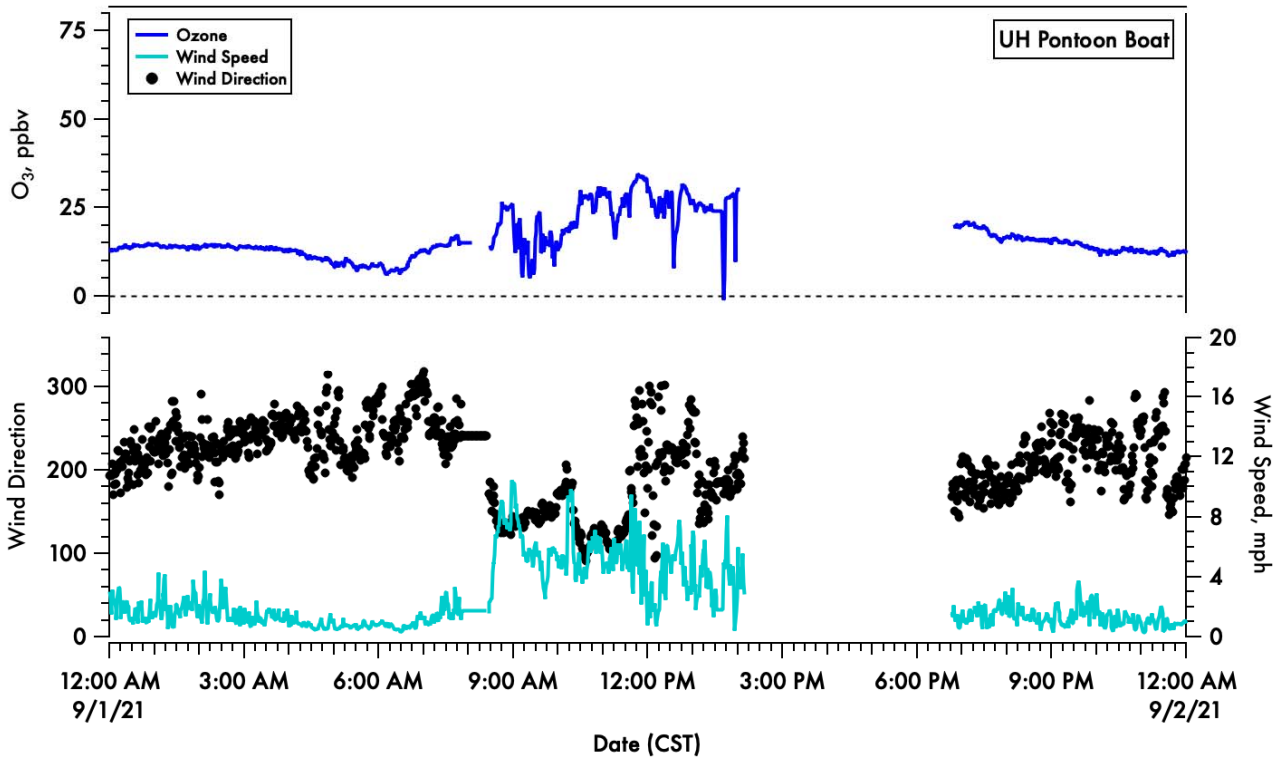

Figure 143. A time-series of 1-minute averaged ozone (blue) on the top panel and wind speed (light blue) and direction (black dots) in the bottom panel.

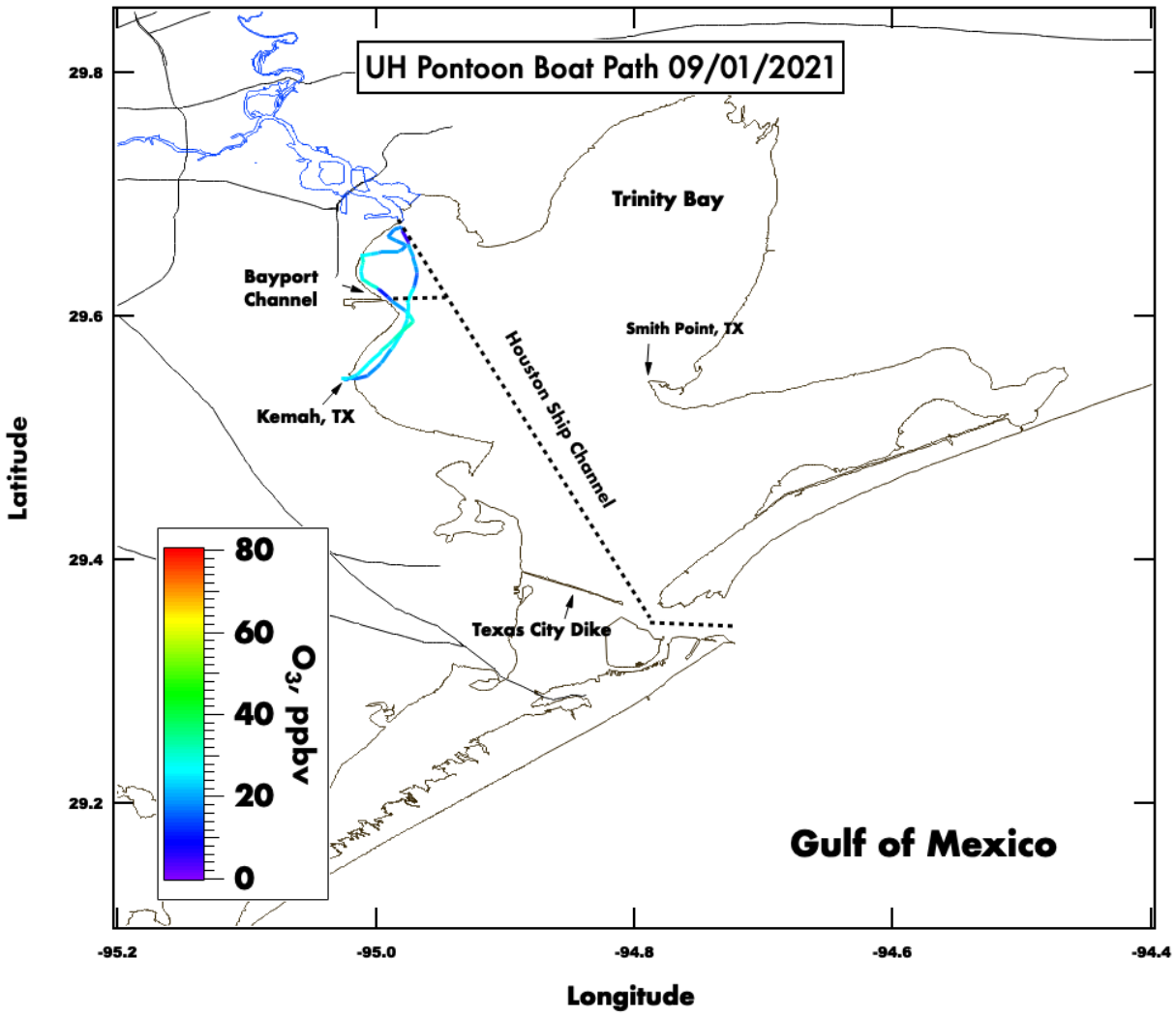

Figure 144. Spatial plot of surface ozone collected from the UH pontoon boat on September 1st, 2021.

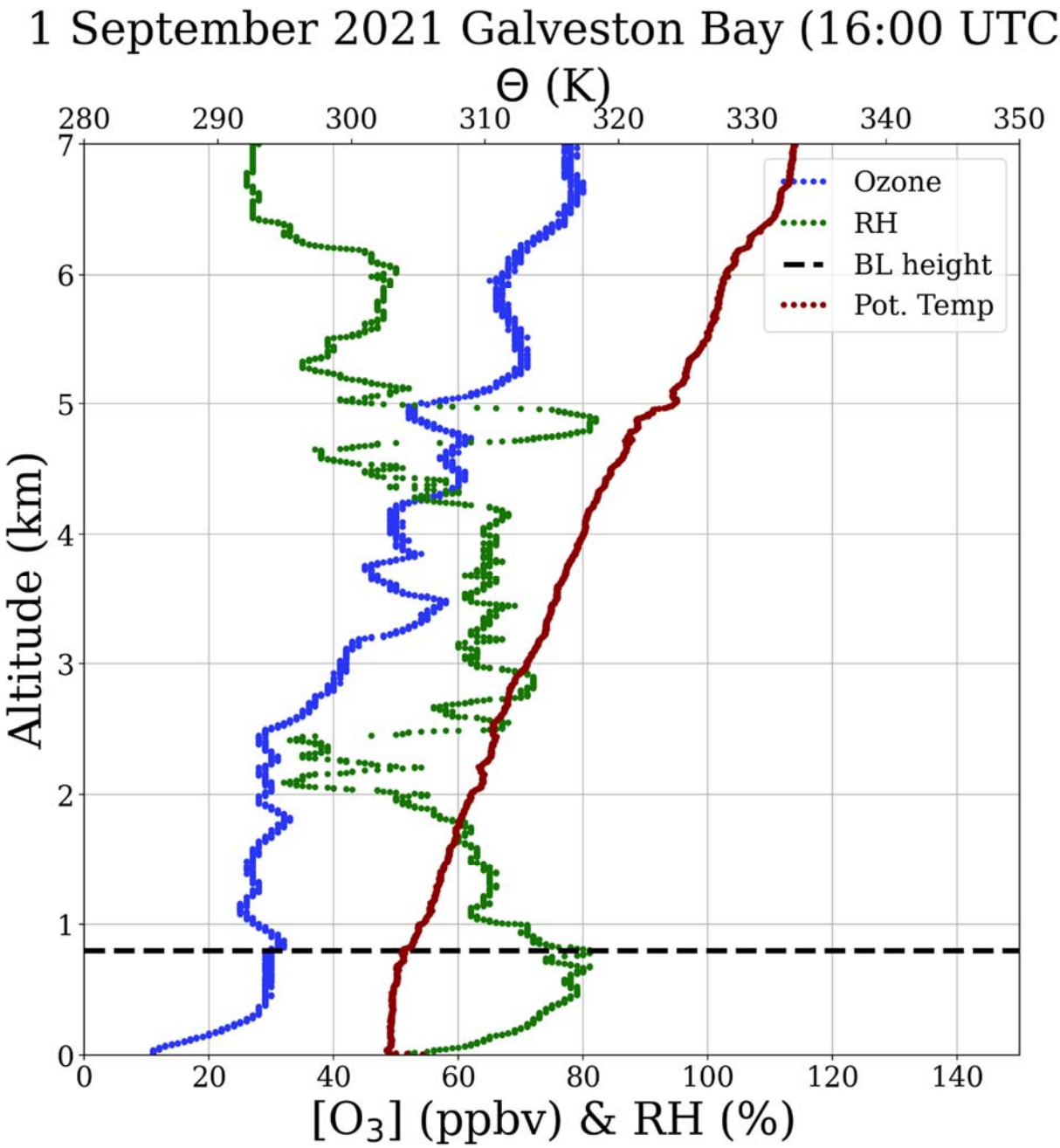

Figure 145. Vertical profiles of ozone (blue), relative humidity (green) and potential temperature (red). The derived boundary layer height is denoted by the horizontal dashed black line.

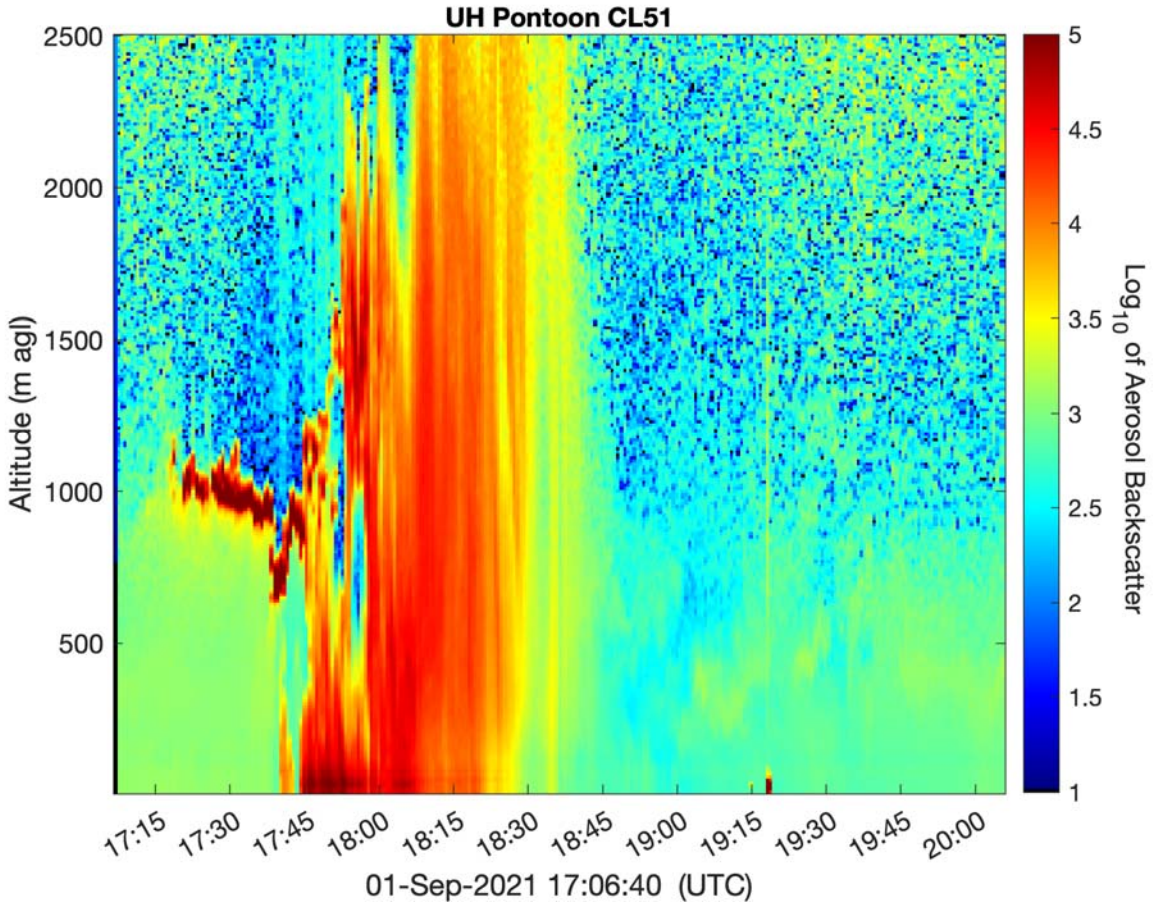

Figure 146. Vertical profile of the aerosol backscatter collected from a Vaisala CL-51 ceilometer mounted on the UH Pontoon boat.

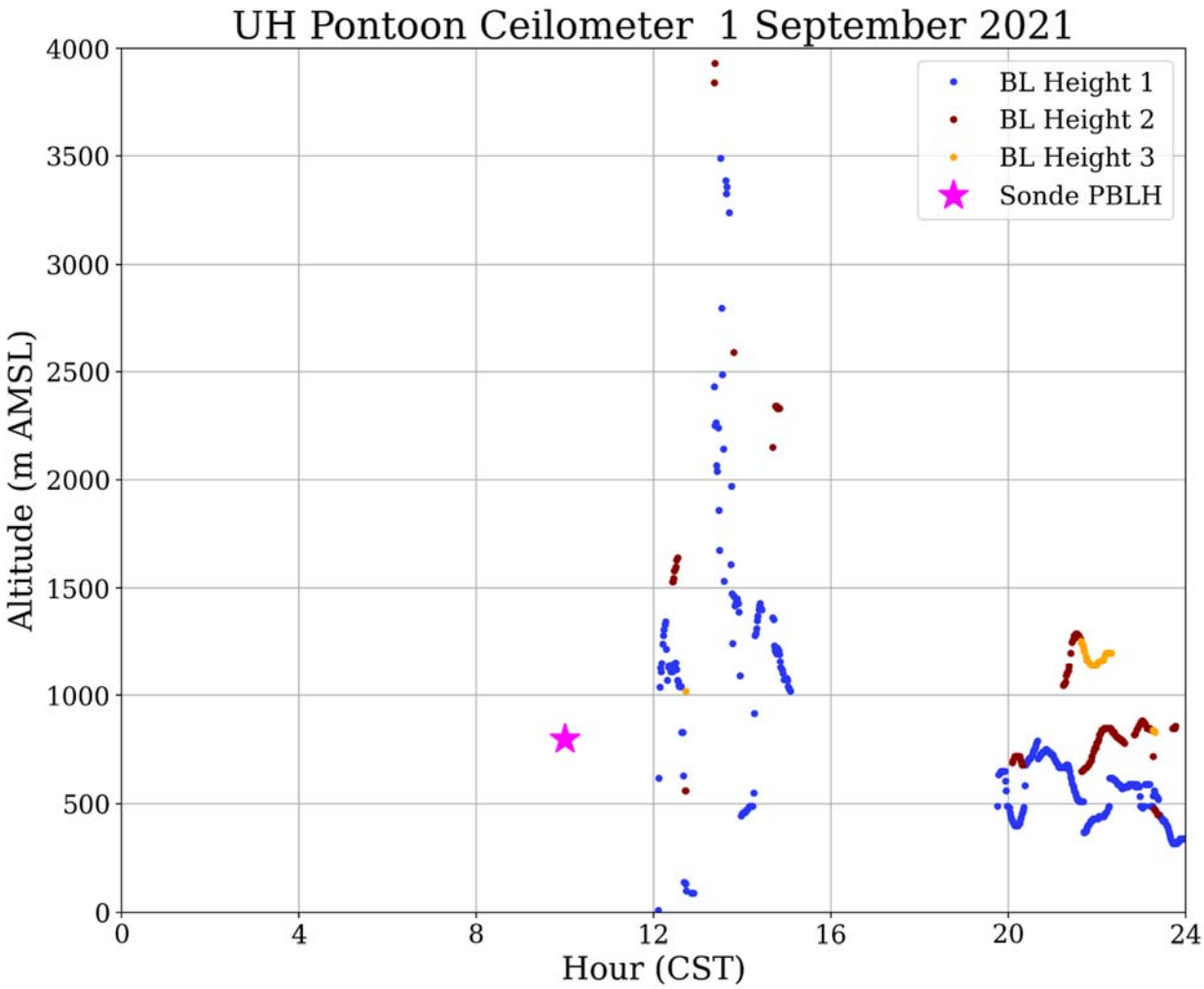

Figure 147. UH Pontoon Vaisala CL-51 ceilometer returned boundary layer heights and boundary layer height from the ozonesonde profile.

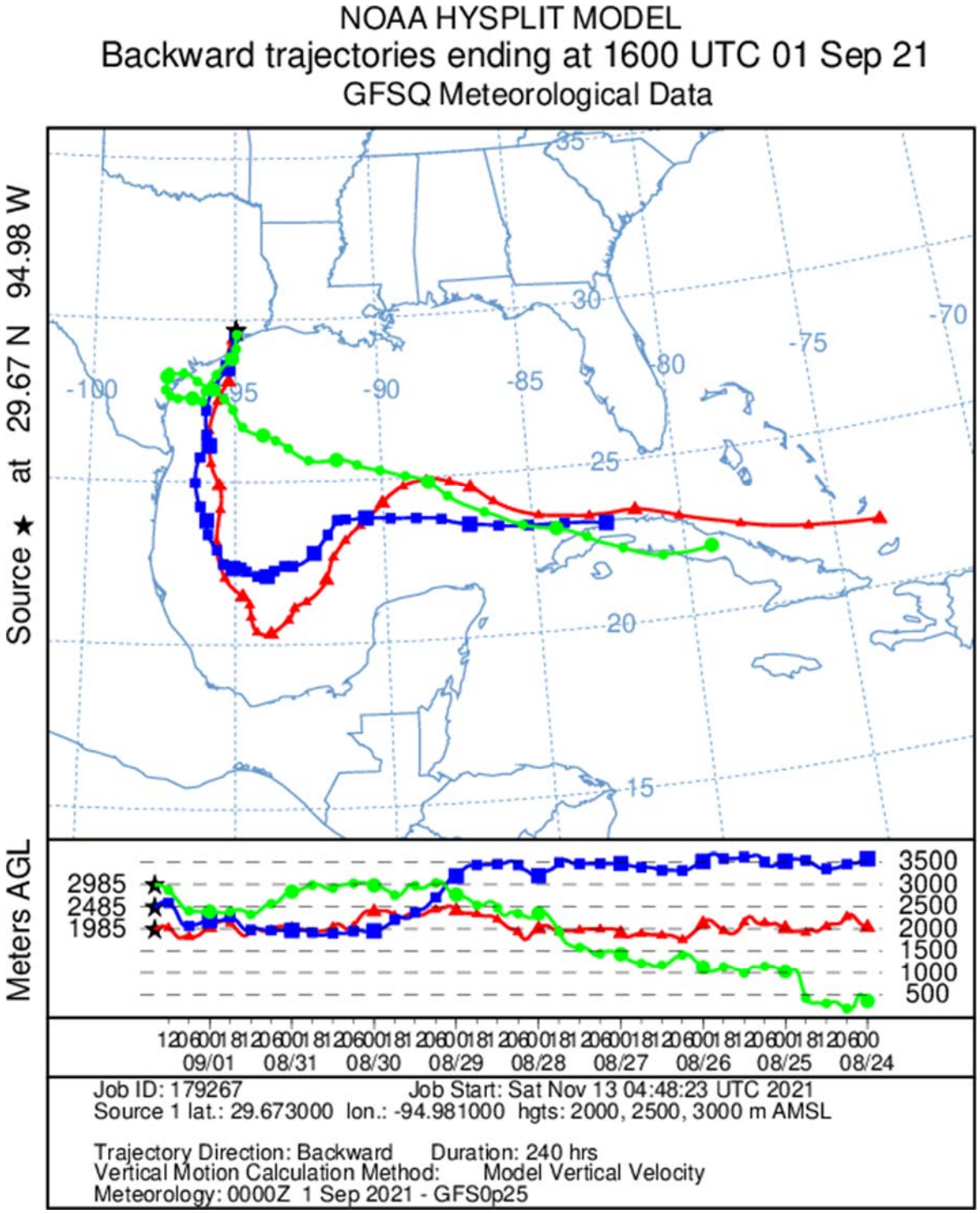

Figure 148. Ten-day HYSPLIT back trajectory for the ozonesonde launch on 1 September 2021 from three heights over the Bay: 500 m (red), 1,000 m (blue), and 1,500 m (green). Each data point is 6 hours apart.

9.13 25 August 2021:

Travis Griggs (UH), Michael Comas (UH), Michael Gray (NASA-Pandora) and Steven Smith (NASA-Pandora) met at the Portofino Marina at 7:00am CST. A main objective for this day was to test the newly installed pandora instrument. The pontoon had some mechanical issues that were addressed before deployment at 10:00am CST. The pontoon headed to the NW section of the bay for surface sampling. After two sampling patterns were completed, the pontoon was taken back to Kemah to be refueled and docked at ~3:00pm CST. The pandora install was successful and it seemed to operate smoothly.

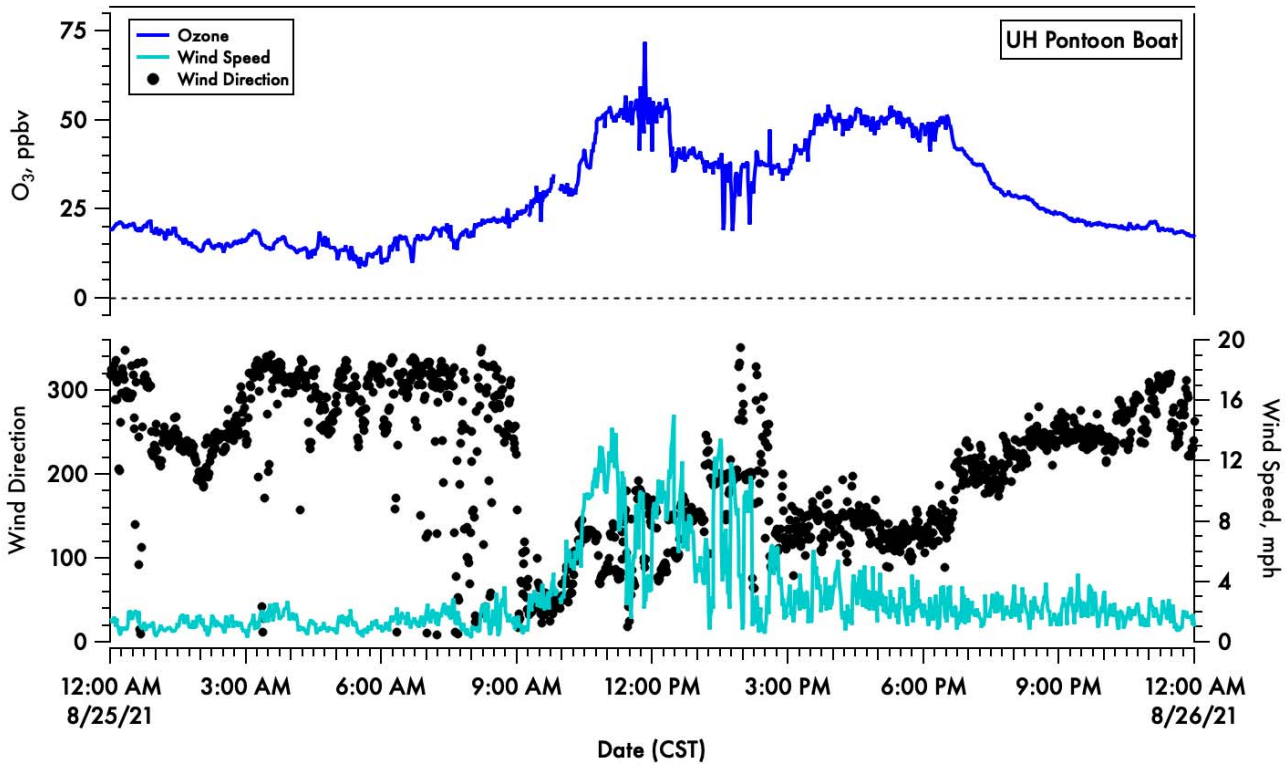

Figure 149. A time-series of 1-minute averaged ozone (blue) on the top panel and wind speed (light blue) and direction (black dots) in the bottom panel.

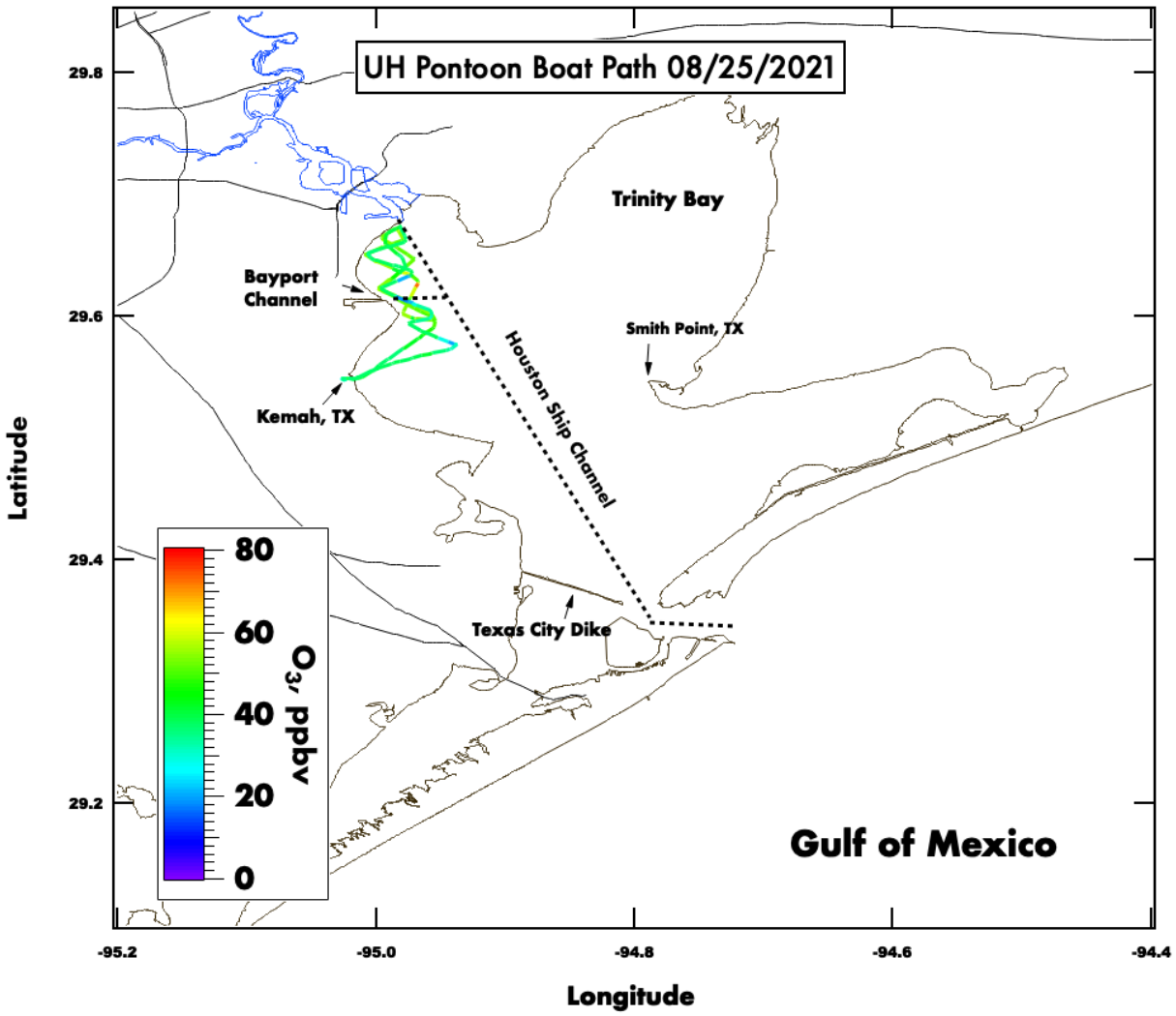

Figure 150. Spatial plot of surface ozone collected from the UH pontoon boat on August 25th, 2021.

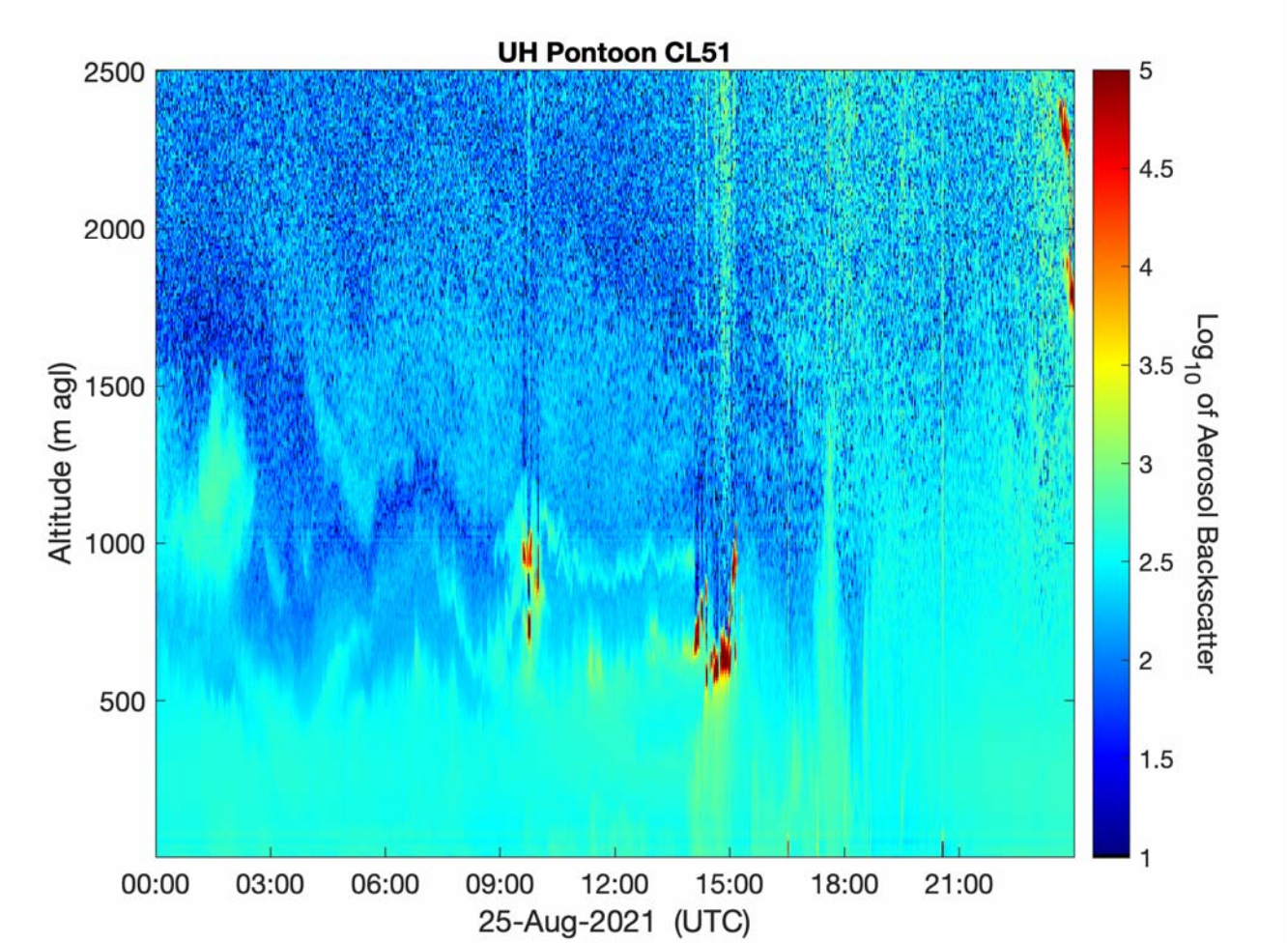

Figure 151. Vertical profile of the aerosol backscatter collected from a Vaisala CL-51 ceilometer mounted on the UH Pontoon boat.

9.14 24 August 2021:

Travis Griggs (UH), Michael Gray (NASA-Pandora), Steven Smith (NASA-Pandora) met at the marina at 7:30am CST. The objective for this day was to finish the install and test the NASA pandora instrument on the Pontoon boat. After troubleshooting the remaining issues, the pontoon was deployed at 12:30pm. The pontoon boat headed to the NW section of the Bay for co-located measurements with the UH MAQL-1 truck. Stationary co-sampling occurred from 2:30pm – 3:45pm. The pontoon was taken back to be refueled and docked at 4:40pm CST.

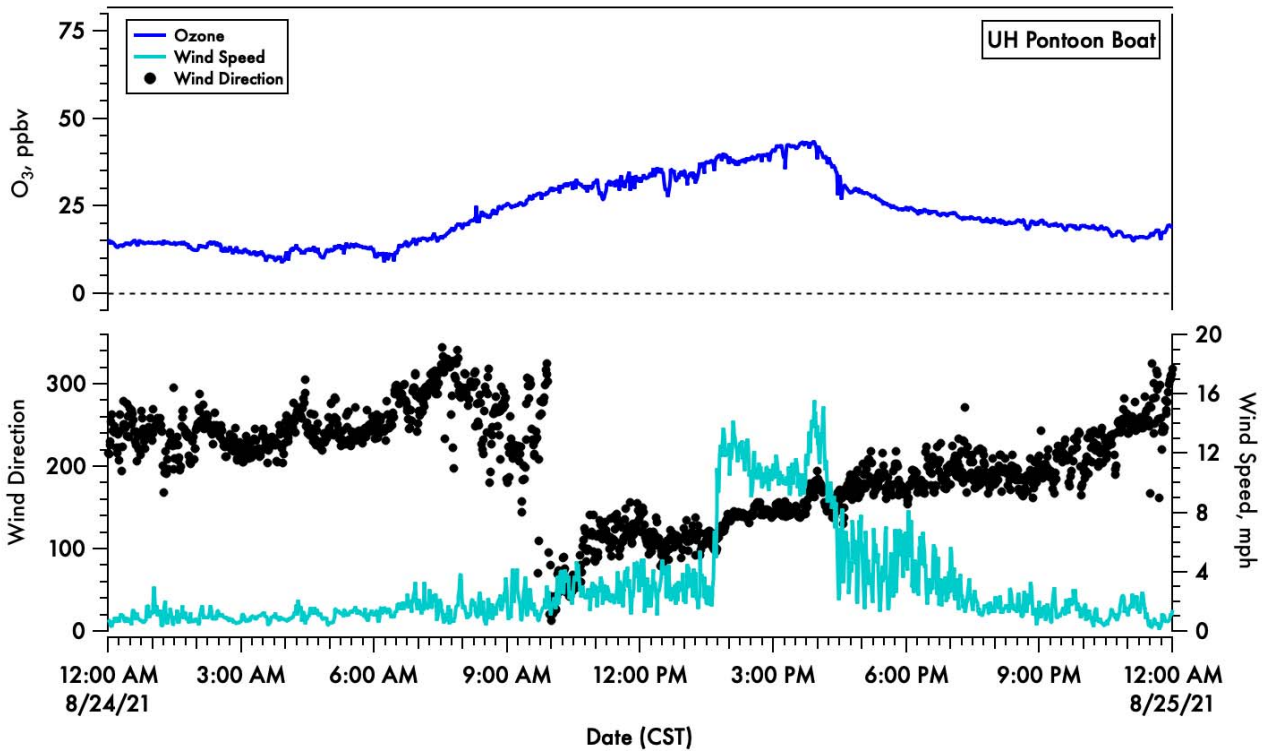

Figure 152. A time-series of 1-minute averaged ozone (blue) on the top panel and wind speed (light blue) and direction (black dots) in the bottom panel.

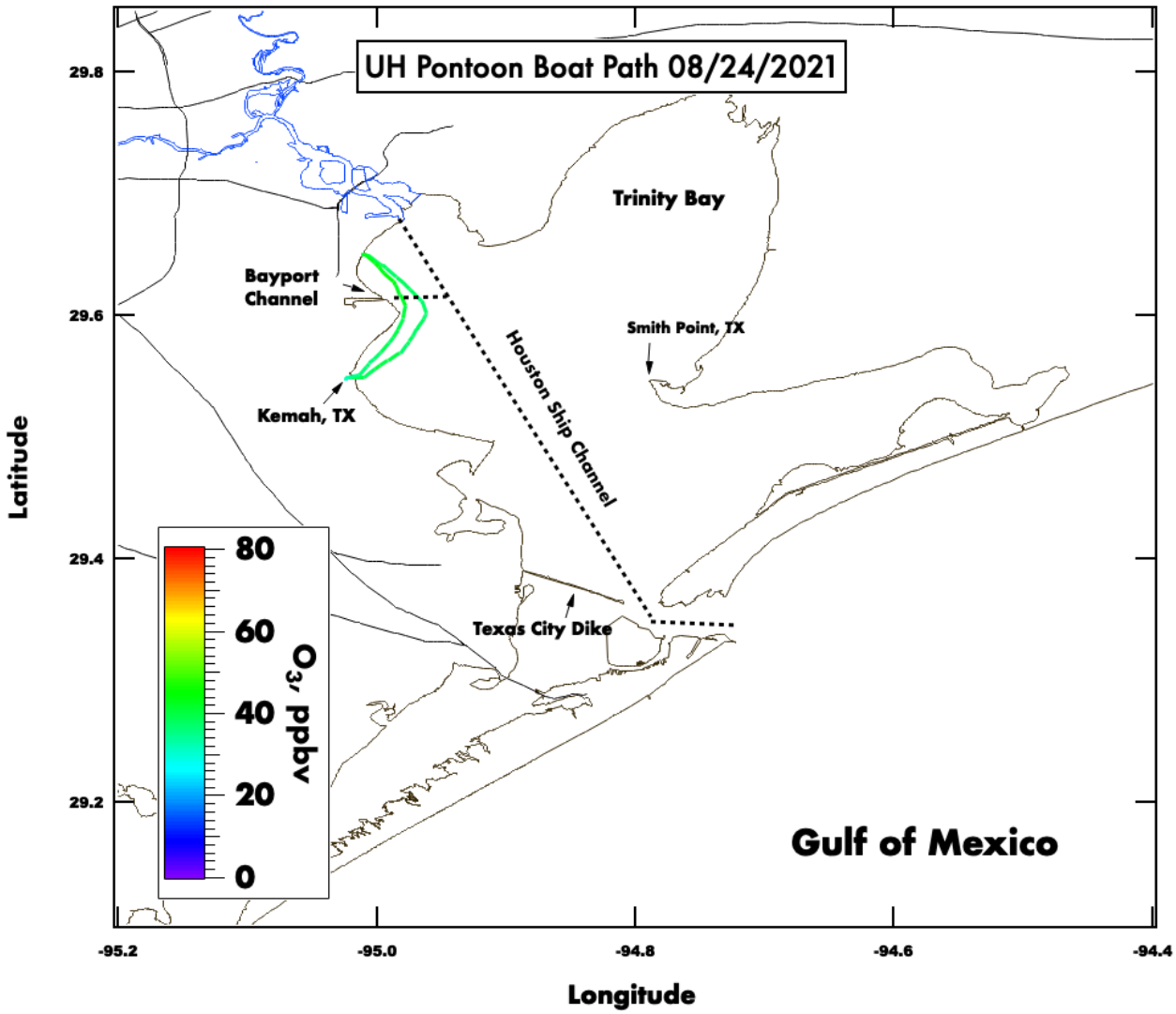

Figure 153. Spatial plot of surface ozone collected from the UH pontoon boat on August 24th, 2021.

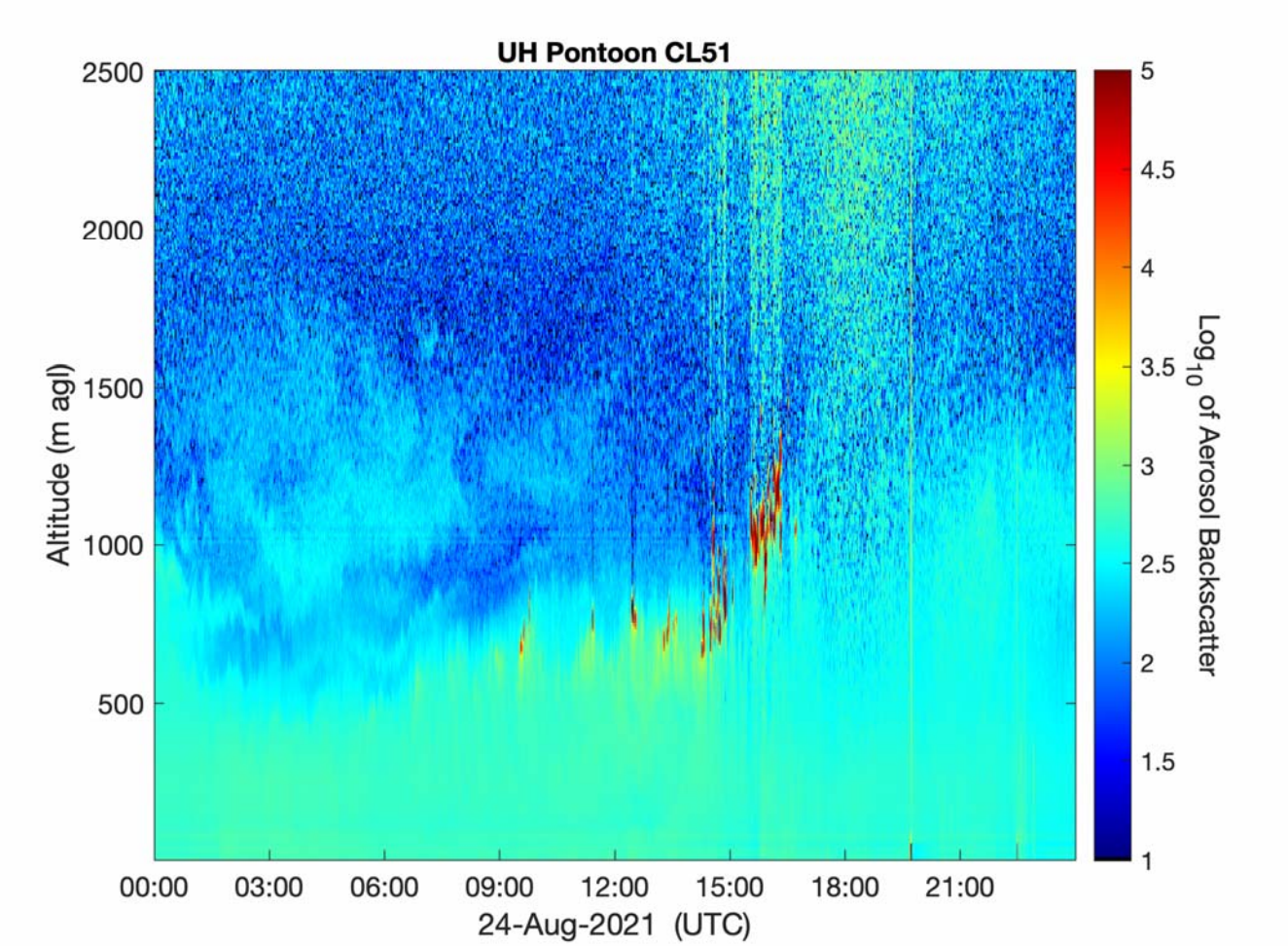

Figure 154. Vertical profile of the aerosol backscatter collected from a Vaisala CL-51 ceilometer mounted on the UH Pontoon boat.

9.15 16 August 2021:

Travis Griggs (UH), Paul Walter (St. Edward's), Michael Comas (UH) and Nadia Partida (UH) met at the Portofino marina at 6:30am and deployed at 07:00am CST. A chemical release that caused a shelter in place in La Porte had occurred overnight. The pontoon initially headed north towards Morgan's Point for an ozonesonde launch that was released at 8:35am CST. The pontoon then conducted surface sampling in the NW section of the Bay and briefly made a pass into north Trinity Bay to attempt to retrieve the morning ozonesonde. The pontoon returned to the same spot near Morgan's point in the afternoon for a second ozonesonde launch that was released at ~1:00pm CST. After the launch the pontoon boat was taken back to Kemah to be refueled and docked at ~2:00pm CST.

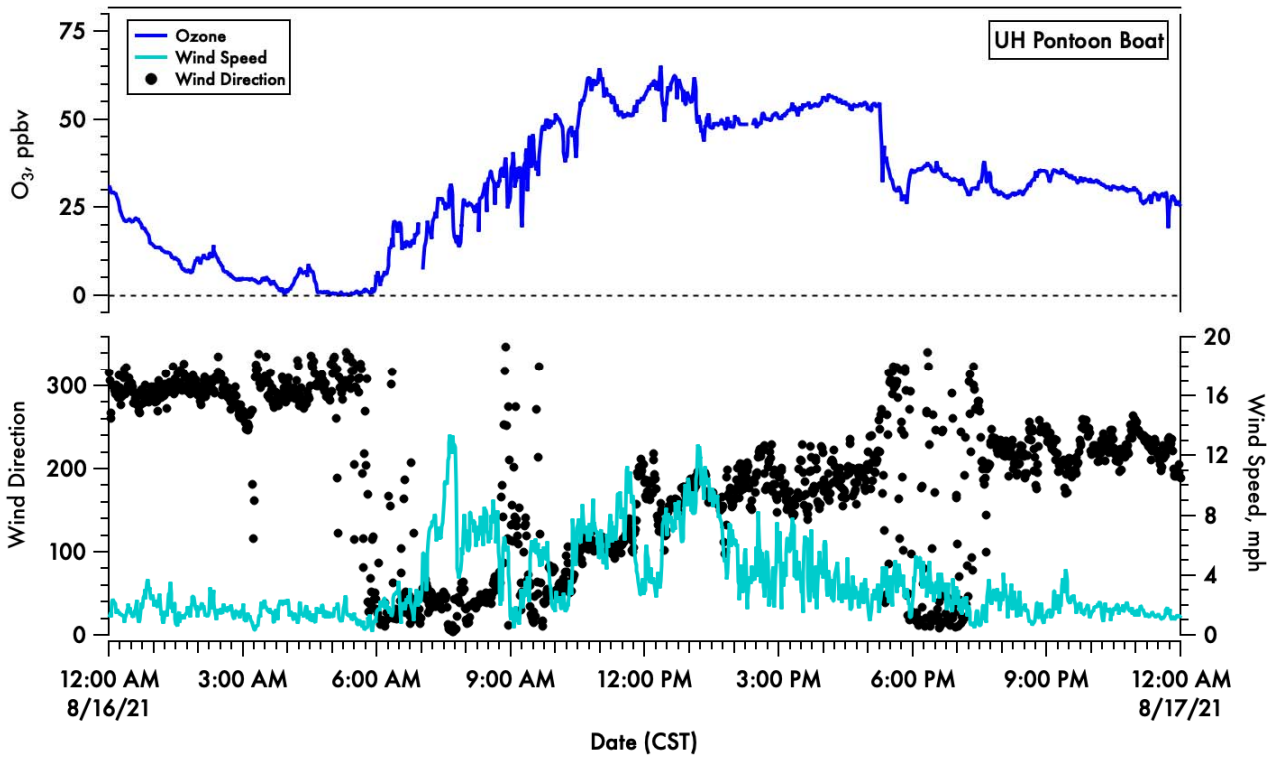

Figure 155. A time-series of 1-minute averaged ozone (blue) on the top panel and wind speed (light blue) and direction (black dots) in the bottom panel.

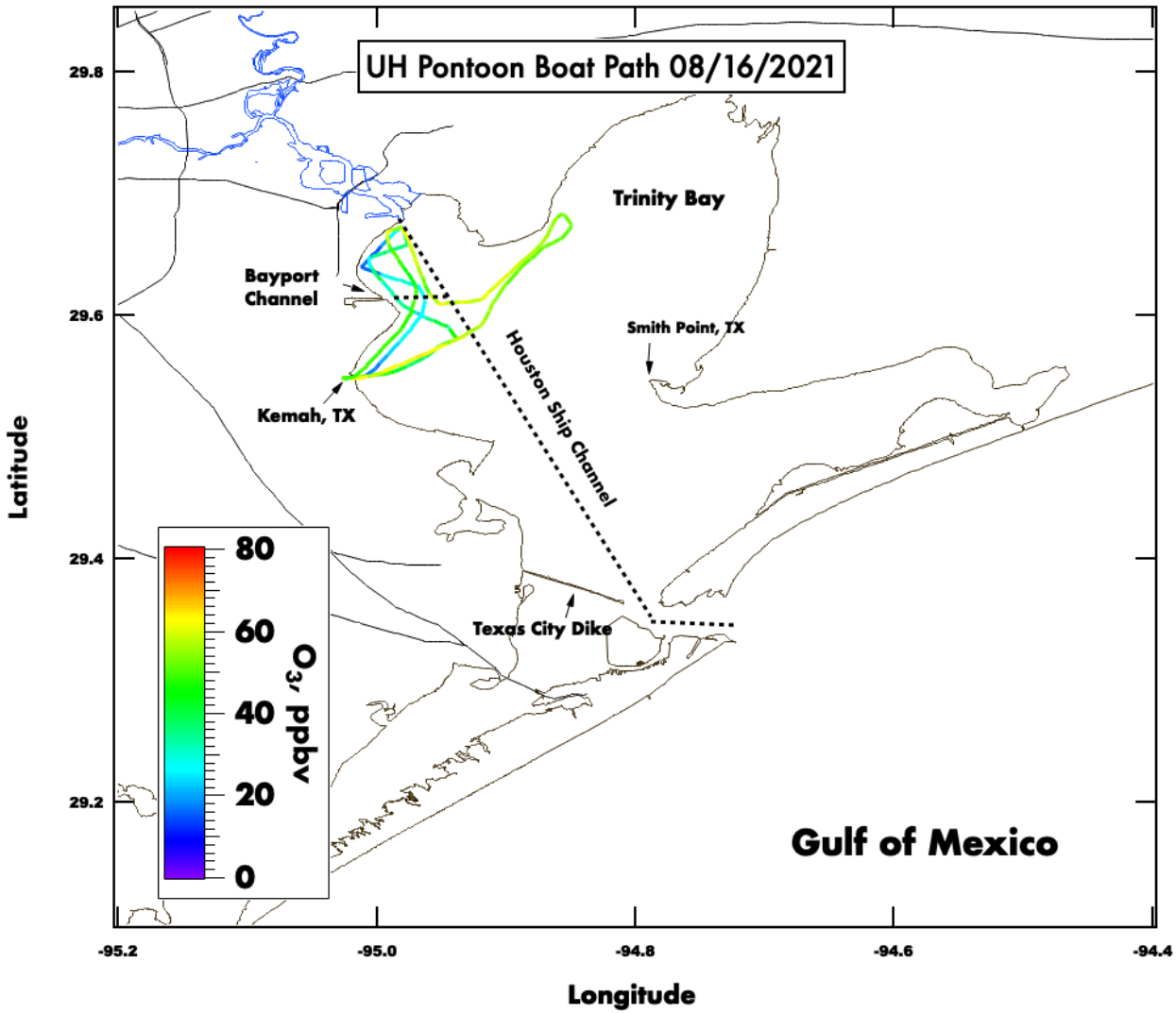

Figure 156. Spatial plot of surface ozone collected from the UH pontoon boat on August 16th, 2021.

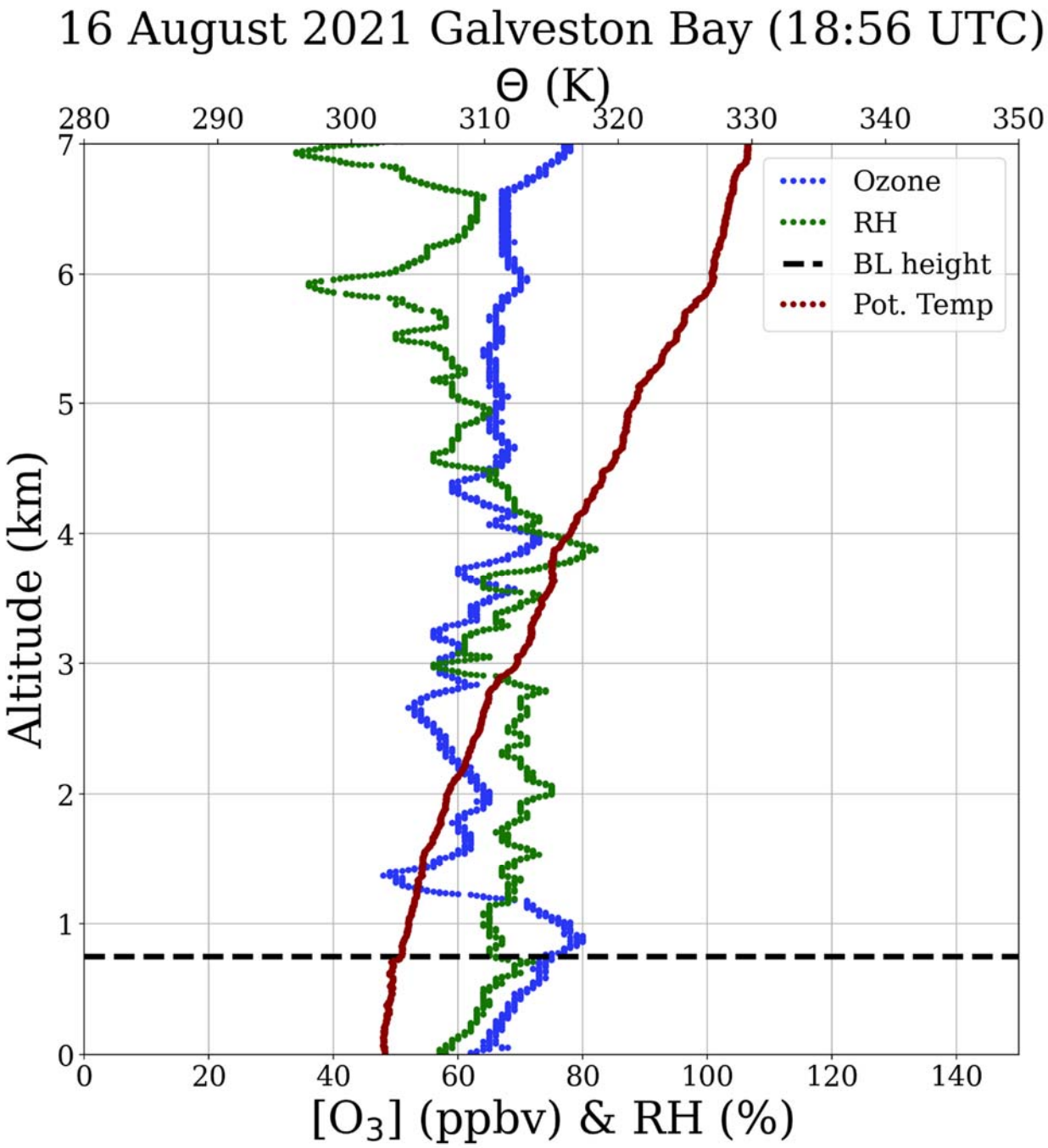

Figure 157. Vertical profiles of ozone (blue), relative humidity (green) and potential temperature (red). The derived boundary layer height is denoted by the horizontal dashed black line.

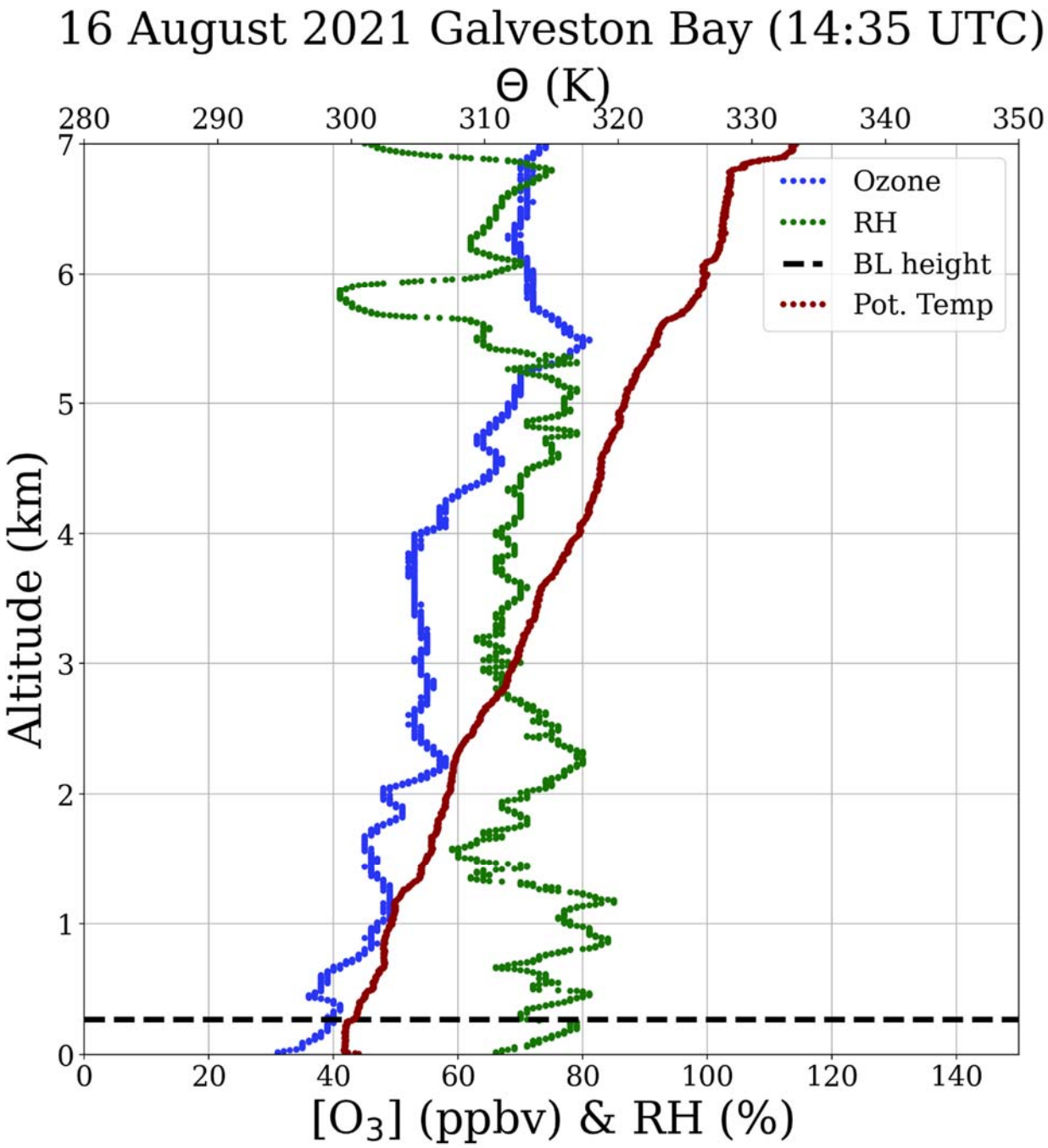

Figure 158. Vertical profiles of ozone (blue), relative humidity (green) and potential temperature (red). The derived boundary layer height is denoted by the horizontal dashed black line.

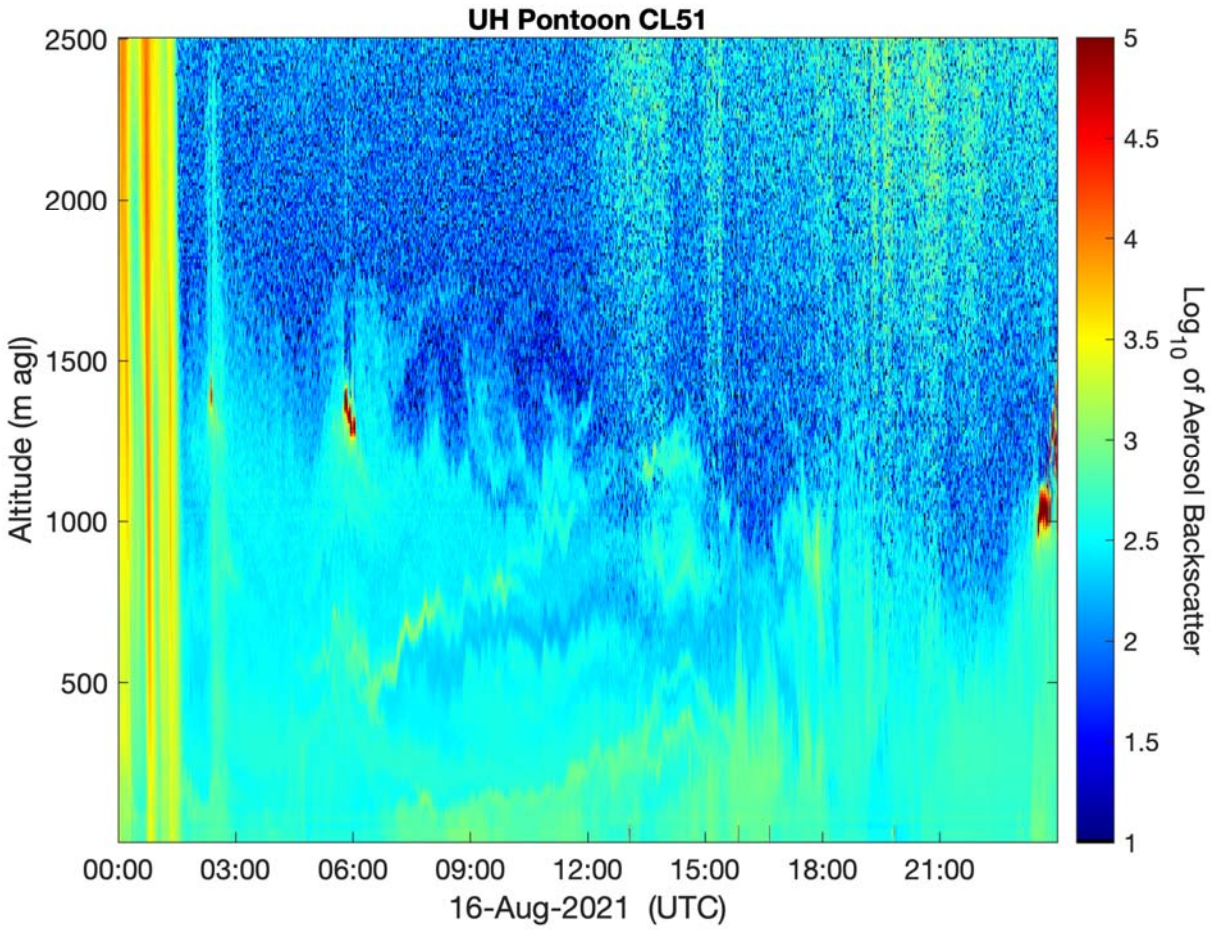

Figure 159. Vertical profile of the aerosol backscatter collected from a Vaisala CL-51 ceilometer mounted on the UH Pontoon boat.

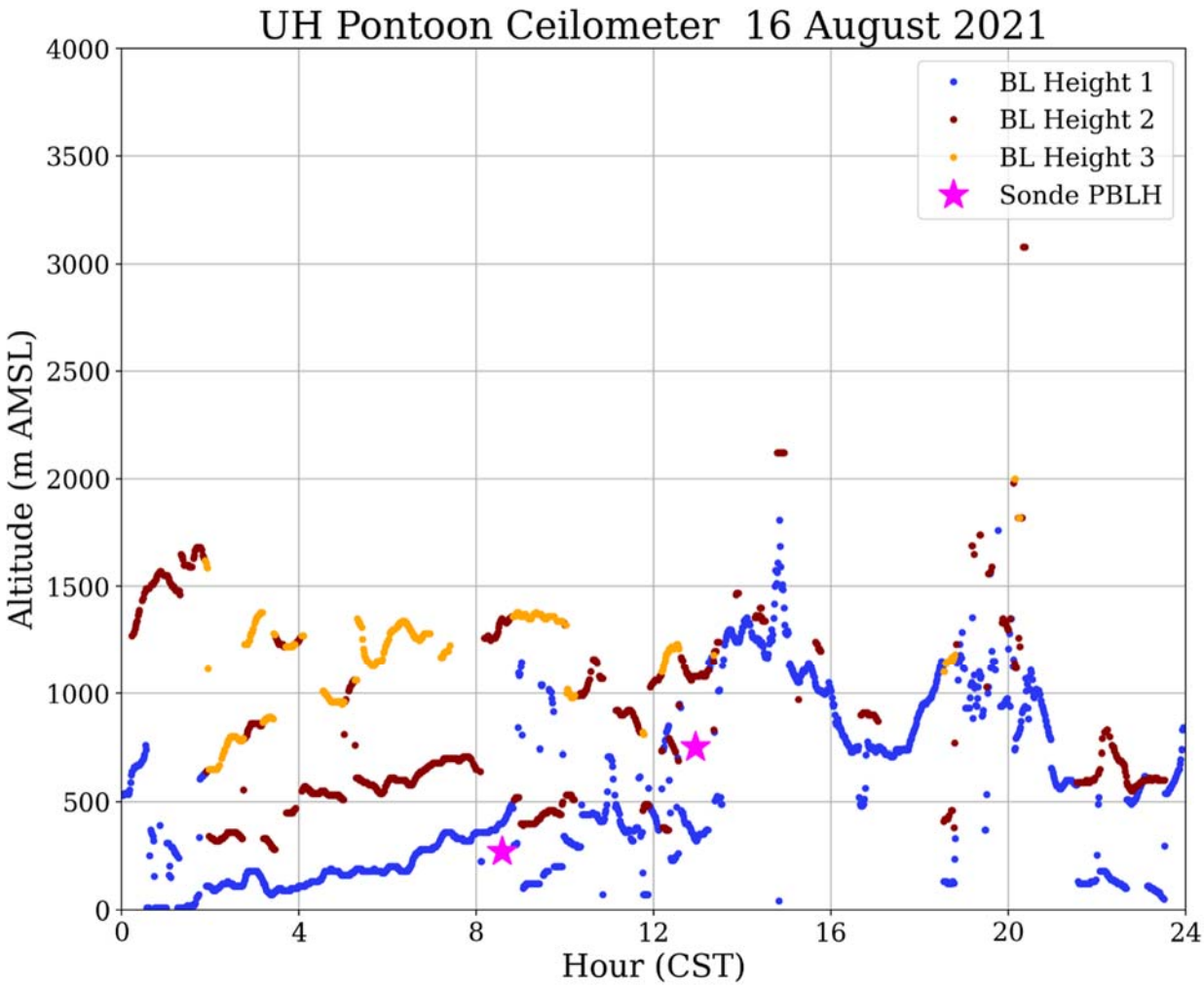

Figure 160. UH Pontoon Vaisala CL-51 ceilometer returned boundary layer heights and boundary layer height from the ozonesonde profile.

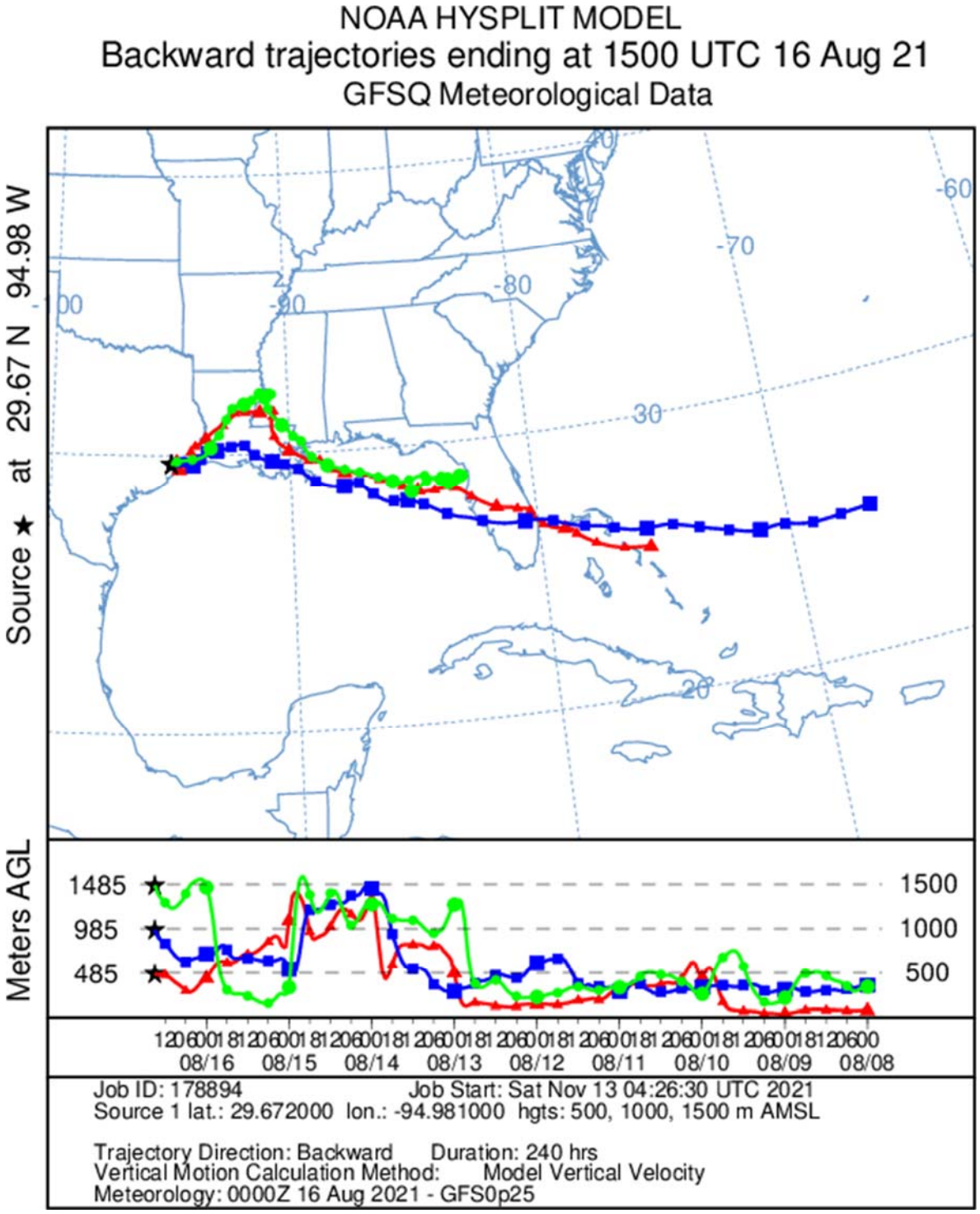

Figure 161. Ten-day HYSPLIT back trajectory for the first ozonesonde launch on 16 August 2021 from three heights over the Bay: 500 m (red), 1,000 m (blue), and 1,500 m (green). Each data point is 6 hours apart.

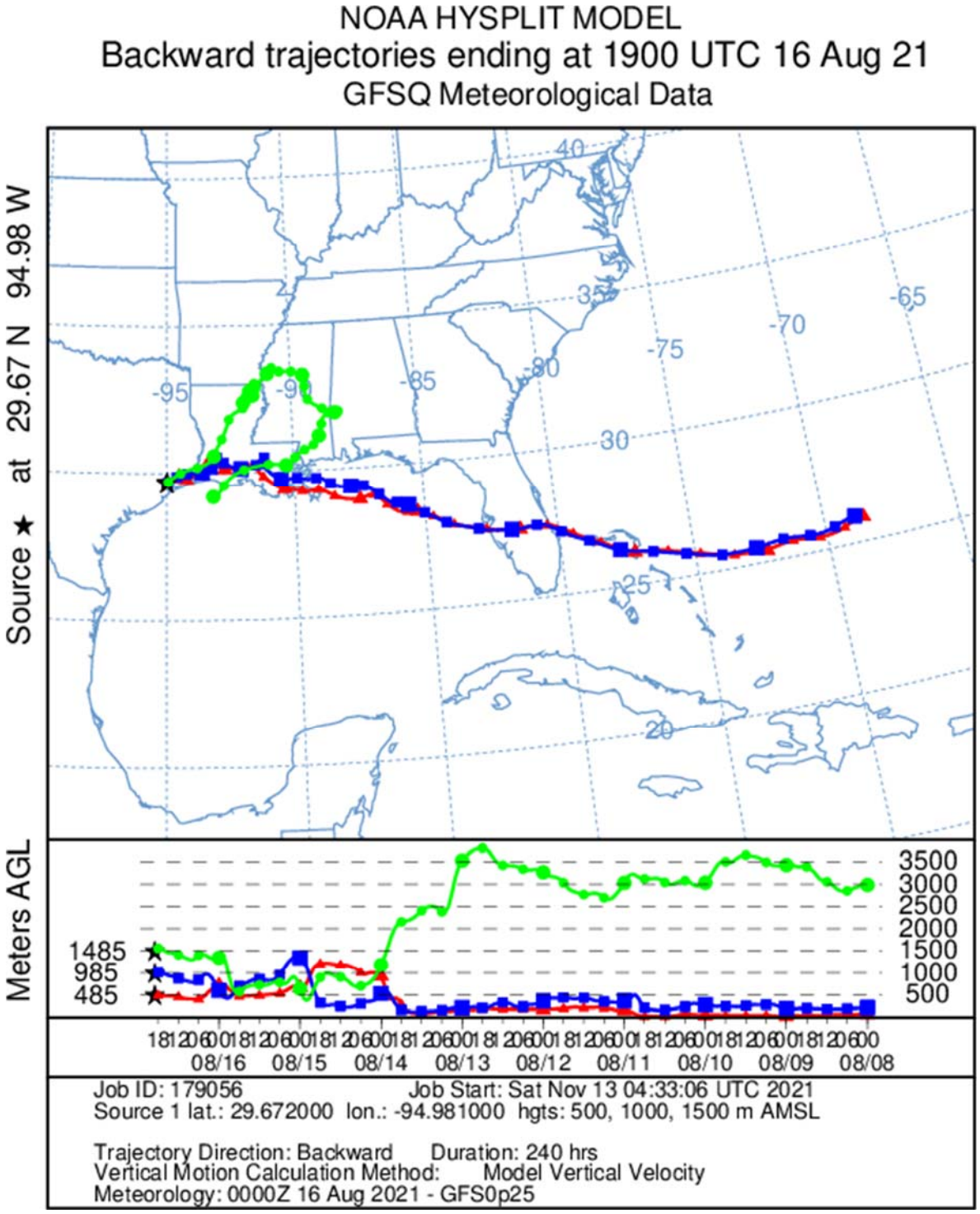

Figure 162. Ten-day HYSPLIT back trajectory for the second ozonesonde launch on 16 August 2021 from three heights over the Bay: 500 m (red), 1,000 m (blue), and 1,500 m (green). Each data point is 6 hours apart.

9.16 12 August 2021:

Travis Griggs (UH), Paul Walter (St. Edward's), Michael Comas (UH), John Sullivan (NASA-Goddard) and Hue (intern - NASA) met at Portofino Marina at 6:00am CST. The daily plan was to head to the SE section of the Bay near Smith Point, TX for a morning ozonesonde launch. The ozonesonde was launched at 8:22am CST. Offshore convection had moved closer to the Bay and the science team decided to call off the afternoon sampling due to the concern over deteriorating Bay conditions. The pontoon was refueled and docked at 10:45am CST.

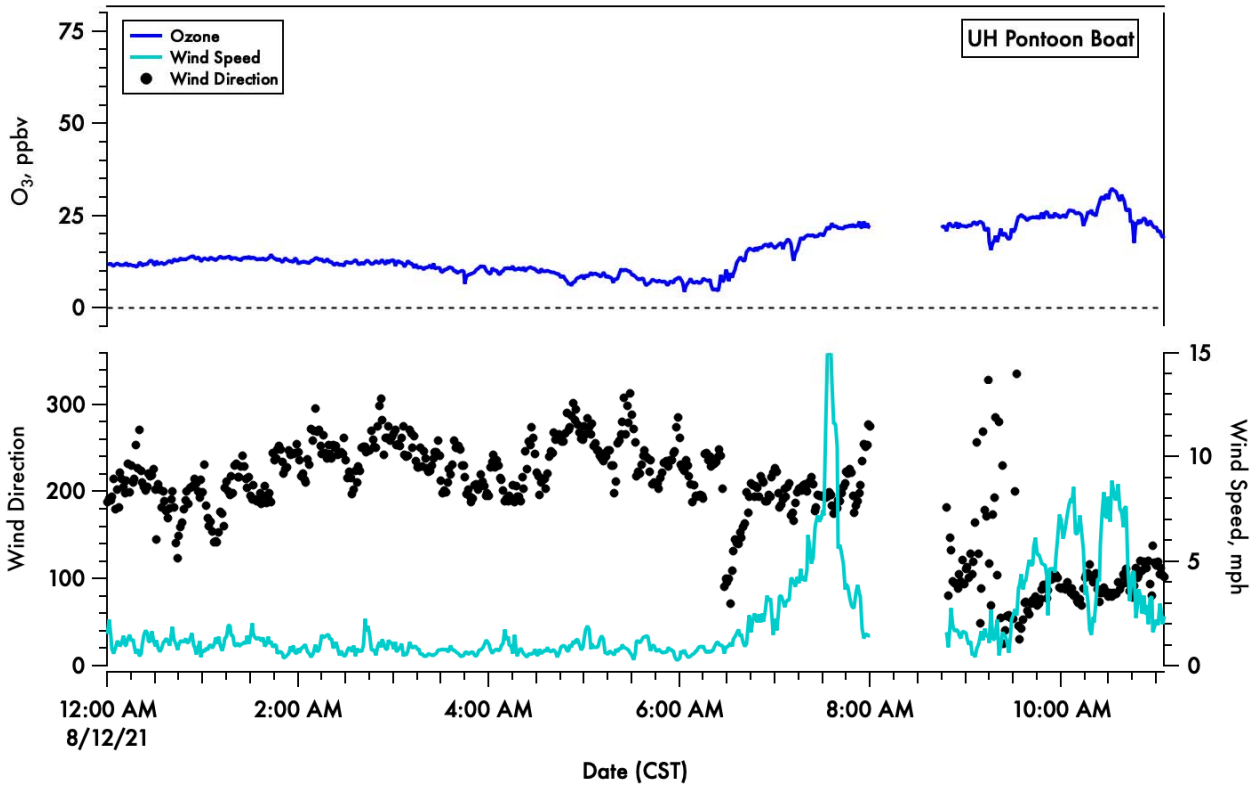

Figure 163. A time-series of 1-minute averaged ozone (blue) on the top panel and wind speed (light blue) and direction (black dots) in the bottom panel.

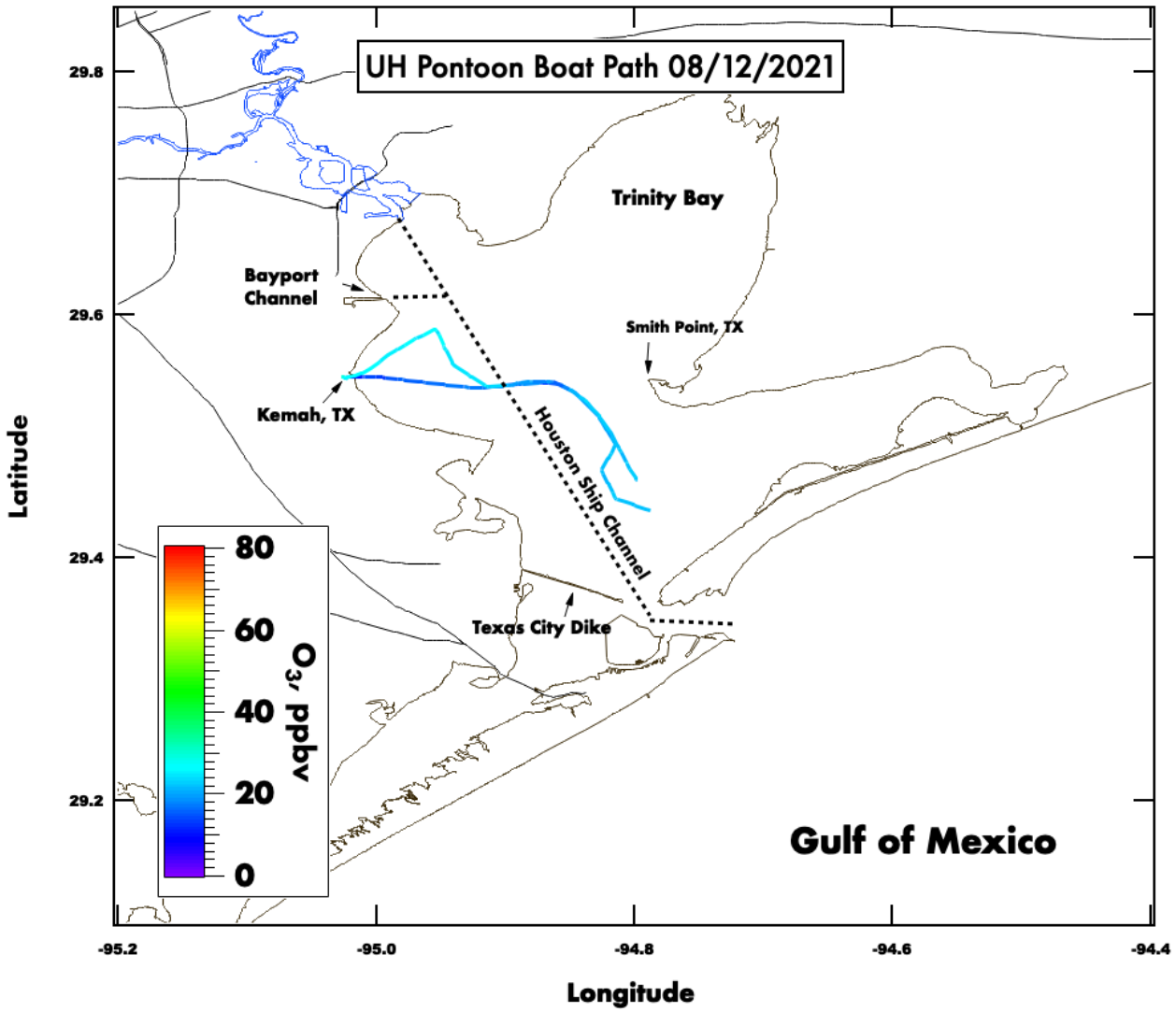

Figure 164. Spatial plot of surface ozone collected from the UH pontoon boat on August 12th, 2021.

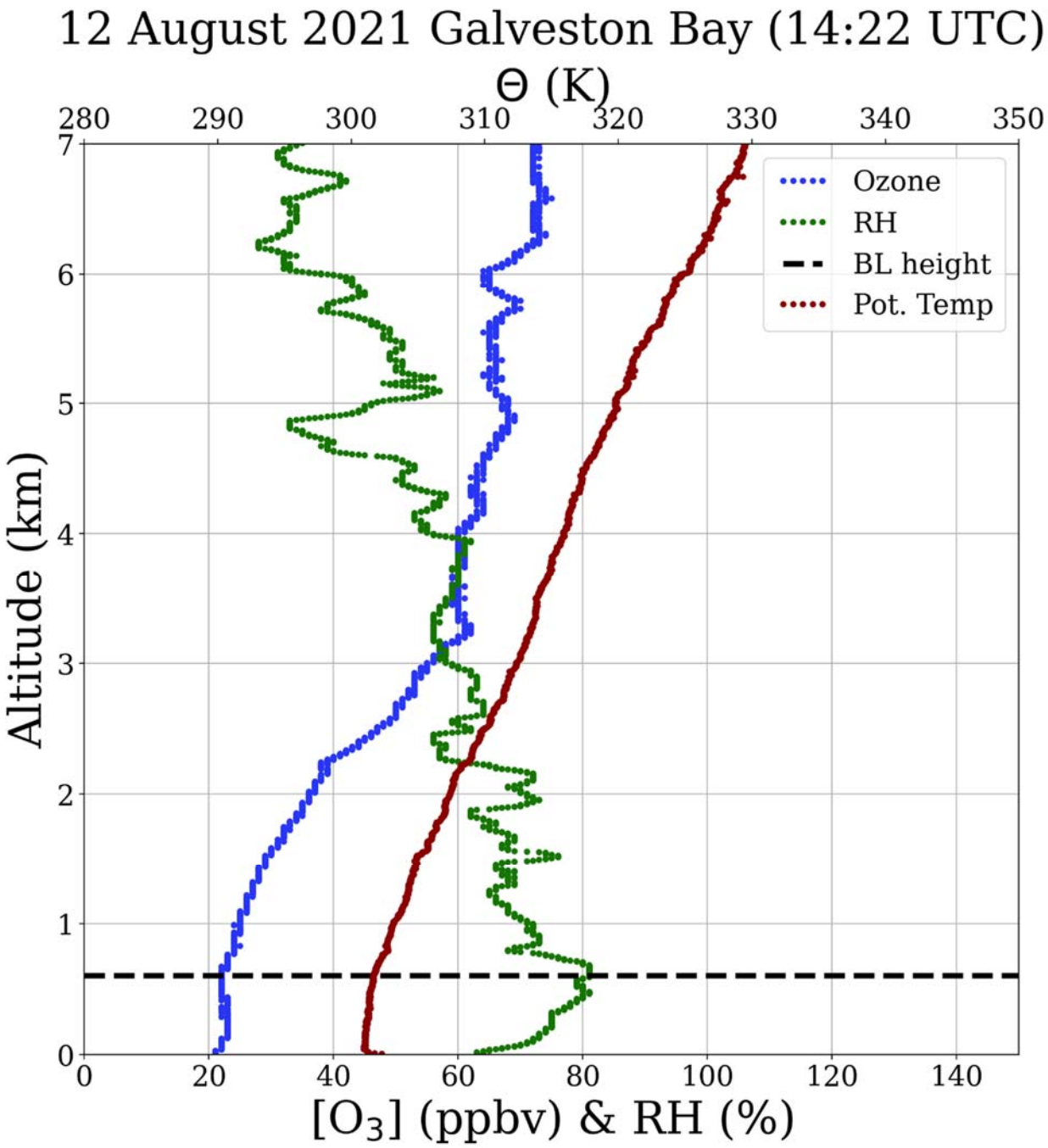

Figure 165. Vertical profiles of ozone (blue), relative humidity (green) and potential temperature (red). The derived boundary layer height is denoted by the horizontal dashed black line.

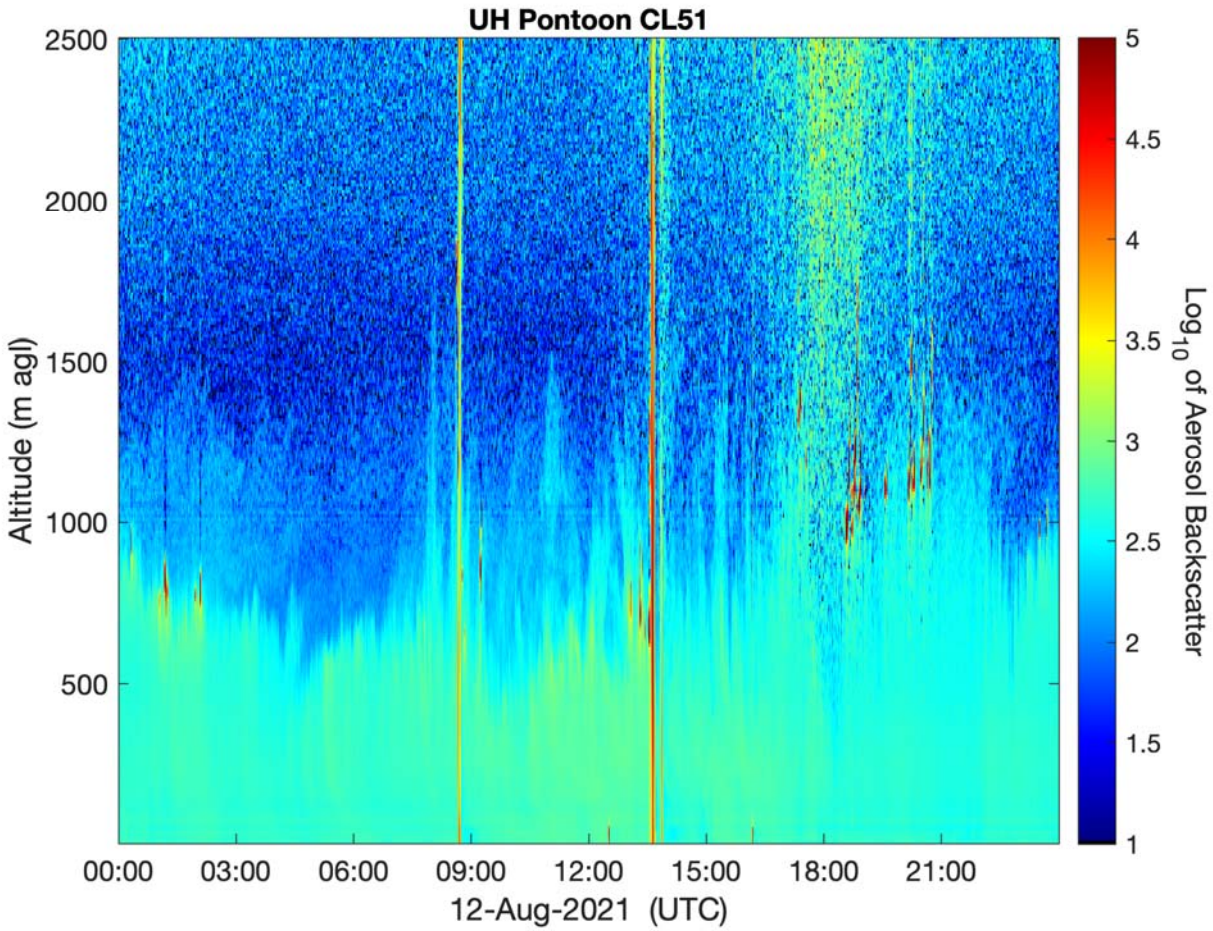

Figure 166. Vertical profile of the aerosol backscatter collected from a Vaisala CL-51 ceilometer mounted on the UH Pontoon boat.

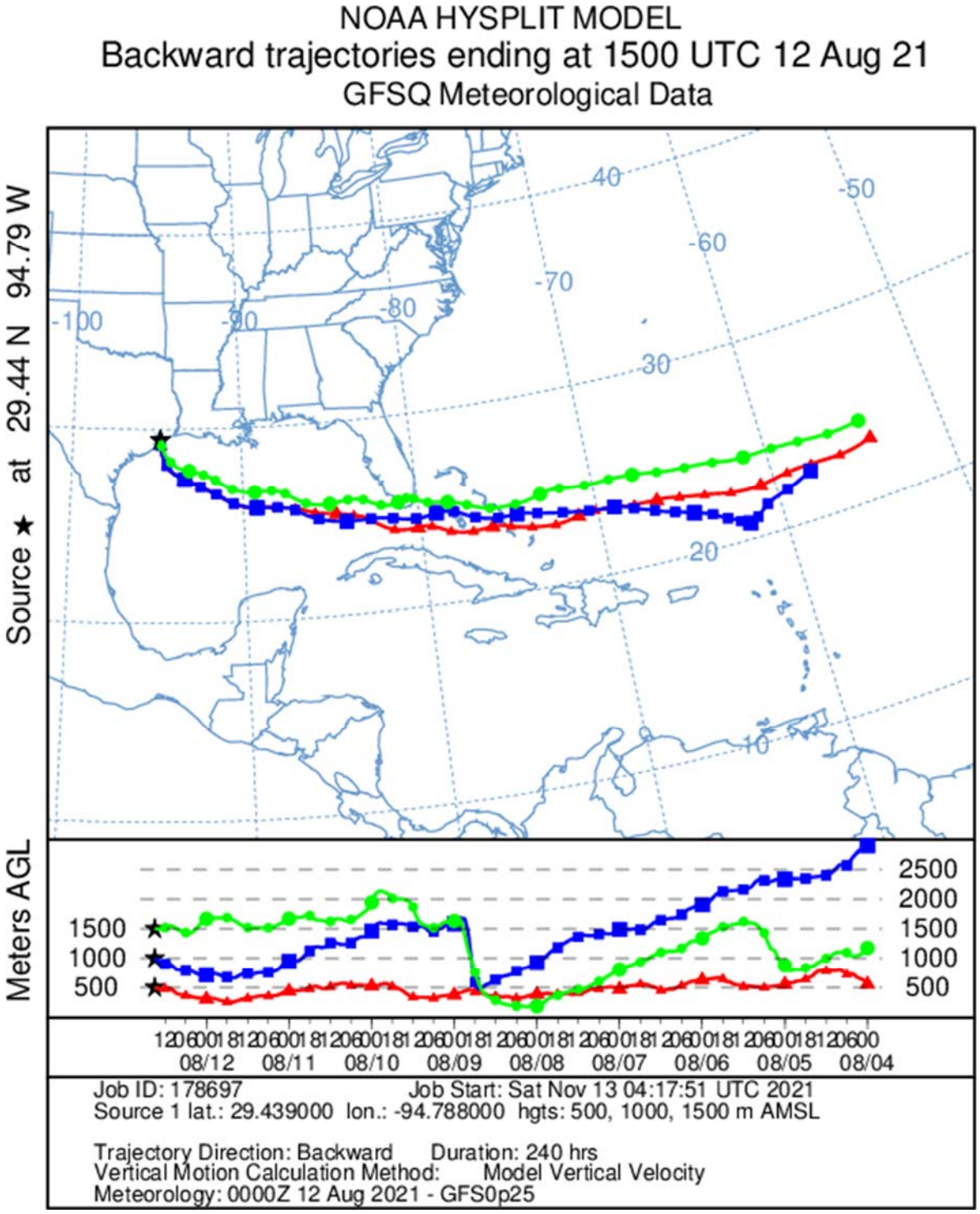

Figure 167. Ten-day HYSPLIT back trajectory for the ozonesonde launch on 12 August 2021 from three heights over the Bay: 500 m (red), 1,000 m (blue), and 1,500 m (green). Each data point is 6 hours apart.

9.17 4 August 2021:

Travis Griggs (UH), Michael Comas (UH) and Gary Morris (St. Edward's) met at the marina at 7:00am CST. Mechanical issues with the boat delayed deployment until 8:45am CST. The pontoon boat initially headed north for surface sampling in the NW section of the bay. Offshore convection moving inland and deteriorating bay conditions shortened this day. The pontoon was refueled and docked at 1:00pm CST.

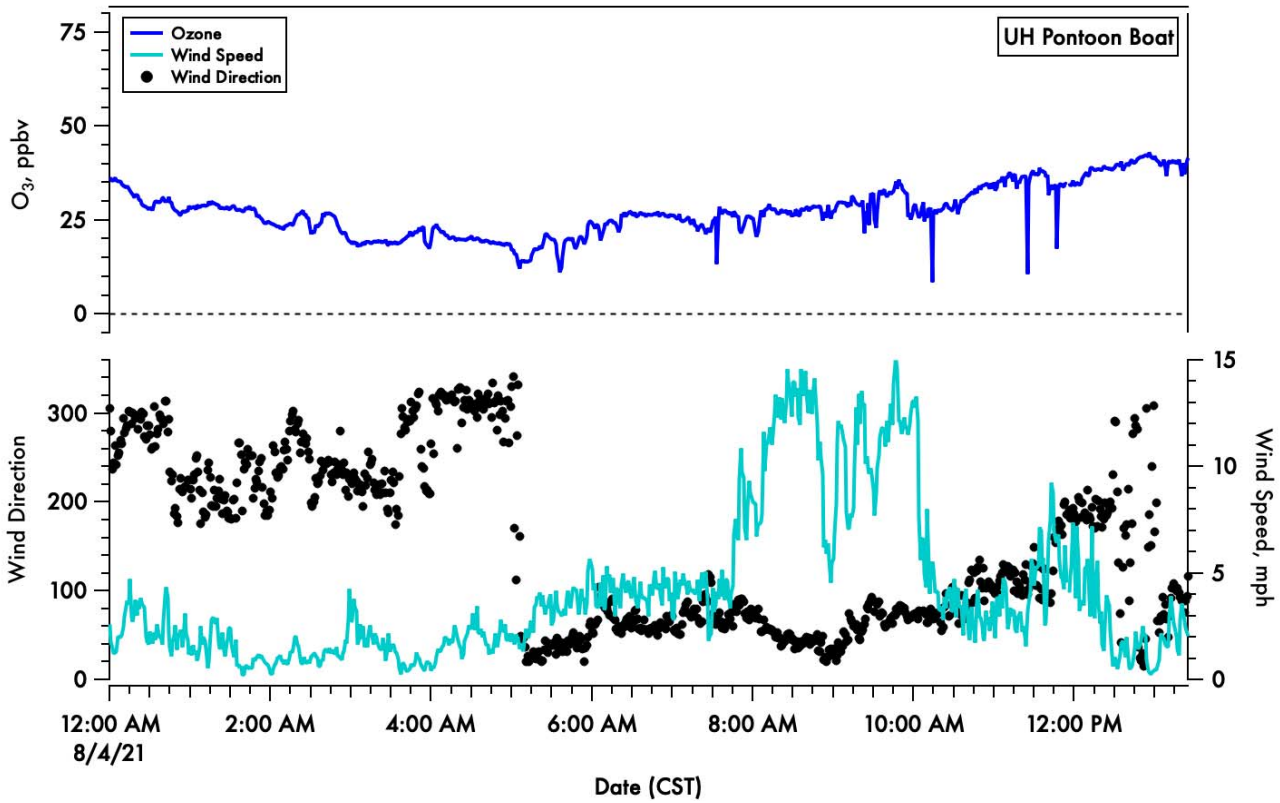

Figure 168. A time-series of 1-minute averaged ozone (blue) on the top panel and wind speed (light blue) and direction (black dots) in the bottom panel.

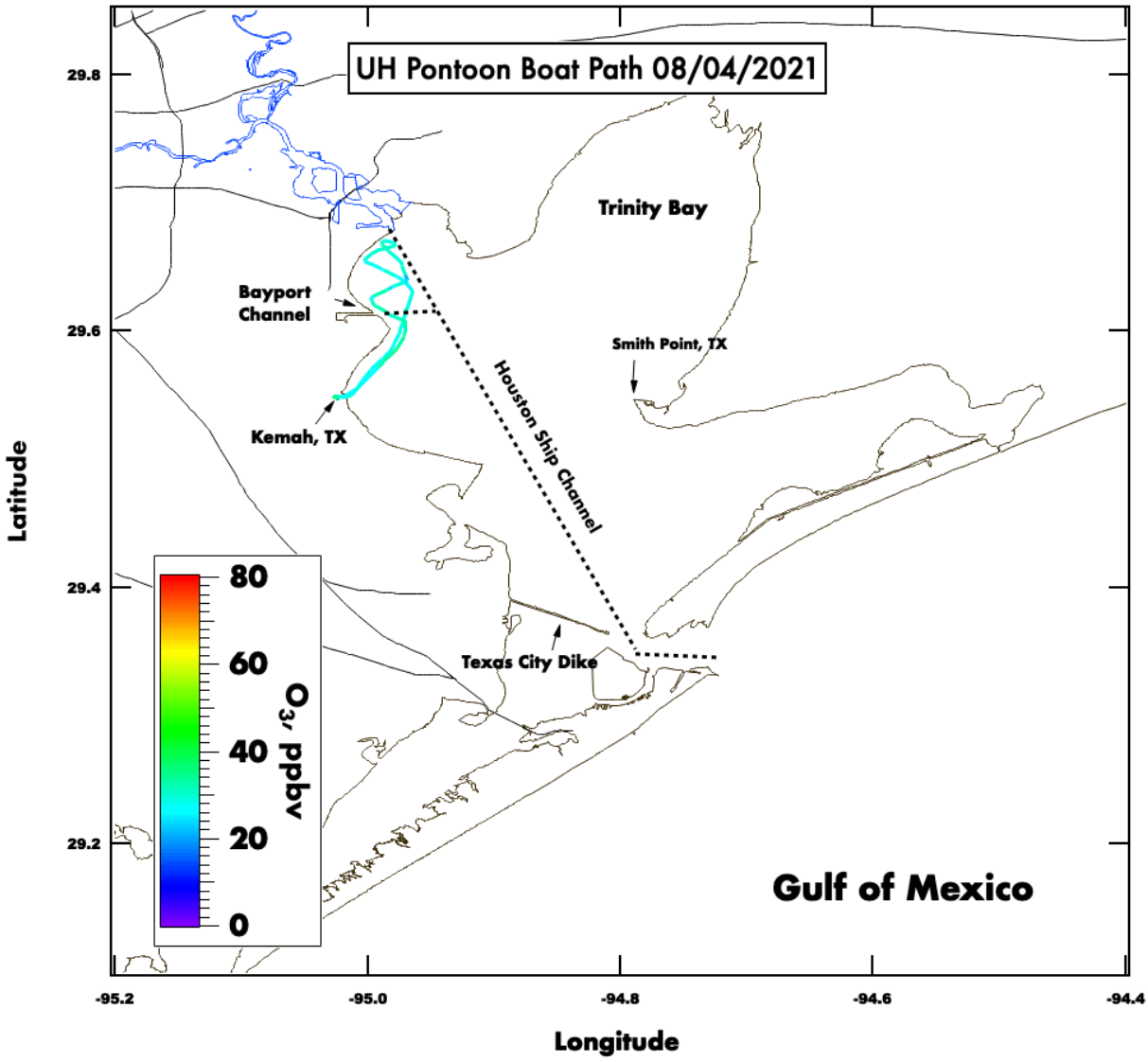

Figure 169. Spatial plot of surface ozone collected from the UH pontoon boat on August 4th, 2021.

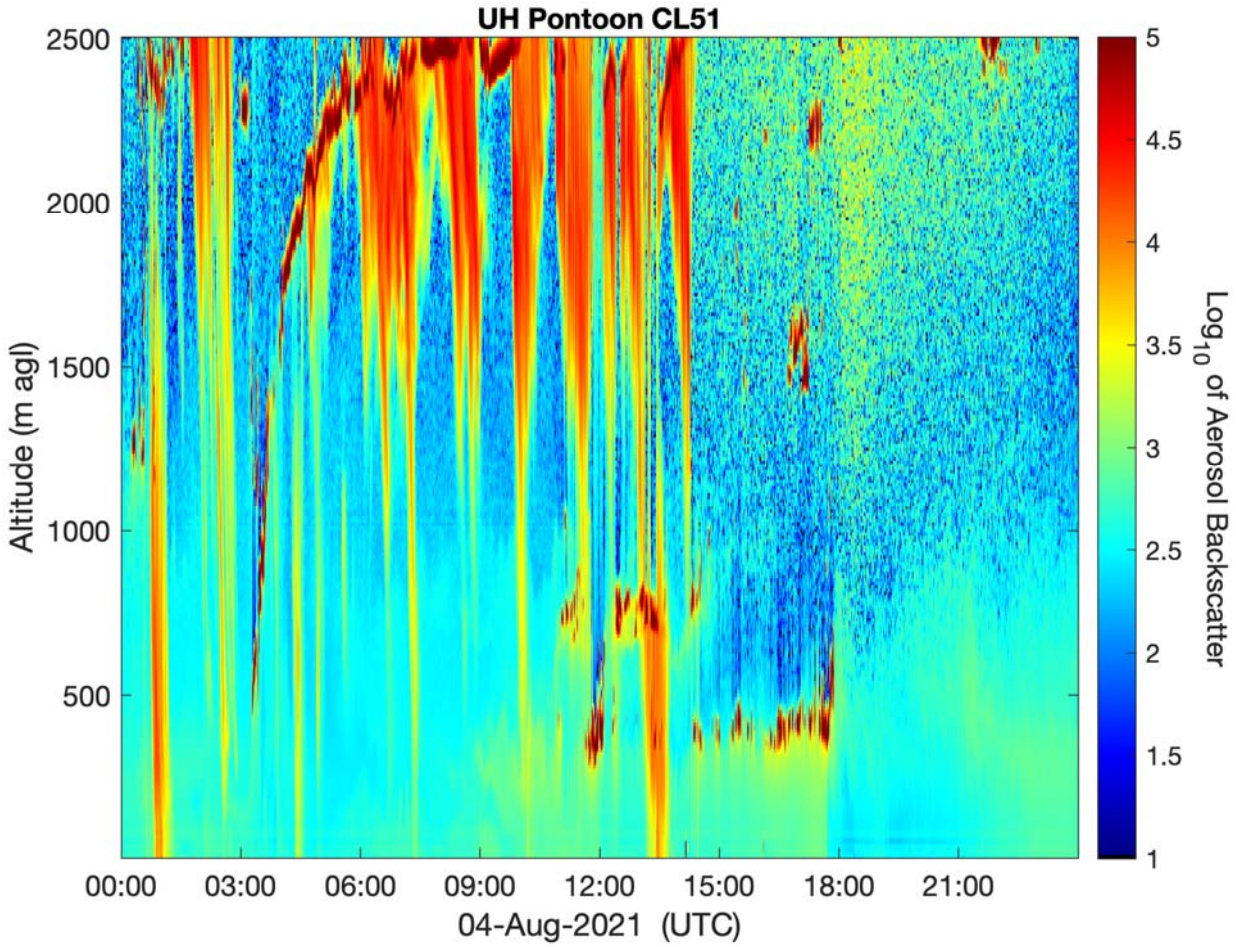

Figure 170. Vertical profile of the aerosol backscatter collected from a Vaisala CL-51 ceilometer mounted on the UH Pontoon boat.

9.18 28 July 2021:

Travis Griggs (UH) and Michael Comas (UH) met at the Marina at 6:15am CST. Initially the pontoon headed to north Trinity Bay and then to the NW section of Galveston Bay for surface sampling. The pontoon was brought back to Kemah to be refueled, when a mechanical issue (broken throttle linkage) caused the boat to be docked for the day at 11:40pm CST.

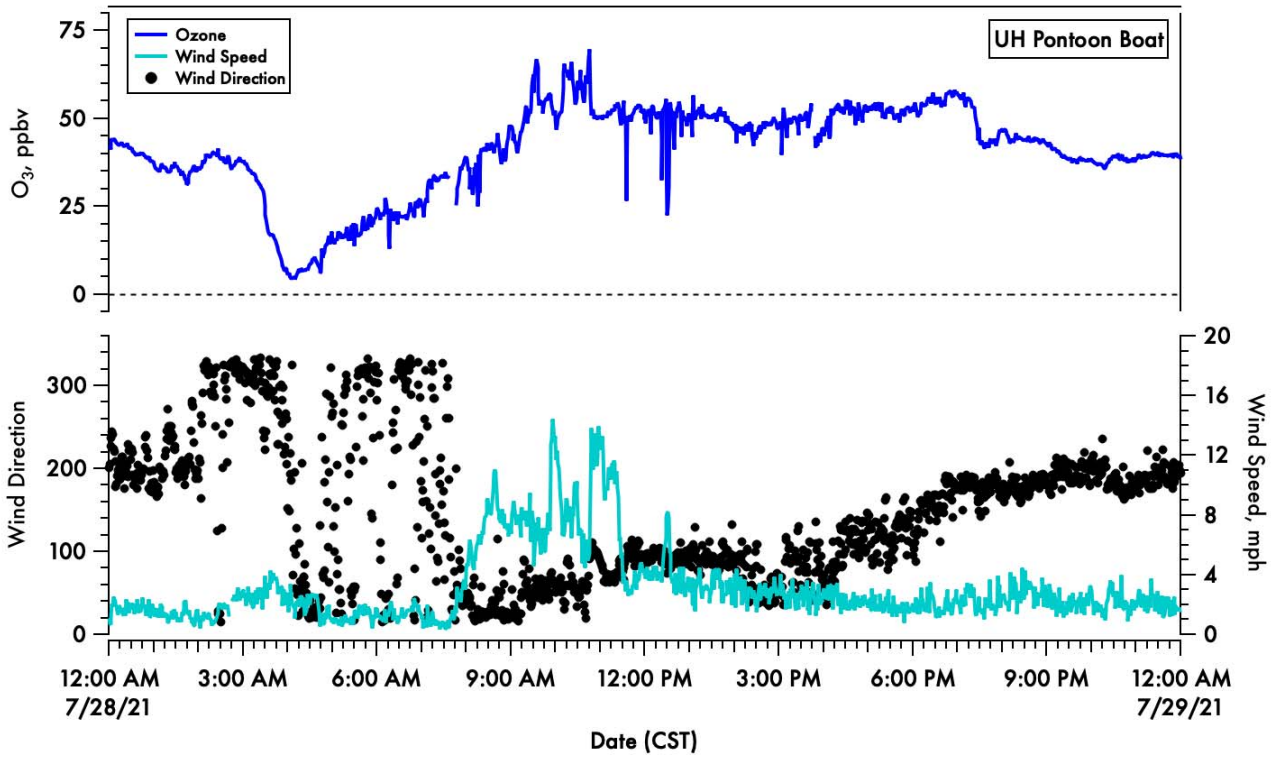

Figure 171. A time-series of 1-minute averaged ozone (blue) on the top panel and wind speed (light blue) and direction (black dots) in the bottom panel.

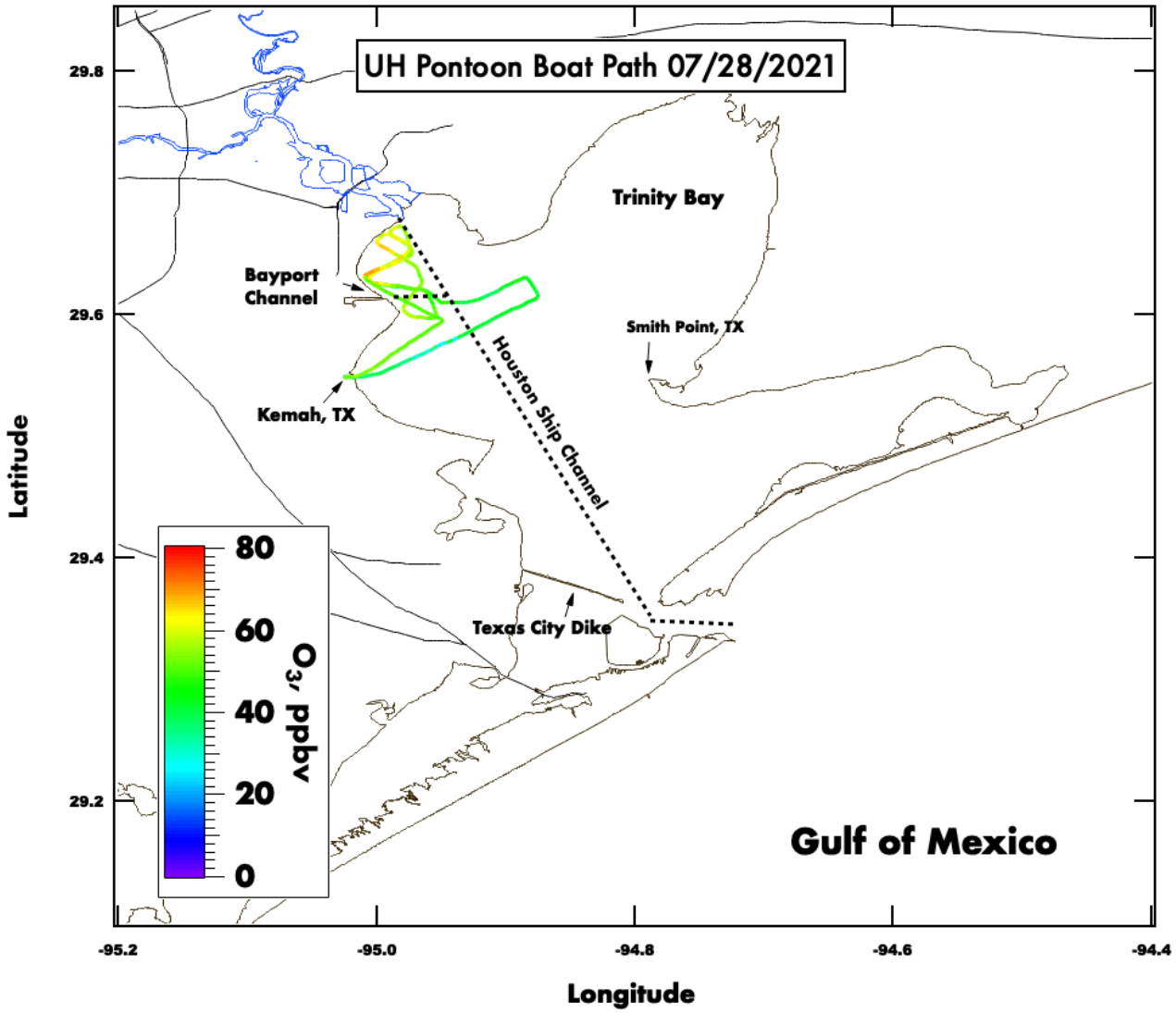

Figure 172. Spatial plot of surface ozone collected from the UH pontoon boat on July 28th, 2021.

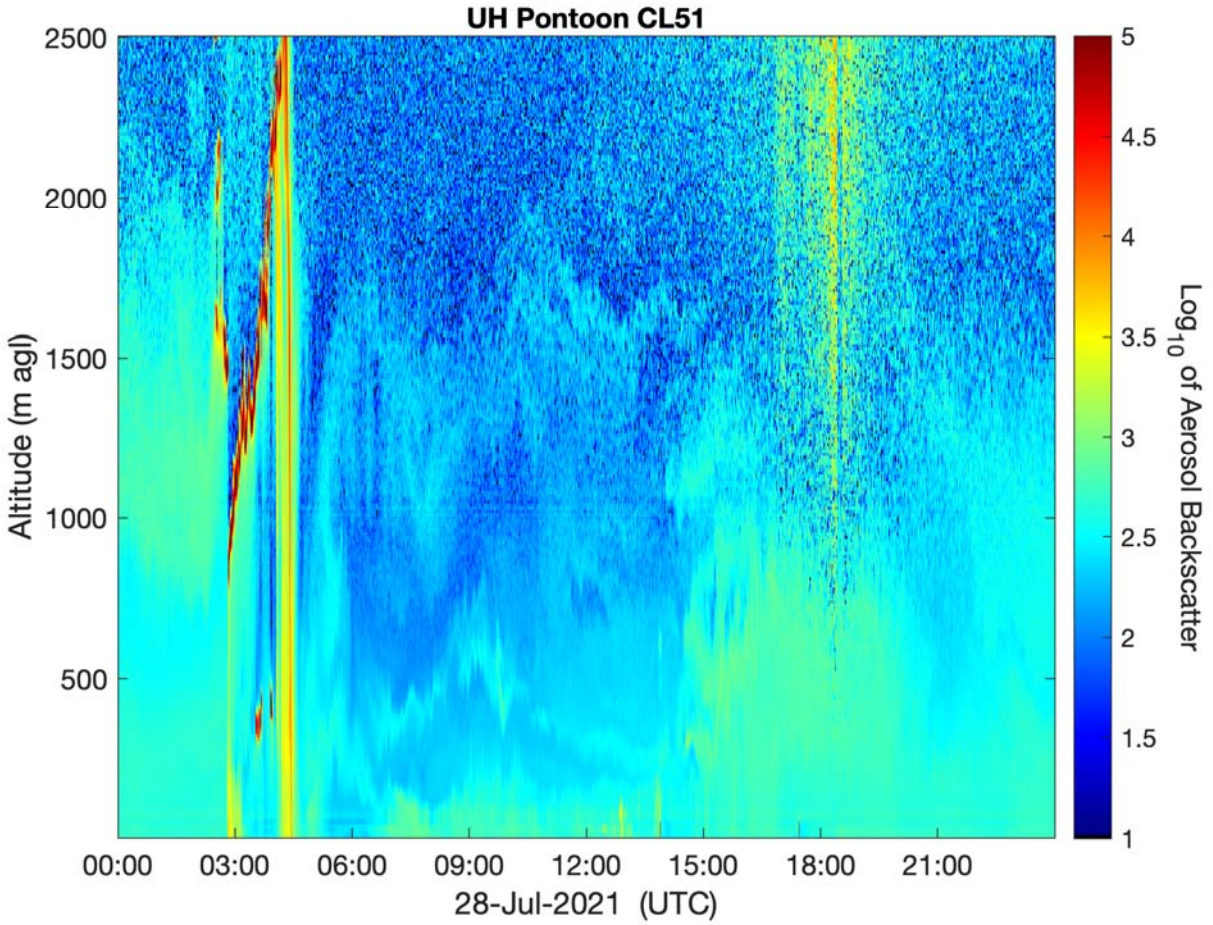

Figure 173. Vertical profile of the aerosol backscatter collected from a Vaisala CL-51 ceilometer mounted on the UH Pontoon boat.

9.19 27 July 2021:

Travis Griggs (UH), Paul Walter (St. Edward's), Claudia Bernier (UH) and Michael Comas (UH) met at the Marina at 7:00am CST. Initially the pontoon boat headed to the SE section of the Bay for a morning ozonesonde launch. The ozonesonde was released at 9:15am CST. The inlet straw for the ozonesonde came loose upon deployment and the radiosonde was the only data profile collected. After the launch the pontoon headed back to the dock to watch nearby storm development. After the passing of the storms a loop into Trinity Bay was made to collect surface measurements. The pontoon was refueled and docked at 2:25pm CST.

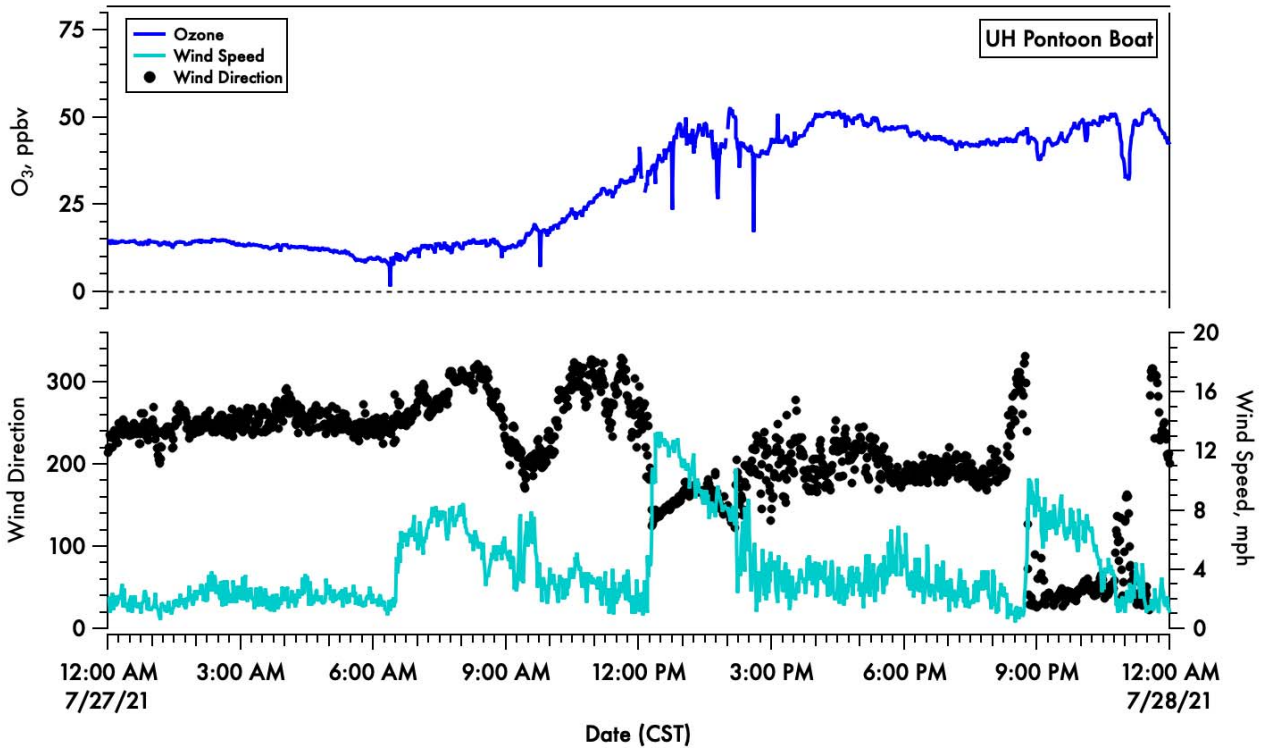

Figure 174. A time-series of 1-minute averaged ozone (blue) on the top panel and wind speed (light blue) and direction (black dots) in the bottom panel.

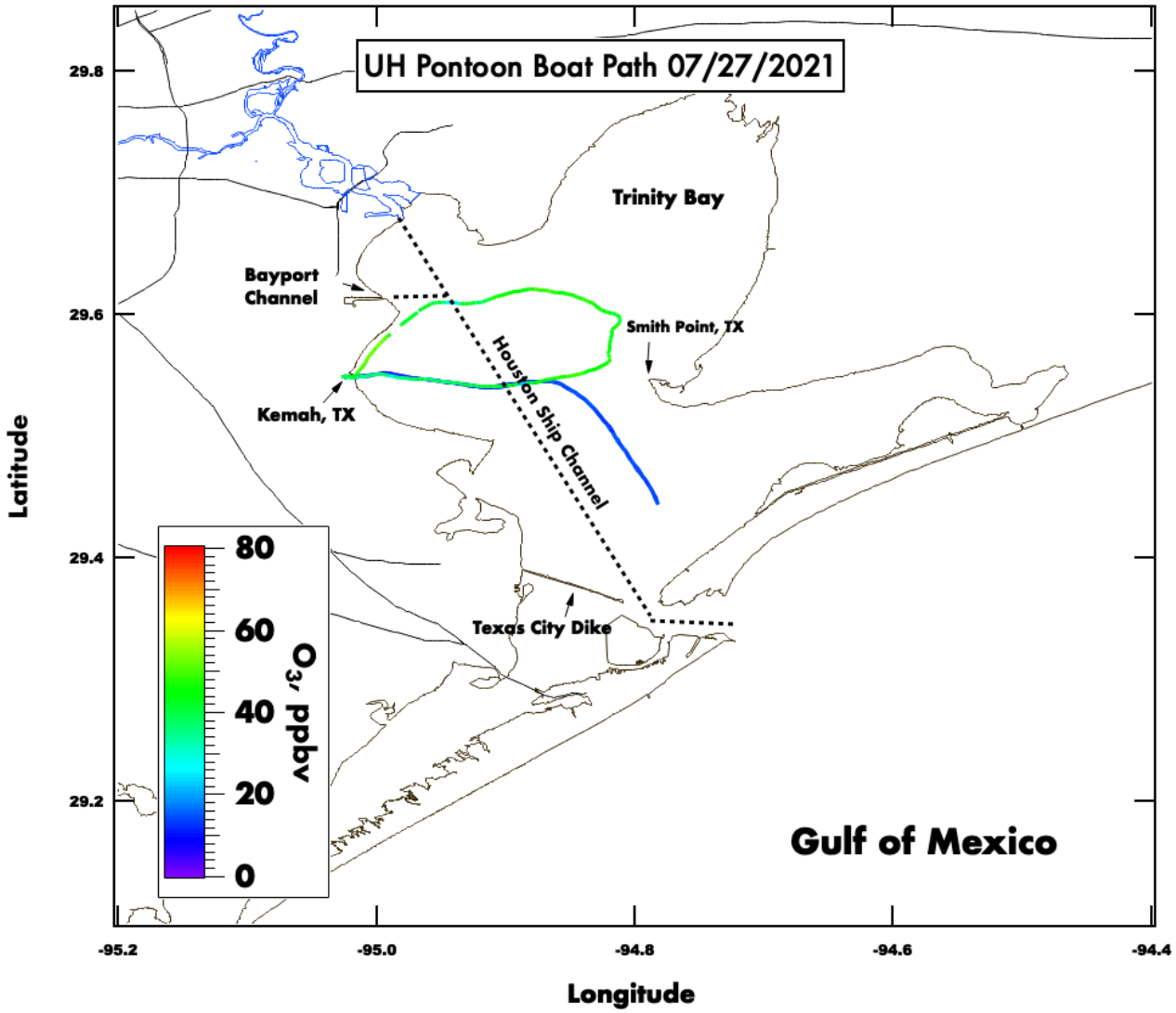

Figure 175. Spatial plot of surface ozone collected from the UH pontoon boat on July 27th, 2021.

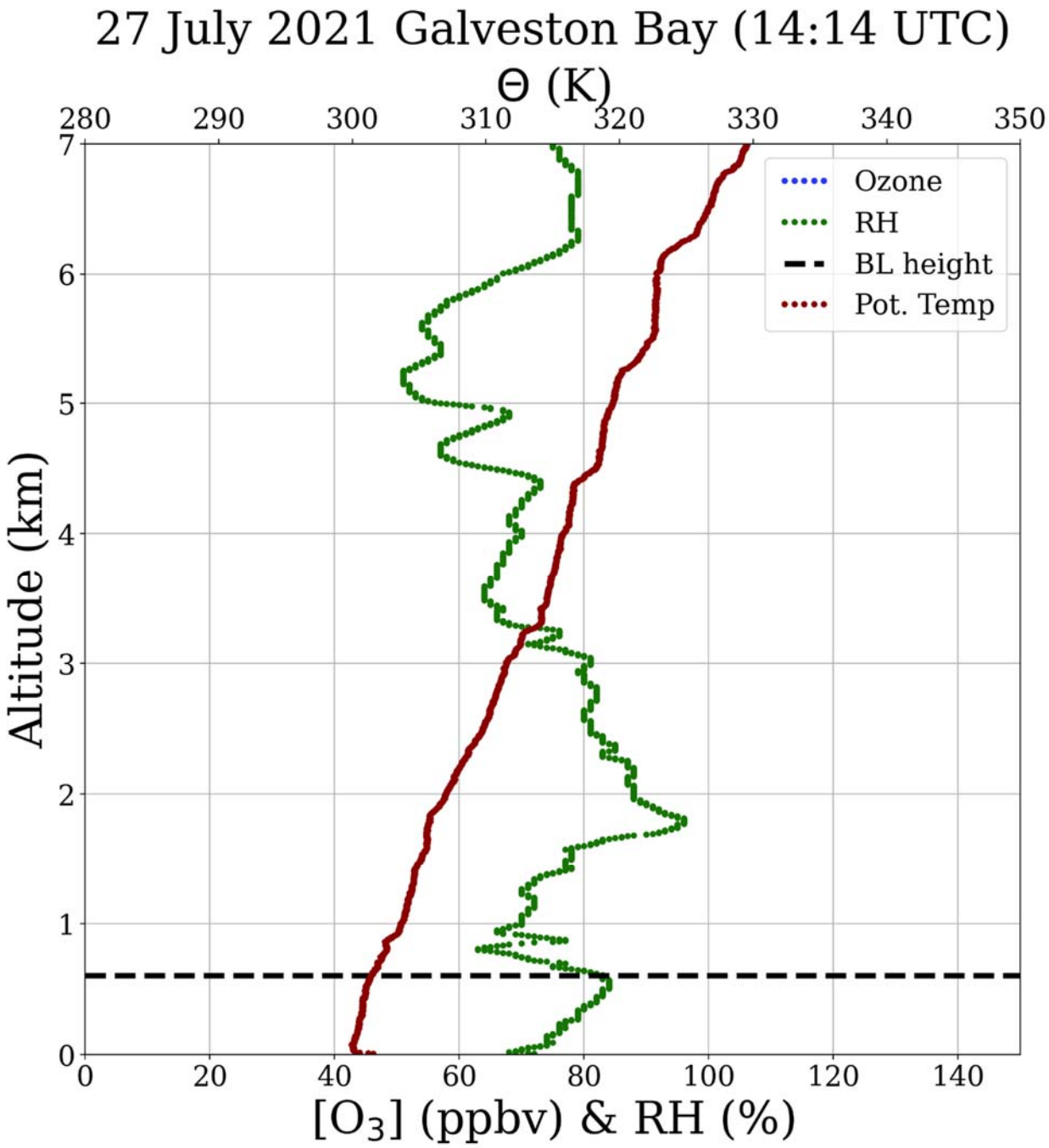

Figure 176. Vertical profiles of ozone (blue), relative humidity (green) and potential temperature (red). The derived boundary layer height is denoted by the horizontal dashed black line.

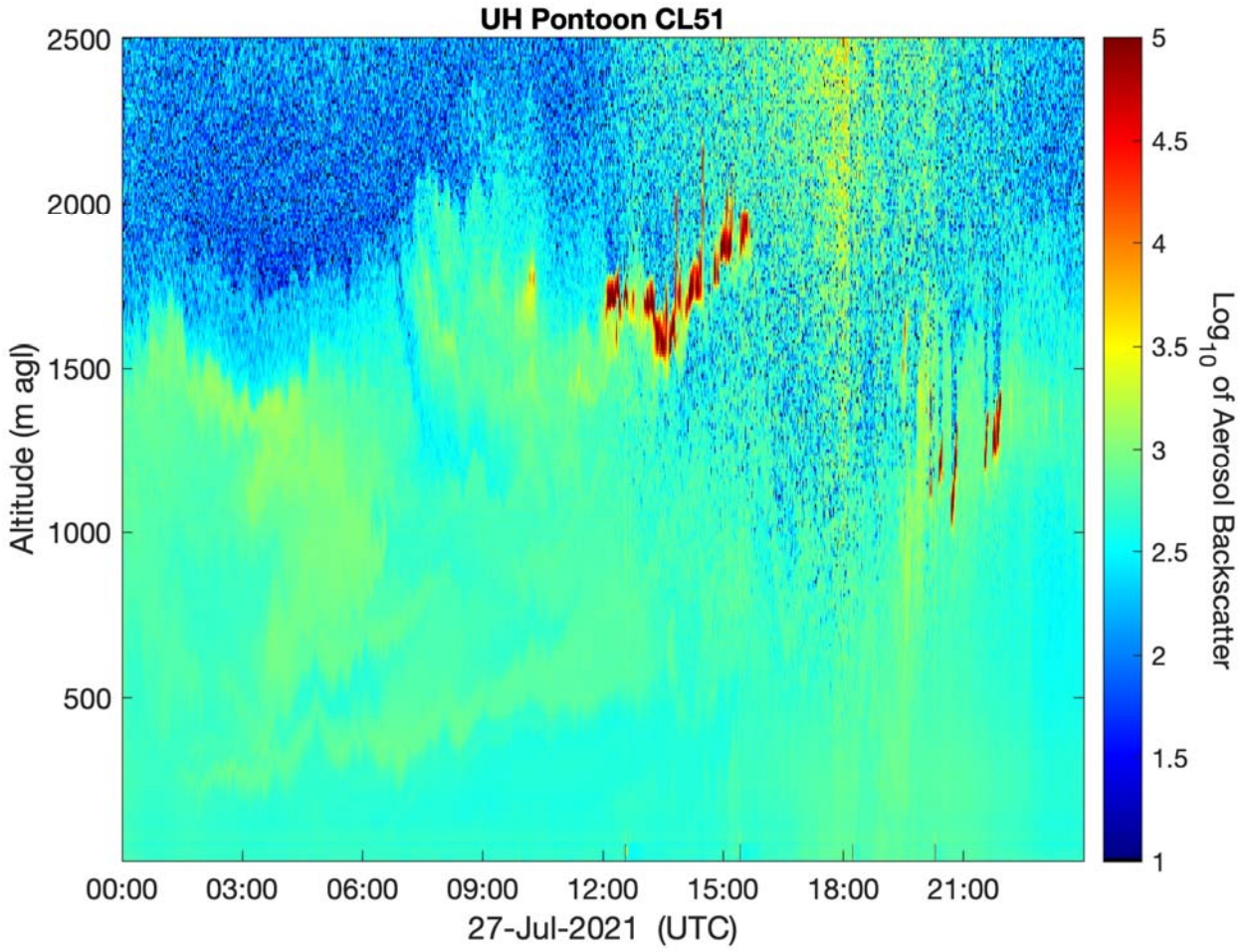

Figure 177. Vertical profile of the aerosol backscatter collected from a Vaisala CL-51 ceilometer mounted on the UH Pontoon boat.

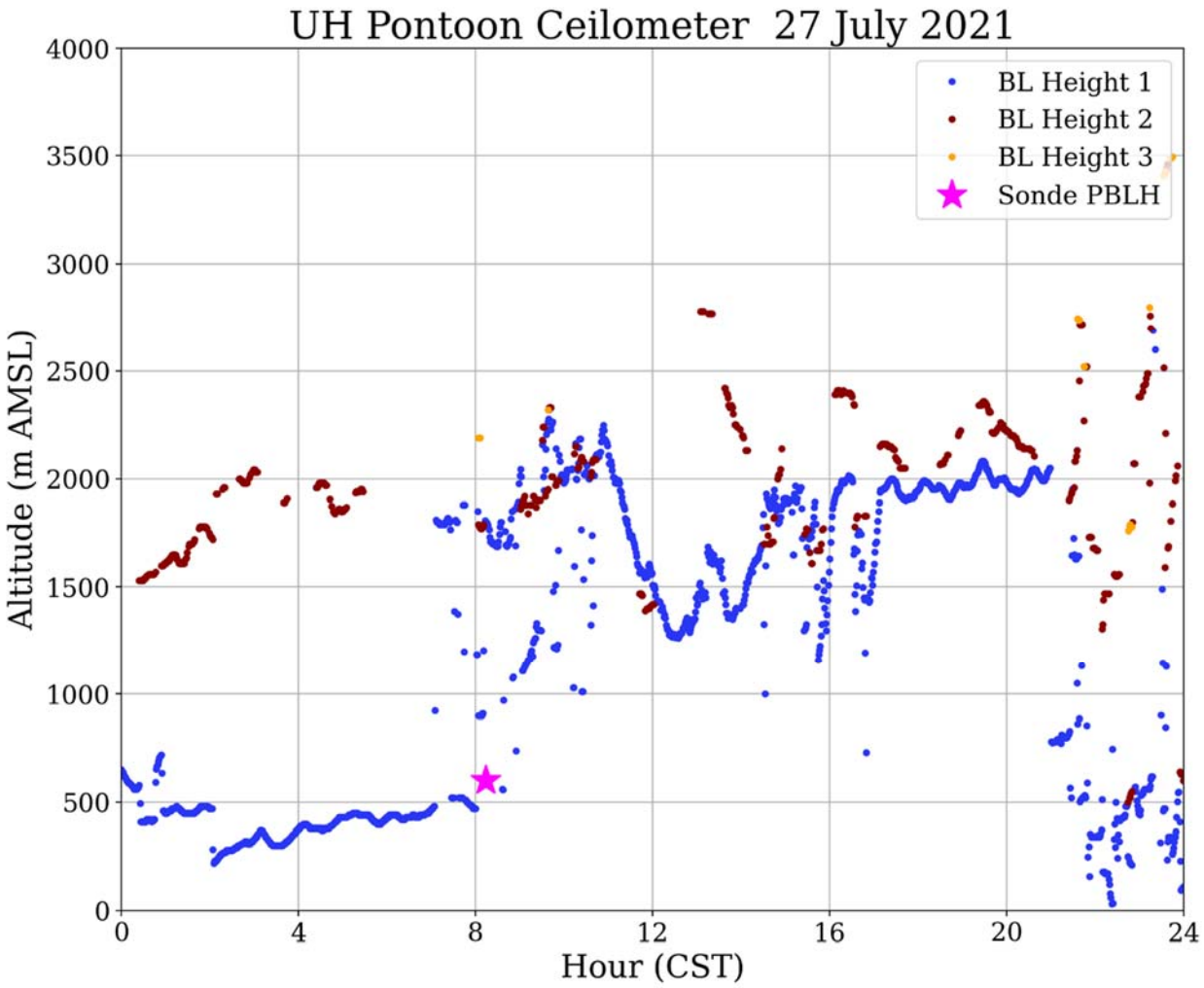

Figure 178. UH Pontoon Vaisala CL-51 ceilometer returned boundary layer heights and boundary layer height from the ozonesonde profile.

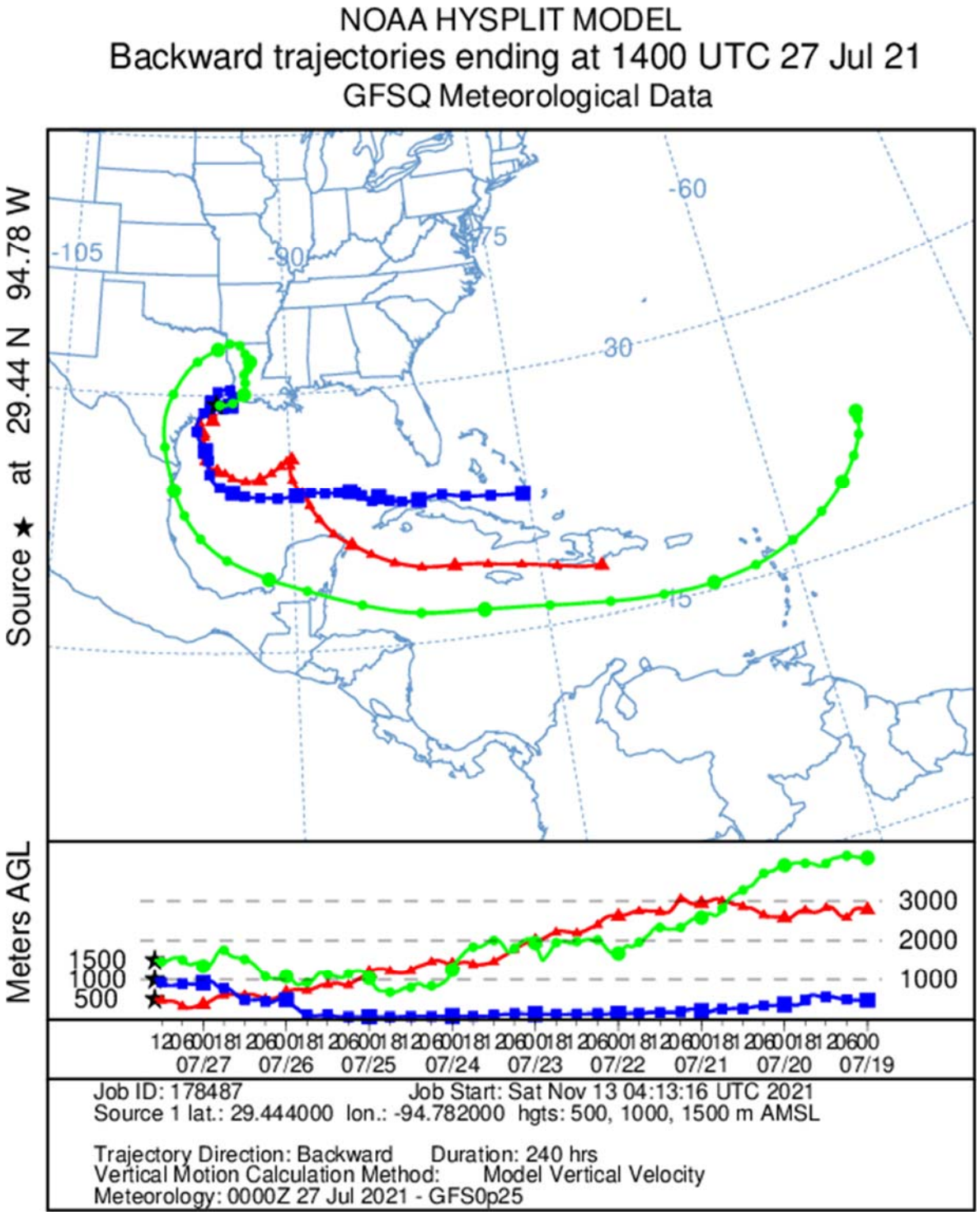

Figure 179. Ten-day HYSPLIT back trajectory for the ozonesonde launch on 27 July 2021 from three heights over the Bay: 500 m (red), 1,000 m (blue), and 1,500 m (green). Each data point is 6 hours apart.

9.20 26 July 2021:

Travis Griggs (UH), Paul Walter (St. Edward's), Claudia Bernier (UH) and Michael Comas (UH) met at the Marina at 6:15am - deployed at 6:47am CST. The pontoon boat initially headed south towards the Texas City Dike for an ozonesonde launch that was released at 8:37am CST. A gradient sampling pattern was conducted in the SW area of Galveston Bay. At 10:15am CST the ozone concentration at Smith Point was 84ppb while the pontoon boat was only measuring 45ppb. The ceilometer on the UH pontoon boat also showing different heights for the lowest mixing layer compared with the Smith Point. A second ozonesonde was launched in the SW area of the Bay at 1:00pm CST, however the ozonesonde malfunctioned and did not record the ozone data. After launching, the pontoon came back to Kemah to refuel and drop off crew members. The science team decided it was a good day for an afternoon deployment and headed to the NW area of the bay for surface sampling. The pontoon was then brought back to Kemah to be refueled and docked at 4:40pm CST.

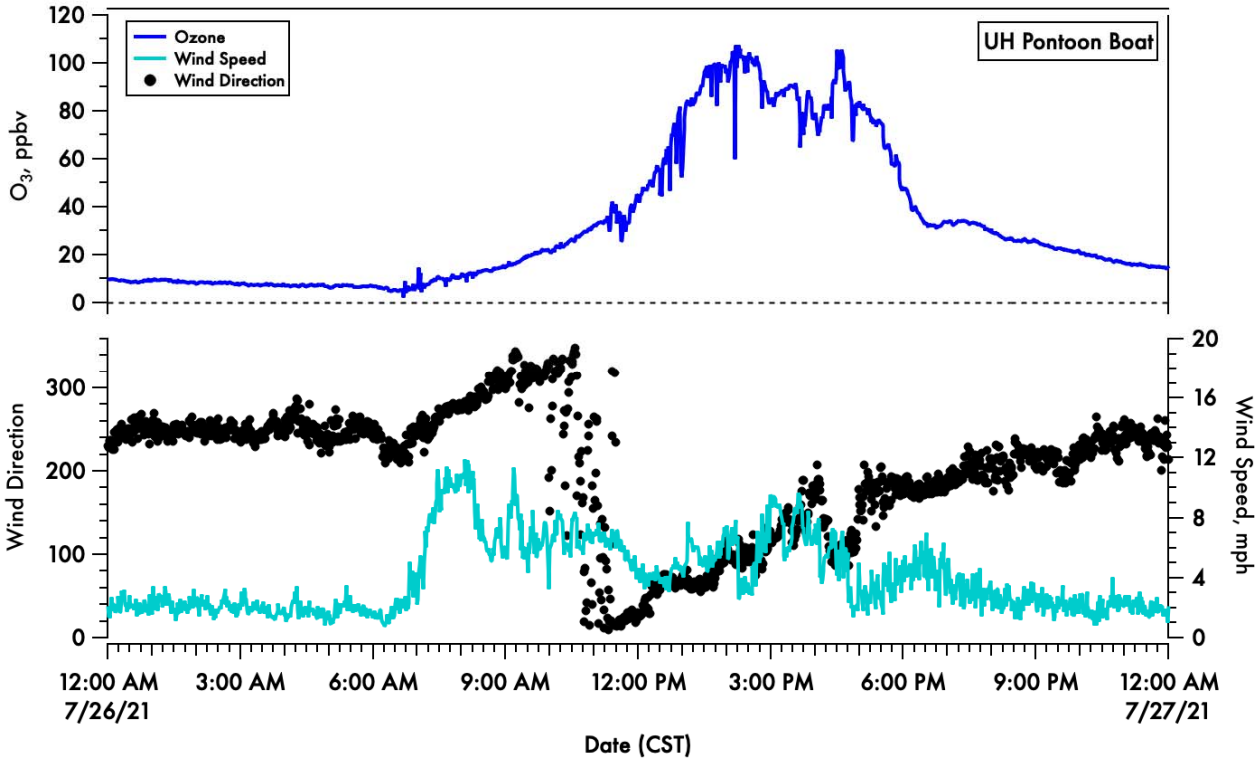

Figure 180. A time-series of 1-minute averaged ozone (blue) on the top panel and wind speed (light blue) and direction (black dots) in the bottom panel.

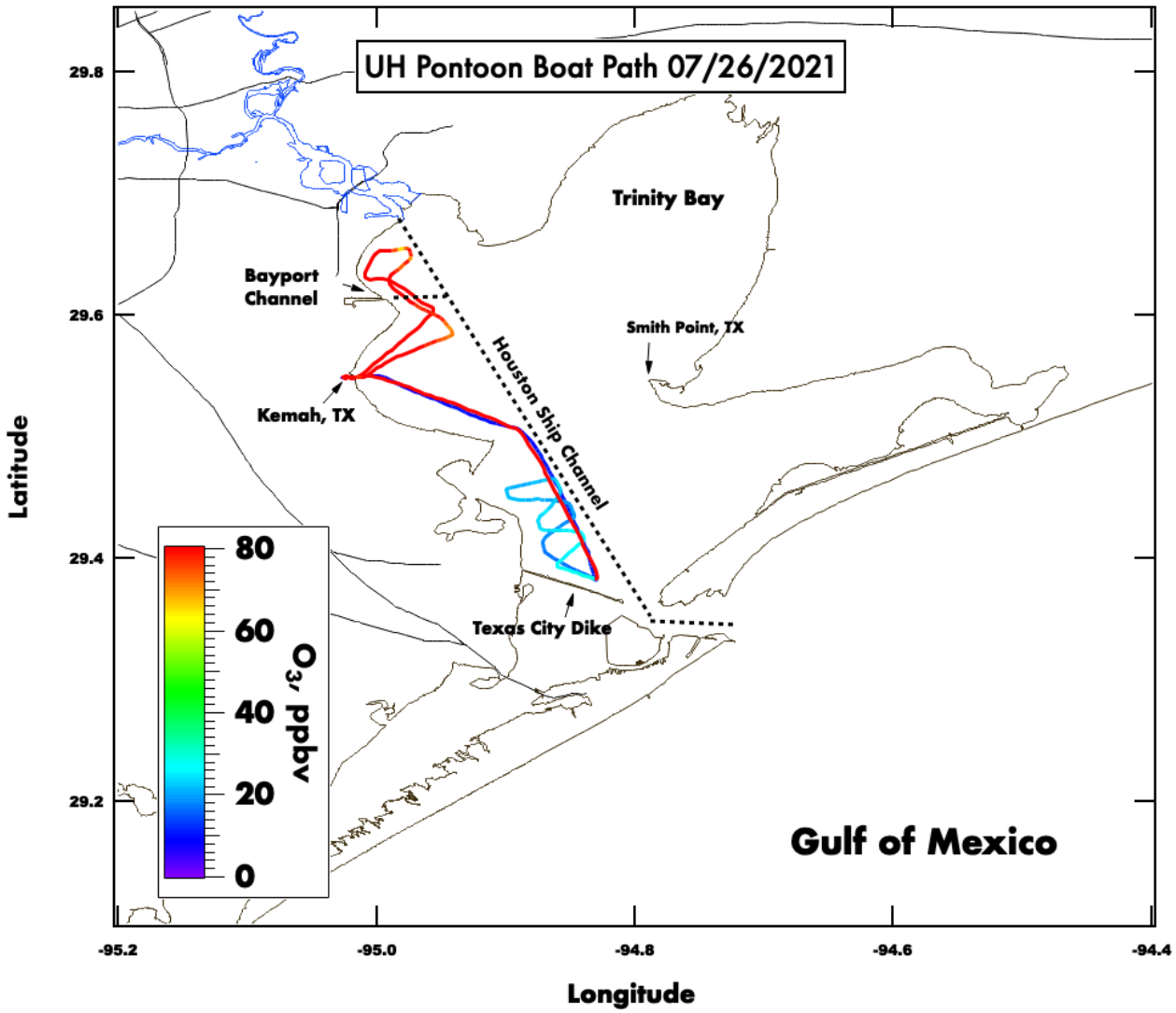

Figure 181. Spatial plot of surface ozone collected from the UH pontoon boat on July 26th, 2021.

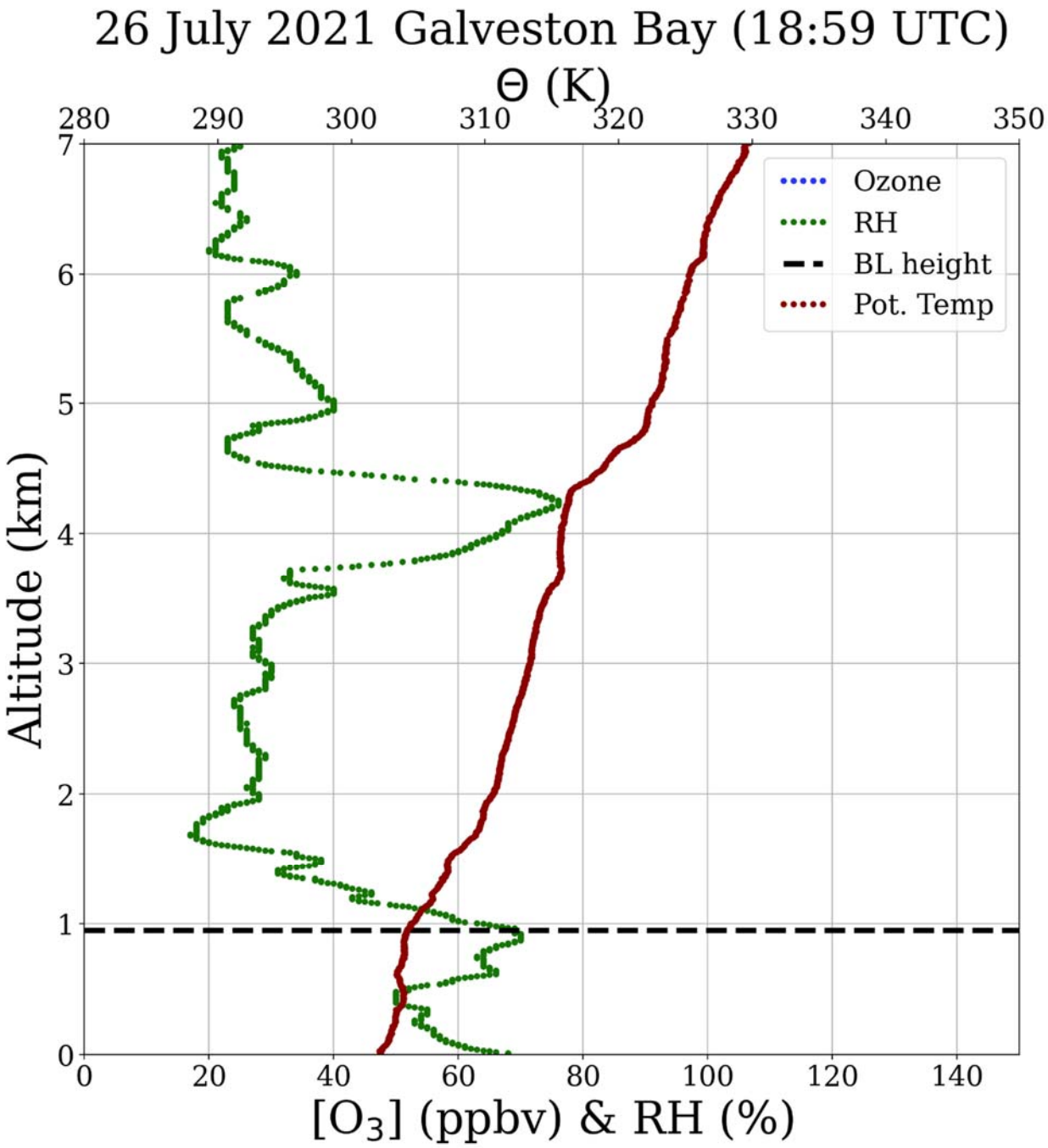

Figure 182. Vertical profiles of ozone (blue), relative humidity (green) and potential temperature (red). The derived boundary layer height is denoted by the horizontal dashed black line.

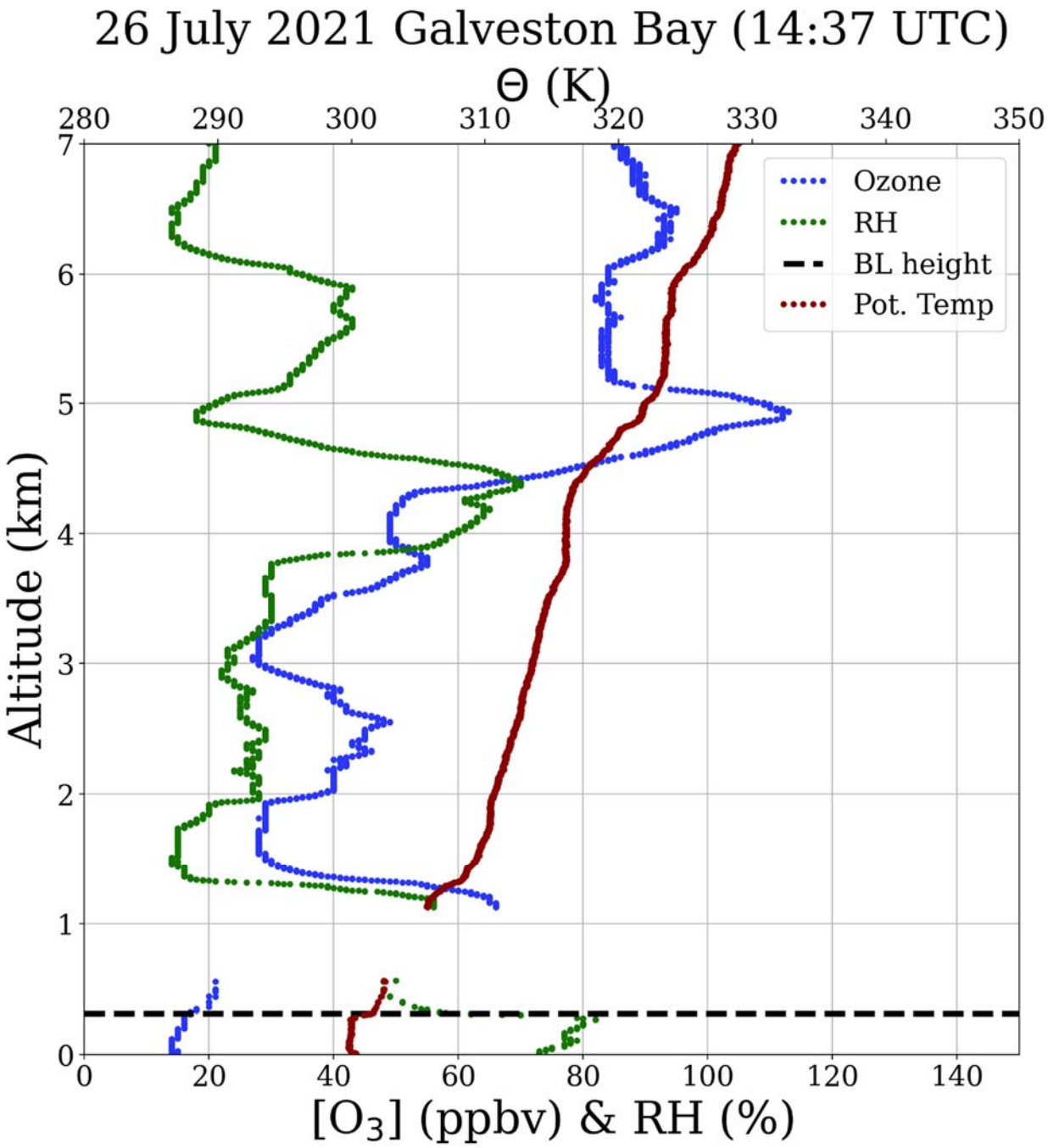

Figure 183. Vertical profiles of ozone (blue), relative humidity (green) and potential temperature (red). The derived boundary layer height is denoted by the horizontal dashed black line.

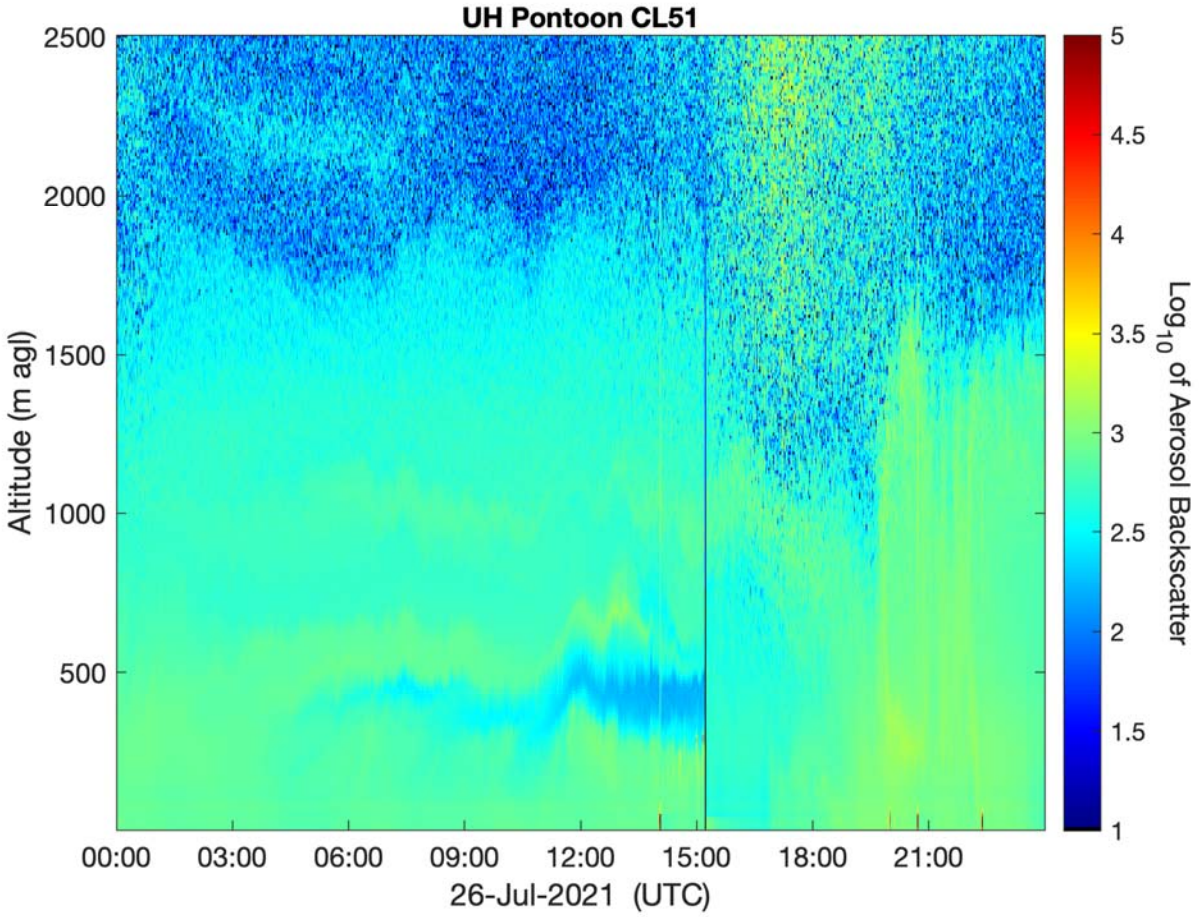

Figure 184. Vertical profile of the aerosol backscatter collected from a Vaisala CL-51 ceilometer mounted on the UH Pontoon boat.

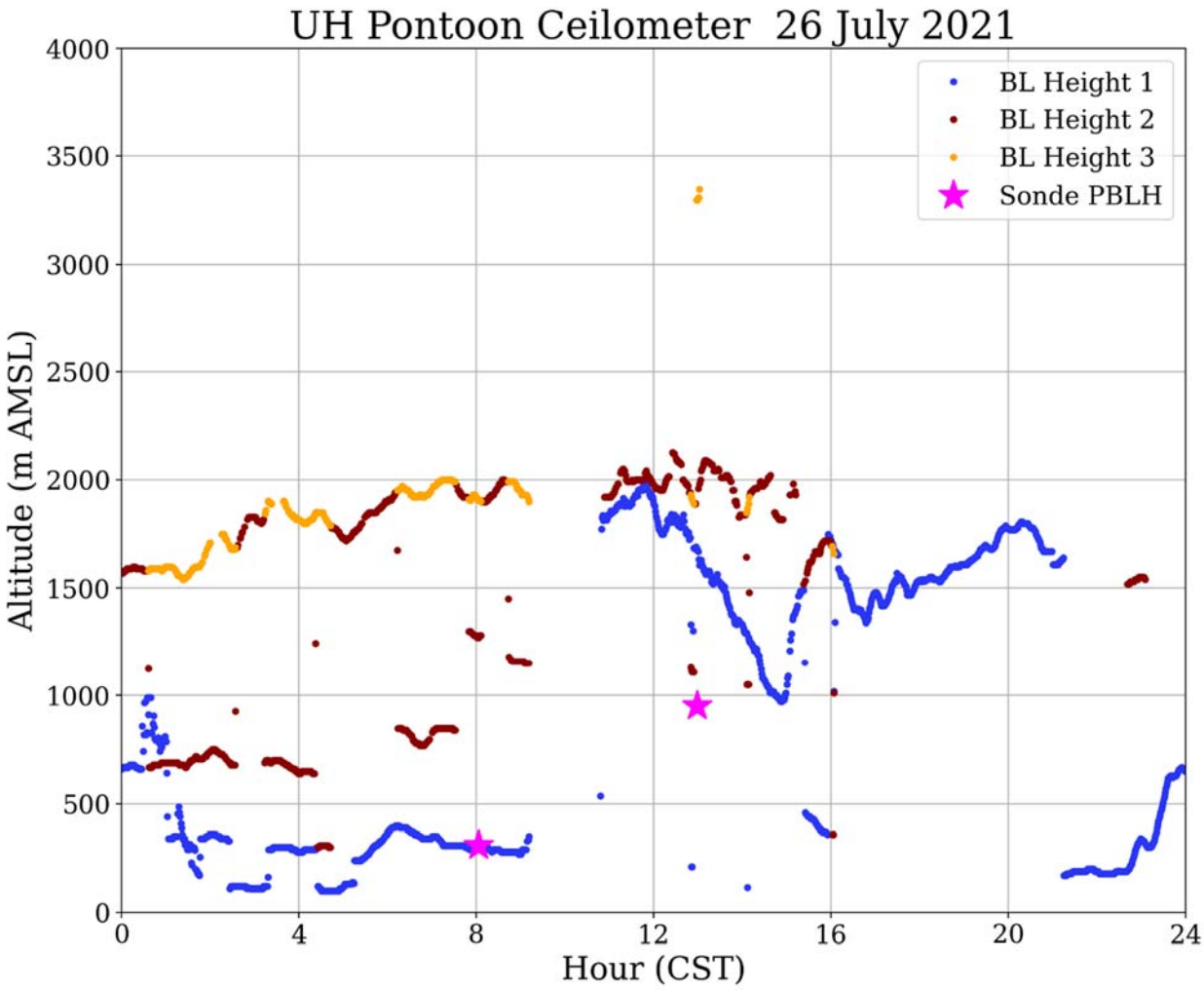

Figure 185. UH Pontoon Vaisala CL-51 ceilometer returned boundary layer heights and boundary layer height from the ozonesonde profile.

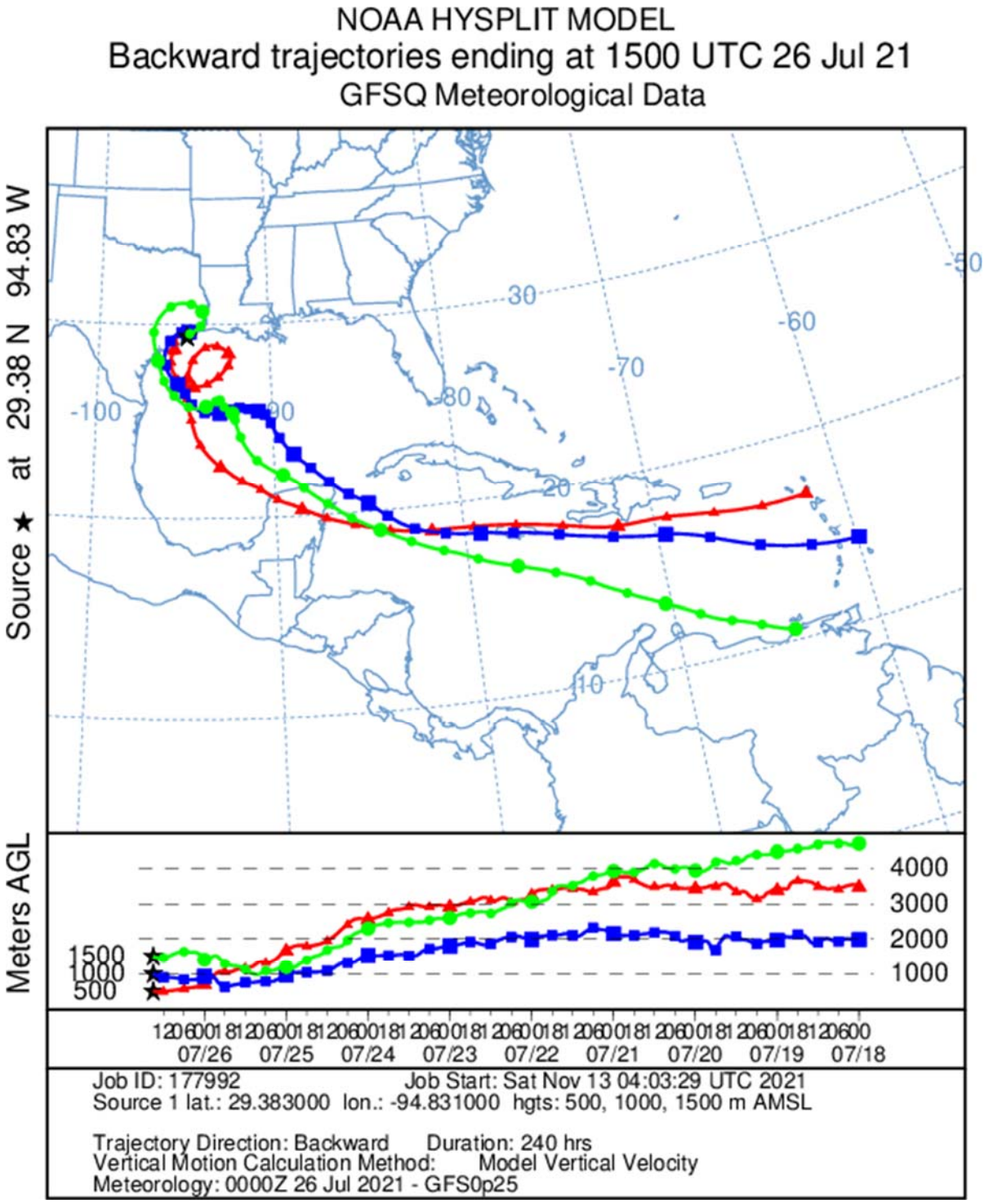

Figure 186. Ten-day HYSPLIT back trajectory for the first ozonesonde launch on 26 July 2021 from three heights over the Bay: 500 m (red), 1,000 m (blue), and 1,500 m (green). Each data point is 6 hours apart.

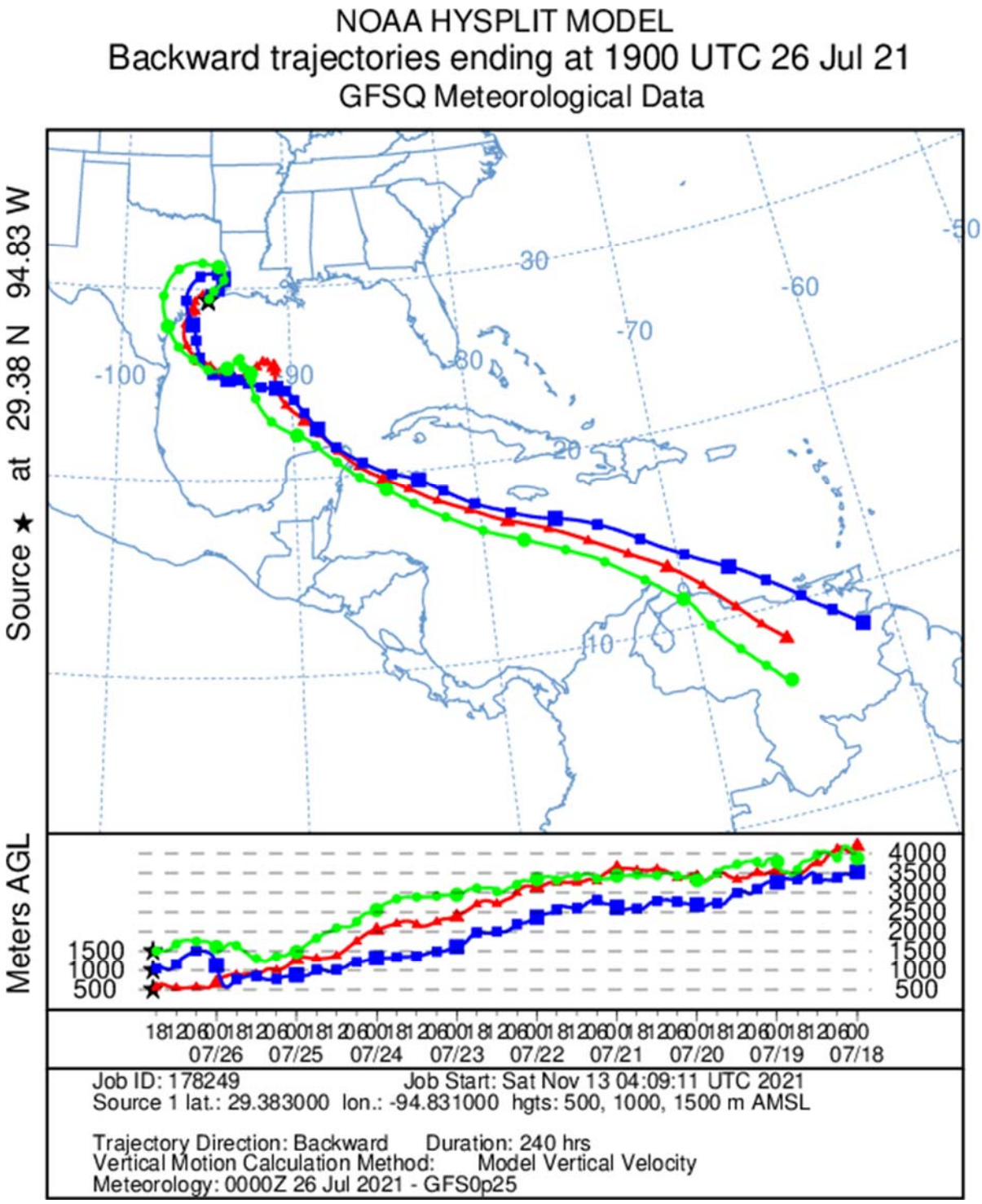

Figure 187. Ten-day HYSPLIT back trajectory for the second ozonesonde launch on 26 July 2021 from three heights over the Bay: 500 m (red), 1,000 m (blue), and 1,500 m (green). Each data point is 6 hours apart.

9.21 22 July 2021:

Travis Griggs (UH), Paul Walter (St. Edward's) and Claudia Bernier (UH) met at the Portofino Marina at 6:30am CST. Initially the pontoon boat headed north towards Morgan Point for an ozonesonde launch that was successfully released at 8:30am CST. Convective storm development nearby the Bay caused the pontoon outing to be ended early. The pontoon was brought back to Kemah to be refueled and docked at 10:00am CST.

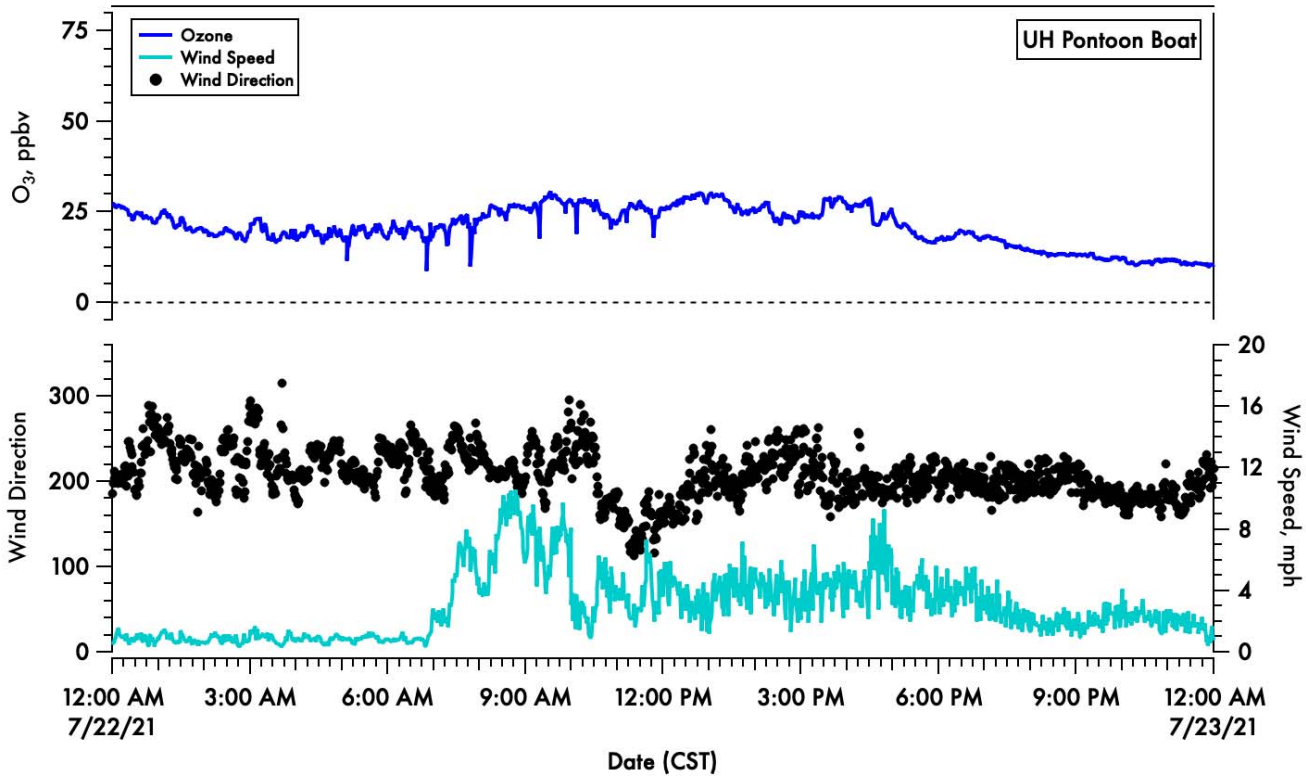

Figure 188. A time-series of 1-minute averaged ozone (blue) on the top panel and wind speed (light blue) and direction (black dots) in the bottom panel.

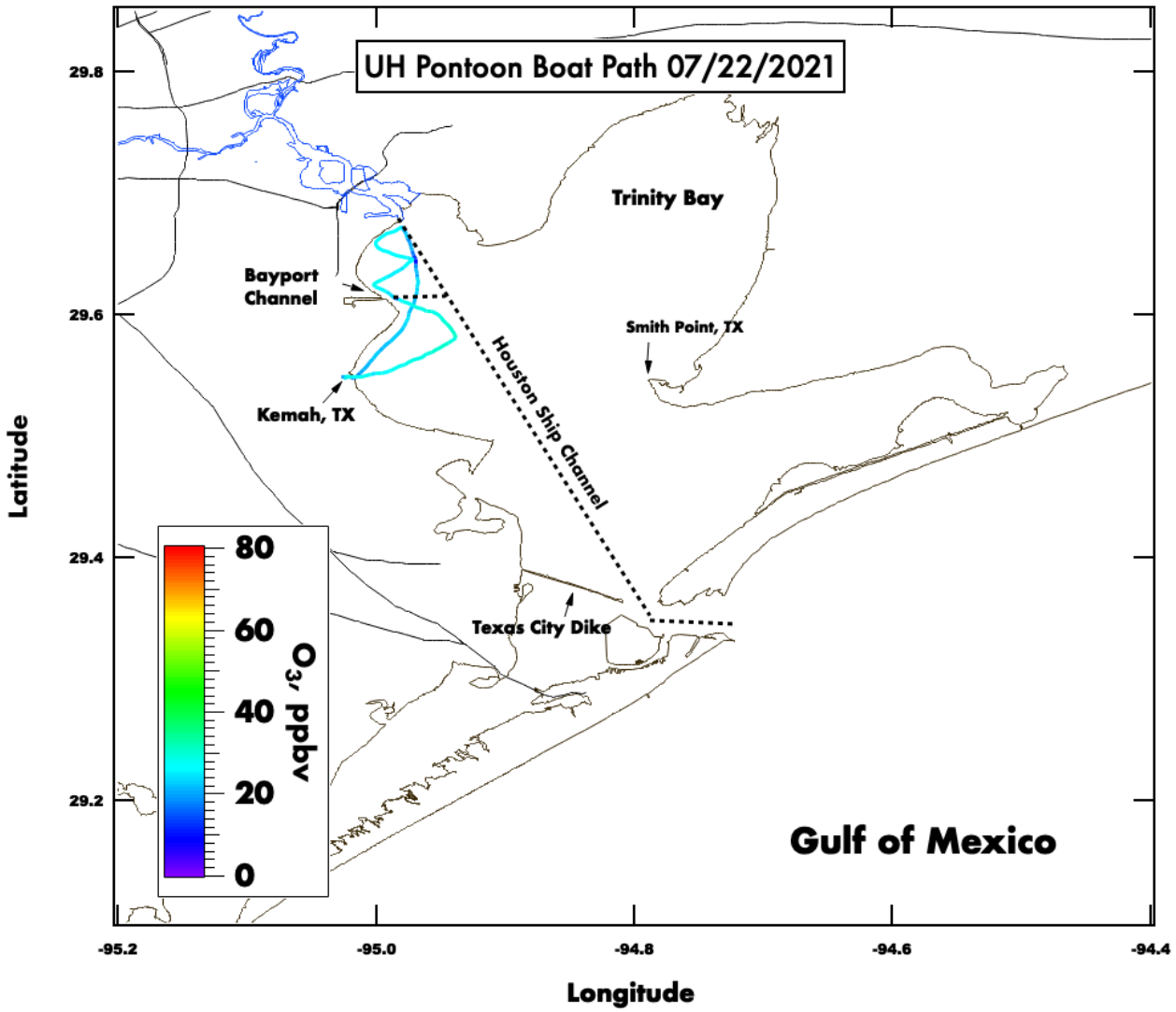

Figure 189. Spatial plot of surface ozone collected from the UH pontoon boat on July 22nd, 2021.

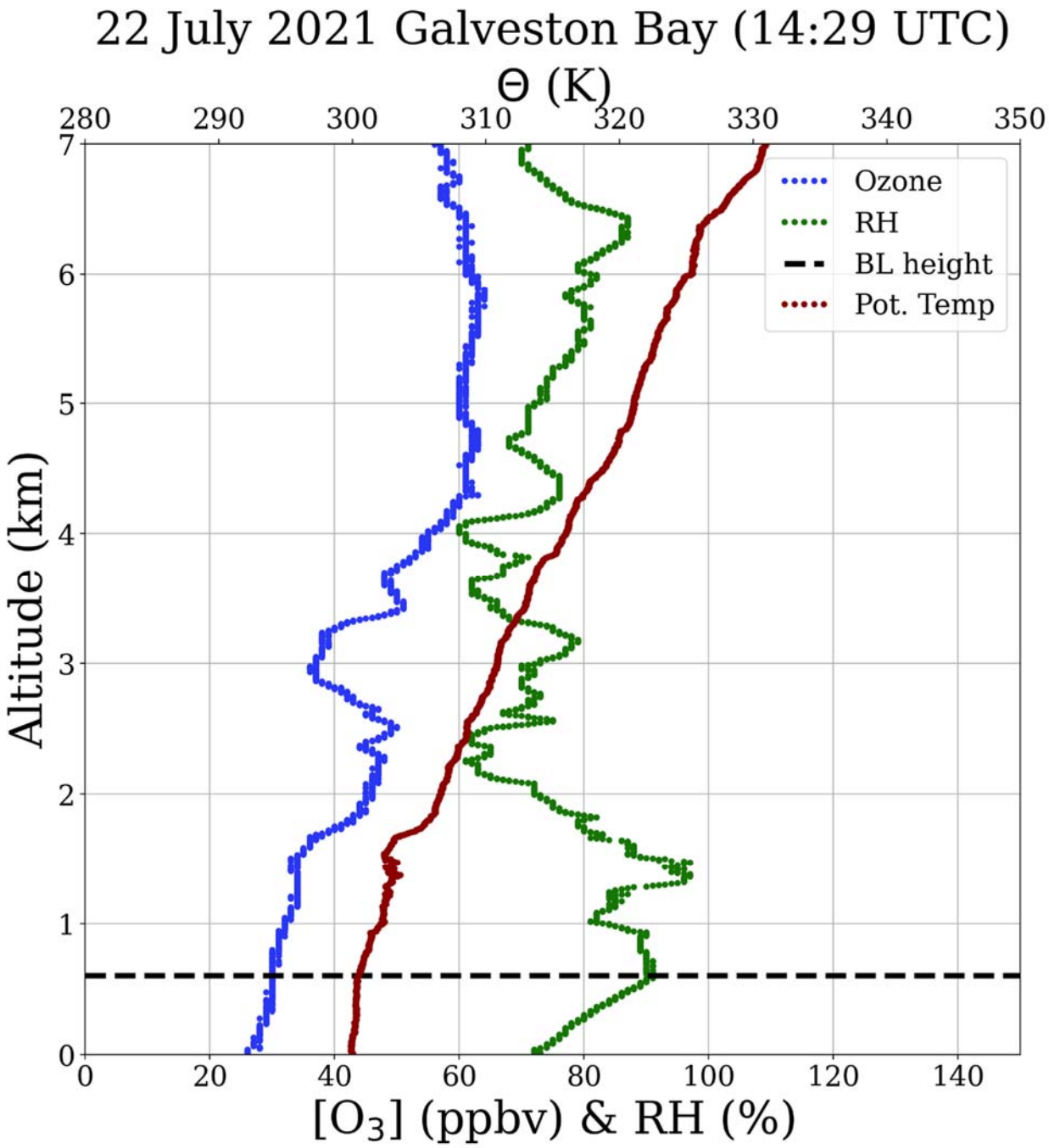

Figure 190. Vertical profiles of ozone (blue), relative humidity (green) and potential temperature (red). The derived boundary layer height is denoted by the horizontal dashed black line.

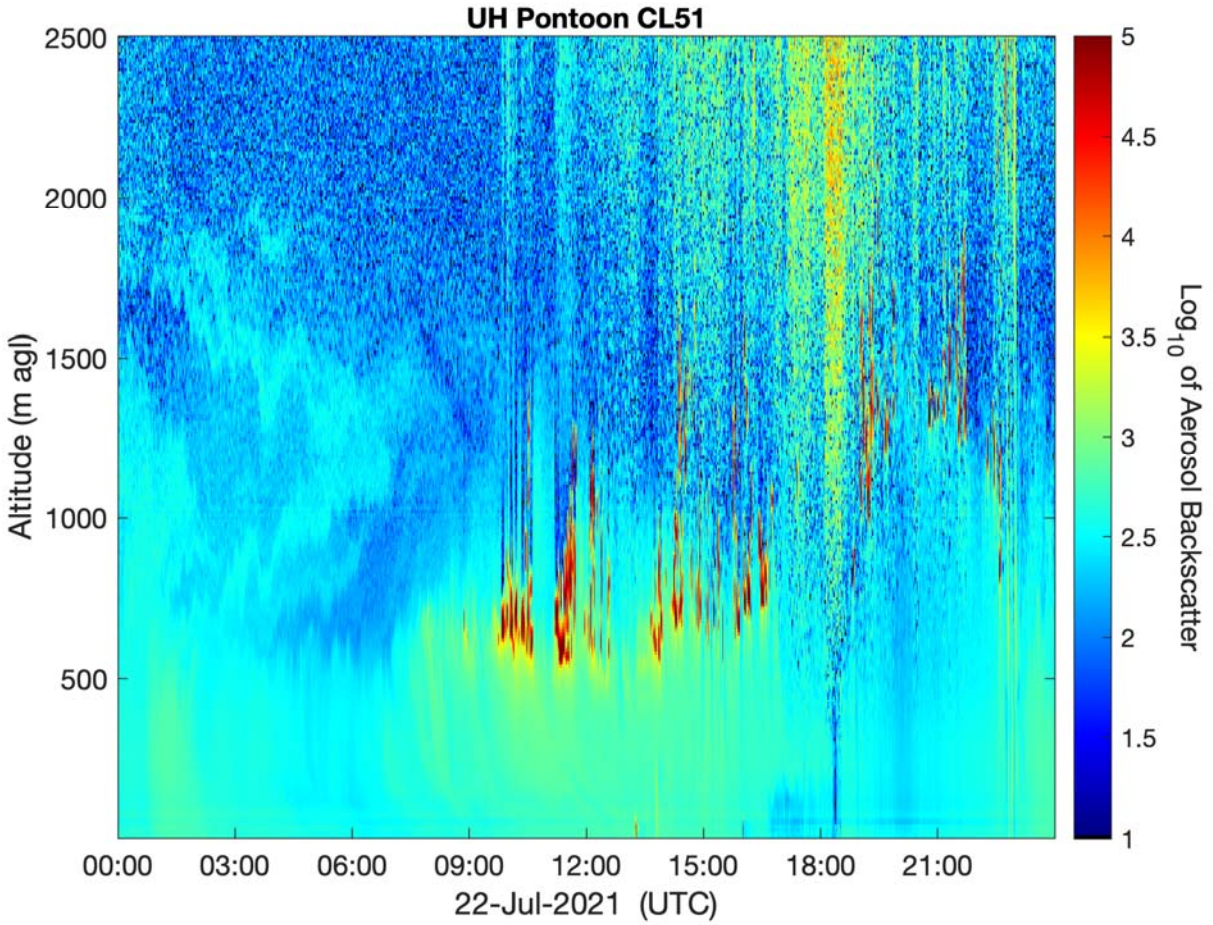

Figure 191. Vertical profile of the aerosol backscatter collected from a Vaisala CL-51 ceilometer mounted on the UH Pontoon boat.

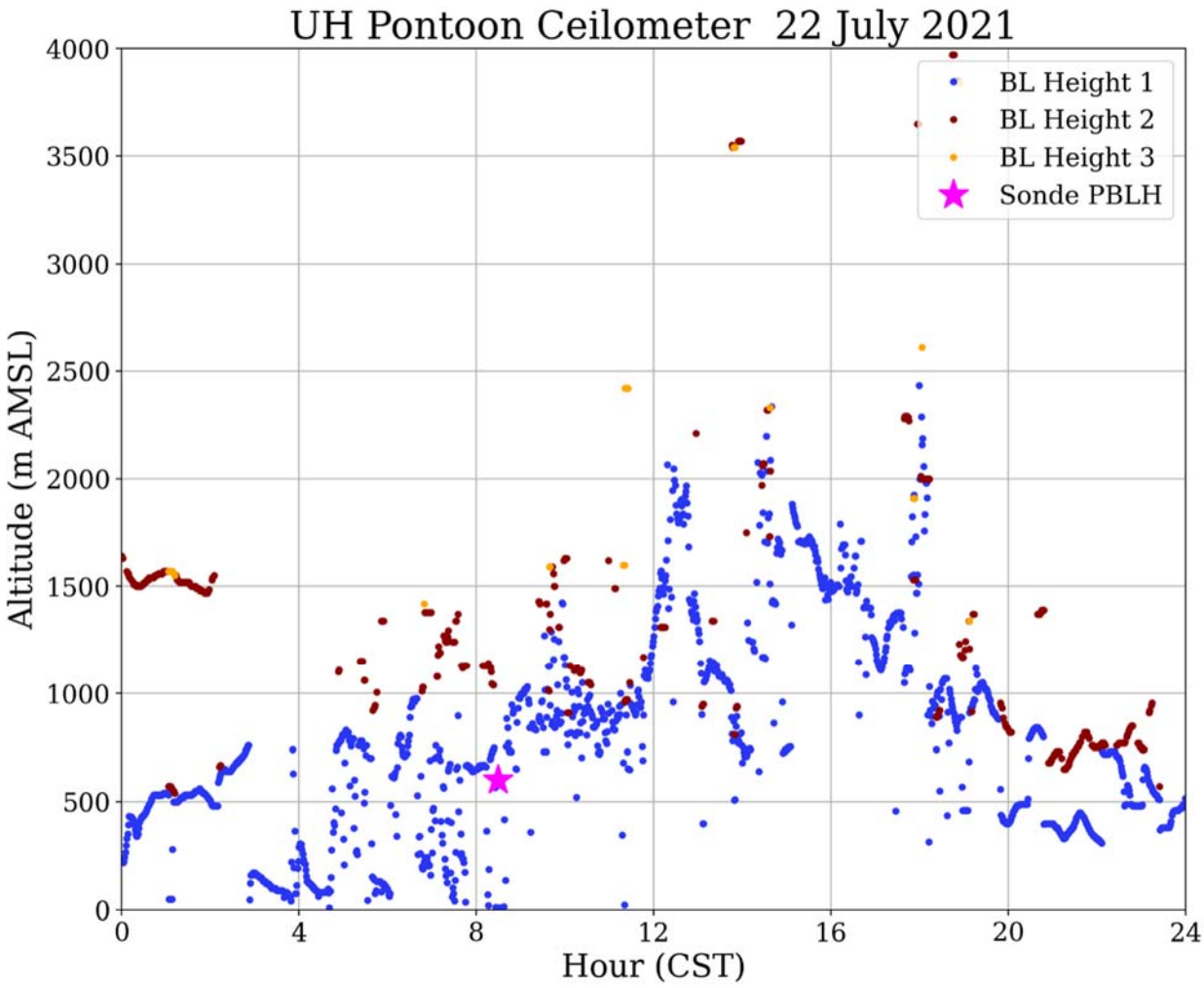

Figure 192. UH Pontoon Vaisala CL-51 ceilometer returned boundary layer heights and boundary layer height from the ozonesonde profile.

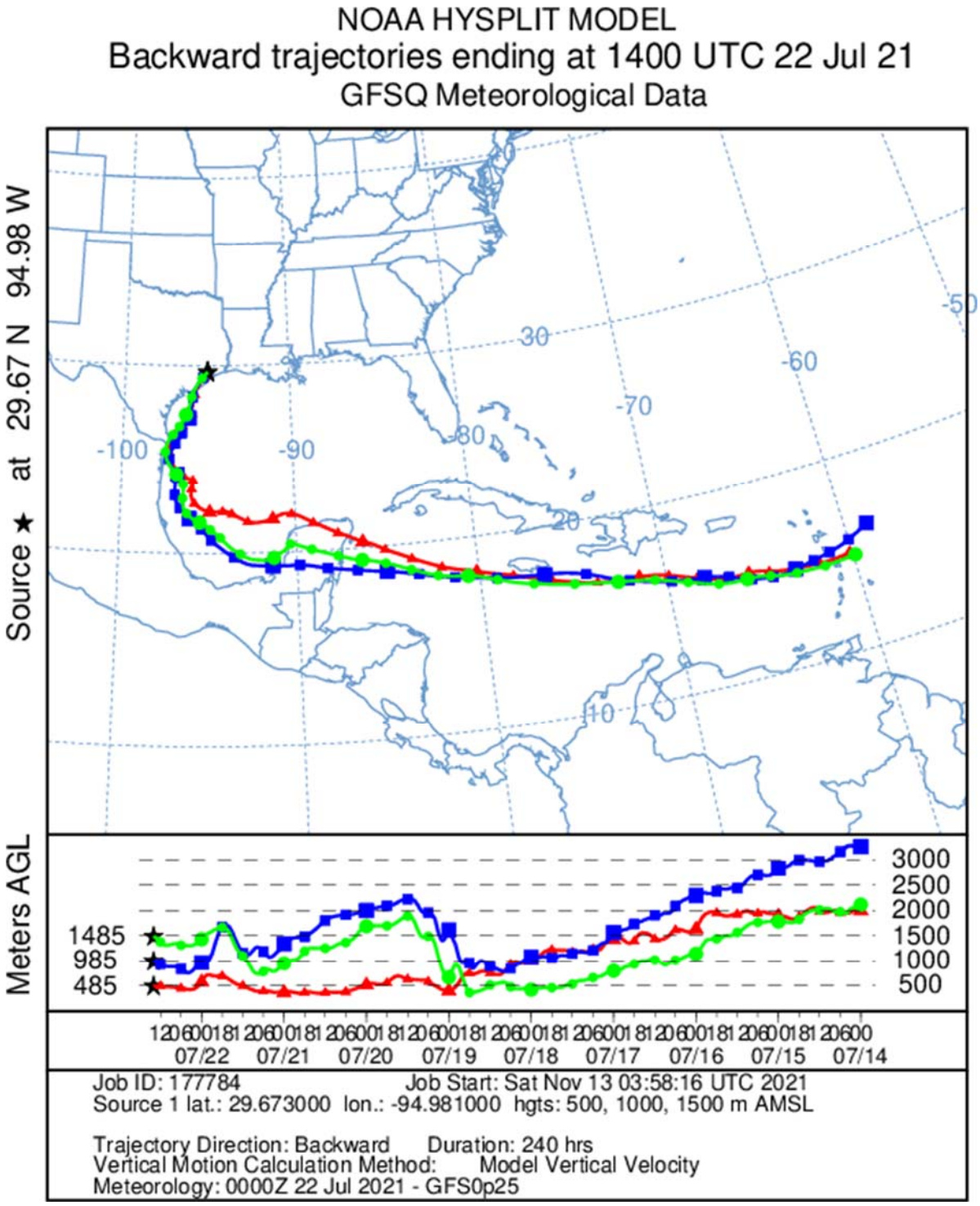

Figure 193. Ten-day HYSPLIT back trajectory for the ozonesonde launch on 22 July 2021 from three heights over the Bay: 500 m (red), 1,000 m (blue), and 1,500 m (green). Each data point is 6 hours apart.

9.22 21 July 2021:

Travis Griggs (UH), Paul Walter (St. Edward's), Michael Comas (UH) and Gabriella Pessoa (UH) met at the marina at 6:30am CST. Initially the pontoon boat headed north towards Morgan's Point for an ozonesonde that was released at 8:52am CST. After the first ozonesonde launch the pontoon came back to the dock in Kemah to resupply on helium and drop off a crew member. The pontoon redeployed to the NW area of the bay for surface sampling and an afternoon ozonesonde launch near Morgan's Point that was successfully released at 12:52pm CST. In preparation for the ozonesonde launch a ship emission plume that titrated the ozone from ~60 to 10 ppbv was observed. The pontoon boat was refueled and docked at 1:45pm CST.

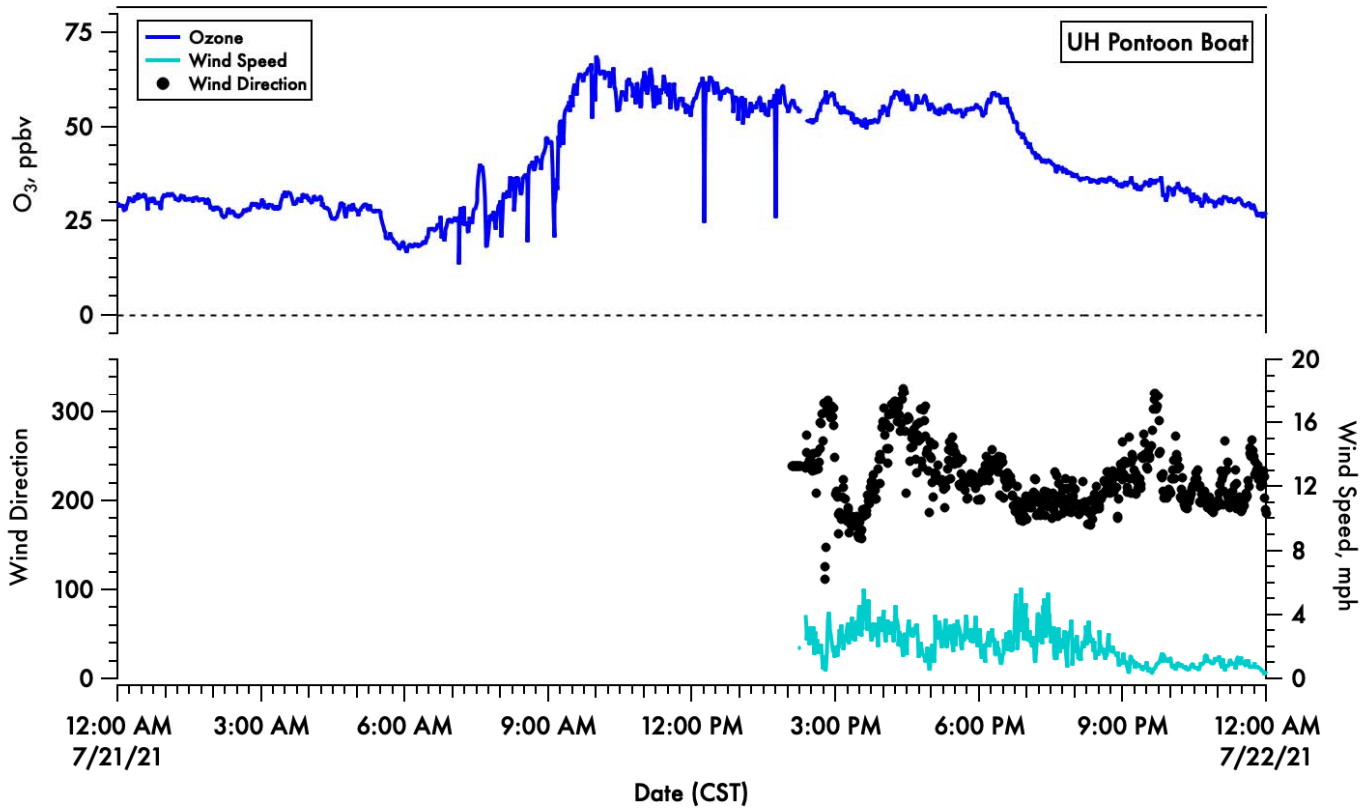

Figure 194. A time-series of 1-minute averaged ozone (blue) on the top panel and wind speed (light blue) and direction (black dots) in the bottom panel.

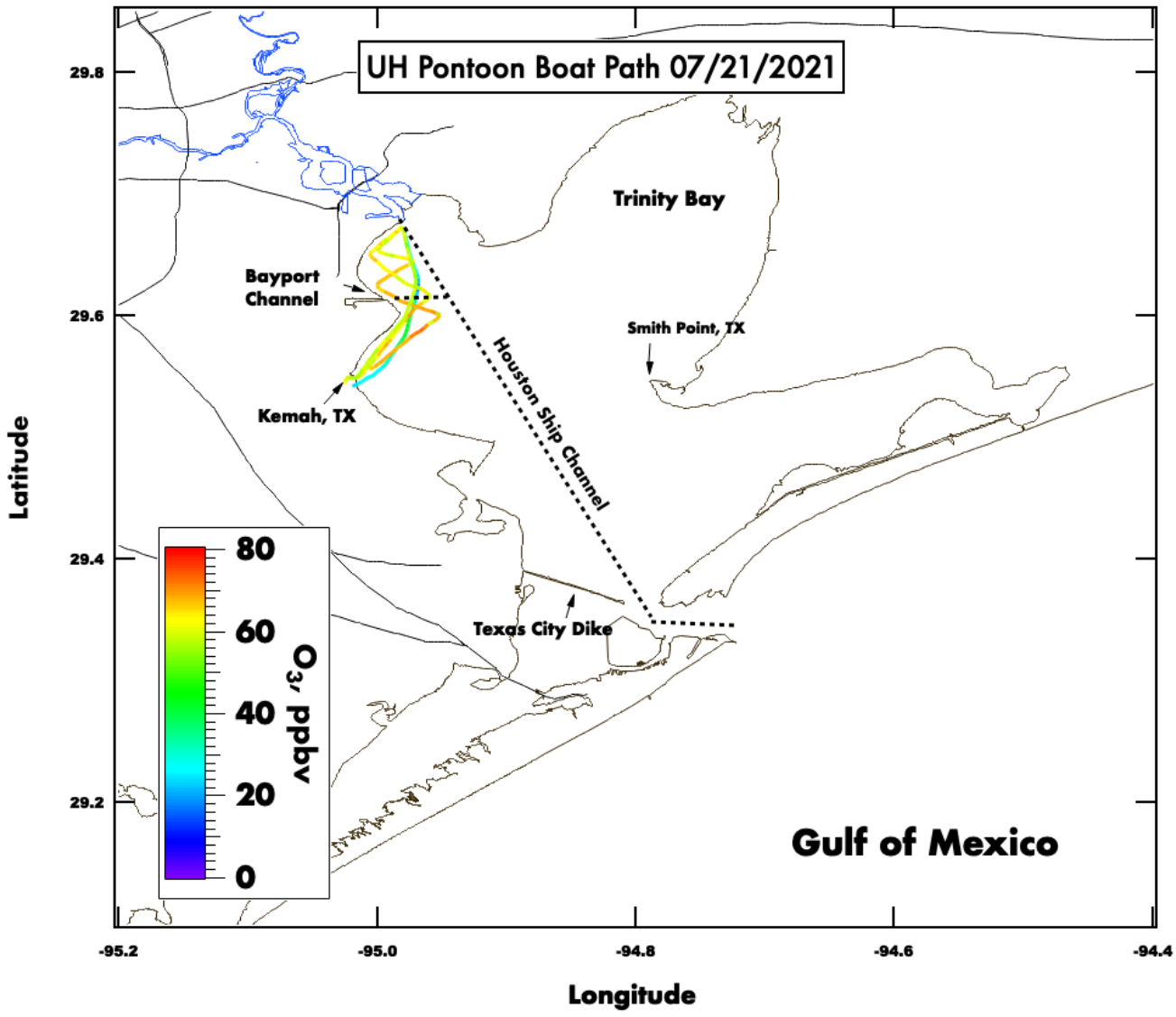

Figure 195. Spatial plot of surface ozone collected from the UH pontoon boat on September 9th, 2021.

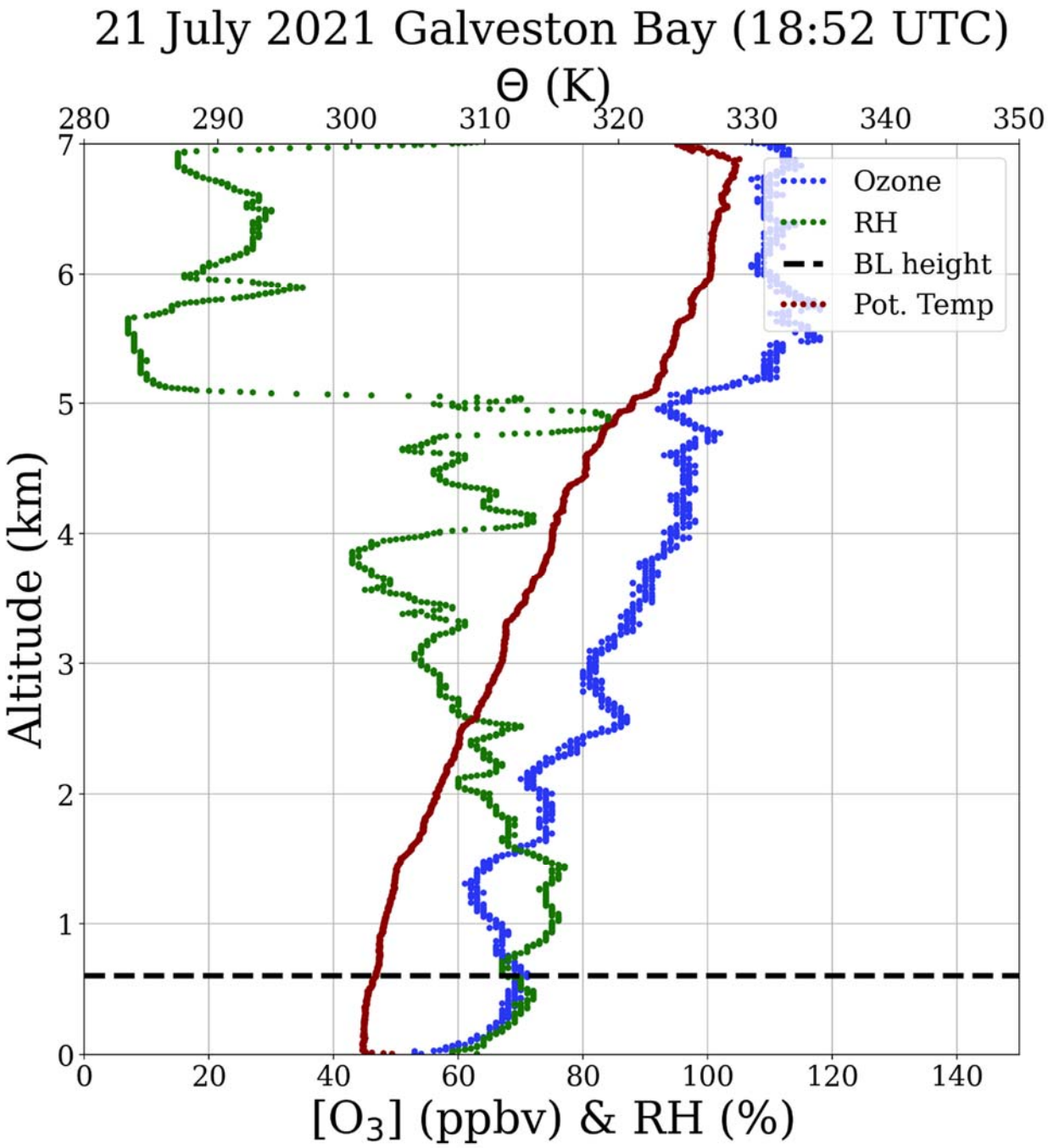

Figure 196. Vertical profiles of ozone (blue), relative humidity (green) and potential temperature (red). The derived boundary layer height is denoted by the horizontal dashed black line.

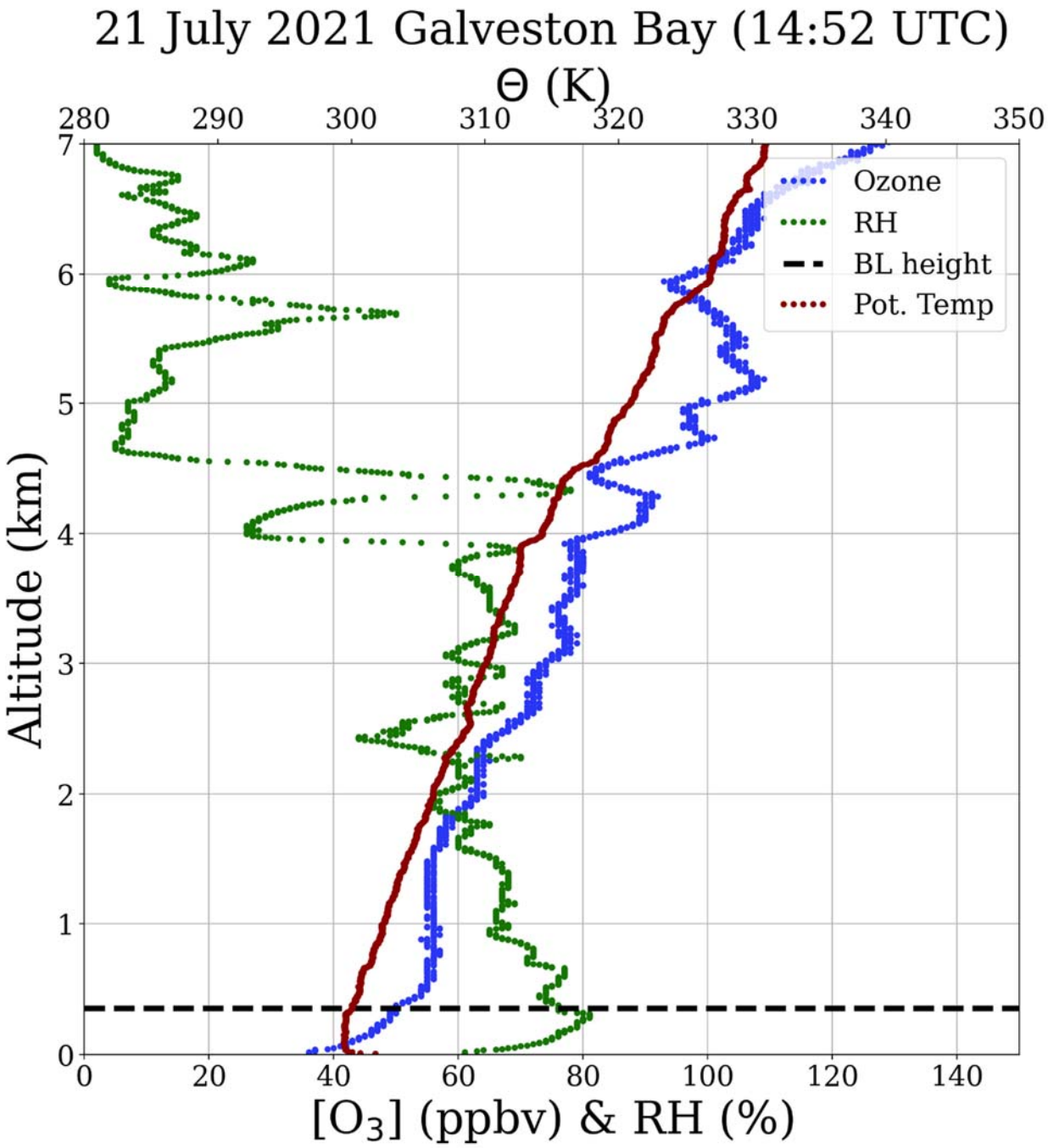

Figure 197. Vertical profiles of ozone (blue), relative humidity (green) and potential temperature (red). The derived boundary layer height is denoted by the horizontal dashed black line.

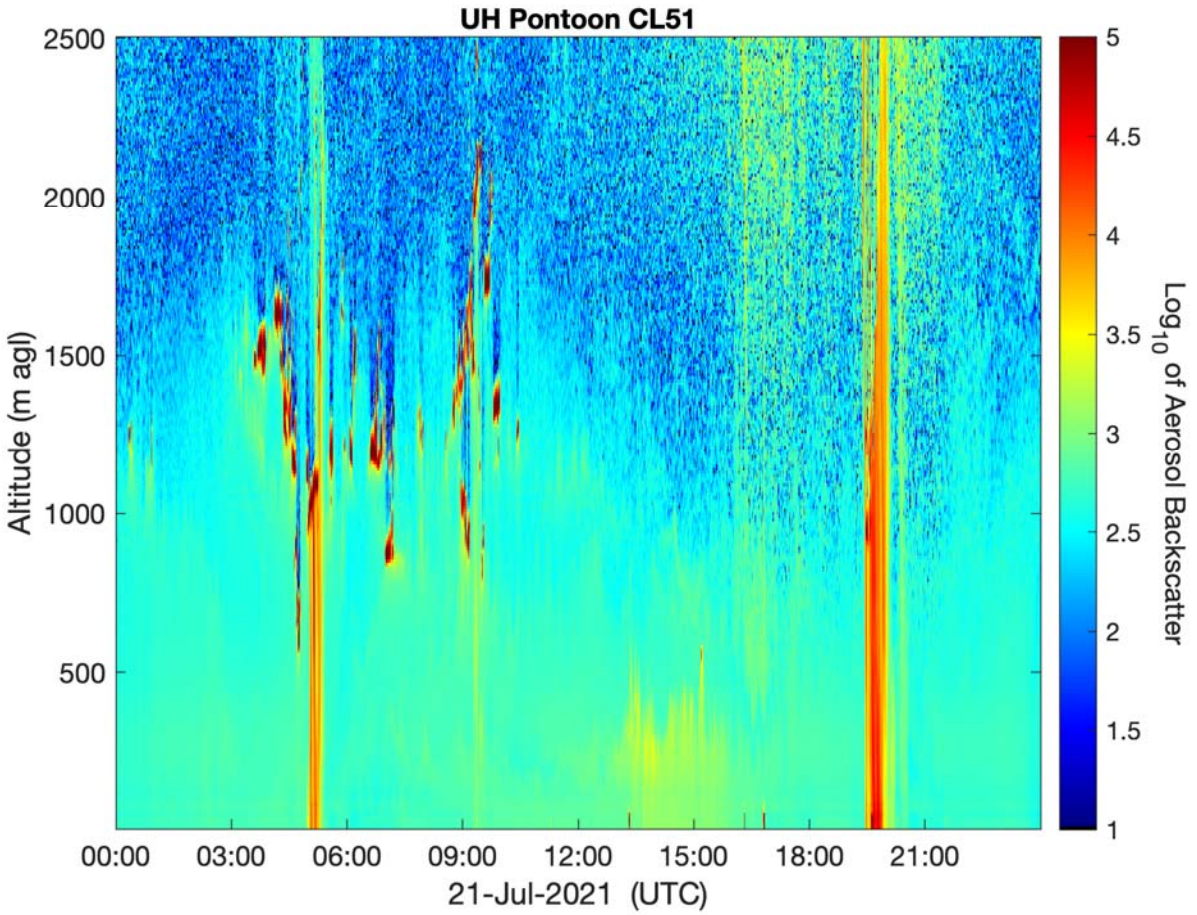

Figure 198. Vertical profile of the aerosol backscatter collected from a Vaisala CL-51 ceilometer mounted on the UH Pontoon boat.

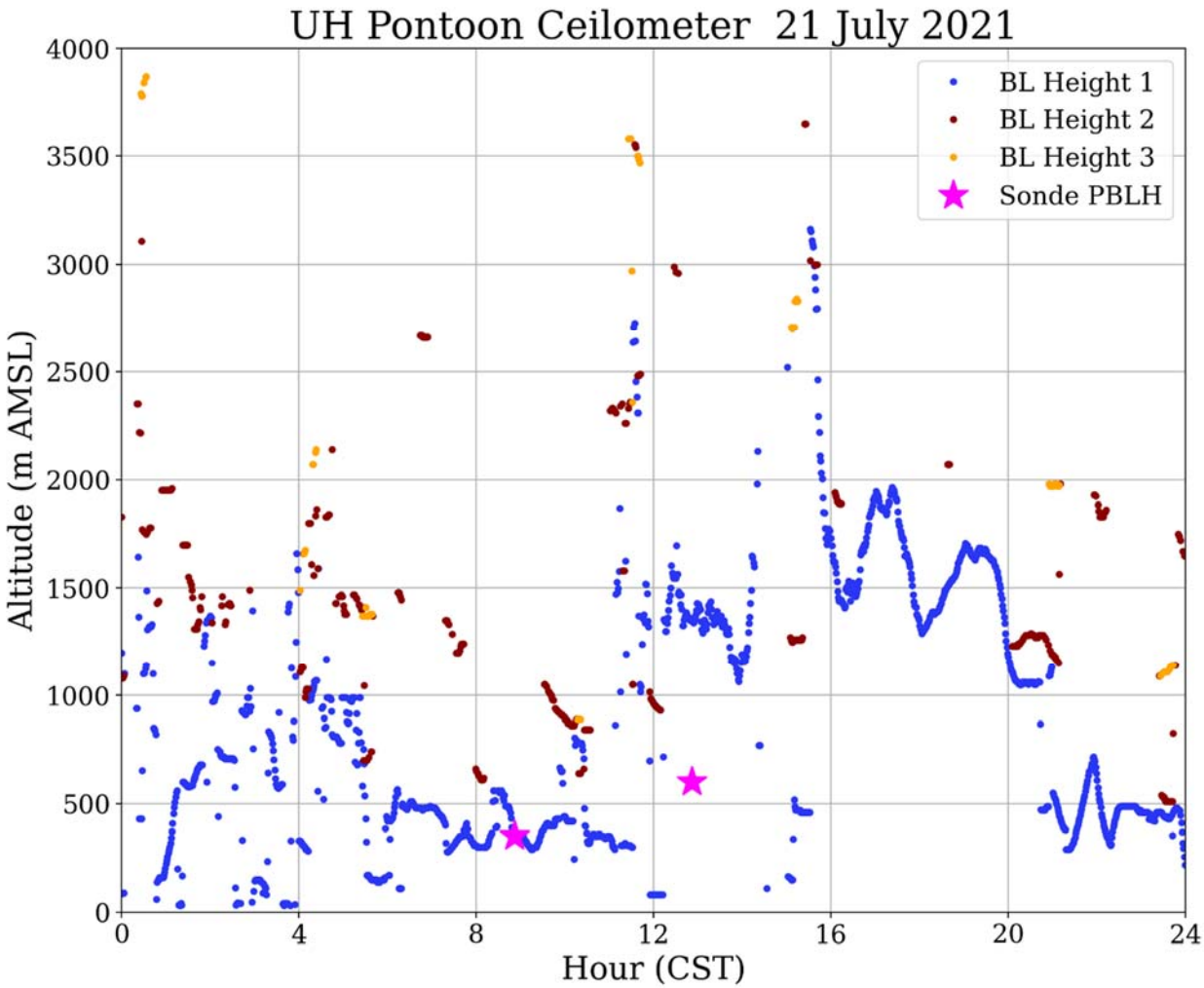

Figure 199. UH Pontoon Vaisala CL-51 ceilometer returned boundary layer heights and boundary layer height from the ozonesonde profile.

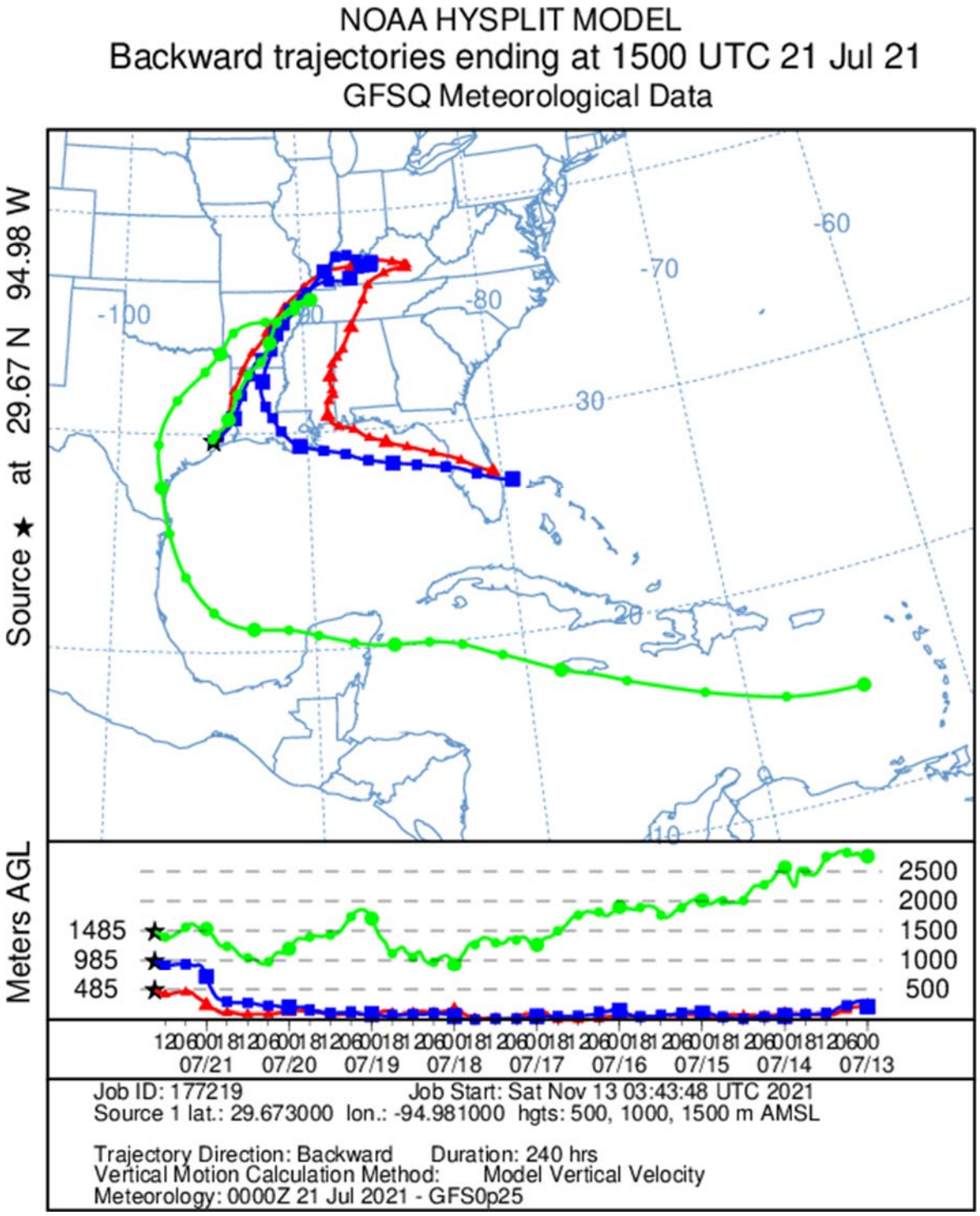

Figure 200. Ten-day HYSPLIT back trajectory for the first ozonesonde launch on 21 July 2021 from three heights over the Bay: 500 m (red), 1,000 m (blue), and 1,500 m (green). Each data point is 6 hours apart.

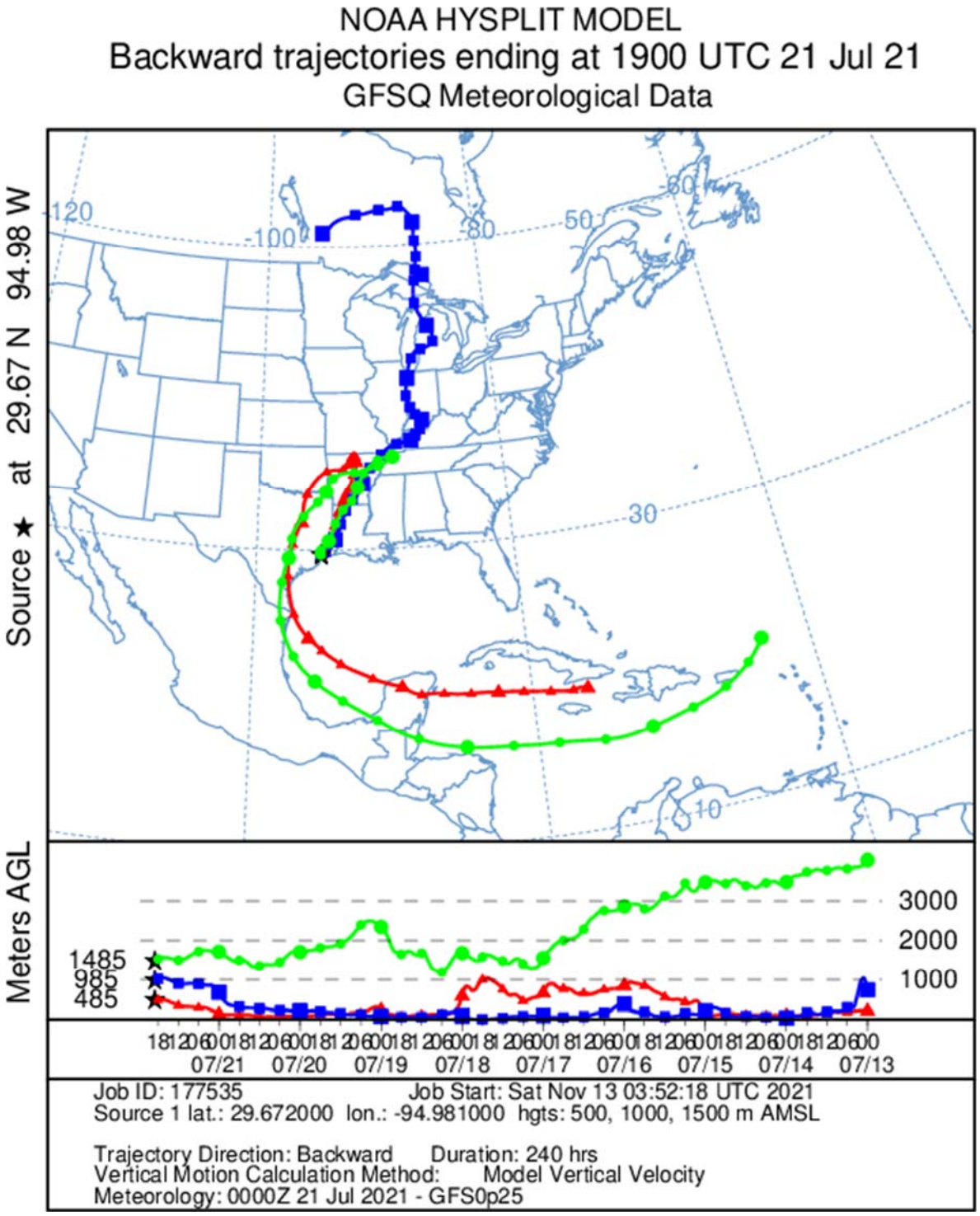

Figure 201. Ten-day HYSPLIT back trajectory for the first ozonesonde launch on 26 July 2021 from three heights over the Bay: 500 m (red), 1,000 m (blue), and 1,500 m (green). Each data point is 6 hours apart.

9.23 18 July 2021:

Travis Griggs (UH), Paul Walter (St. Edward's) and Michael Comas (UH) met at the Portofino marina at 6:00am CST. The daily plan was to go to the SW region of the Bay to target a 'low' ozone day to compare with previous work done near San Luis Pass (Tuite 2018). Initially the pontoon boat headed south towards the Texas City Dike for a morning ozonesonde launch that was released at 8:54am CST. A circle surface sampling pattern was conducted in the SW area of the bay before an afternoon ozonesonde launch that was released at 12:09pm CST. After the afternoon launch the pontoon boat was brought back to Kemah and docked at 1:45pm CST.

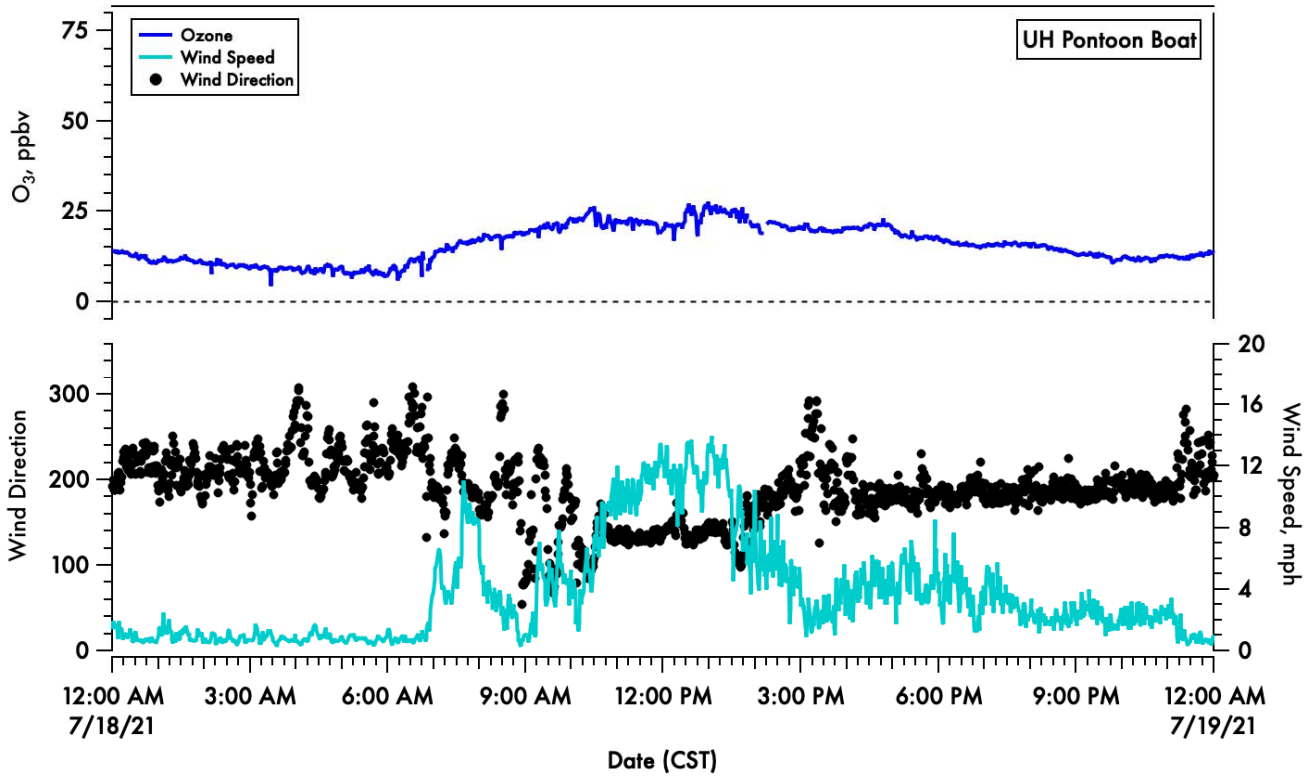

Figure 202. A time-series of 1-minute averaged ozone (blue) on the top panel and wind speed (light blue) and direction (black dots) in the bottom panel.

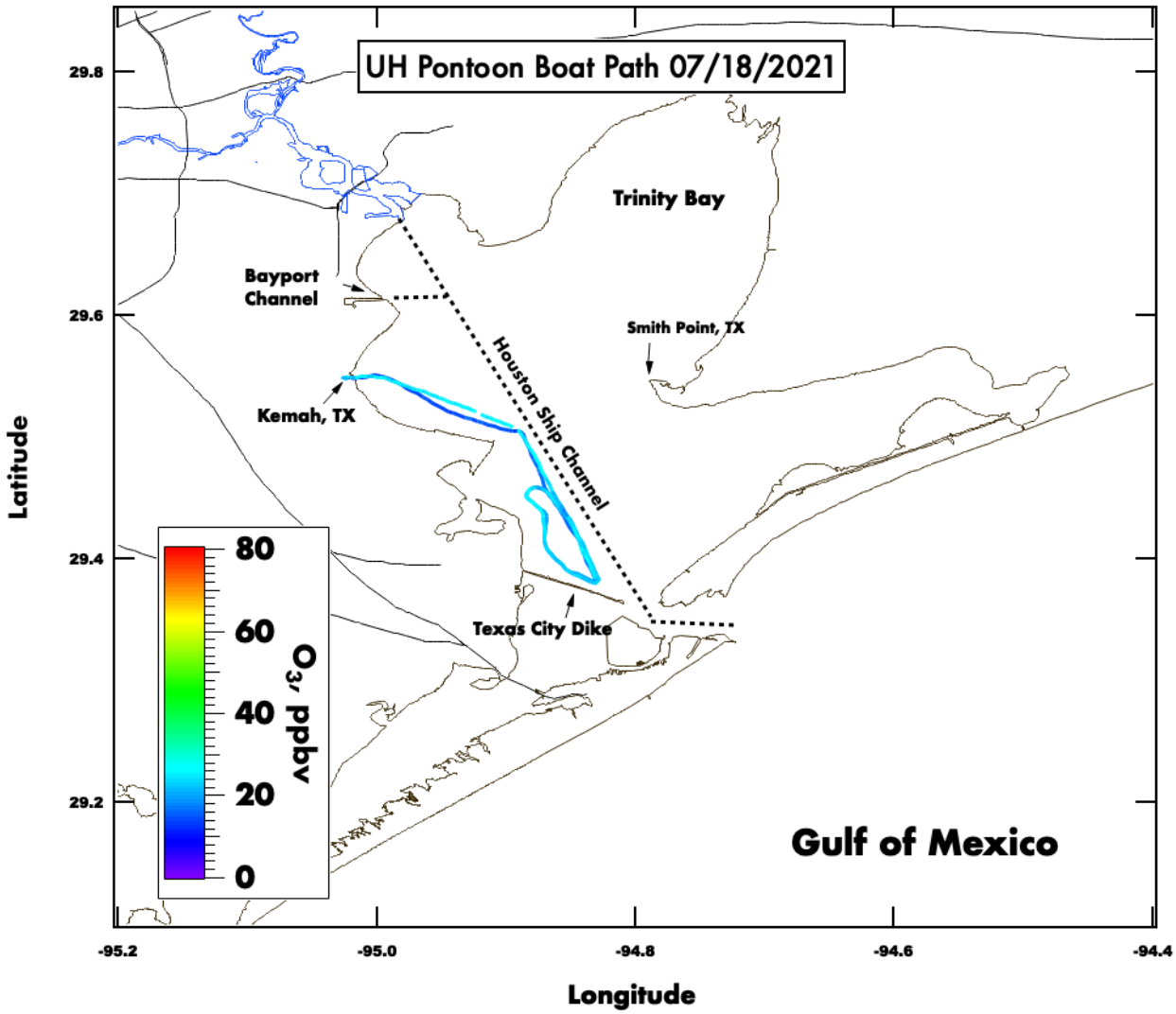

Figure 203. Spatial plot of surface ozone collected from the UH pontoon boat on July 18th, 2021.

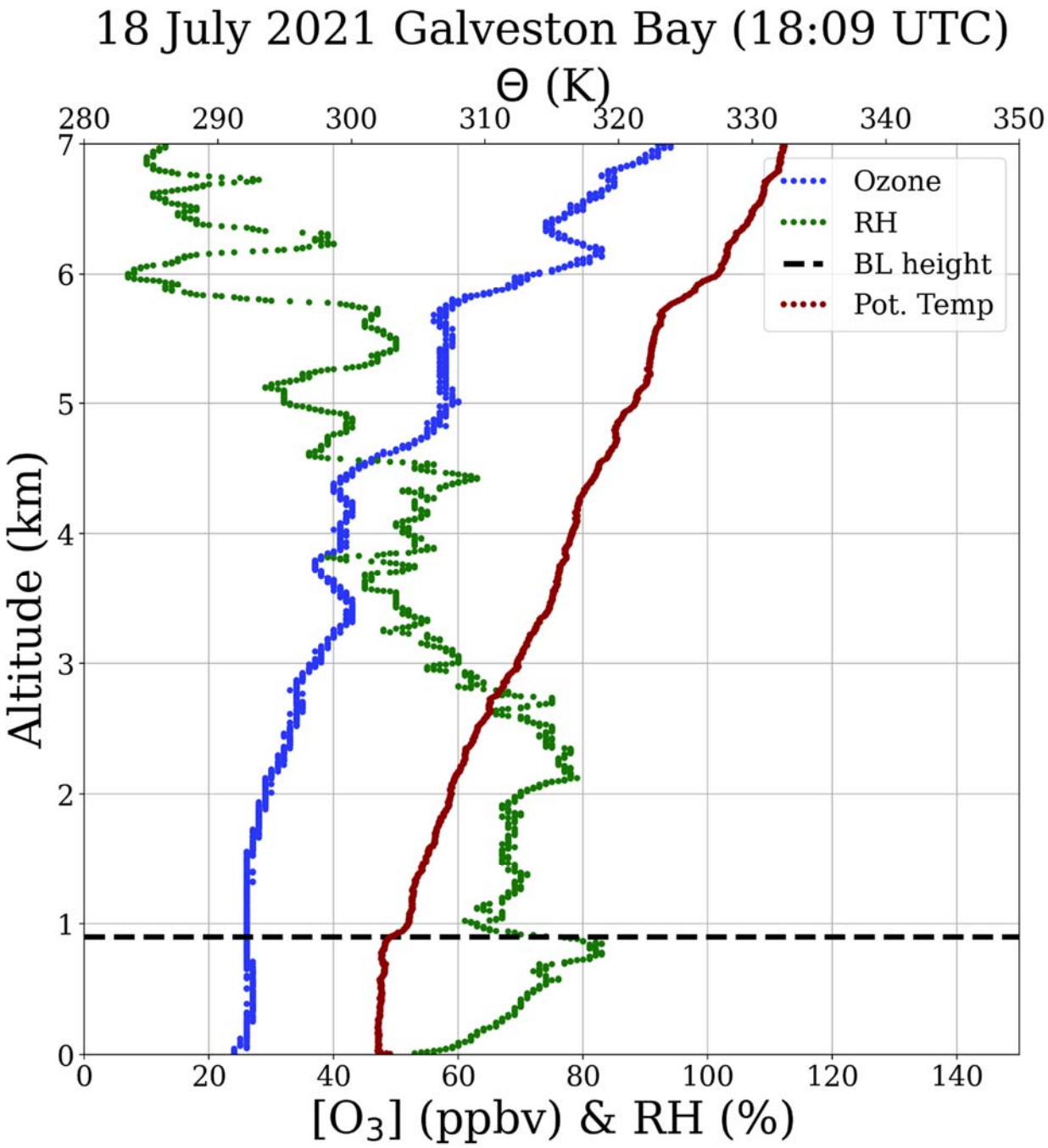

Figure 6.23.3. Vertical profiles of ozone (green), relative humidity (blue) and potential temperature (red). The derived boundary layer height is denoted by the horizontal dashed black line.

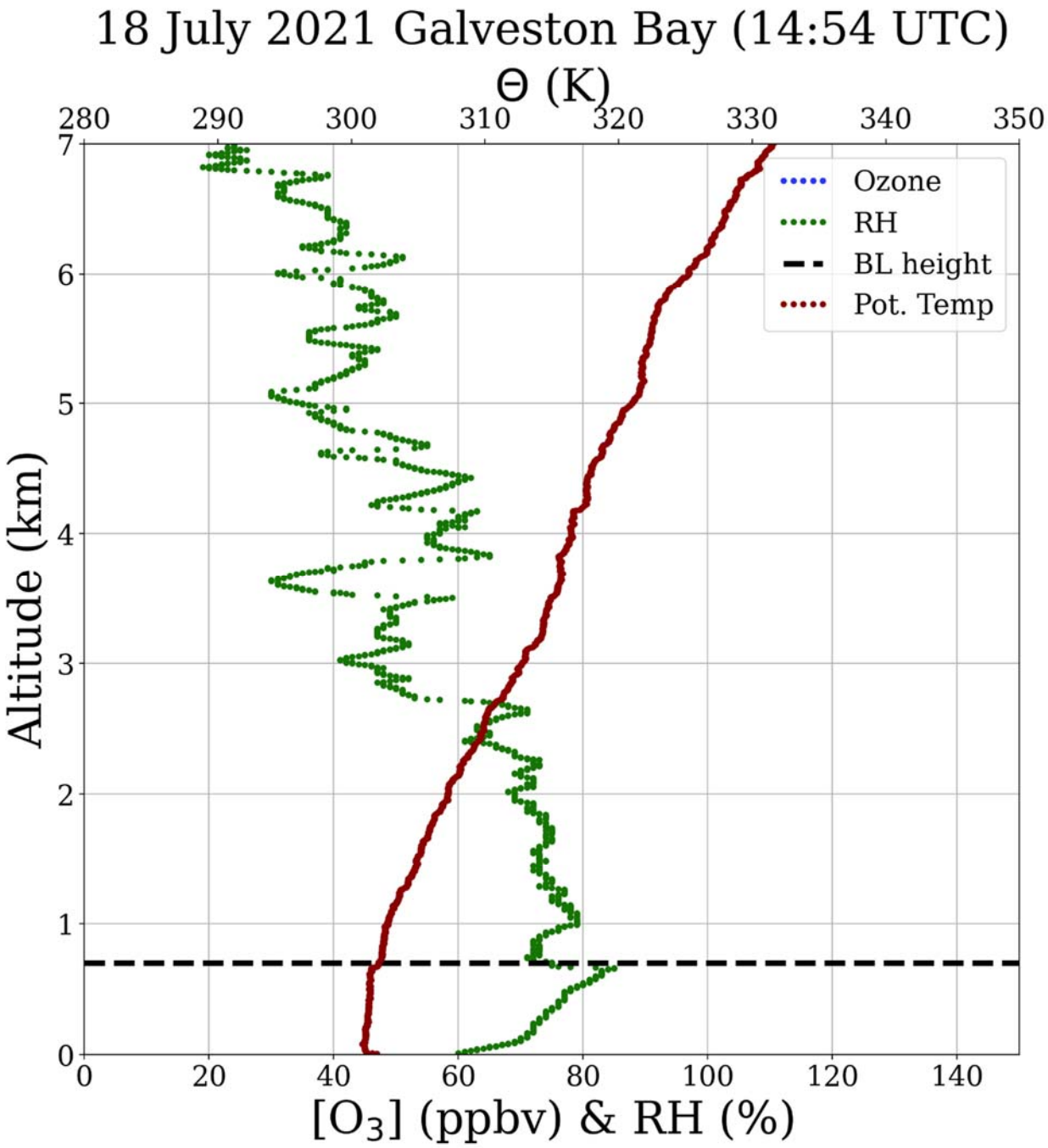

Figure 204. Vertical profiles of ozone (blue), relative humidity (green) and potential temperature (red). The derived boundary layer height is denoted by the horizontal dashed black line.

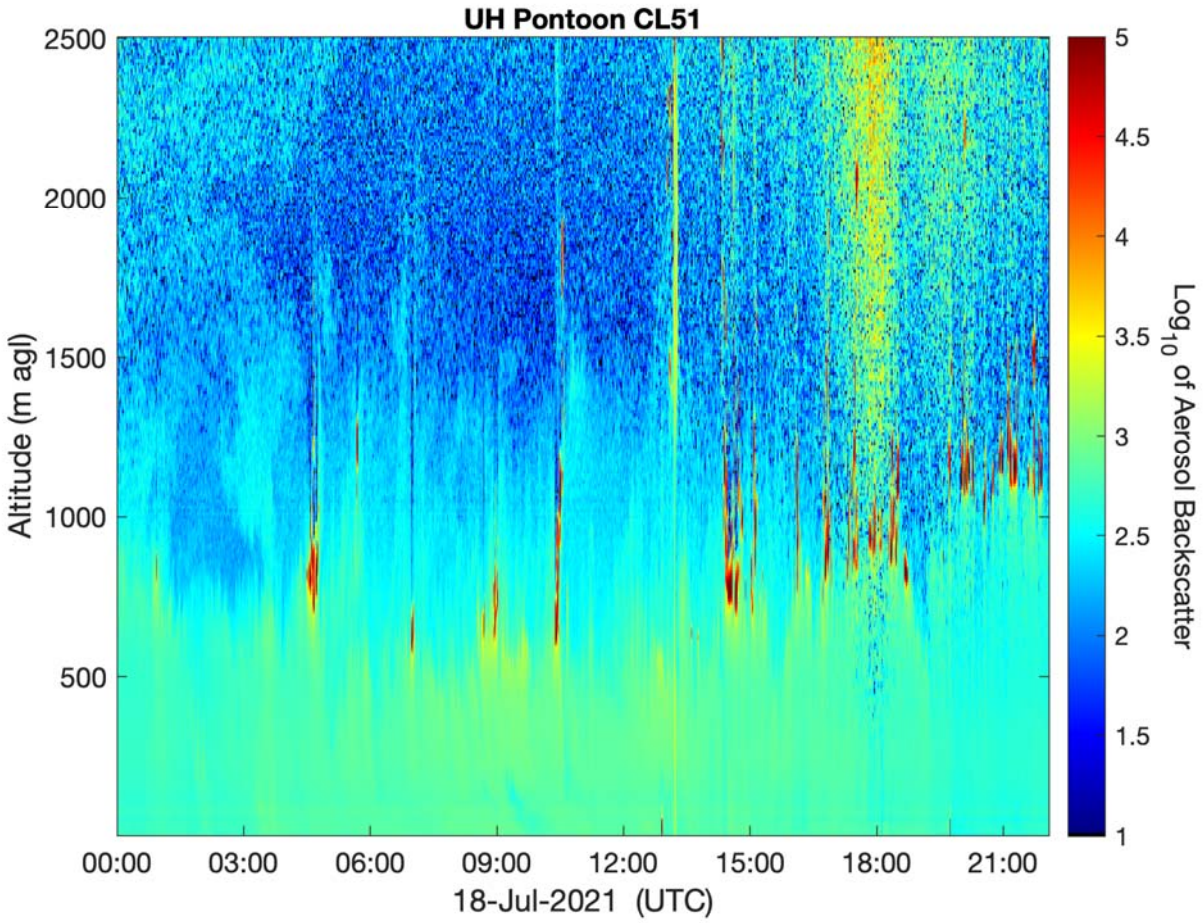

Figure 205. Vertical profile of the aerosol backscatter collected from a Vaisala CL-51 ceilometer mounted on the UH Pontoon boat.

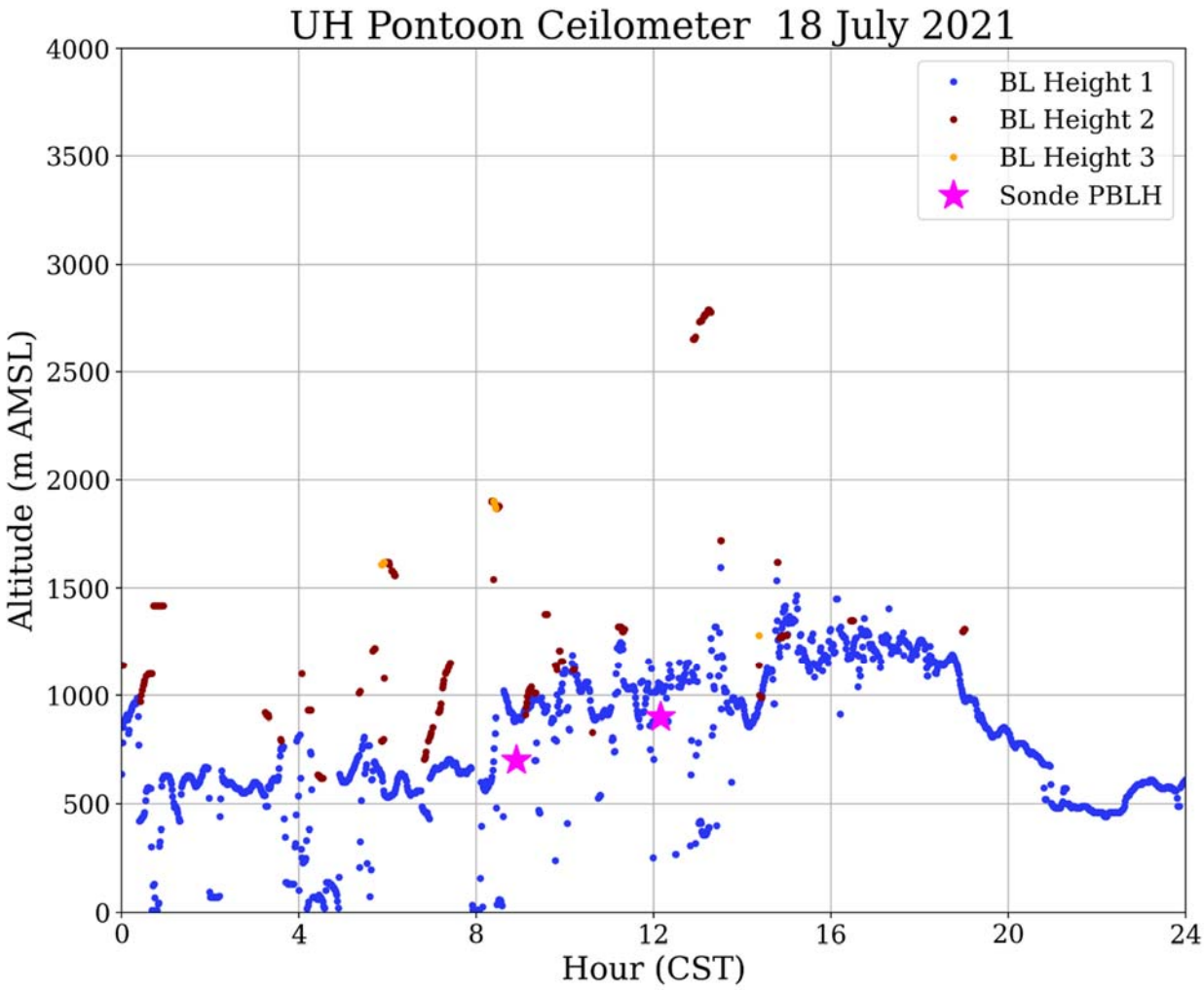

Figure 206. UH Pontoon Vaisala CL-51 ceilometer returned boundary layer heights and boundary layer height from the ozonesonde profile.

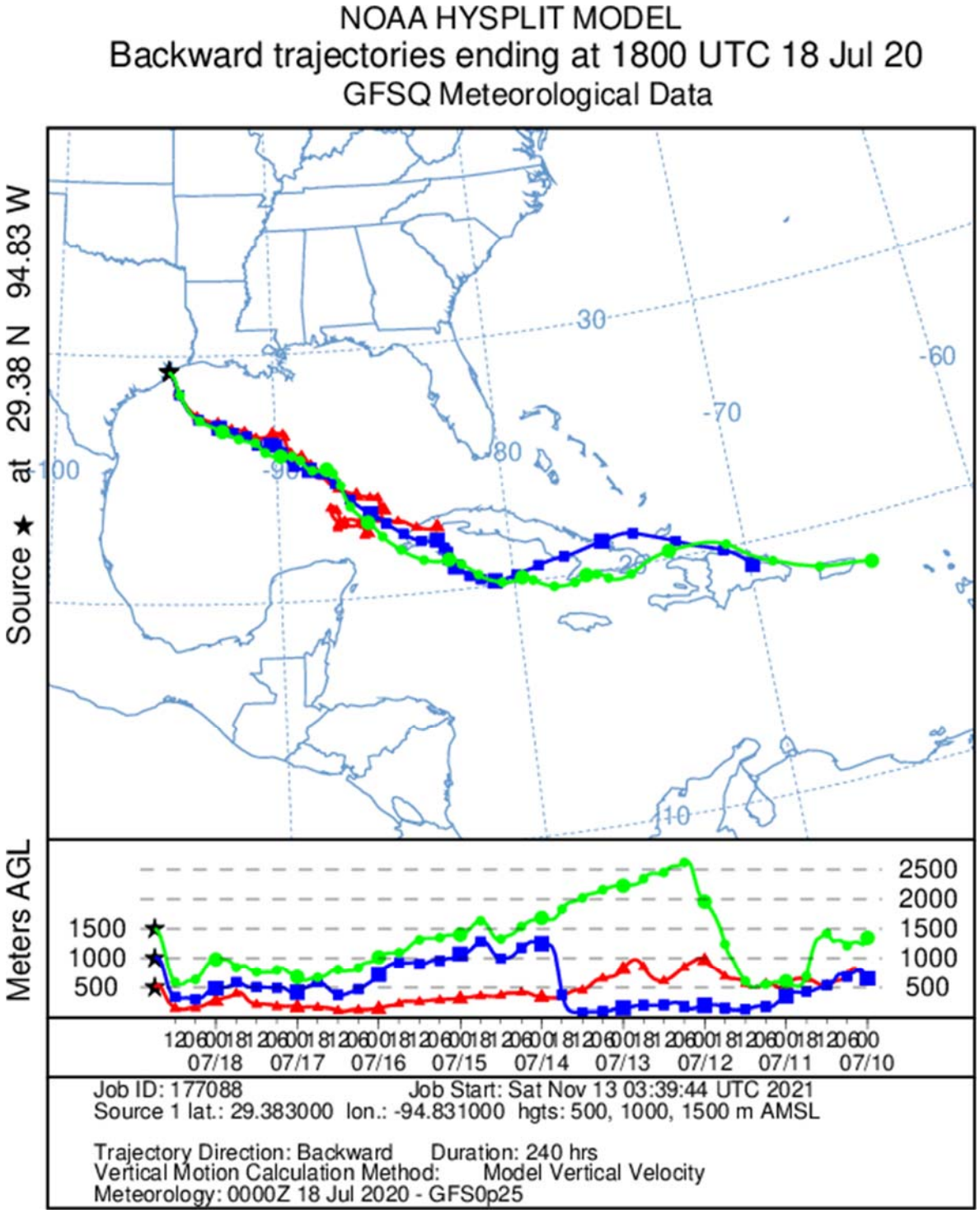

Figure 207. Ten-day HYSPLIT back trajectory for the ozonesonde launch on 18 July 2021 from three heights over the Bay: 500 m (red), 1,000 m (blue), and 1,500 m (green). Each data point is 6 hours apart.

9.24 14 July 2021:

Travis Griggs (UH), Paul Walter (St. Edward's) and Michael Comas (UH) met at the Portofino marina at 7:00am CST. Initially the pontoon boat headed to the NW area of the bay for surface sampling. The pontoon boat then attempted to go to the SW area of the bay, but water conditions were rougher than the crew felt comfortable with. Another pass in the NW area of the Bay was conducted before heading back to Kemah to be refueled and docked at 12:00pm CST.

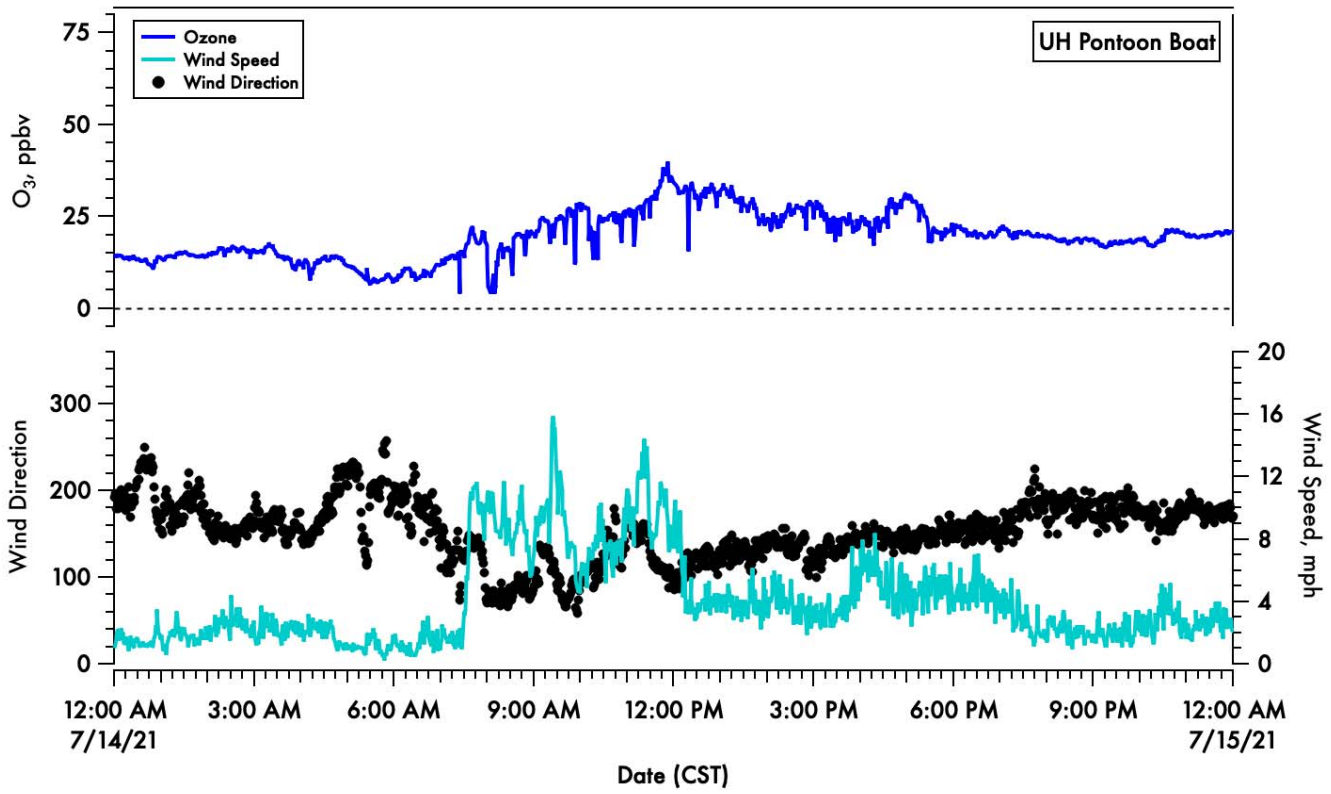

Figure 208. A time-series of 1-minute averaged ozone (blue) on the top panel and wind speed (light blue) and direction (black dots) in the bottom panel.

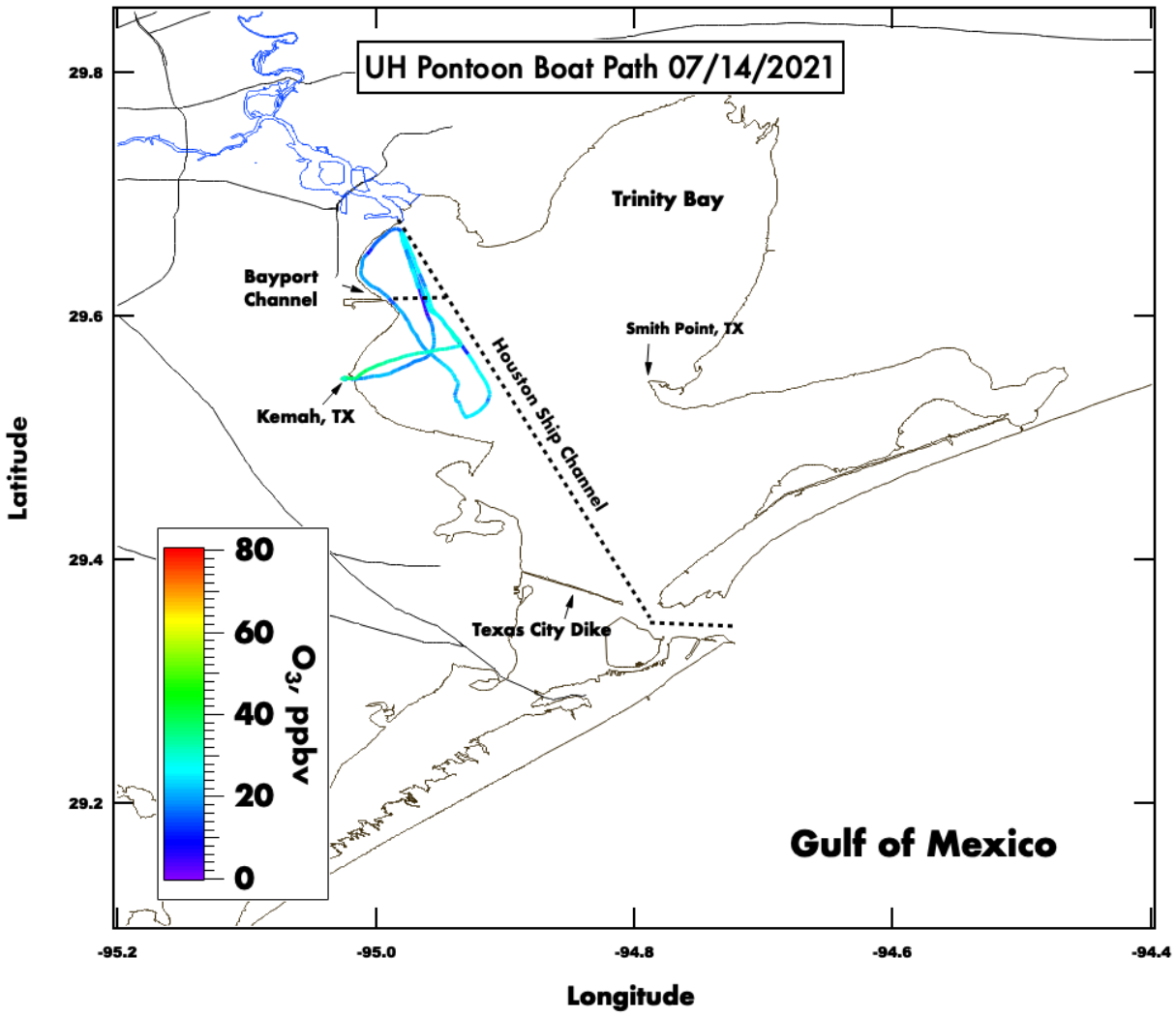

Figure 209. Spatial plot of surface ozone collected from the UH pontoon boat on July 14th, 2021.

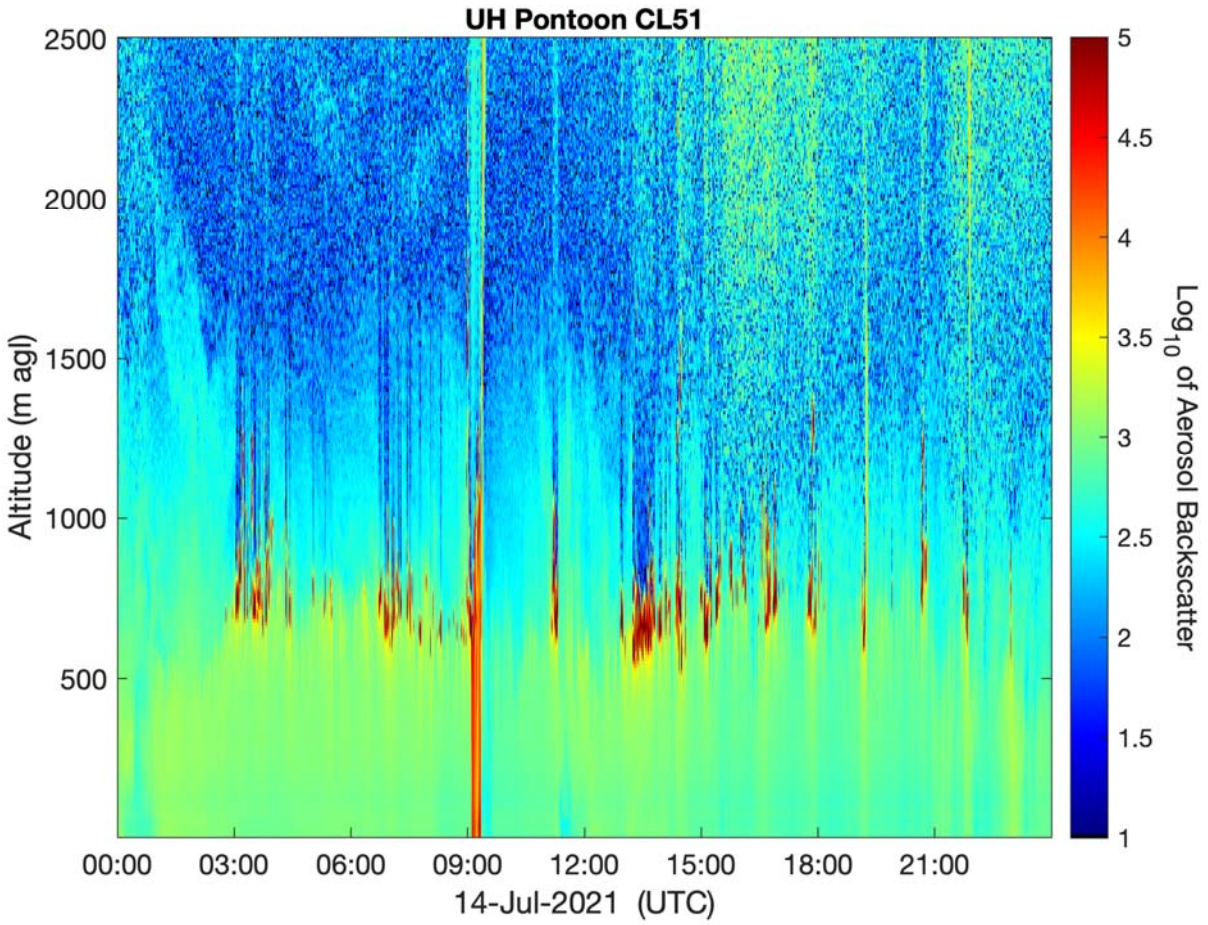

Figure 210. Vertical profile of the aerosol backscatter collected from a Vaisala CL-51 ceilometer mounted on the UH Pontoon boat.

9.25 13 July 2021:

Travis Griggs (UH), Paul Walter (St. Edward's), Michael Comas (UH) and Gabriella Pessoa (UH) met at the Portofino Marina at 06:00am CST. Bay conditions were forecast as smooth with 5-10 knot winds. The daily plan was to cross the HSC at the south cut and head to the SE portion of Galveston Bay. The balloon launch was successfully released at 9:04 am CST, aided using a soccer net to control the balloon during fill and pre-launch checks. After the balloon descent, a loop around the SE portion of Galveston Bay was made monitoring surface ozone, meteorological and ceilometer data. An afternoon ozonesonde launch at the same spot in the Bay was successfully released at 2:04 pm CST. After the afternoon launch the pontoon boat headed back to Kemah and was docked at ~ 4:00 pm CST.

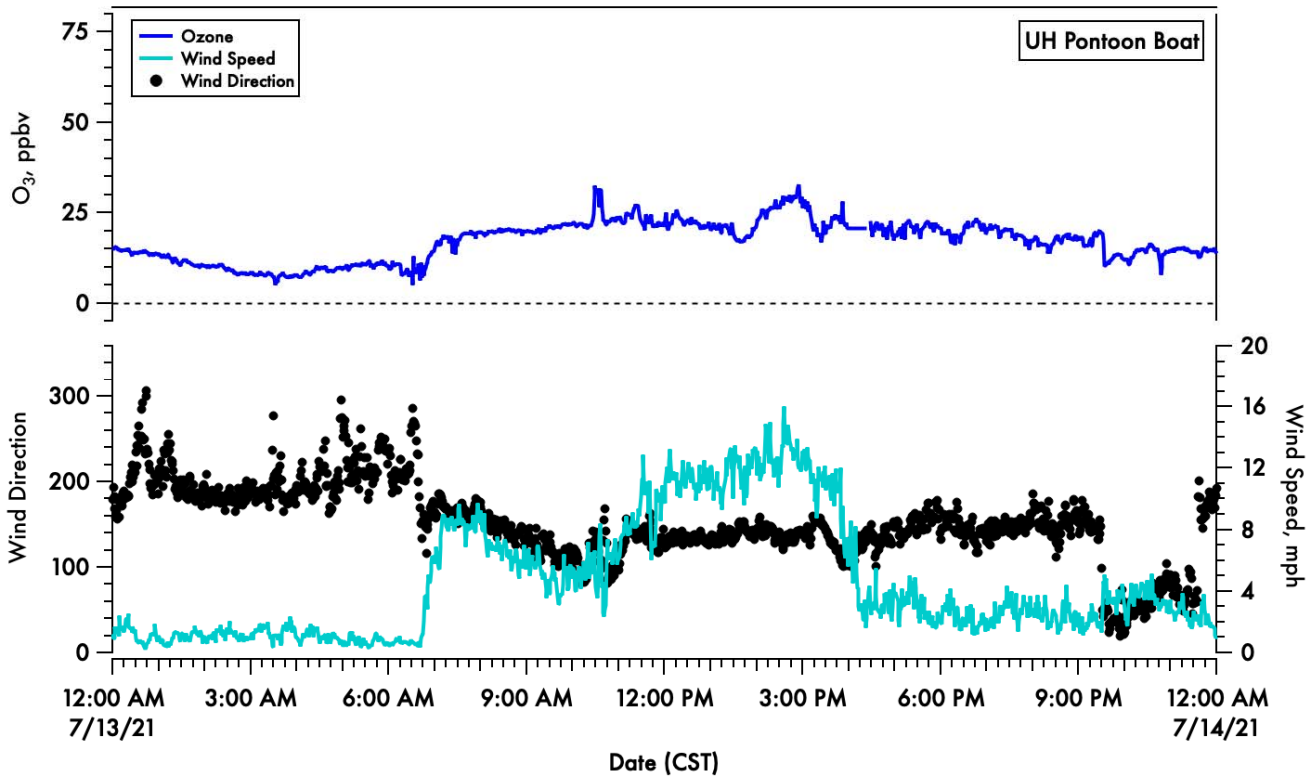

Figure 211. A time-series of 1-minute averaged ozone (blue) on the top panel and wind speed (light blue) and direction (black dots) in the bottom panel.

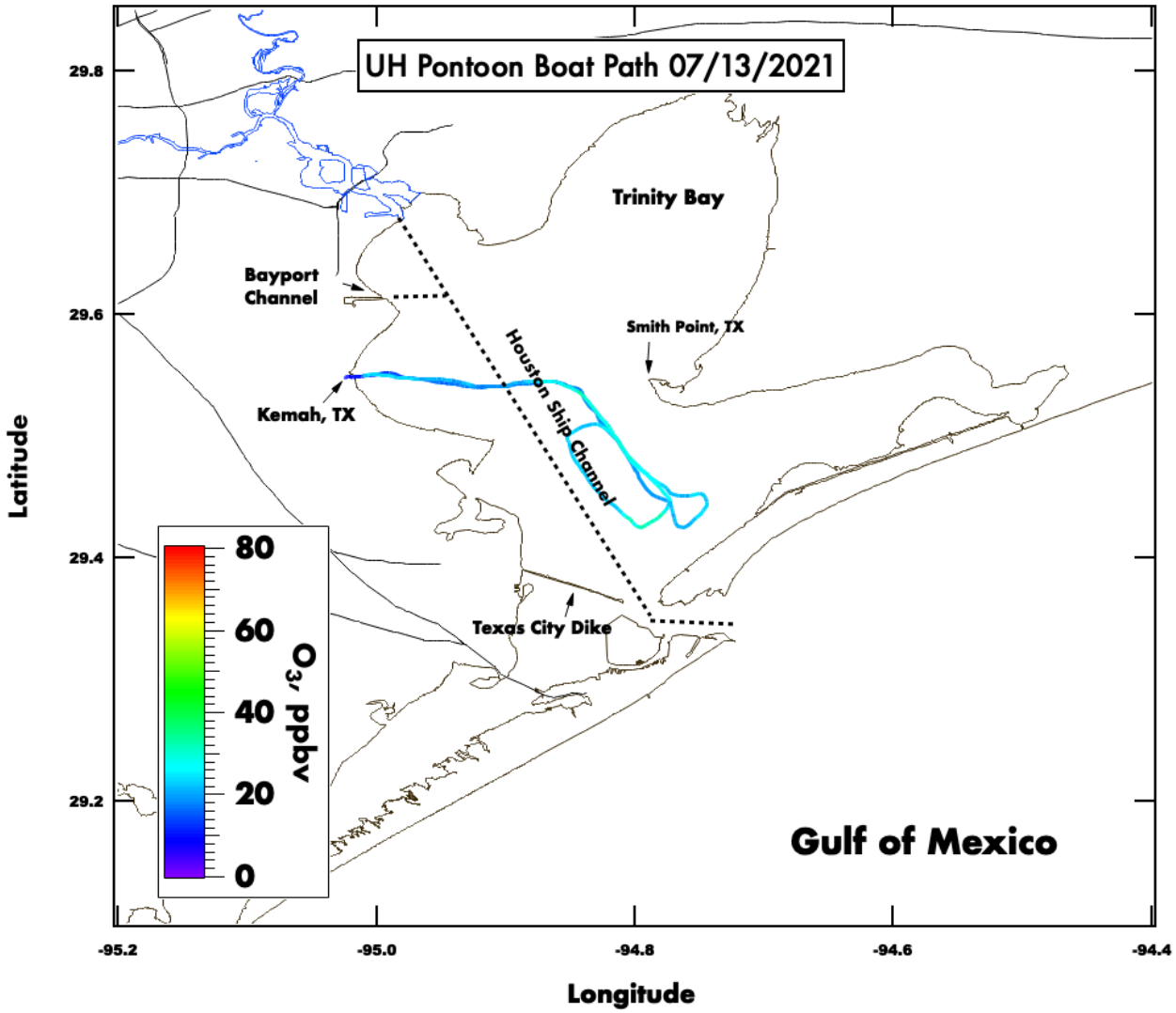

Figure 212. Spatial plot of surface ozone collected from the UH pontoon boat on July 13th, 2021.

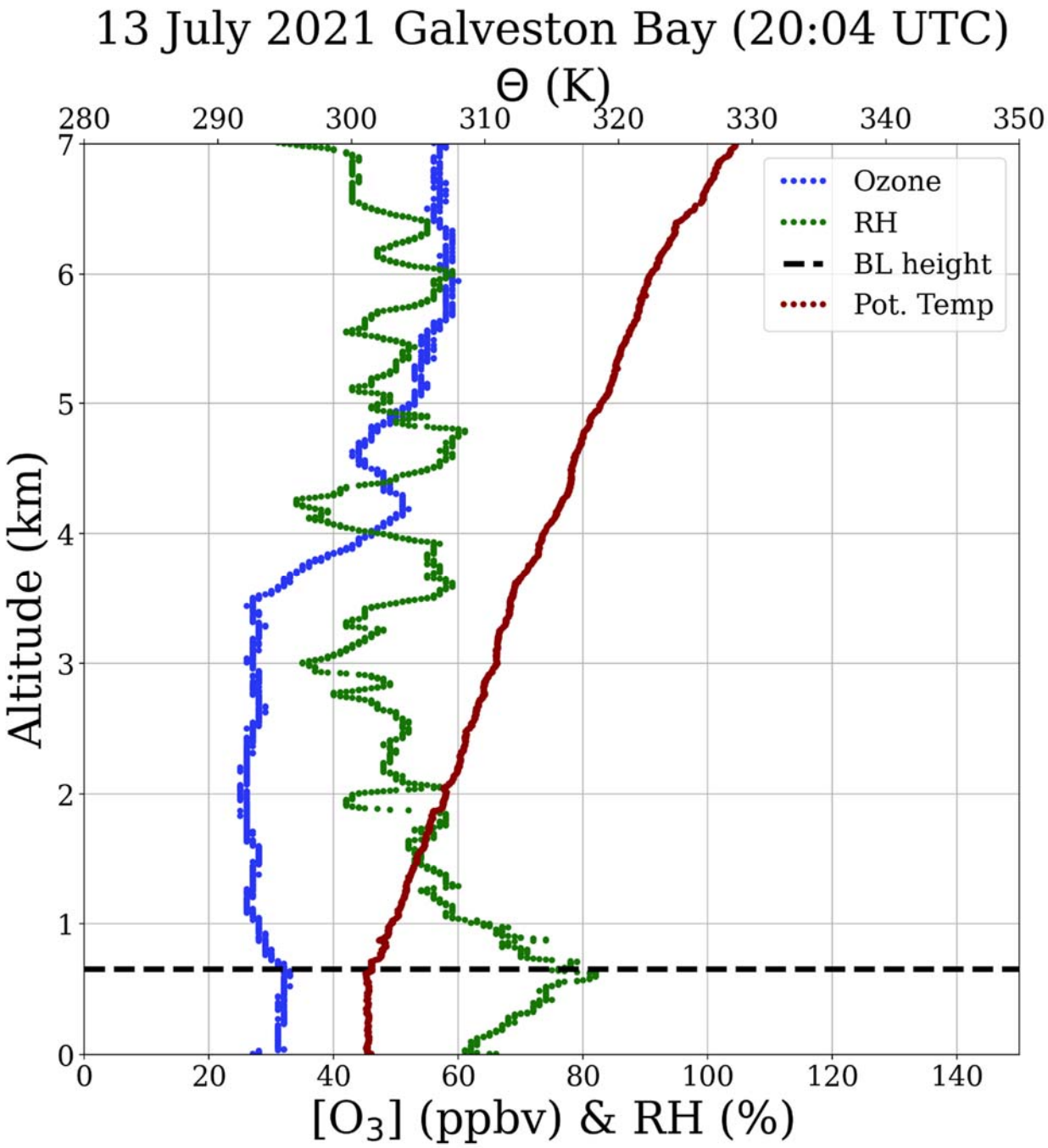

Figure 213. Vertical profiles of ozone (blue), relative humidity (green) and potential temperature (red). The derived boundary layer height is denoted by the horizontal dashed black line.

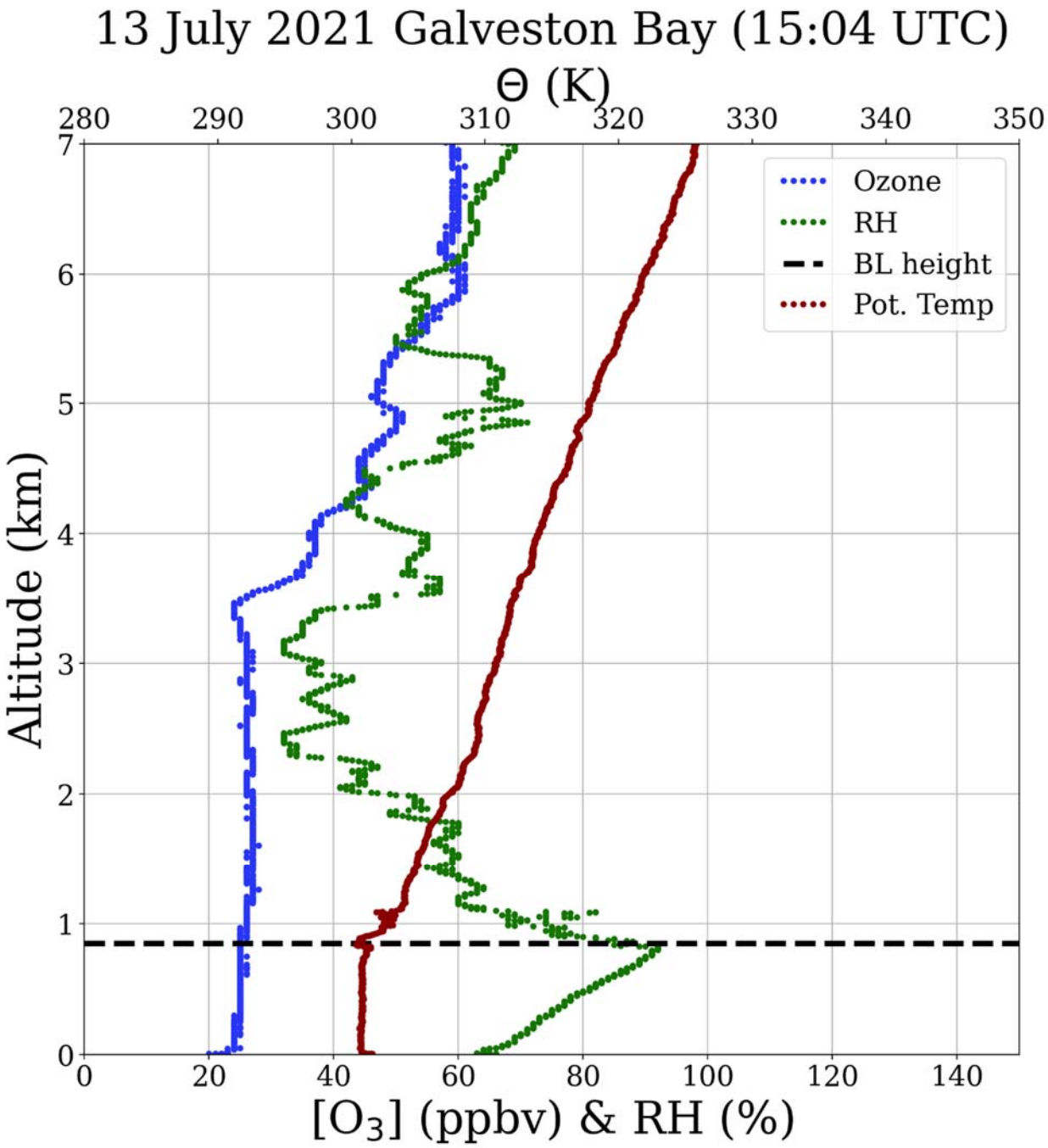

Figure 214. Vertical profiles of ozone (blue), relative humidity (green) and potential temperature (red). The derived boundary layer height is denoted by the horizontal dashed black line.

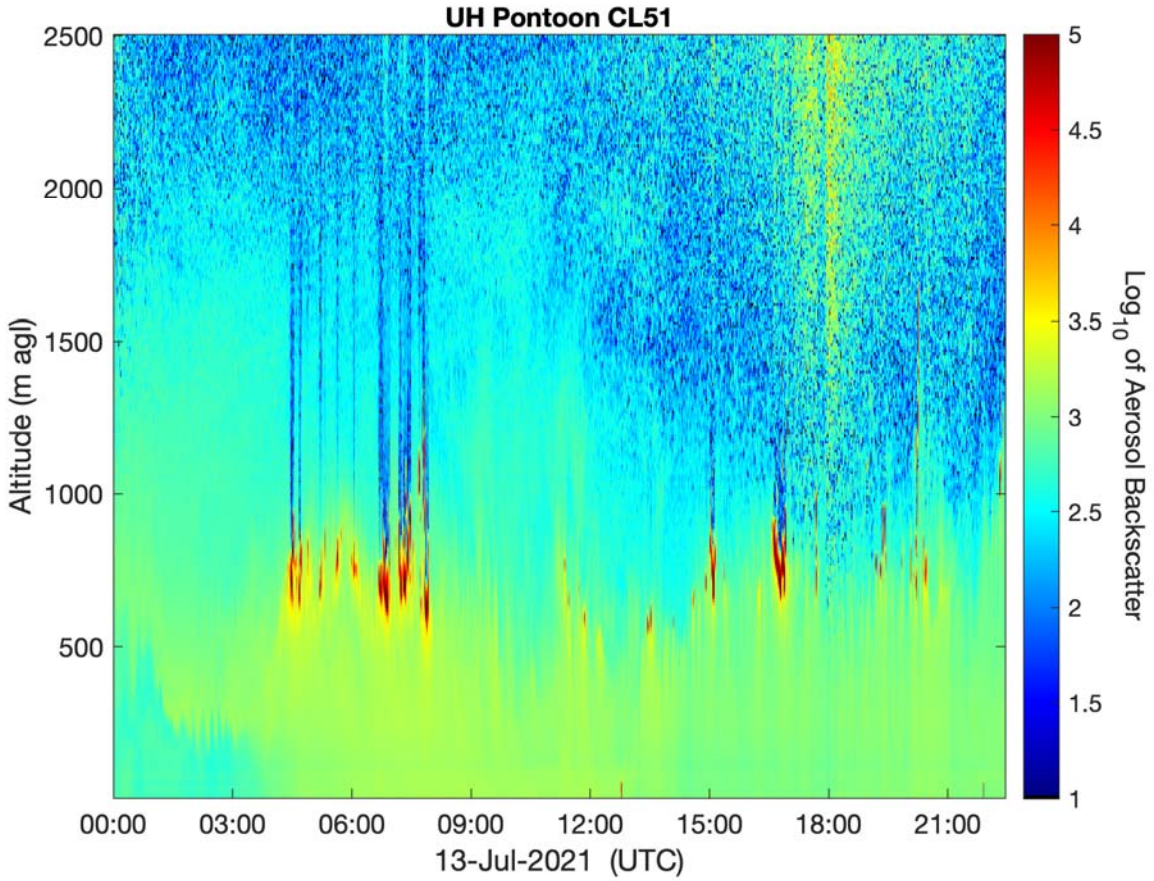

Figure 215. Vertical profile of the aerosol backscatter collected from a Vaisala CL-51 ceilometer mounted on the UH Pontoon boat.

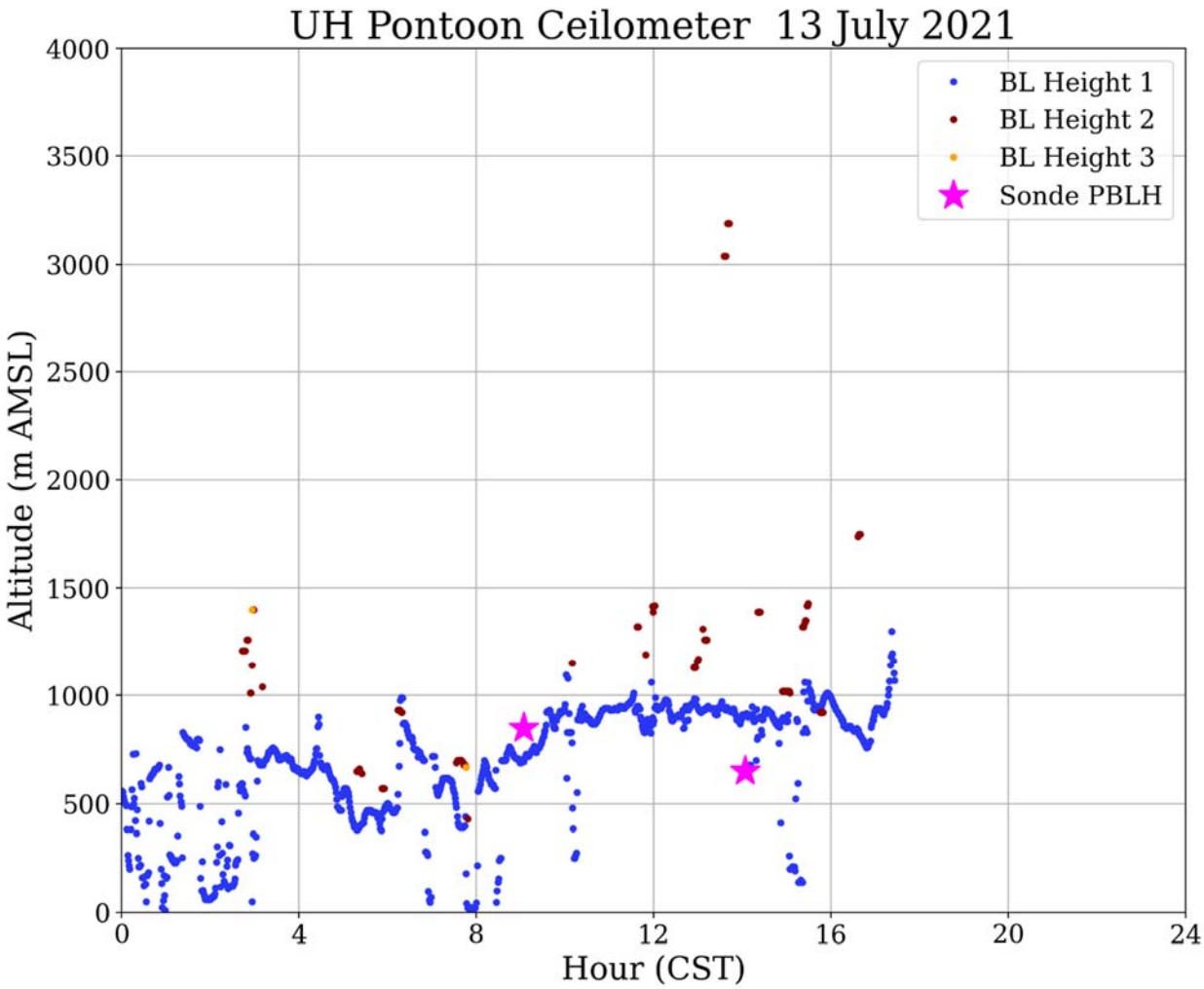

Figure 216. UH Pontoon Vaisala CL-51 ceilometer returned boundary layer heights and boundary layer height from the ozonesonde profile.

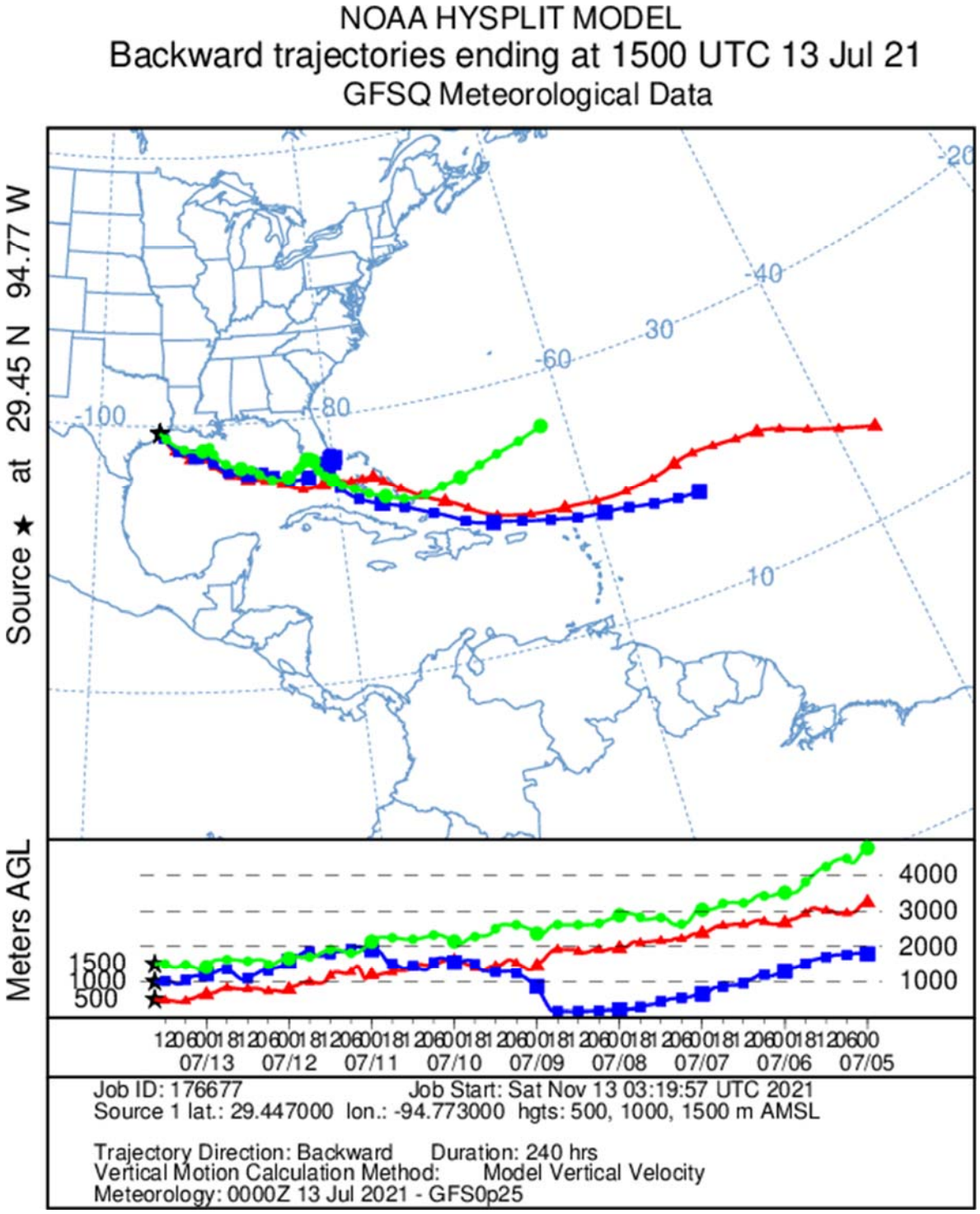

Figure 217. Ten-day HYSPLIT back trajectory for the first ozonesonde launch on 13 July 2021 from three heights over the Bay: 500 m (red), 1,000 m (blue), and 1,500 m (green). Each data point is 6 hours apart.

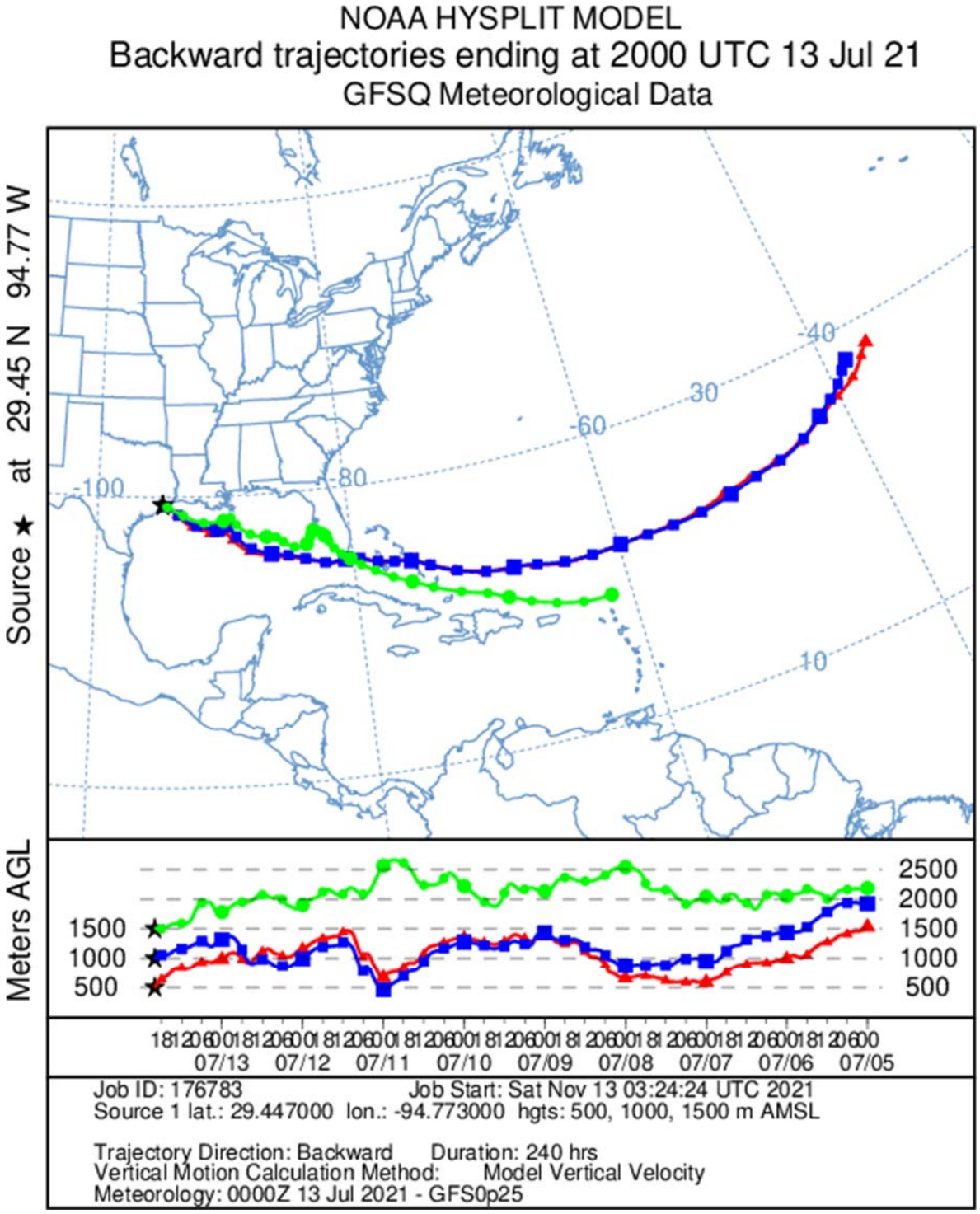

Figure 218. Ten-day HYSPLIT back trajectory for the second ozonesonde launch on 13 July 2021 from three heights over the Bay: 500 m (red), 1,000 m (blue), and 1,500 m (green). Each data point is 6 hours apart.